Optimization and Control of Voltage in Active Distribution Networks

Mohammed Alshehri

Submitted in fulfilment of the requirements for the
Degree of Doctor of Philosophy (Ph.D.)

Electronics and Electrical Engineering
James Watt School of Engineering
University of Glasgow

February 2026

Abstract

The global transition towards decarbonized and decentralized energy systems is driving the rapid integration of Distributed Energy Resources (DERs), such as solar photovoltaic (PV) systems and wind turbines, into electricity distribution networks. This evolution transforms traditionally passive networks into Active Distribution Networks (ADNs), characterized by bidirectional power flows, voltage fluctuations, and increased operational complexity. Voltage regulation emerges as a paramount challenge in this context, as the stochastic nature of renewable generation can lead to voltage violations, elevated power losses, and significant phase unbalance, particularly in inherently unbalanced three-phase low-voltage networks. While traditional devices like On-Load Tap Changers (OLTCs) provide a foundational means of voltage control, they lack the speed and flexibility to manage the spatial and temporal variations introduced by high DER penetration.

This thesis addresses these challenges by proposing and validating a series of integrated optimization frameworks that leverage the capabilities of power electronic-based Soft Open Points (SOPs) and Energy Storage Systems (ESS). The core of this research lies in the coordinated operation of these advanced technologies with traditional infrastructure to enhance the technical and economic performance of ADNs. A convex semidefinite programming (SDP) approach is used to optimize voltage profiles, reduce power losses, and improve phase balancing. Furthermore, the work introduces an economic model that includes grid purchase cost, battery degradation, and PV curtailment to ensure financially efficient operation. To tackle large-scale and time-coupled optimization, accelerated variants of the Alternating Direction Method of Multipliers (ADMM) are applied. Case studies on IEEE 13-bus and 123-bus systems validate the proposed methods. The results demonstrate the effectiveness of the coordinated operation of OLTC and SOP-ES in reducing losses, enhancing voltage quality, and minimizing economic cost.

Acknowledgements

This thesis is dedicated to the memory of my beloved father. His values, prayers, and quiet strength continue to light my path. I carry this work in his honour.

I would like to express my deepest gratitude to my supervisor, Professor Jin Yang, for his guidance, patience, and unwavering support. His insight and high standards shaped both the direction of this research and my development as a researcher. I am truly fortunate to have learned under his supervision.

My sincere thanks go to the Royal Commission for Jubail and Yanbu (RCJY), Saudi Arabia, for sponsoring my postgraduate studies at the University of Glasgow. Their support made this journey possible.

To my mother, whose constant prayers, care, and encouragement sustained me throughout the most challenging times—thank you. To my wife, Reem, whose love, patience, and daily support were the foundation of this achievement—this PhD belongs as much to you as it does to me. And to my wonderful children, Oday and Jumanah, your smiles and hugs gave me the strength to keep going; this accomplishment is dedicated to you.

Contents

List of Tables

List of Figures

Abbreviations and Nomenclature

ADN	Active Distribution Network
ADMM	Alternating Direction Method of Multipliers
AADMM	Adaptive-penalty ADMM
BESS	Battery Energy Storage System
DSM	Demand-side Management
DICOPT	Discrete and Continuous OPTimizer
FAADMM / N-ADMM	Fast / Nesterov-type Accelerated ADMM
GAs	Genetic Algorithms
GAMS	General Algebraic Modeling System
BFM	Branch Flow Model
SDP	Semidefinite Programming
OPF	Optimal Power Flow
SOCP	Second-Order Cone Programming
AC	Alternating Current
DER	Distributed Energy Resource
PV	Photovoltaic (generation)
DG	Distributed Generation
ESS / ES	Energy Storage System / Energy Storage
RES	Renewable Energy Source
SOP	Soft Open Point
SOP-ES	Soft Open Point Integrated with Energy Storage

OLTC	On-Load Tap Changer
OpenDSS	Open Distribution System Simulator
VUC	Voltage Unbalance Condition
VSCs	Voltage Source Converters
VVO	Volt/VAR Optimization
YALMIP	MATLAB modeling toolbox for optimization
LMIs	Linear Matrix Inequalities
MILP	Mixed-Integer Linear Programming
MINLP	Mixed-Integer NonLinear Programming
MISDP	Mixed-Integer Semidefinite Programing
MOPSO	Multi-Objective Particle Swarm Optimization
MOSEK	Commercial conic/SDP optimization solver
IEEE	Institute of Electrical and Electronics Engineers
MOPSO	Multi-Objective Particle Swarm Optimization
PSO / GA	Particle Swarm Optimization / Genetic Algorithm
MISOCP / MIQP / MILP	Mixed-Integer SOCP / Quadratic / Linear Programming
NSGA-II	Non-dominated Sorting Genetic Algorithm II
MPC	Model Predictive Control
TOU	Time-of-use

Nomenclature (symbols & variables)

$P_{\varphi,i,t}^{\mathrm{SOP-ES}}, P_{\varphi,j,t}^{\mathrm{SOP-ES}}$	Active power injection by SOP converters at nodes i, j on phase φ at period t
$P_{m,t}^{\mathrm{SOP-ES}}$	Active power injection by ES converter at nodes m at period t

$P_{\varphi,i,t}^{\mathrm{SOP-ES,L}}, P_{\varphi,j,t}^{\mathrm{SOP-ES,L}}$	Active power loss of SOP converters at nodes i, j on phase φ at period t
$\mathrm{P}_{\mathrm{m,t}}^{\mathrm{SOP-ES}}$	Active power injection by ES converter at nodes m at period t
$P_{m,t}^{\mathrm{SOP-ES,L}}$	Active power loss of ES converters at nodes m at period t
$P_{m,t}^{\mathrm{ch-ES}}, P_{m,t}^{\mathrm{dis-ES}}$	Charging and Discharging power of ES battery at period t
$\mathrm{P}_{\mathrm{m,t}}^{\mathrm{ES,L}}$	Power loss of ES battery at period t
$A_i^{\mathrm{SOP-ES}}$, $A_j^{\mathrm{SOP-ES}}$, $A_m^{\mathrm{SOP-ES}}$	Loss coefficient
$\mathrm{Q}_{\varphi,i,\mathrm{t}}^{\mathrm{SOP-ES}}$, $\mathrm{Q}_{\varphi,\mathrm{j,t}}^{\mathrm{SOP-ES}}$	Reactive power injection by SOP converters at nodes i, j on phase φ at period t
$\mathrm{S}_{\mathrm{max}}^{\mathrm{AC-DC}}$	Rating of AC-DC converters
$\mathrm{S}_{\mathrm{max}}^{\mathrm{DC-DC}}$	Rating of DC-DC converters
$\overline{\mathrm{Q}}_{\varphi,\mathrm{i}}^{\mathrm{SOP-ES}}$, $\overline{\mathrm{Q}}_{\varphi,\mathrm{j}}^{\mathrm{SOP-ES}}$	Upper limit of reactive power provided by SOP on phase ϕ at bus i, and j
$\underline{\mathrm{Q}}_{\varphi,\mathrm{i}}^{\mathrm{SOP-ES}}$, $\underline{\mathrm{Q}}_{\varphi,\mathrm{j}}^{\mathrm{SOP-ES}}$	Lower limit of reactive power provided by SOP on phase ϕ at bus i, and j
SoC	State of charge (SoC) of the battery
$-\mathrm{P}_{\mathrm{max}}^{\mathrm{ES}}$, $\mathrm{P}_{\mathrm{max}}^{\mathrm{ES}}$	Power rating of energy storage
Tap_{ϕ}	Tap position of voltage regulator [−16,+16]
$V_{\mathrm{sec}}^{a}, V_{\mathrm{sec}}^{b}, V_{\mathrm{sec}}^{c}$	Secondary voltage of voltage regulator at phase a,b,and c
$V_{\mathrm{pri}}^{a}, V_{\mathrm{pri}}^{b}, V_{\mathrm{pri}}^{c}$	Primary voltage of voltage regulator at phase a,b,and c
$v_{i,t}$	Second-order decision variable of voltage at node i at time t
$l_{ij,t}$	Second-order decision variable of current from node i to node j at time
$S_{ij,t}$	Second-order decision variable of power from node i to node j at time t
V_0^{ref}	Nodal voltage vector at the source node

v_0^{ref}	Second-order decision variable at the source node
$I_{ij,t}$	Branch current vector from node i to node j at time t
$V_{i,t}$	Nodal voltage vector at node i at time t
V_{nominal}	Nominal voltage at node i
$\bar{v_i}$, $\underline{v_i}$	Upper / Lower limit for second-order decision variable of voltage at node i
z_{ij}	Branch resistance from node i to node j
y_j	Nodal shunt capacitance of node i
T	Number of time periods.
Δt	Duration of a single time period.
W_L, W_U, W_D	Weight coefficients associated with each term in objective function.
φ	Phase A, B or C (a, b, or c)
012	Symmetrical components
H	Hermitian transpose
abc	Phase components
χ_g	Feasible set for local area g
$f_g(\cdot)$	Local objective (loss, voltage deviation, control effort) in area g
A_g	Selector for boundary (consensus) variables in area g
z	Global consensus copy of boundary variables
λ_g	Dual variables for area g (unscaled)
$\mathrm{u}_g = \lambda_g/\rho$	Scaled duals
ρ	ADMM penalty parameter
$r_{\text{pri}}, r_{\text{dual}}$	Primal/dual residual norms
$\theta_k \in [0,1)$	Nesterov momentum weight at iteration k

ϕ_k	Nesterov state $\left(\phi_{k+1} = \frac{1+\sqrt{1+4\phi_k^2}}{2}\right)$
$\varepsilon_{\text{abs}}, \varepsilon_{\text{rel}}$	Absolute/relative tolerances for hybrid stopping
$\mathcal{N}(i)$	Neighbour set of bus i
Ω_b	Set of all network branches

Chapter 1

Introduction

1.1 Research Background and Motivation

The architecture of electrical power systems has undergone a profound transformation since its inception. The 20th century was dominated by the Centralized Model, characterized by large-scale, fossil-fuel or nuclear power plants located remotely from load centers. Power flowed unidirectionally from these high-voltage transmission networks through sub-transmission and finally to passive distribution networks, which acted as simple conduits to deliver electricity to end-users. In this paradigm, distribution networks were designed to be passive; voltage and power flow were controlled by a handful of centralized devices like On-Load Tap Changers (OLTCs) at substations and switched capacitor banks, operating based on predictable, slow-changing load patterns.

This model began to shift in the late 20th and early 21st centuries, driven by the global imperatives of climate change, energy security, and technological advancement. The transition towards a cleaner, more sustainable energy economy has catalyzed the rapid deployment of Distributed Energy Resources (DERs), primarily solar photovoltaic (PV) systems and wind turbines, but also including small-scale combined heat and power (CHP) and flexible loads. Unlike traditional central generation, these resources are connected directly to the distribution grid, often at the medium- and low-voltage levels. This integration marks the evolution from a passive to an Active Distribution Network (ADN), defined by bidirectional power flows, active management, and a generation mix that is decentralized, stochastic, and power-electronics interfaced [1].

The modern ADN represents the current frontier in power system development, but its emergence has introduced a new set of complex operational challenges that legacy systems were not designed to handle.

The intermittent and location-specific nature of renewable generation, particularly rooftop PV, causes significant voltage fluctuations. During periods of high generation and low load, reverse power flow can lead to voltage rise violations at the end of feeders. Conversely, during peak demand with low generation, voltage drop remains a concern [2]. Furthermore, the unequal connection of single-phase DERs and loads exacerbates voltage unbalance, leading to inefficiencies and potential equipment overheating [3].

Traditional voltage regulation devices like OLTCs and capacitor banks, while robust, lack the speed and granularity of control required for modern ADNs. OLTCs have a slow mechanical response and operate on a discrete step basis, making them ineffective at managing rapid voltage variations caused by passing clouds or sudden load changes [4]. Their operation is typically based on the voltage or current at a single point (the substation), providing a coarse, network-wide adjustment that may not resolve localized voltage issues elsewhere in the feeder.

To address these limitations, the state-of-the-art has turned to power electronics. Soft Open Points (SOPs) are a key innovation in this domain. An SOP is a power electronic device installed to replace a normally open point (NOP) between two feeders or adjacent substations [5]. It provides fully controllable, bidirectional active and reactive power flow, enabling real-time rebalancing of loads and generation across feeders. This offers unprecedented spatial flexibility, allowing Distribution System Operators (DSOs) to manage power flows and mitigate voltage problems with a precision impossible for traditional switches or regulators [6].

While SOPs manage power flow in space, Energy Storage Systems (ESS) manage energy across time. By co-locating ESS with SOPs to form an SOP-ES unit, the benefits are amplified. The ESS can store excess renewable energy during periods of high generation and feed it back into the network during periods of high demand [7]. This "energy time-shifting" provides temporal flexibility, further alleviating voltage issues, reducing peak demand on the substation transformer, and maximizing the utilization of renewable energy that might otherwise be curtailed [8].

Effectively coordinating these diverse assets—traditional OLTCs, power-electronic SOPs, and distributed storage in a complex, unbalanced three-phase network demands mathematically rigorous optimization models. Semidefinite Programming (SDP) has emerged as a powerful tool for convexifying the non-convex Optimal Power Flow (OPF) problem, allowing for accurate and efficient computation of optimal setpoints [9]. However, as the number of controllable components grows, centralized solutions become computationally intensive for large-scale networks. This highlights the need for distributed optimization methods like the Alternating Direction Method of Multipliers (ADMM), which can decompose the problem for parallel computation, enhancing scalability and real-time applicability [10].

The principal motivation for this thesis is to bridge the gap between the advanced capabilities of modern grid technologies like SOP-ES and the sophisticated optimization frameworks required to unlock their full potential. While the individual components have been studied, a holistic approach that coordinates traditional OLTCs with SOP-ES in unbalanced networks, validated through both technical and economic lenses, and solved using scalable optimization techniques, remains a critical research need. This thesis aims to contribute this integrated solution, developing the models and strategies necessary for the secure, efficient, and economically viable operation of the next-generation Active Distribution Network.

1.2 Research Aim and Objectives

The principal aim of this thesis is to develop an integrated, multi-objective optimization framework for the coordinated control and operation of OLTCs, SOPs, and SOP-ES units in Active Distribution Networks.

To achieve this aim, the research is guided by the following specific objectives:

- To model and optimize the operation of SOP-ES units using Semidefinite Programming in unbalanced, three-phase distribution networks with high renewable energy penetration (chapter 3).

- To develop a coordination framework for OLTCs and SOP-ES systems that mitigates voltage unbalance and minimizes system losses, while ensuring operational feasibility (chapter 4).

- To formulate an economic operation model that integrates grid purchase costs, energy storage degradation, and renewable energy curtailment, and to minimize the total cost using convex optimization (chapter 5).

- To implement and test accelerated distributed optimization algorithms, specifically FAADMM and AADMM, to enhance the real-time applicability and scalability of the proposed optimization frameworks (chapter 6).

1.3 Contributions of the Thesis

This thesis presents the following contributions, specifically in the coordination, integration,

and implementation of methods for three-phase BFM–SDP distributed OPF:

- First, the thesis develops a comprehensive three-phase, multi-period Semidefinite Programming (SDP) model specifically for scheduling Soft Open Points integrated with Energy Storage (SOP-ES). Unlike previous works that often simplify network unbalance or treat storage separately, this model explicitly captures the asymmetrical nature of distribution systems under realistic load and generation profiles. The use of a convex SDP relaxation guarantees globally optimal solutions for the relaxed problem, ensuring both computational efficiency and high solution quality in complex, unbalanced environments for radial distribution networks.

- A second key contribution is the formulation of a convex modeling technique for On-Load Tap Changers (OLTCs) and their seamless integration with SOP-ES within a unified voltage control framework. This approach transforms the traditionally discrete tap-changing problem into a continuous convex formulation compatible with SDP. The resulting coordinated strategy demonstrates a critical cooperation, significantly improving voltage profiles and system losses while dramatically reducing OLTC switching operations, thereby extending the operational life of this critical asset.

- Third, the thesis introduces a comprehensive cost-based optimization model that effectively balances economic and technical performance in ADN operations. This model uniquely integrates time-of-use grid purchase costs, a detailed battery degradation cost model, and PV curtailment penalties into a single objective function. This holistic economic analysis quantitatively demonstrates that SOP-ES is not merely a technical asset but also a source of substantial cost savings, providing a more complete justification for its deployment.

- Finally, to enable fast, scalable control on realistic feeders, the thesis successfully applies advanced distributed optimization techniques. By implementing accelerated variants of the Alternating Direction Method of Multipliers (ADMM), including Fast ADMM (FADMM) and Adaptive ADMM (AADMM), this work addresses the scalability challenge inherent in centralized optimization. These algorithms decompose the large-scale problem into manageable sub-problems, achieving near-optimal solutions with significantly enhanced convergence speed, thus making the proposed frameworks applicable to real-world, large-scale distribution networks.

Comparative analysis of OLTC-only, SOP-only, SOP-ES-only, and coordinated OLTC + SOP-ES scenarios, quantifying benefits in terms of power loss, voltage deviation, and unbalanced indices.

1.4 Organization of the Thesis

This thesis is structured into seven chapters, each focusing on a critical aspect of the proposed optimization framework:

Chapter 2 presents a comprehensive literature review that synthesizes recent advancements in voltage regulation techniques for ADNs, categorizing them into analytical and computational methods, and identifying key research gaps in the integration of Soft Open Points and energy storage.

Chapter 3 develops the network modeling and the convex OPF formulation adopted in this thesis. Using the branch-flow model (BFM) and SDP relaxation, it formalizes bus/branch variables, operational limits, and objective terms (loss minimization and voltage quality), used as the baseline throughout the thesis.

Chapter 4 introduces and analyzes a coordinated control strategy between traditional On-Load Tap Changers (OLTCs) and SOP-ES systems, demonstrating how their synergistic operation enhances voltage quality, reduces power losses, and minimizes OLTC switching operations to extend device lifespan.

Chapter 5 formulates and solves a comprehensive economic operation model that integrates grid purchase costs under time-of-use tariffs, battery degradation costs, and PV curtailment penalties, quantifying the significant cost savings achieved by the SOP-ES configuration.

Chapter 6 proposes and evaluates accelerated ADMM strategies tailored to the SDP consensus setting. The chapter introduces hybrid (absolute + relative) stopping thresholds, adaptive penalty updates with clipping (AADMM), and Nesterov-type Fast ADMM (FAADMM) with monotone restart. Extensive experiments on IEEE-13 (two areas) and IEEE-123 (four areas) quantify iteration counts, wall-clock time, residual decay, and solution quality relative to centralized benchmarks.

Chapter 7 summarizes the findings and outlines directions for future research, including stochastic modeling, real-time control, and hardware-in-the-loop validation.

Publications

1. Alshehri, Mohammed, and Jin Yang. "Voltage optimization in active distribution Networks—Utilizing analytical and computational approaches in high renewable energy penetration environments." *Energies* 17, no. 5 (2024): 1216.

2. Alshehri, Mohammed, Jin Yang, Chengwei Lou, and Liang Min. "Optimal Operation in Active Distribution Networks Using Soft Open Point Integrated with Energy Storage." In *2025 IEEE Texas Power and Energy Conference (TPEC)*, pp. 1-6. IEEE, 2025.

3. Alshehri, Mohammed, and Jin Yang. "A Unified SDP Framework for Coordinated Operation of Soft Open Points with Energy Storage and OLTCs in Unbalanced Distribution Networks". (Under Preparation).

Chapter 2

Literature Review

2.1 Introduction

The evolving dynamics of power distribution systems, increasingly influenced by the integration of RESs, have necessitated innovative strategies for voltage regulation in active distribution networks (ADNs). The review delves deeply into various methodologies that have emerged to address the challenges posed by high photovoltaic (PV) penetration and other renewable energy sources (RESs), with a particular focus on two primary types of optimization methods: Analytical Methods and Computational Methods.

2.1.1 Review Methodology

This literature review aims to synthesize recent research related to voltage optimization techniques in active distribution networks, specifically focused on analytical and computational methods. The key questions that guided the paper selection process are:

- What are the recent techniques used for voltage regulation in distribution grids with high penetration of renewable energy sources?

- How are analytical and computational optimization methods applied to manage voltage fluctuations and improve network efficiency?

- What are some of the current limitations and challenges in this research domain?

Analytical Methods are crucial in understanding and solving optimization problems within power systems. These methods involve mathematical formulations and theoretical frameworks that provide insights into the fundamental principles governing the system operations. They are instrumental in devising control strategies for voltage regulation, power flow management, and loss minimization in a more deterministic manner. This review explores how analytical methods are applied to develop algorithms for reactive power control, voltage stability assessment, and the efficient dispatch of PV inverters in distribution networks.

In contrast, Computational Methods have gained prominence with the advent of advanced computing technologies and the increasing complexity of power networks. These methods cover a wide range of algorithms and heuristic approaches, including genetic algorithms (GAs), particle swarm optimization (PSO), and other metaheuristic methods. Computational Methods are particularly effective in dealing with the non-linear, multi-objective, and often stochastic nature of modern power systems. They offer robust solutions for real-time control and optimization in scenarios where traditional analytical approaches may fall short because of the high fluctuations and unpredictability of RES.

Analytical techniques based on mathematical modelling and deterministic analysis as well as computational data-driven methods offer complementary strengths for addressing the multifaceted voltage regulation challenges in modern distribution systems. Hence this review accentuates both categories of optimization approaches from recent literature.

2.1.2 Keywords and Search Strategy

The primary keywords used in our database searches included voltage optimization, voltage

regulation, voltage control, active distribution networks, renewable energy integration, photovoltaic (PV) systems, analytical optimization methods, and computational optimization methods. These keywords were carefully selected to capture the essence of the research domain, focusing on innovative strategies for managing the complexities introduced by the high penetration of RESs in ADNs.

The paper selection methodology involved keyword-based searches on databases like IEEE Xplore, ScienceDirect, and SpringerLink to filter for peer-reviewed articles from the past 5-10 years. Specific exclusion criteria included grey literature sources without rigorous analysis, centralized control techniques lacking optimization algorithms, and solutions tailored for transmission grid operations. Out of the 86 cited references, 41 papers employ analytical optimization strategies, while 45 leverage various computational methods like metaheuristics and machine learning. This indicates the nearly equal prominence given to both methodologies in contemporary research on voltage control for distribution systems. Figure 2.1 presents a timeline graph depicting the distribution of cited papers by their year of publication over the previous decade. Among the 86 references cited, 79 have clearly identifiable publication years. The graph highlights that the first paper dates back to 2010, with a significant majority of the papers being published from 2016 onward. The rapidly increasing publications over the past 5 years, with a peak in 2020, provides quantitative evidence for the growing relevance and importance of voltage optimization techniques in active distribution networks. It validates the need for a comprehensive literature review synthesizing the latest advancements in this area to guide future research.

The cited literature for this chapter reflects a systematic review conducted up to mid-2023, as this chapter was developed during the initial stages of the research. Therefore, publications from late 2023 and onward are not represented in Figure 2.1. More recent studies (2024–2025) are reviewed and incorporated in later chapters where relevant to specific methodological developments (e.g., SDP-based SOP-ES coordination, accelerated

ADMM). The strong upward trend from 2016 to 2022 nevertheless highlights the accelerating research interest in voltage optimization for active distribution networks.

The filtered papers provide the basis for a targeted synthesis of diverse voltage regulation techniques that offer promising capabilities like decentralized control, enhanced integration of renewable sources, reduced power losses etc. But they also outline key limitations and gaps in translating these solutions to large-scale practical implementations. The summarized insights aim to direct future explorations in this crucial area of power distribution optimization to address grid stability and efficiency challenges.

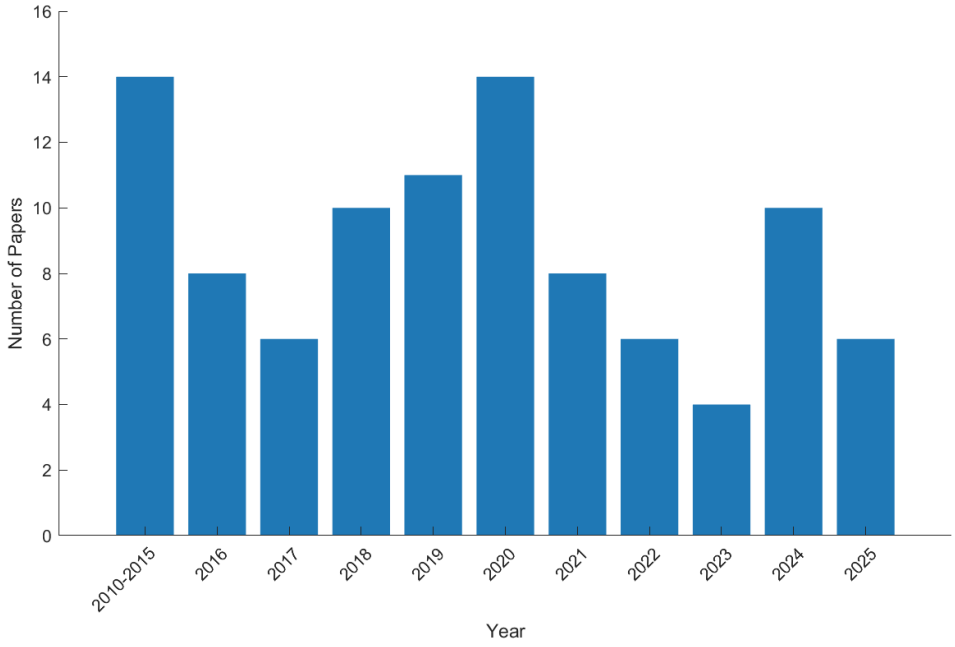

Figure 2.1 Distribution of cited papers by year of publication

2.1.3 Technological Innovations in Voltage Regulation

Smart inverters represent a significant area of focus within both analytical and computational optimization frameworks. These devices not only convert solar energy into grid-compatible power but also play a pivotal role in providing dynamic voltage support and reactive power compensation where the output reactive power of smart inverter is following the Volt/Var

and power capability curves in Figure 2.2.

A PV smart inverter's operational behavior is defined by two key characteristic curves, as illustrated in Figure 2.2. The Volt/Var curve (a) governs the inverter's reactive power (Q) response based on measured grid voltage. Voltage thresholds (V1–V4) establish a deadband (V2–V3) where minimal reactive power is exchanged; outside this range, the inverter injects or absorbs Q up to its maximum capability (±Qmax) to support grid voltage stability.

The power capability curve (b) defines the inverter's operational envelope in terms of real (P) and reactive (Q) power. Bounded by its apparent power rating (S), the curve illustrates the trade-off between P and Q: when real power output is below maximum, surplus capacity can be allocated to reactive support without exceeding the inverter's rated capacity. Together, these curves enable the inverter to function as a grid-supportive asset, providing dynamic voltage regulation while adhering to its hardware limits.

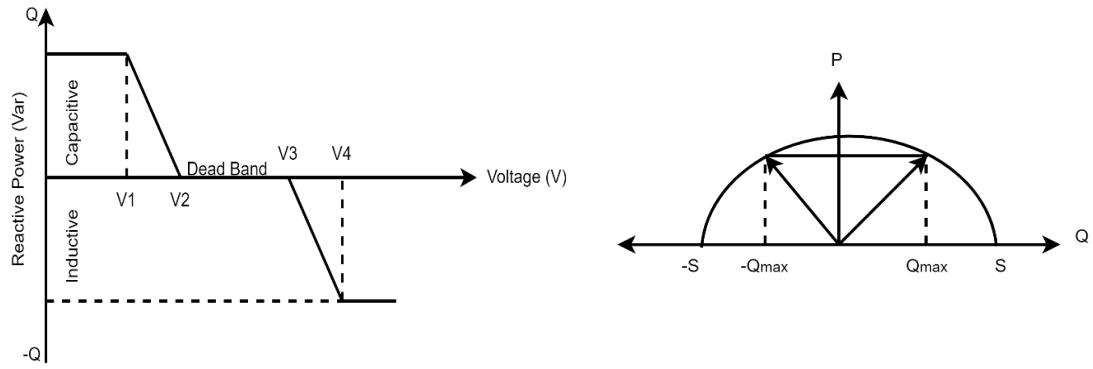

(a) (b)

Figure 2.2 PV smart inverter curve: (a) Volt/Var curve; (b) power capability curve.

This review examines various studies that utilize both analytical and computational methods to enhance the functionality of smart inverters in power distribution systems. Another critical aspect of this review is the integration and optimization of battery energy storage system

(BESS) in conjunction with smart PV inverters. The coordination between these systems is essential for managing the intermittency of renewable sources and maintaining grid stability. This paper reviews different bi-level optimization methods and metaheuristic algorithms that leverage the capabilities of BESS and PV inverters, highlighting how analytical and computational approaches can be combined for effective voltage regulation.

Furthermore, the paper discusses decentralized control algorithms, emphasizing the shift from traditional centralized methods to more efficient, localized control strategies. These algorithms, developed using both analytical and computational methods, demonstrate their effectiveness in managing voltage deviations and reducing line losses in complex power systems with high PV penetration.

Advancements in multi-objective optimization techniques, particularly Multi-Objective Particle Swarm Optimization (MOPSO), are also a significant focus of this review. These techniques address the complexities introduced by high levels of RES penetration, aiming to balance operational efficiency with system stability and reliability. Studies employing these methods showcase significant improvements in reducing power loss, minimizing voltage deviation, and optimizing the operation of various grid components such as on-load tap changers (OLTC) and shunt capacitors (SCs).

Lastly, the chapter explores the impact of sophisticated control mechanisms like soft open points (SOPs) and distributed static compensators (DSTATCOMs) in enhancing grid functionality. These technologies contribute to improved voltage profiles, reduction in power losses, and better management of the challenges posed by the integration of rooftop PV systems in low-voltage distribution networks.

In summary, this literature review chapter provides a comprehensive analysis of the advanced strategies and methodologies in voltage regulation for ADNs, underlining the

importance of both Analytical and Computational Methods. By exploring the applications of these two optimization approaches, the review highlights the significant advancements in managing the complexities introduced by renewable energy integration, setting a foundation for future developments in efficient and resilient power grid management.

2.2 Voltage Related Optimization Methods

2.2.1 Analytical Methods

2.2.1.1 Robust Optimization

Voltage levels can be maintained within acceptable limits through the control of reactive power, which can be produced or absorbed by PV inverters. In [11] the author presents a decentralized method for reactive power control in PV-integrated distribution networks. Utilizing linear decision rules based on PV real power output, the approach uses an adjustable robust optimization framework, employing convex quadratic programming to ensure optimal voltage and power loss management. Demonstrated as more effective than traditional local control methods via Monte Carlo simulations, this approach offers a practical, robust solution for modern grid management with renewable energy integration; however, its dependency on accurate PV output predictions might reduce the method's effectiveness. Reference [12] presents an innovative approach to integrating PV systems into voltage and reactive power (Volt/Var) control in distribution networks. Adhering to the new IEEE 1547-2018 standard [13] , this method involves formulating local decision rules for PV inverters, allowing them to adjust reactive power based on real power output. The paper introduces two techniques for determining these rules: one based on linear programming for minimizing voltage deviations and another based on closed-form solutions from distributionally robust chance constraints. Demonstrated through simulations on networks

with up to 3146 nodes, the approach effectively reduces voltage violations but with minimal increase in network power loss. The authors in [14] propose a novel decentralized algorithm for power flow optimization in active distribution grids with high Distributed Energy Resources (DERs) integration. This approach, known as Increment-Exchange-Based Decentralized Mult-objective Optimal Power Flow (MO-OPF), addresses the complexities of coordinating network operators and DER owners. The key innovation lies in its ability to solve the MO-OPF problem in a decentralized manner without compromising private DER data. The algorithm is based on quadratic functions of coupling variables' increments, facilitating efficient and privacy-preserving interactions between stakeholders. Demonstrated through simulations on IEEE 33-bus and a real 266-bus distribution systems, the method shows its effectiveness in providing distributed Pareto-optimal solutions, offering a scalable and privacy-conscious solution for optimizing power distribution in grids with significant DER penetration. To address the challenges in voltage and VAR control within distribution networks heavily integrated with PV sources, the paper [15] introduces a multi-objective adaptive robust optimization (MOARO) approach, focusing on minimizing voltage deviations and power loss in the presence of high PV penetration. This approach is notable for its robustness in handling the uncertainties inherent in such networks. The effectiveness of this method is validated through extensive simulations on the IEEE 123-bus system, showcasing its efficiency and robustness. Comparative analysis with other multi-objective programming algorithms highlights the superiority of the proposed method in operational robustness and efficiency. This paper contributes significantly to the field of power systems, offering an innovative solution for managing complex challenges in high-PV penetrated distribution networks. A robust optimization method is proposed in [16] for controlling the active and reactive power injections of distributed generators (DGs) in coordination with transformers' OLTC. The mixed-integer linear programming (MILP) problem formulation accounts for uncertainties in the network admittance matrix and utilizes sensitivity coefficients for optimization. In contrast, the paper in [17], addresses voltage regulation in similar systems but emphasizes robust optimization under the uncertainties of

DG and load variations. This paper uses a mixed-integer nonlinear programming (MINP) approach and validates its methodology on a modified IEEE 123 bus system, demonstrating effective voltage control despite uncertain and fluctuating generation and load conditions.

2.2.1.2 Advanced Optimization Techniques in Power Systems

The Alternating Direction Method of Multipliers (ADMM) is a powerful optimization technique that combines elements of dual decomposition and augmented Lagrangian methods for solving complex problems. It is particularly effective for solving large-scale optimization problems that can be decomposed into smaller, more manageable subproblems. ADMM achieves this by breaking down the original problem into parts, solving each part separately, and then iteratively refining these solutions to converge to an optimal solution. This method is well-suited for distributed optimization problems common in power systems, where it can significantly reduce computational burden and handle communication constraints effectively. Several studies have effectively employed ADMM in optimizing power distribution systems. Reference [18] presents a distributed approach for Conservation Voltage Reduction (CVR) in distribution systems with high PV penetration. It introduces a multi-objective optimization model that coordinates the operation of PV inverters with traditional voltage regulation devices using a modified ADMM to address non-convex optimization challenges, ensuring quality solutions, and computational efficiency. In [19], a convex quadratic program (QP) optimization model for both balanced and unbalanced systems is developed, utilizing ADMM for distributed optimization. The model, suitable for large-scale applications, includes a two time-scale architecture for controlling DERs. Its simplicity and linear constraints ease computation, though its static nature can limit effectiveness in dynamic scenarios. The paper in [20], proposes a novel linearized voltage model for AC optimal power flow (AC-OPF) problems, leading to a tractable quadratic constrained quadratic program (QCQP), further simplified under certain conditions. The Scalable Optimal Inverter Dispatch (SOID) algorithm, which uses ADMM for distributed

implementation, efficiently adjust inverter dispatch to reduce power losses and effectively correct voltage deviations. Further, the author in [21], introduces a method for optimally setting transformer tap positions in distribution systems using a rank-constrained semidefinite program (SDP). ADMM is applied to solve this relaxed SDP, demonstrating its effectiveness through case studies on single- and three-phase distribution systems, showcasing advantages over centralized methods. The work in [22], develops decentralized methods for optimal power setpoints in residential PV inverters, also employing ADMM. This paper addresses conventional PV inverter limitations by incorporating voltage regulation and network loss minimization, demonstrating the adaptability and efficiency of ADMM in tackling various distributed optimization challenges in power systems. Another utilizing of ADMM but with energy storage system (ESS) is introduced in [23], the paper proposes a multi-objective procedure that considers various ancillary services provided by ESSs, such as voltage support and network loss minimization, along with minimizing the cost of energy from the external grid and managing congestion.

2.2.1.3 Advanced Hierarchical and Predictive Control

The paper in [24] introduces a groundbreaking approach to optimize power flow (OPF) in power systems, emphasizing real-time application. The authors propose a multi-stage quadratic flexible OPF (MQFOPF) framework, characterized by an object-oriented device modelling approach. This methodology allows for seamless integration of various power system devices, enhancing the flexibility of the OPF process. A key innovation of the paper is the development of an efficient Sequential Linear Programming (SLP) algorithm, designed to solve the OPF problem in real-time using a rolling horizon scheme. This scheme takes into account changing forecasts, enabling dynamic optimization of the power system's operations. The effectiveness of this framework is demonstrated through a case study on a real distribution feeder, showcasing its potential in managing power systems with diverse and evolving requirements. The paper also acknowledges opportunities for further

optimization, particularly in improving the speed and convergence quality of the SLP algorithm. The recent advancements in voltage regulation techniques for ADNs are well-captured in several innovative studies. The study [25] proposes real-time Volt/Var control using two-stage. The first stage schedules OLTC and capacitor banks (CBs), while the second stage uses a data-driven method to assess voltage violation risks and control the dispatch of electric vehicles (EVs). Additionally, a rule-based strategy is employed for coordinating PVs and CBs, enhancing reactive power reserve. While in [26] the study introduces a double-time-scale voltage control scheme using model predictive control (MPC) in distribution networks with DGs. The slow-time-scale control aims to rectify long-term voltage deviations, while the fast-time-scale control efficiently manages rapid voltage fluctuations and maximizes renewable energy capture. The control problem is solved using a sophisticated branch-and-bound algorithm, with an ADMM based solver for mixed-integer quadratic programming (MIQP) problems. Reference [27], introduces a novel strategy for reactive power and voltage optimization over multi-periods, featuring a decoupling rolling approach. This approach accounts for the strong time-based interconnections between different devices, including PVs and OLTC. The strategy employs Bender's decomposition algorithm to separate the mixed-integer voltage optimization model into a master problem which addresses long-period for OLTC, and multiple short-period subproblems for PV power. Utilizing MPC, these subproblems are then modified into a series of rolling subproblems within the time window, facilitating an efficient and smooth transition from the existing state to the optimal state. The paper focuses on achieving fast computation and effective voltage regulation by employing a simplified discrete equation for the adjustments of OLTC tap, and utilizes a linearized sensitivity matrix among power and voltage.

2.2.1.4 Soft Open Point (SOP) Utilization in Voltage Regulation

A soft open point (SOP) is a power electronic device that is fully controllable. It has the capability to precisely manage the active power transfer between the interconnected feeders

on each side and provide certain reactive power and voltage support as shown in Figure 2.3. The paper [4] introduces a method for addressing voltage and reactive power challenges in ADNs with high DG penetration. This method centers around the use of SOP, which offers more precise and real-time control compared to traditional voltage regulation devices.

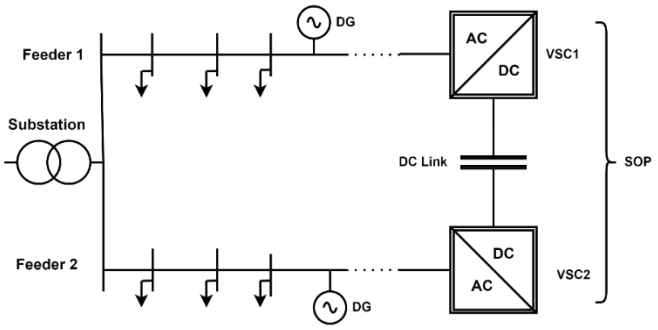

Figure 2.3 Network with SOP connection.

The paper's key contribution is a time-series optimization model that coordinates SOP with traditional regulation devices like OLTC and CBs. This model, which aims to minimize operational costs and eliminate voltage violations, employs linearization and conic relaxation techniques to transform the complex MINP problem into a more tractable mixed integer second-order cone programming (MISOCP) model. Reference [28] proposes the innovative Phase-Changing Soft Open Point (PC-SOP) to address three-phase imbalances in distribution networks, often exacerbated by uneven distributed generation. The PC-SOP connects soft open points in a novel way to control active and reactive power, balancing the power flow among phases. Key contributions include developing an optimized operational strategy for unbalanced ADNs that combines SOP regulation, ESS dispatch, and DG curtailment. This approach effectively reduces power losses and improves voltage regulation. The paper transforms the complex optimization problem into a more tractable second-order cone programming (SOCP) model.

In [29] a novel approach is presented to address voltage violations in networks with high DG

integration. The strategy combines decentralized and local control of SOPs to effectively manage voltage fluctuations. Key features include a locally tuned Q/V control curve for intra-area reactive power regulation, reducing system complexity and communication needs. Additionally, decentralized coordination regulates active power transmission among areas, accommodating DG output fluctuations. The study in [30] focuses on using SOPs in networks with high distributed generation. The paper introduces a Jacobian matrix-based sensitivity method to determine SOP operating regions under varying load and generation conditions. Three optimization objectives are considered: voltage profile improvement, balancing line utilization, and minimizing energy losses. The study provides a graphical representation of SOP operating regions and quantifies the impacts of different optimization objectives, aiding Distribution Network Operators in SOP control and operation. For fully utilizing the regulation ability of SOPs, a robust optimization method is proposed in [31]. This method involves a two-stage adjustable robust optimization model that generates robust operation strategies for SOPs. These strategies aim to reduce voltage violations and minimize power losses in ADNs. The robust optimization model is formulated as a SOCP to improve accuracy and computational efficiency. However, the effectiveness of the model relies on accurately predicting the uncertainties associated with PV generation. Any inaccuracies in these predictions could impact the performance of the SOPs. A two-stage optimization method for distribution networks based on an integration of energy storage with SOP is proposed in [32]. The first stage involves day-ahead optimization using interval optimization (IO) for optimizing the OLTC and the state of charge (SOC) selections of the BESS in every Energy Storage Integrated Soft Open Point (E-SOP). In the second one, an intra-day optimization model is utilized, which is based on the rolling optimization algorithm. This model is designed to optimize both the active and reactive power across each side of E-SOP, as well as manage the charging and discharging power of the BESS within each E-SOP. The approach aims to reduce comprehensive operating costs, control nodal voltage within desired ranges, and improve voltage profiles and load balancing indexes in distribution networks with high levels of DGs. The authors in [33] proposes a novel voltage regulation

framework utilizing SOPs and reactive powers of DG inverters. The approach is based on linearized DistFlow equations, creating a biconvex problem that minimizes voltage deviation through a coordinated scheme for SOPs and DGs. This problem can be efficiently solved by an alternative convex search algorithm. The paper's contributions include modelling various types of SOPs and power electronic devices as nodal or line variables in a universal voltage regulation model, offering coordinated reactive power support in distribution systems. The papers [34, 35] explore innovative strategies for voltage regulation in ADNs in the context of increasing DG penetration. Reference [34] introduces a combined strategy, where the active power of SOPs is centrally adjusted using global network information, complemented by local reactive power control based on real-time data. This approach aims to effectively manage voltage profiles and reduce power losses, employing convex relaxation to simplify the optimization model. While [35], in contrast, proposes a decentralized strategy using the ADMM algorithm. This method optimizes the transmission power of SOPs across network partitions, achieving near-global optimal solutions without heavy computational demands. Both strategies underscore the critical role of SOPs in enhancing operational flexibility and voltage stability in ADNs, each employing distinct methodologies to navigate the challenges posed by high DG integration.

2.2.1.5 Local and Coordinated Voltage Control

Paper [36], proposes a coordinated local control strategy for integrating DG based on RESs into distribution networks. It emphasizes a collaborative approach between distribution system operators and independent power producers for voltage regulation and maximizing active power production. The control method, formulated as a nonlinear constrained optimization problem, is solved using Sequential Quadratic Programming (SQP). The coordination of two voltage control algorithms is proposed in [37], where the first one based on control rules and the other utilizing optimization. The paper compares the network effects and costs of both algorithms and discusses their practical implementation issues. This

approach offers a cost-effective solution to the traditional method of network reinforcement for mitigating voltage rise issues due to distributed generation integration. The authors in [38] presents a novel two-stage optimization method to regulate voltage in unbalanced distribution networks with DG, like solar power. It focuses on the coordination between OLTC and Static Var Compensators (SVC). The method's efficiency is demonstrated by its ability to solve problems that were previously unsolvable due to computational burden, completing tasks in less than 10 minutes that could take over 8 hours. This is achieved through a two-stage process: a one-day-ahead optimization using forecasted load and generation values, followed by a real-time local optimization based on current load and generation.

2.2.1.6 Convexification and Relaxation

Paper in [39] presents a multi-objective optimization problem for optimally allocating Dispersed Storage Systems (DSSs) in ADNs. This study aims to find the optimal balance between technical and economic goals, addressing congestion in feeders and lines, network losses, network voltage deviations, and the cost associated with supplying loads, alongside the stochastic nature of load demands and renewables productions. To address these challenges, it uses a convex formulation of an AC-OPF problem which is then structured as MISOCP problem. A novel method for managing voltage control in ADNs with high DG integration has been proposed in [40]. This approach involves a centralized model for tuning the parameters of local control curves of DG inverters, focusing on optimizing reactive and curtailed active power based on local voltage measurements. Utilizing MISOCP, the method effectively converts complex MINP challenges into more tractable problems. This paper makes a significant contribution by offering an innovative solution for enhancing voltage control and reducing power losses in ADNs, emphasizing the crucial role of DG inverters in modern power systems. While the centralized-based method for parameter tuning is effective, its complexity might increase significantly with the scale of the network, potentially

impacting its applicability in very large or complex distribution systems. In contrast, the paper [41] introduces an Optimal Tap Control (OTC) method to regulate OLTCs by minimizing voltage profile deviation and reducing the number of tap operations. This method employs a linearization technique to convexify the optimization problem, allowing it to be solved efficiently at operational timescales. The study in [42] introduces an optimization method that integrates VAR optimization with network reconfiguration to minimize power losses and prevent voltage violations. This approach involves formulating reactive power of DGs, VAR compensators, tap-changer positions, and branch states as decision variables in a MISOCP model. The method successfully transforms a non-convex three-phase model into this format using techniques like second-order cone relaxation and piecewise linearization, including a detailed linearization of the typically neglected non-linear transformer model. This developed method showcases substantial improvements in reducing network losses and mitigating voltage violations, positioning it as an effective tool for active distribution network management. Reference [43] introduce an innovative approach to optimizing energy dispatch in distributed PV systems, aimed at enhancing Advanced Distribution Management Systems (ADMS). The study proposes a convex optimization model that controls smart inverters in distributed PV systems for voltage regulation and conservation voltage reduction. This model, which employs linearized power flow and the gradient projection algorithm, is tested on an open-source ADMS platform, demonstrating its effectiveness in improving grid operations. The paper also outlines a control architecture for coordinating smart inverter outputs, supported by simulations that validate the approach. The paper [44] presents a novel approach to voltage regulation in networks with high penetration of DERs. It formulates the issue as an optimization program to minimize network losses, considering constraints on bus voltage, power injections, and transmission line limits. The paper establishes conditions for solving this problem through convex relaxation and semidefinite programming. A key contribution is the development of a distributed algorithm robust against communication failures, efficient for large-scale networks.

2.2.1.7 Other Optimization Frameworks

The authors in [45] propose a novel approach using simplified linear equations to represent the characteristics of voltage control devices. This approach involves formulating the voltage equations of the distribution network using QP, which incorporates the control ranges of voltage devices and operating voltage ranges of the network. The method utilizes MIQP for deriving optimal solutions. The results were compared with the optimal results of a global search method and were almost identical to the optimal solution, however, the use of simplified linear equations may not capture the full complexity of real-world distribution networks, especially under varying load and generation conditions. A probabilistic optimization strategy for the effective use of PV generators in voltage regulation of distribution networks is introduced in [46]. This strategy incorporates probabilistic scenarios of PV output into a constrained optimal load flow planning analysis, aiming to minimize a voltage deviation index that reflects the quality of voltage regulation. The novel aspect of this approach lies in using the PV generators as capacitors and inductors, scheduling their reactive power compensation monthly to be in sync with the high-voltage/medium-voltage (HV/MV) substation OLTC settings. A key feature of this strategy is its independence from a communication infrastructure and the absence of feedback voltage control. In [47] an innovative optimization strategy that controls both reactive and real power of single-phase PV inverters is presented. This approach aims to enhance voltage profiles and voltage balance while reducing network losses and the costs associated with generation. The authors formulate a multi-objective OPF problem, solved using a global SQP method. The paper in [48] presents a multi-objective optimization approach which can effectively coordinate the reactive power provided by smart inverters and tap operations of OLTCs in multi-phase unbalanced distribution networks. The primary objectives are to reduce voltage deviations and the number of OLTC tap actions. The paper introduces a novel linearization method for power flow equations, which helps to convexify the optimization problem, ensuring convergence and reducing computational costs. This approach is modelled and solved using

MILP. In [49] a framework for optimizing distribution systems using linearized power-flow equations is proposed. The optimization addresses control variables such as adjustable capacitors, voltage regulators (VRs), and configuration of the system to achieve objectives like loss minimization and voltage profile improvement. The problem is formulated as MIQP, which guarantees optimal solutions. The framework incorporates system operational constraints including feeder capacities, drop in the voltage level, and switching operations. Key advantages of the proposed method include its general applicability to distribution system optimization, efficient solution algorithms, known optimality gaps providing effective stop criteria, and realistic load modelling accounting for voltage dependency. However, the use of linearized power-flow equations, while simplifying the optimization process, might not capture all the non-linear dynamics of real-world distribution systems, potentially affecting the accuracy of the optimization results. Reference [50], presents a sophisticated approach to managing and controlling distributed generation in electric distribution systems. It introduces a two-stage short-term scheduling procedure, integrating a day-ahead scheduler and an intra-day scheduler, to optimize the production of various energy and control resources, including embedded generators, reactive power compensators, and transformers with on-load tap changers. The day-ahead scheduler plans the distribution of resources for the next day, while the intra-day scheduler adjusts these plans every 15 minutes based on the operational requirements and constraints of the network. The intra-day scheduler employs MILP algorithm to solve a non-linear multi-objective optimization problem, with linearization achieved using sensitivity coefficients derived from three-phase power flow calculations. A decentralized control algorithm in [51] was presented for optimizing reactive power in electrical distribution networks with PV sources. The main focus of the paper is on developing a control strategy that minimizes voltage deviations and line losses by optimally dispatching the reactive power of PV inverters. This is achieved by correlating the optimal reactive power dispatch with locally measurable quantities, such as node voltage, reactive power consumption, and PV generation. The paper demonstrates that a near-optimal local control strategy, derived from global optimization problem solutions

under various operating conditions, performs effectively. It closely matches central optimal solutions and shows potential for real-time voltage control in complex power systems with high PV penetration. However, it is still need for further research in more general scenarios, including varying levels of PV penetration and different line characteristics.

2.2.2 Computational Method

2.2.2.1 Heuristic Optimization Methods

Recent advancements in voltage regulation for ADNs with high PV penetration have led to innovative strategies to minimize voltage fluctuations and optimize network performance. The paper [52] introduces a method based on worst-case voltage scenarios (WCVSs) using MINP. This approach, which coordinates CBs, OLTCs, and PVs plants, aims to minimize operational losses, limit voltage variations, and reduce the flow of reactive power through OLTCs and decrease the number of switch operations in substation CBs. Similarly, the research detailed in [53] proposes a centralized-decentralized voltage regulation method, considering the optimization of substations while regulating voltage variations. Both papers employ multi-objective MINP models and solve them utilizing the non-dominated sorting genetic algorithm II (NSGA-II). Additionally, they incorporate decision-making algorithms to choose optimal solutions from Pareto front. These studies emphasize the importance of sophisticated optimization techniques in improving the stability and efficiency of power distribution networks in the era of renewable energy integration.

Several papers emphasise the effectiveness of GAs in optimizing power distribution systems with smart inverters. Reference [54] propose a multi-objective GA to optimize smart inverter Volt/Var curves for voltage regulation and loss minimization. Tested on an IEEE 13 node feeder model, optimized curves reduced system losses and improved voltage profile compared to a baseline curve. Minimizing reactive power injection showed more significant

loss reduction than absorption minimization. However, only one PV system size/location is evaluated, thus optimization results could vary for different PV sizes and distribution on the network. In [55], the author presents a novel co-optimization technique using a GA for managing voltage fluctuations in power distribution networks with high PV penetration. This technique integrates individual optimization algorithms for Load Tap-Changing (LTC) transformers, SCs, and smart inverters to determine their optimal settings. The primary goal is to minimize system power losses while optimizing the smart inverter power factor settings and ensuring conservative voltage reduction. In [56], a novel algorithm, utilizing GAs, to optimize the parameters of Volt/Var curves in smart inverters is introduced. This optimization aims to enhance the performance of distributed generation systems. The key objectives of the algorithm include minimizing voltage deviation, reducing network loss, and limiting the peak of reactive power. The algorithm addresses various limitations of previous studies by incorporating a multi-objective optimization function that adjusts Volt/Var curve parameters, considering service transformers' effects, and analyzing system improvements based on the number of parameters optimized. The approach also evaluates the implementation of optimized Volt/Var curves during practical periods and assesses suitable Volt/Var curves for clustered photovoltaic generators. The study [57] introduces a deep reinforcement learning (DRL)-based algorithm for coordinating multiple smart inverters. This approach balances voltage regulation and reactive power utilization, adapting to varying conditions without the need for extensive network model knowledge. It demonstrates near-optimal performance in maintaining grid voltage limits and significantly reducing PV production curtailment.

A coordination between BESS and smart PV inverters is proposed in [58]. The study introduces a voltage management approach with two controlling stages: using BESS and smart PV inverters' reactive power injection capabilities. The core of this strategy is a bi-level optimization method, leveraging metaheuristic optimization algorithms (MOA) such as Social Spider Optimization (SSO), Particle Swarm Optimization (PSO), and Cuckoo

Search Optimization (CSO). This approach regulates voltage levels by managing BESS charging and discharging rates. The method aims to increase the utilization of energy from PVs and wind resources, along with enhancing voltage profiles. A notable aspect of this research is its consideration of uncertainties in PV system generation, integrating PV generation forecasts to enhance the decision-making process for BESS operation. The results demonstrate that appropriate coordination between BESS and smart PV inverters can significantly enhance distribution system operations, enabling seamless integration of PV and wind energy. However, employing three different MOAs for which there is no comprehensive comparison in the literature. This lack of comparative data might impact the ability to fully assess the effectiveness of these algorithms in the specific context of electrical distribution systems with high renewable integrations. The paper in [59] presents a novel optimization technique known as Locust Search (LS) for addressing the Optimal Capacitor Placement (OCP) issue in radial distribution networks. This problem, characterized by its complexity due to high multi-modality, discontinuity, and non-linearity, involves strategically installing capacitor banks within electrical distribution systems. Proper allocation of these banks can significantly improve the feeder's voltage profile and reduce power loss, leading to substantial energy savings and cost reductions. The LS algorithm, inspired by swarm optimization, was tested on several IEEE radial distribution test systems, and compared against other techniques. The results indicate that the LS-based method effectively addresses the OCP problem, demonstrating high accuracy and robustness in optimizing capacitor placement for improved network performance.

Reference [60] introduces a novel approach to enhance voltage control in distribution systems by utilizing end-users' reactive power capable devices. This integration is aimed at providing substantial support to the grid's voltage profile. The study develops a Centralized Support Distributed Voltage Control (CSDVC) algorithm that decomposes the distribution system into different areas using ε-decomposition. It identifies Q-C buses, or candidate buses, which are optimal for reactive power injection. The approach calculates the optimum

reactive power injection for each of these candidate buses in every area, along with the necessary tap position of the regulator, using a GA. The CSDVC algorithm is particularly designed to address inaccuracies in load forecasting and potential faults in control area centers, ensuring secure and reliable reactive power control. This advanced technique exhibits potential for application in current electrical distribution systems. However, the use of end-users as reactive power support introduces uncertainty due to their stochastic behavior. Changes in consumption patterns can lead to insufficient reactive power in local regions, posing challenges for maintaining voltage stability. Additionally, if a local control center fails, the entire control system for that region may become inoperable. An optimization model using the Grey Wolf Optimization (GWO) heuristic search method is proposed in [61]. This model aims to coordinate various distribution controllers, including tap changing transformers, capacitors, and PV inverters, to minimize voltage deviations and ensure that all voltages stay within specified limits. The effectiveness of the GWO method was compared with other heuristic-based optimization methods: Differential Evolution and Harmony Search, where DE evolves solutions through vector differences, while HS improvises them like musical harmonies. The results from simulations indicated that GWO method was effective in managing voltage fluctuations and maintaining operational limits in these distribution networks. Another work using the coordination between PV inverters and tap position of OLTC in the distribution network is presented in [62] as schedule method. This scheduling is based on a pattern search optimization algorithm, which utilizes predicted load demand and PV active power generation. The primary objectives are to reduce bus voltage deviation and minimize the losses of the network while keeping the number of tap operations within a predefined limit. Additionally, the paper includes a stochastic analysis to assess the effectiveness of this optimal scheduling method in the presence of inaccurate forecasting in load demand and PV generation, highlighting the robustness of the work approach under uncertain conditions.

2.2.2.2 SOPs and PSO Algorithm in Voltage Regulation

The paper [63] proposes a novel control method for regulating voltages in unbalanced three-phase electrical distribution systems. This method addresses a constrained optimization problem that aims to minimize voltage deviations and maximize the active power output of DERs. The harmony search algorithm is employed to solve this optimization problem. To demonstrate the efficacy of this approach, the IEEE 13 Bus distribution test system was modified and tested in three scenarios: a) a system controlled only by voltage regulators, b) a system controlled solely by DERs, and c) a system controlled by both voltage regulators and DERs. The simulation results indicate that systems with a combination of voltage regulators and DER control achieve a better voltage profile, highlighting the potential of integrating DERs into voltage regulation strategies for improved system performance. The parameters of the harmony search algorithm are carefully selected, and the convergence criterion is based on the change in the best objective function value. However, setting these parameters and determining the appropriate convergence criteria can be challenging, and may impact the efficiency and accuracy of the algorithm.

The use of SOPs and the PSO algorithm as key tools for addressing the challenges in electrical distribution networks, has been as a common thread in several research, especially in the context of high levels of DG and the integration of RESs, such as PV systems and wind turbines. In the study [64] a multi-objective optimization framework is proposed. This framework leverages SOPs—advanced power electronic devices adept at managing precise active and reactive power flows. The research employs an enhanced version of the PSO algorithm, the MOPSO, combined with a local search technique, the Taxi-cab method which is a local search strategy using Manhattan distance to explore neighboring solutions in grid-like steps, often applied in combinatorial or mixed-integer optimization alongside metaheuristics like PSO. This approach aims to optimize various operational aspects, including power loss reduction, feeder load balancing, and voltage profile improvement,

demonstrating its effectiveness in a 69-bus distribution network. Similarly, Reference [65] investigates the complexities in distribution networks arising from renewable energy integration. It identifies key issues like overvoltage, load imbalances, and fluctuating power outputs, proposing the installation of SOPs. The PSO algorithm is utilized to determine the optimal operating parameters for SOPs, focusing on minimizing bus voltage deviations and total line losses. Moreover, in [66], the enhancement of ADNs through the integration of DG units is discussed. The paper aims to improve energy efficiency by reducing power system losses and optimizing voltage profiles while adhering to system constraints. The methodology involves network reconfiguration, including strategic control over the quantity, size, and placement of DG units and the use of SOPs for advanced power flow control. Once again, a modified PSO algorithm is employed to determine the best system configuration, encompassing the optimal sizing and positioning of DG units and the allocation and dimensioning of SOPs. Additionally, the paper [67] explores the integration of DG units and the control of SOPs in ADNs. This study aims to enhance system efficiency by reducing power losses, improving voltage profiles, and balancing feeder loads. It presents a strategy for reconfiguring the network through the optimal determination of the number, location, and size of DGs and optimally managing SOP operations. A Modified Particle Swarm Optimizer (MPSO) is used as a crucial tool for handling the variables involved. The paper in [68] introduces a Mutation Fuzzy Adaptive Particle Swarm Optimization (MF-APSO) algorithm to solve the multi-objective optimization problem, effectively balancing the mitigation of overvoltage issues and reduction in total line loss. The methodology is demonstrated using numerical results, showing that the proposed multi-objective optimization method outperforms conventional methods, enabling enhanced utilization of high-penetration PV systems with reduced power curtailment due to improved voltage regulation and line-loss minimization.

On the other side ESSs have become pivotal in voltage optimization within power networks, especially in the context of integrating RESs, PSO plays a key role in these developments.

Reference [69], proposes a two-stage methodology to optimize reactive-voltage control in distribution networks with PV and ESSs. It addresses the challenge of voltage control due to the unpredictability of DGs by combining network reconfiguration with reactive resources. The first stage involves finding an optimal network topology with minimal line loss and reconfiguration, while the second stage determines the output of reactive power devices for each hour, including PV inverters and energy storage devices. While in [70], the study introduces an improved particle swarm optimization (I-PSO) method for optimizing both active and reactive power of the BESS to mitigate voltage fluctuations. This approach is demonstrated to be more effective than the standard PV smoothing mode. In [71], the author introduces an improved MOPSO algorithm for determining the optimal capacity and locations of ESSs. The algorithm aims to minimize voltage deviation and ESSs capacity costs. A novel two-stage majorization configuration model to optimize a hybrid energy storage system (HESS) in ADNs is presented in [72]. The model specifically addresses the challenges posed by volatile energy sources like wind and solar. By integrating both lead-acid batteries and supercapacitors, the study aims to balance cost, network loss, and node voltage deviation. The unique aspect of this paper is the use of a revised MOPSO approach to solve capacity configuration challenges, further enhanced by a quantum particle swarm optimization with a chaotic mechanism for operational optimization. Reference in [73] integrates the reactive power control function of PV inverters with the charge/discharge characteristics of ESSs to optimize voltage deviation. The study employs an improved adaptive PSO algorithm based on distributed information, demonstrating through simulations that this methodology more effectively improves voltage deviation in distribution networks compared to existing reactive power optimization strategies. This approach highlights the potential of coordinated control strategies in managing voltage issues in modern power systems with significant renewable energy integration. However, in grids where such storage systems are not widely deployed or are of limited capacity, the effectiveness of the approach could be reduced.

The papers [74, 75] both employ the NSGA-II genetic algorithm for optimizing ESS in ADNs. Where paper in [74] focuses on reducing power loss and voltage violation risk through extended reactive power optimization, considering the output of PV-storage systems. In contrast, the paper in [75] aims at optimal placement and capacity sizing of battery storage systems, targeting overall cost, load, and voltage fluctuation reduction.

Recent research employs diverse optimization algorithms to effectively manage voltage stability and efficiency in power networks with varying levels of renewable energy integration. Study In [76], introduces decentralized optimization methods as an alternative to traditional centralized methods, overcoming challenges like high computational cost and data privacy concerns. The study focuses on optimizing the operation of voltage regulators and energy storage devices through decentralized coordination. It employs two methods: the Advanced Arithmetic Optimizer algorithm and the Profile Steering approach, aiming to improve the reliability and efficiency of optimization processes while minimizing communication and computational costs. While in [77], the paper explores optimal sizing and siting of DG units to improve voltage profiles and reduce power losses. It also examines the role of BESS in peak shaving. The paper utilizes a Harris Hawks Optimization (HHO) algorithm for finding near-optimal solutions, tested on 33 and 141 bus distribution test systems. The paper in [78], introduces a method for voltage regulation in distribution networks using BESS units. It focuses on optimizing BESS units' operation in networks with high solar PV penetration. The method uses sparse optimization techniques for minimal unit engagement and power output variation. A distributed Lagrangian primal-dual sub-gradient algorithm is employed for decentralized decision-making. A stochastic multi-objective framework for daily control of Volt/Var in distribution networks is proposed in [79]. The objective is to lower power losses, minimize voltage deviations, reduce the costs of energy, and decrease overall emissions. The approach incorporates uncertainties in hourly demand, wind energy, and solar radiation within a scenario-driven probabilistic model and utilizes an evolutionary algorithm through a Modified Teaching-Learning Algorithm (MTLA) to solve

the MINP problem.

2.2.2.3 Multi-Objective Optimization

Recent advancements in active distribution network optimization emphasize the integration of sophisticated multi-objective optimization techniques, particularly MOPSO, focusing on managing the complexities introduced by high RES penetration levels. In [80] the author proposes a novel approach for Volt/Var optimization in ADNs with RESs. This approach employs a two-timescale multi-objective coordinated control system, focusing on minimizing power loss and reducing the number of control actions required for OLTC and SCs over a 24-hour period. The paper introduces a three-step method, including local search, global search, and user preference, to address the multi-objective MINP problem. The optimization is performed every 6 hours, considering the variability in day-ahead predications of RES, and every 15 minutes for the reactive power control of RES, explicitly accounting for RES uncertainties. The strategy employs a group-based MOPSO for global search and the Interior Point Method (IPM) for local search and real-time optimization. The efficacy of this methodology is demonstrated using the IEEE 33-bus distribution network, showcasing significant improvements in power loss reduction and effective voltage regulation in the presence of RES uncertainties. Similarly, reference [81] presents a comprehensive approach to reactive power control in ADNs. This approach involves formulating a multi-objective mixed-integer nonlinear optimization problem focusing on reducing active power loss and minimizing voltage deviation. The solution employs a group-based MOPSO and fuzzy logic to find Pareto optimal solutions and select a preferred compromise solution. A composite load model, including plug-in electric vehicles, static induction motors, and ZIP loads, is used to better represent load behaviour. Further in [82], the application of MOPSO is employed for an optimal reactive power dispatch (ORPD) strategy. This strategy focuses on reducing active power losses and minimizing voltage deviation by effectively coordinating OLTC transformers, CBs, and DGs. The paper

highlights the efficacy of MOPSO algorithm in handling nonlinear functions, continuous and discrete variables, and multiple constraints. By utilizing this method, the authors demonstrate improved active power loss reduction and voltage profile optimization in distribution systems, offering a valuable contribution to the field of smart grid technology and renewable energy integration. In [83] the paper introduces a multistage, multi-objective Volt/Var control strategy incorporating high solar PV penetration in smart grids. It focuses on enhancing energy efficiency through CVR in distribution networks. The strategy comprises a dual approach: a slow time scale control for planning and a fast time scale control for real-time operations. In the planning stage, the paper employs a Discrete Multi-objective Particle Swarm Optimization (DMOPSO) for stochastic multi-objective Volt/Var optimization, addressing uncertainties and inaccuracies in predicting load demand and PV generation. For real-time operations, it utilizes an adaptive Volt/Var droop-controlled approach to manage voltage fluctuations induced by sudden variations in PV output. The research demonstrates significant improvements in reducing peak demand, daily energy demand, and system losses, offering a comprehensive control strategy for modern power systems with significant renewable energy integration. A mathematical model for reactive power regulation based on MPC is presented in [84]. The model proposes a multiple-timescale optimal reactive voltage control method, specifically designed to lower the impact of uncertainties from wind and photovoltaic energy sources on voltage control. To validate this approach, the study employs the IEEE-57 node system integrated with RESs. The efficiency of the model is exhibited using the Whale Optimization Algorithm combined with Simulated Annealing (WOASA). The results from this approach show that the multiple-timescale control method significantly enhances the operational safety of the power grid and effectively leverages the potential of reactive power regulation.

The paper [85], proposes a novel Volt/Var (VV) co-optimization strategy for managing the challenges of PV integration in low-voltage distribution networks. It addresses the limitations of traditional models that assume a single voltage level and balanced networks.

The study introduces a three-stage approach, coordinating the operation of medium-voltage switched capacitors and low-voltage PV inverters, to improve voltage profiles and reduce power losses, and solved by employing improved direct load flow and MPSO methods.

The work in [86], investigates the impact of integrating DSTATCOMs and PV units in Tala city, Egypt's distribution network. Using an improved sine cosine algorithm, the study assesses the network at varying PV penetration levels and optimizes the placement of DSTATCOMs and PV units to minimize power losses and improve voltage stability. Results show significant enhancements in power loss reduction and system stability when combining PV units with DSTATCOMs, demonstrating the effectiveness of this integrated approach.

2.2.2.4 Control and Optimization Integration

Reference [87], introduces a two-stage optimization strategy to manage voltage fluctuations and minimize power losses in distribution systems with high PV penetration. The first stage involves a day-ahead optimal strategy focused on minimizing total voltage deviations and power losses, constrained by the maximum allowable operations of OLTCs and SCs. The second stage involves real-time inverter reactive power control to adjust for the uncertainties in PV output and load demand. This stage utilizes an artificial neural network (ANN) to estimate system states. Both optimization problems are formulated as nonlinear problems and are solved using direct search algorithms. The effectiveness of this method is validated using a Hardware-In-the-Loop (HIL) simulation platform on IEEE 34-node test feeder.

The increasing integration of RESs into power systems has led to the advent of advanced technologies like smart inverters, which are instrumental in maintaining voltage stability and efficiency. Smart inverters, primarily used in PV systems, convert the variable direct current (DC) output of solar panels into a grid-compatible alternating current (AC). Beyond this basic function, they are increasingly recognized for their capability to provide dynamic

voltage support and reactive power compensation, which are essential for stabilizing the grid amidst the variable nature of solar energy. In light of this context, the paper [88] addresses a critical aspect of modern power distribution systems: the coordination of these smart inverters with traditional Volt/Var control (VVC) devices. The paper proposes a coordinated methodology for Volt/Var optimization (VVO) that combines the rapid response capabilities of smart inverters with the established functionality of traditional VVC devices including shunt capacitor banks (SCBs), OLTC, and VRs. This approach is aimed at effectively managing voltage fluctuations that occur because of the variable nature of RES, changes in network configurations, and varying load demands. The methodology encompasses both centralized and local control algorithms with an objective to reduce the total cost of operating, while considering CVR and the voltage deviation of nodes. Additionally, the study examines the influence of BESS on the overall system performance. To tackle this multi-objective optimization challenge, the fuzzy decision-making technique and ϵ-constraint method are applied. The efficiency of the proposed VVO methodology is verified through its application to a well-known 33-bus distribution system, showcasing significant improvements in energy consumption efficiency, reduction of OLTC switching operations, and voltage stabilization. The subsequent study, [89] focuses on enhancing distribution system performance by optimizing the Volt/Var function in smart inverters. This method addresses voltage deviations caused by DG connections, aiming to reduce voltage deviation and minimize the loss of lines without affecting distributed generation output. The algorithm's effectiveness is demonstrated through a case study on the South Korean distribution system, confirming the significant improvement in system performance through optimized smart inverter settings. Author in [90], addresses the challenges of increased line loss and voltage deviation in distribution networks due to high PVs and EVs penetration. The study proposes new reactive power regulation methods, utilizing the potential of PVs and EVs, to alleviate these challenges. It establishes reactive power regulation models for PVs and EVs, along with methods to evaluate their reactive power adjustable capacity dynamically. The paper employs five different algorithms for optimization, with deep learning used to approximate

the optimization objectives of minimizing line loss and voltage deviation. The results demonstrate the effectiveness of deep learning in accurately fitting the Pareto front achieved by intelligent algorithms in practical applications.

2.2.2.5 Other Optimization Techniques

Using the Sparrow Search Algorithm (SSA), the study in [91] coordinates the OLTC, VR, smart inverter settings, and switched capacitor bank to optimize the unbalance and variation of voltage. The approach addresses individual phase voltage regulation, considering the operational dynamics of these devices and the unbalanced load conditions. The results show significant improvements in voltage variation and unbalance, demonstrating the efficacy of the SSA in optimizing the system's performance. [92] employs probability distribution models to estimate power generation and network load demands, considering the fluctuations in load, along with the variability in solar radiation and wind speed. It utilizes the Open Distribution System Simulator (OpenDSS) for modelling ADNs and aims to reduce network voltage deviation and minimize power loss. The paper introduces numerous novel metamodel-based global optimization (MBGO) methods, comparing them with traditional metaheuristic global optimization (GO) methods to identify their respective advantages, limitations, and weaknesses. Simulations on different bus systems demonstrate that MBGO methods are more suited for small-and medium-scale ADNs, while metaheuristic GO algorithms perform better in large-scale ADNs with simpler objective functions. In [93], a multi-objective hierarchically-coordinated VVC method that utilizes droop-controlled PV inverters is proposed. The approach is designed to reduce the voltage deviation and power loss through the optimization of reactive power setpoints and droop control functions in PV inverters. It includes a comprehensive modelling of the droop control characteristics of PV inverters, including voltage ranges and droop slope gradients. To tackle the random variations in PV power generation, the paper applies Taguchi’s orthogonal array testing technique. The effectiveness of this method is demonstrated through tests on two distribution

systems, showing improved control performance compared to existing methods. The papers in [94-96], highlight innovative methods and algorithms to optimize and control ADNs, ensuring stable operation and efficient integration of renewable energy sources. In [94], the author proposes a technique using big bang-big crunch (BB-BC) optimization and reactive power compensation to control voltage profiles in distribution systems, thereby avoiding active power curtailment in DGs. The method involves optimizing regulator taps and reactive power contributions of capacitors and DGs, implemented by a central control unit for effective voltage management and increased DG penetration. On the other hand, paper in [95], presents a scheme for their optimal placement in distribution networks to enhance system performance. The strategy employs the artificial bee colony (ABC) optimization approach, focusing on reducing voltage deviation, power losses, and line loading, contributing to improved voltage profiles and network functionality. While paper in [96], proposes a strategy for optimal voltage control in distribution networks, coordinating various distributed equipment like transformers, voltage regulators, and compensators. The strategy uses a GA to manage operations effectively, tested on a network model with photovoltaic generation to validate its efficacy in voltage control.

2.3 Discussions on Optimization Strategies, Methods, and Practicality

The integration of RESs, especially PV systems, into power distribution networks introduces a complex blend of opportunities and challenges in voltage regulation and system stability. This paper's exploration of various optimization strategies and technologies provides an insight into the evolving landscape of active distribution network management.

2.3.1 Common Trends: Objectives, Algorithms, Architectures, and Benchmark Case Studies

In analyzing the various analytical and computational techniques applied for voltage

regulation, some key commonalities emerge in the optimization objectives and algorithms adopted across studies reflecting contemporary research priorities. The cumulative percentages provided in the analysis reflect the proportion of papers focusing on specific optimization objectives, algorithms, architectures, and test systems, offering insights into the research trends and focal points within the domain.

2.3.1.1 Objectives Analysis

a) Voltage Deviation Minimization:

Minimizing voltage deviations, emphasized by 64% of the studies, underscores the critical importance of stability in power systems. This focus reflects the pivotal role that voltage stability plays in ensuring the reliable operation of electrical devices and maintaining the integrity of the power grid. The significant attention on this objective demonstrates an ongoing effort within the research community to enhance grid reliability and performance under varying load conditions.

b) Active Power Loss Reduction:

Around 53% targeting the reduction of active power loss is indicative of a broader push towards efficiency in power distribution. By minimizing losses, utilities can achieve significant energy savings and reduce operational costs, which is essential in the context of growing energy demands and the push for sustainable energy practices.

c) Correlation Between Voltage and Loss Reduction:

There is about 44% overlap between papers focusing on minimizing voltage deviations and reducing power losses indicates a significant intersection in research objectives,

demonstrating that nearly half of the studies in this domain consider these two issues concurrently. This overlap highlights the intertwined nature of voltage stability and efficiency in power systems, where addressing one often contributes to improvements in the other.

d) Conservation Voltage Reduction:

Although less emphasized, 12% of the papers focus on conservation voltage reduction (CVR) signifies an interest in demand-side management strategies. CVR can be an effective tool for reducing peak demand, thereby enhancing the overall efficiency of the power system and potentially deferring the need for new generation capacity.

2.3.1.2 Algorithms Analysis

a) Metaheuristic Algorithms:

Over 67% of papers leverage metaheuristic algorithms for handling complex, non-convex problems. The popularity of metaheuristic algorithms, including Particle Swarm Optimization (PSO), Genetic Algorithm (GA), and Multi-Objective PSO (MOPSO), reflects their flexibility in navigating complex, multi-dimensional search spaces. These algorithms are well-suited for optimizing non-linear, multi-objective problems characteristic of voltage regulation tasks, where trade-offs between different objectives might need to be carefully balanced.

b) Convex Optimization:

Almost 32% of papers apply convex relaxation/convexification techniques. The use of convex optimization techniques, such as Second Order Cone Programming (SOCP),

Semidefinite Programming (SDP), and the Alternating Direction Method of Multipliers (ADMM), points to a methodological approach aimed at simplifying complex optimization problems. By reformulating or approximating non-linear, non-convex problems as convex ones, researchers can leverage powerful mathematical tools to find globally optimal solutions more efficiently.

2.3.1.3 Benchmark Case Studies

A number of benchmark case studies are recurrently used within the literature, including IEEE bus systems (e.g., IEEE 33-bus, IEEE 69-bus) and real-world network models. However, the IEEE 33 node feeder and IEEE 123 node models are frequently adopted benchmarks to compare voltage regulation techniques. These case studies serve as common grounds for validating and comparing the effectiveness of different optimization strategies.

2.3.1.4 Common Optimization Architecture

Recent studies have increasingly focused on decentralized and distributed optimization approaches, highlighting a shift towards more scalable and resilient voltage regulation solutions that can better accommodate the distributed nature of renewable energy resources. However, the centralized optimization at a system level still adopted architecture. The performance of centralized optimization strategies relies heavily on having accurate system data and forecasts. A few papers do analyze the impact of uncertainties and inaccuracies in the inputs [31, 52, 80, 87]. The lack of studies analyzing the impact of false or uncertain data represents a gap in validating the real-world performance of proposed centralized optimization schemes. More research is likely required to enhance optimization robustness under data inaccuracies.

2.3.2 Efficiency and Application: Analytical vs. Computational Methods in Voltage Optimization

A detailed comparison between analytical and computational methodologies is presented, focusing on advantages, limitations, key applications, and notably their time efficiency and processing speed. Outlined in Table 2.1, the analysis illuminates the distinct capabilities and performance of both approaches in addressing voltage optimization challenges in active distribution networks. This evaluation aims to assist researchers and practitioners in selecting the most suitable technique based on the problem's complexity, available computational resources, and time constraints.

Table 2.1: Efficiency and Application Comparison of Analytical and Computational Techniques

Category	Advantages	Limitations	Key Applications	Time Efficiency
Analytical Approaches	Provide deterministic analysis grounded in mathematical rigor, crucial for capturing physical system behaviors and constraints.	May struggle with complex system dynamics and large network computational tractability.	- Decentralized control algorithm design - Local voltage stability assessment - Coordination of OLTC, capacitor banks, and PV inverters	Faster for simpler, well-defined problems through direct mathematical formulations
Computational Methods	Leverage big data and machine learning to navigate complex optimization landscapes, offering adaptability to intricate objective functions.	Sometimes suffer from limited explainability and dependence on input data patterns.	- Large-scale renewable generation coordination - Probabilistic multi-objective optimization - Metaheuristic volt-VAR optimization	Slower initial setup but adaptable to complex, non-linear systems, potentially requiring more computational time

2.3.3 Voltage Optimization Techniques: A Research Taxonomy

The taxonomy of reviewed papers as shown in Table 2.2 provides a structured overview of research spanning references [11,12,14-96] on voltage optimization in ADNs. It details diverse strategies, from analytical to computational, highlighting their impact on grid

stability and the integration of RES. This section outlines key methods, their benefits, and limitations, offering insights for future research and practical applications in enhancing power system resilience and efficiency.

Table 2.2 Taxonomy of reviewed papers

Ref.	Category	Method	Description	Limitations and Gaps
[11]	Analytical	Decentralized reactive power control	Uses adjustable robust optimization and convex quadratic programming to determine decentralized decision rules for PV inverter reactive power control	Depends on accurate PV output predictions. Effectiveness reduced by inaccurate forecasts.
[12]	Analytical	Robust distributed PV inverter control	Develops local decision rules for PV inverter reactive power control based on distributionally robust optimization to minimize voltage deviations	Focused only on PV-based Volt/Var control. Did not consider coordination with other DERs
[14]	Analytical	Increment-exchange decentralized optimization	Enables decentralized multi-objective optimization through quadratic functions of coupling variable increments while preserving privacy	Trading off some optimality for privacy preservation - solutions are not perfectly Pareto optimal
[15]	Analytical	Multi-objective adaptive robust optimization	Handles uncertainties using robust optimization to minimize voltage deviations and losses with high PV penetration	Unclear if approach handles all types of uncertainties.
[16]	Analytical	Robust optimization for DG reactive power control	Handles uncertainties using robust MILP optimization approach for control of DG reactive power injection	Sensitive to errors in network admittance matrix

[17]	Analytical	Robust optimization, MINP	Robust optimization formulation using MINP to handle uncertainty in DG and loads	Effectiveness depends on accurate load & generation forecasting
[18]	Analytical	Distributed CVR using ADMM optimization	Distributed optimization model for conservation voltage reduction using Alternating Direction Method of Multipliers	Suboptimal solutions possible compared to centralized optimization.
[19]	Analytical	Quadratic programming	Develops quadratic programming (QP) model for optimal reactive power dispatch in balanced and unbalanced systems; two time-scale architecture for controlling DERs	Needs coupling with slow time-scale control for comprehensive system management.
[20]	Analytical	SOID algorithm for inverter optimization using ADMM	Linearized voltage model enables quadratic optimization of inverter dispatch using ADMM	Have not been extensively benchmarked with other methods like SOCP. Testing limited to balanced networks.
[21]	Analytical	Transformer tap optimization using SDP and ADMM	Determines optimal tap positions through rank constrained SDP, solved via ADMM	Issues with algorithmic efficiency, system-wide applicability, and dynamic response handling
[22]	Analytical	Decentralized PV inverter setpoint optimization with ADMM	Develops decentralized methods for optimizing inverter power setpoints using ADMM algorithm	Limited testing on more complex system configurations.

[23]	Analytical	Multi-objective optimization for ESS ancillary services with ADMM	Optimizes various objectives related to ESS services using ADMM-based multi-objective procedure	Need for advanced algorithms in dynamic grid conditions. Aligning strategy with ESS capabilities and constraints.
[24]	Analytical	Multi-stage quadratic flexible OPF framework	Proposes real-time OPF framework using object-oriented device models and SLP algorithm for sequential optimization	Need for speed and convergence quality improvement in MQFOPF
[25]	Analytical	Two-stage optimization	Two-stage real-time Volt/Var control method using data-driven model for voltage violation risk assessment and EV dispatch	Balancing different optimization objectives in real-time control.
[26]	Analytical	Model predictive control, Mixed-integer quadratic programming	Double time-scale voltage control scheme utilizing model predictive control (MPC) and specialized mixed-integer quadratic programming solver	Does not consider the voltage deviation in unbalanced system.
[27]	Analytical	Decoupling rolling multi-period optimization	Uses Benders decomposition and MPC for decoupled optimization of OLTC and PV systems across time periods	Could be computationally intensive, especially for larger networks

[4]	Analytical	SOP coordination using MISOCP	Coordinates SOP with OLTC and capacitors through linearization and conic relaxation into MISOCP	Centralized approach may struggle with computational, and communication demands in larger ADNs.
[28]	Analytical	SOP optimization for unbalanced networks	Introduces phase-changing SOP concept and employs conic relaxation strategies for optimization	Need for further study on coordination and timing between PC-SOP and other phase transfer techniques
[29]	Analytical	Decentralized SOP optimization	Develops decentralized and local control schemes for coordinating multiple SOPs	Can only achieve near-global optimal solutions, not absolute optimality.
[30]	Analytical	Sensitivity analysis for SOP optimization	Uses Jacobian matrix sensitivity analysis to quantify SOP optimization tradeoffs	Inherent trade-offs in the control scheme, such as improved voltage profile leading to increased energy losses.
[31]	Analytical	Robust SOP optimization via SOCP	Employs adjustable robust optimization model transformed into computationally efficient SOCP	Potential moderate complexity in computation for larger networks. Performance under larger uncertainty conditions is yet to be fully assessed.

[32]	Analytical	Interval and rolling optimization for E-SOPs	Two-stage scheme using interval optimization for day-ahead planning and rolling optimization for real-time E-SOP control	The method mainly targets long-term optimization, needing research on short-term (5-15 min) control strategies.
[33]	Analytical	Biconvex optimization for SOPs and DGs	Universal SOP and DG coordination method based on biconvex relaxation solved using alternative convex search	The ACS algorithm achieves a local optimum but may not reach the global best solution.
[34]	Analytical	Convex relaxation for centralized & local SOP control	Combined centralized SOP control though convex relaxation and local decentralized reactive power control	Additional comprehensive assessment across a wider range of network performance metrics is needed
[35]	Analytical	SOP optimization using ADMM	Employs ADMM algorithm for decentralized optimization of SOP power transmission between networks	Achieves near-global optimal solutions but may miss the absolute best solution.
[36]	Analytical	Coordinate PV & voltage control co-optimization	Formulates nonlinear constrained optimization problem for coordinating PV and voltage control systems solved using SQP	Requires close cooperation between DSOs and IPPs for data sharing, which could be a challenge in terms of data privacy, security, and operational coordination.

[37]	Analytical	Analytical algorithms	Coordination of two analytical voltage control algorithms - one rule-based, one optimization-based; compares network effects and costs	Effectiveness reliant on sufficient controllable resources in the network.
[38]	Analytical	Two-stage optimization	Two-stage optimization coordinating OLTC and SVC using forecast data in day-ahead stage and local optimization in real-time stage	Focus on specific OLTC and SVC operation strategies, possibly overlooking other effective approaches.
[39]	Analytical	Dispersed storage optimization mixed integer SOC model	Determines optimal allocation of dispersed storage systems using mixed integer SOC programming model	Effectiveness demonstrated on a modified IEEE 34-bus test feeder; broader applicability needs more validation.
[40]	Analytical	Centralized tuning of local inverter control	Uses MISOCP optimization to determine parameters for local voltage-based inverter reactive and active power control	The need for frequent parameter adaptation could lead to increased communication requirements, posing a challenge in terms of system efficiency and resource utilization.
[41]	Analytical	OLTC control via convex optimization	Employs linearization to enable convex optimization formulation for optimal tap changing transformer control	OTC's performance heavily relies on accurate solar and power demand forecasts.

[42]	Analytical	MISOCP optimization integrating VAR devices	Transforms non-convex AC OPF to MISOCP using convexification techniques to optimize VAR devices	Moderate computational burden suggests potential for optimization, especially for complex networks.
[43]	Analytical	Smart inverter optimization model for ADMS	Convex optimization model to control smart inverters for voltage regulation and conservation voltage reduction	Limited applicability in diverse energy resource scenarios beyond PV systems.
[44]	Analytical	Convex relaxation for DER voltage regulation	Establishes sufficient conditions to enable voltage regulation as a convex optimization program	Need to explore the coupling between this method and conventional voltage regulation devices across different time-scales.
[45]	Analytical	Quadratic programming voltage control model	Formulates voltage control model of distribution network as quadratic program using simplified linear voltage equations	The method relies on approximation for solutions, which may not be optimal in all scenarios.
[46]	Analytical	Probabilistic optimization for voltage regulation	Incorporates probabilistic PV generation scenarios into constrained optimal load flow problem formulation for voltage regulation	Potential challenges in accurately predicting real-time PV output and sudden variability.

[47]	Analytical	Multi-objective OPF for PV inverter optimization	Develops multi-objective OPF solved with SQP to optimize inverter real and reactive power control	Strategy based on the widespread availability of advanced communication systems. Reliance on a centralized system to collect data and control inverter settings.
[48]	Analytical	MILP for coordinated inverter & OLTC control	Linearization approach enables MILP formulation for coordinating inverters and OLTCs	Primarily compared with conventional AVR, lacking broader comparisons with other voltage regulation methods.
[49]	Analytical	MIQP optimization model with linearized power flow	Uses MIQP optimization of control variables based on linearized power flow equations	Challenges in tuning MIQP problem-solving software for specific distribution system issues.
[50]	Analytical	Two-stage scheduling and control procedure	Employs MILP optimization and sensitivity analysis for day-ahead and intra-day scheduling of distributed energy resources and control devices	Potential oversimplification of network dynamics due to linearization in the MILP problem-solving process.
[51]	Analytical	Decentralized reactive power optimization	Derives near-optimal decentralized inverter control from global optimization solutions to minimize voltage deviations and losses	Further research required for more general scenarios beyond the study's current parameters.

[52]	Computational	MINP for worst-case voltage scenarios	Handles OLTC, capacitor banks and PV plants using MINP optimization for worst-case voltage scenarios to limit variations and losses	Heavy dependence on communication for coordinating controllable units.
[53]	Computational	Centralized-decentralized voltage regulation	Employs multi-objective MINP optimization and NSGA-II algorithm for centralized-decentralized voltage control	Potential issues with frequent switching of substation capacitors and power factor violations.
[54]	Computational	Multi-objective GA for smart inverter Volt-VAR curves	Employs genetic algorithm to optimize smart inverter Volt-VAR curves for loss reduction and voltage regulation	Prioritizes specific objectives like voltage profile and system loss minimization, but may not capture trade-offs in more complex scenarios.
[55]	Computational	PV device coordination using GA	Integrates individual optimization algorithms for tap changers, capacitors and inverters using genetic algorithm	Encountered trade-offs where lower voltages for CVR benefits slightly increase system losses.
[56]	Computational	Parameter optimization for smart inverters using GA	Genetic algorithm used to optimize volt-var curve parameters to improve distributed generation system performance	Service Transformer Integration: Inclusion in the model not fully assessed for different network types.

[57]	Computational	Deep reinforcement learning algorithm for smart inverters	Online coordination of smart inverters using deep reinforcement learning for voltage regulation	Comparison with Other Methods: While effective, the proposed shows a slight increase in PV curtailment compared to OPF due to more reactive power use.
[58]	Computational	Bi-level optimization for battery & inverter coordination	Combines metaheuristic algorithms in bi-level optimization strategy for battery storage and smart inverter voltage control	The effectiveness of voltage control may be constrained by the limited capacities of BESS and smart inverters.
[59]	Computational	Locust search algorithm	Optimizes capacitor placement using locust swarm optimization algorithm to improve voltage profile and reduce losses	LS's distinct method of avoiding concentration around best solutions needs further real-world scenario testing.
[60]	Computational	ε-decomposition, Genetic algorithm	Centralized support distributed voltage control algorithm utilizing ε-decomposition and genetic algorithm for optimization	Variable Effects in Different Grid Types: Shows differing impacts of local region increases in systems with and without constant voltage DG, suggesting dependency on specific grid characteristics.

[61]	Computational	Grey wolf optimization algorithm	Coordinates control devices using grey wolf optimization to minimize voltage deviations	Focuses on numerical accuracy and simulation speed, but overlooks aspects like scalability and robustness in variable network conditions.
[62]	Computational	Schedule optimization using pattern search algorithm	Schedules tap changer and inverter setpoints based on forecast load and generation to regulate voltage and minimize losses	Relies on day-ahead predictions of PV generation and load demand, with effectiveness potentially impacted by forecast accuracy.
[63]	Computational	Harmony search algorithm	Employs harmony search to optimize voltage regulator and DER reactive power control for voltage regulation	Focuses on three specific control scenarios, potentially overlooking other operational configurations and their impacts.
[64]	Computational	Enhanced PSO for optimization with SOPs	Uses multi-objective particle swarm optimization enhanced with local search to optimize networks with soft open points	Improved results over conventional MOPSO, yet broader comparisons with other optimization techniques are not conducted.

[65]	Computational	PSO to determine SOP parameters	Employs particle swarm optimization to find optimal control parameters for soft open points	The study ignores the impact of the SOP capacity on power transfer efficiency and voltage control in the network.
[66]	Computational	Modified PSO algorithm for DG & SOP optimization	Optimizes size, placement of DG units and allocation of SOPs using adapted particle swarm algorithm	The study's general approach to DG challenges isn't thoroughly assessed for its adaptability to changing grid technologies and requirements.
[67]	Computational	Reconfiguration optimization using modified PSO	Network reconfiguration involving DGs and SOPs based on modified particle swarm optimization method	Compares results with existing literature but could benefit from a wider range of comparative studies with different optimization methods.
[68]	Computational	Mutation fuzzy adaptive particle swarm optimization	Balances overvoltage mitigation and loss reduction using adapted meta-heuristic particle swarm algorithm	Significant energy savings are noted, but adaptability in different grid environments isn't extensively examined.
[69]	Computational	Two-stage optimization algorithm for ESS & reactive power	Methodology with separate optimizations for network topology and reactive resource dispatch including ESS	The paper's effectiveness in dynamic or highly variable grid conditions isn't fully explored.

[70]	Computational	Improved particle swarm optimization	Optimizes battery active and reactive power to smooth PV fluctuations using adapted particle swarm algorithm	Compares the I-PSO approach mainly with the PV smoothing mode, lacking a broader range of comparisons with other advanced methods. Also, Did not consider the insufficient BESS capacity.
[71]	Computational	PSO algorithm to optimize ESS capacity & placement	Employs improved particle swarm optimization to determine optimal ESS size and locations	Need for further research on scalability and adaptability.
[72]	Computational	Multi-objective PSO for hybrid ESS configuration	Uses enhanced multi-objective particle swarm optimization for optimizing hybrid energy storage configuration	Addresses power fluctuation smoothing and voltage improvement but doesn't deeply examine performance in extreme operational scenarios.
[73]	Computational	Coordination of ESS & PV using improved PSO	Integrates ESS and PV control capabilities using adaptive particle swarm optimization variant	Centers on PV inverter reactive power and energy storage optimization, not exploring interactions with other network components.

[74]	Computational	NSGA-II algorithm for PV-storage optimization	Focuses on reactive power optimization and risk reduction using genetic algorithm with PV-storage systems	Mainly focuses on PV-storage systems in DNs, potentially limiting its relevance for networks with different energy sources.
[75]	Computational	NSGA-II method for ESS placement and sizing	Evolves Pareto optimal solutions for energy storage placement and capacity using NSGA-II	The NSGA-II heuristic algorithm introduces randomness, leading to variability and subjectivity in selecting the optimal solution.
[76]	Computational	Decentralized optimization algorithms	Examines decentralized optimization methods as alternatives to centralized approaches	Advantages in privacy and cost, but potential trade-offs in effectiveness and robustness.
[77]	Computational	Harris hawks optimization algorithm	Employs bird-inspired metaheuristic optimization for optimal sizing and siting of DG	The study limits DG units and BESS capacity to 1 MW, which might not be applicable in different regions with varied capacity requirements.

[78]	Computational	Distributed optimization algorithm for battery optimization	Develops distributed Lagrangian optimization scheme for coordinating battery storage units	A gap in multi-time period optimization, indicating limitations in current handling of long-term voltage regulation.
[79]	Computational	Multi-objective stochastic optimization & evolutionary algorithm	Handles uncertainties using scenario-based stochastic scheme optimized with teaching-learning based evolutionary algorithm	Dividing control variables into centralized and local groups may not fully address dynamic network interactions.
[80]	Computational	MOPSO & interior point method for coordinated optimization	Two-timescale scheme using MOPSO for global search and interior point method for real-time reactive power optimization	Effective voltage/var optimization (VVO) relies on accurate forecasts, with errors potentially impacting results.
[81]	Computational	Pareto optimization using MOPSO and fuzzy logic	Multi-objective PSO combined with fuzzy logic to obtain and select compromise solutions	Further extension to include forecasting errors and wider network evaluations are necessary.
[82]	Computational	MOPSO algorithm for optimal reactive power dispatch	Employs multi-objective particle swarm optimization for coordinated dispatch of reactive power resources	While the model offers multiple solutions, it might not provide a comprehensive understanding for all operational scenarios.

[83]	Computational	Multi-stage stochastic MOPSO optimization	Planning stage uses discrete MOPSO under uncertainties, operating stage uses adaptive droop-based Volt/Var mechanism	Impact of flexible electric vehicle charging loads on algorithm performance unexplored.
[84]	Computational	Whale optimization & simulated annealing algorithm	Hybrid whale optimization with simulated annealing used to solve predictive control optimization model	Requires further research to improve system reliability and expand the scope of reactive power regulation.
[85]	Computational	Multi-stage optimization for coordinated volt-var control	Proposes 3-stage approach integrating modified PSO for coordinating volt-var control devices	The pre-set threshold OFmax is assumed constant, not accounting for dynamic network conditions.
[86]	Computational	Optimizing DSTATCOMs & PV using improved sine cosine algorithm	Assesses placement of DSTATCOMs & PV units using enhanced sine cosine optimization algorithm	The study is limited to a specific case study (Tala City), which may not generalize to other distribution networks with different characteristics.
[87]	Computational	Two-stage direct search optimization	Performs day-ahead optimization to minimize voltage deviations and losses, along with real-time ANN-based inverter reactive power control	The ANN-based state estimation method depends on the availability and accuracy of measurements; its performance might be limited in scenarios with insufficient data.

[88]	Computational	Hierarchical coordinated VVO	Uses ε-constraint and fuzzy decision-making optimization methods for coordinating inverters, OLTCs, VRs and capacitor banks	The study doesn't thoroughly address how the proposed scheme adapts to evolving grid conditions and increasing DER penetration over time.
[89]	Computational	Smart inverter VVO parameter optimization	Optimization method to determine optimal parameters for smart inverter volt-var control functionality	Need for precise weight settings in optimization, challenging optimal balance under varying system conditions.
[90]	Computational	Deep learning approximation of optimization objectives	Uses deep learning to fit Pareto fronts from multi-objective optimization algorithms	Long computation time for data acquisition and network training, and potential infeasible solutions due to DL's poor generalization with insufficient data.
[91]	Computational	Device coordination using sparrow search algorithm	Employs sparrow search algorithm to optimize individual phase voltage regulation from various control devices	The approach may neglect the interactions and cumulative effects of phase imbalances on the entire network's voltage stability

[92]	Computational	Comparison of metaheuristic & metamodel optimization methods	Compares performance of metaheuristic algorithms with metamodel-based global optimization techniques	High-dimensional problems in large ADNs pose significant challenges, requiring new approaches or enhancements to existing methods.
[93]	Computational	Optimization using taguchi's orthogonal array testing	Applies taguchi experimental design within solution algorithm for Volt/Var control optimization	Need for broader testing in diverse network scenarios.
[94]	Computational	Coordinated real-time voltage control using BB-BC optimization	Proposes technique using big bang-big crunch optimization method combined with reactive power compensation to control voltages	Reliance on the specific performance of the modified BB-BC optimization method.
[95]	Computational	Optimal placement of ESSs units using ABC algorithm	Determines optimal placements of distributed ESSs using artificial bee colony metaheuristic optimization to enhance system performance	Additional studies needed on intelligent ESS control, comprehensive sizing, and power quality improvements post-ESS implementation.
[96]	Computational	Genetic algorithm	Optimal distribution voltage control method coordinating various devices, solved using genetic algorithm	Centralized control requires a robust communication system. If it fails, devices revert to self-information-based control, limiting system-wide optimization.

2.3.4 Approach Methods: An Overview

Decentralized control algorithms emerge as a significant theme, demonstrating considerable potential in managing voltage fluctuations and reducing line losses in networks with high PV penetration level. These algorithms offer an alternative to centralized control methods, which can be limited by computational complexities and data privacy concerns. The decentralized approach, utilizing local measurements and decision-making, shows promise for real-time voltage control and system optimization. However, their effectiveness heavily relies on the accuracy of local measurements and the speed of decision-making. Future systems should incorporate edge computing technologies to bolster the real-time processing capabilities of decentralized frameworks.

Smart inverters have emerged as a pivotal technology in grid management, providing dynamic voltage support and reactive power compensation. The increasing capabilities of these inverters, particularly when combined with BESS, enable more efficient management of the variable nature of solar energy. The paper highlights various optimization methods that leverage these technologies, underscoring their critical role in enhancing grid resilience and stability. We believe that the next generation of smart inverters should integrate machine learning algorithms for predictive control, adapting to grid conditions dynamically. This integration not only improves voltage regulation but also optimizes energy storage usage, paving the way for a more resilient grid.

Another key aspect is the application of both computational and analytical optimization methods. Computational methods like GAs and PSOs provide robust solutions for the complex, multi-objective problems typical of modern power systems. Conversely, analytical methods offer deterministic approaches, essential for understanding fundamental operational principles and developing theoretical control strategies. However, the practical application of analytical methods might be constrained by simplifications and assumptions. In contrast,

computational methods, especially those employing artificial intelligence and machine learning, present promising solutions to these constraints by adapting to the complexities of real-world scenarios.

The review underlines the significance of multi-objective optimization techniques in balancing various operational goals, such as minimizing power loss, maintaining voltage stability, and optimizing renewable energy utilization. These techniques, especially MOPSO, are instrumental in addressing the intricacies introduced by high RES penetration levels. Though, the advancement of multi-objective optimization techniques, especially those incorporating environmental and economic objectives, is critical. Future research should explore optimization frameworks that integrate cost analysis and carbon footprint assessment to support decision-making.

Moreover, despite technological advancements, challenges remain, particularly in terms of scalability and adaptability to diverse and dynamic grid conditions. Overcoming these challenges requires a holistic approach that considers not just technological solutions but also regulatory frameworks, market mechanisms, and infrastructure upgrades. Additionally, the development of standardized protocols for grid management systems will facilitate the integration of new technologies and enhance system adaptability.

Practical implementation issues, including economic, scalability, and regulatory factors, also need careful consideration. Theoretical and simulation-based studies, while promising, may encounter various barriers in real-world applications. Navigating these economic and regulatory challenges is crucial for the successful deployment of these strategies.

In conclusion the chapter navigates through a spectrum of optimization strategies employed for voltage regulation in active distribution networks with high renewable energy penetration. Table 2.3 outlines different approaches, from robust optimization to customized techniques,

each with specific merits and limitations. It highlights the diversity of strategies in managing voltage within power systems, emphasizing the balance between effectiveness and the challenges posed by dynamic grid conditions. This summary aims to provide a clear comparison, aiding in the identification of suitable methods for addressing voltage regulation challenges.

Table 2.3 Approach Methods: Advantages and Disadvantages

Research Focus & Citations	Methodological Approach	Pros	Cons	Keywords
Robust Optimization [11,12,14-17]	Uses adjustable robust optimization models to ensure optimal voltage and power loss management under uncertainties	Effective handling of uncertainties; Provides robust solutions	Relies on accurate PV output predictions, which may not always be available	Active Distribution Networks, Robust Optimization, Uncertainty Management, Voltage Regulation, Power Loss Management
Advanced Optimization Techniques in Power Systems [18-23]	Utilizes ADMM for distributed optimization problems in power systems	Computationally efficient; Flexible framework	Static models may have limitations in dynamic scenarios	Advanced Distribution Management Systems, Distributed Optimization, ADMM, Power Systems, Efficiency, Energy Storage System
Advanced Hierarchical and Predictive Control [24-27]	Employs predictive control and rolling horizon optimization for real-time optimization	Adaptive to changing conditions; Enables dynamic optimization	Algorithm speed and convergence improvements needed	Predictive Control, Hierarchical Control, Real-Time Optimization, Rolling Horizon Optimization
Soft Open Point (SOP) Utilization in Voltage Regulation [28-36]	Leverages SOPs to actively manage voltage and power flow	More flexibility than traditional devices; Handles DG effectively	Increased complexity for large networks	Soft Open Points, Voltage Regulation, Distributed Generation, Power Flow Management
Local and Coordinated Voltage Control [28-36]	Coordinates local and distributed control elements for voltage regulation	Cost-effective; Reduces network reinforcement need	Limitations in high DG penetration scenarios	Voltage Control, Distributed Energy Resources, Local Control, Coordinated

Convexification and Relaxation Techniques [37-42]	Uses conic relaxation and linearization to convexify optimization problems	Computationally efficient; Ensures convergence	May not fully capture distribution network dynamics	Convexification, Relaxation Techniques, SOCP, SDP, Linearization, Conic Relaxation, Optimization Problems
Flexible Optimization Frameworks [43-49]	Employs various techniques for adaptable optimization frameworks	Adaptable to multiple problem formulations	Simplified models may reduce accuracy	Optimization Frameworks, Flexibility, Adaptability, Model Simplification
Heuristic Optimization Methods [50-59]	Utilizes algorithms like NSGA-II, GA, DRL, PSO for complex problems	Handles complex problems effectively; Manages uncertainties	Performance dependent on parameter tuning	Heuristic Methods, Metaheuristic Algorithms, NSGA-II, GA, DRL, PSO, Uncertainty Management
SOP and PSO-based Optimization [60-66]	Leverages SOPs and PSO for power flow optimization	Precise power flow control; Computationally efficient	May be outperformed by other methods	Soft Open Points, Particle Swarm Optimization, Power Flow Optimization
Multi-Objective Optimization [60-85]	Employs MOPSO for trade-off optimization between competing objectives	Balances multiple objectives; Flexible	Complex problem formulation; Scalability issues	Multi-Objective Optimization, MOPSO, Trade-Off Analysis, Competing Objectives
Control and Optimization Integration [86-89]	Combines optimization models with control algorithms like ANN and deep learning	Adaptive control; Handles uncertainties	Reliant on accurate system state estimators	Integration of Control and Optimization, ANN, Deep Learning, Uncertainty Management
Customized Optimization Techniques [90-96]	Diverse algorithms tailored for specific applications	Specialized solutions; Tailored approaches	Narrow scope; Limited generalizability	Sparrow Search Algorithm, Metamodel-Based Global Optimization, Big Bang-Big Crunch Optimization, Artificial Bee Colony

2.3.5 Future Directions and Emerging Technologies

The analysis of current strategies and methodologies in voltage regulation within ADNs with high penetration of PV and RES underscores the complexity and evolving nature of modern power systems. The reliance on metaheuristic and convex optimization algorithms has demonstrated substantial success in navigating these complexities. However, this focus also signals the necessity for ongoing innovation and adaptation in algorithm development to meet future challenges and opportunities. Below are key areas for future directions and emerging technologies in voltage regulation:

- Hybrid Optimization Techniques

The exploration of hybrid optimization techniques represents a significant opportunity for advancing voltage regulation strategies. Combining the strengths of analytical models and computational algorithms could yield more effective and efficient solutions. Such hybrid methods would benefit from the precision and theoretical foundations of analytical models while harnessing the flexibility and adaptability of computational algorithms, especially in dealing with non-linear, dynamic problems in ADNs.

- Impact of Emerging Technologies

Emerging technologies, including blockchain and the Internet of Things (IoT), hold the potential to dramatically transform voltage regulation practices. Blockchain technology could offer secure, transparent, and efficient mechanisms for energy transactions and data management within ADNs. It enables peer-to-peer energy trading between prosumers without intermediaries, ensures transparency and auditability of all exchanges, and automates processes via smart contracts (e.g., settling payments when solar generation is verified), and facilitating better demand response and distributed energy resource

management. Similarly, the IoT could enhance grid monitoring and control capabilities, providing real-time data for more responsive and adaptive voltage regulation strategies.

- Conservation Voltage Reduction (CVR)

The relatively low emphasis on CVR in current research suggests room for expanded exploration, especially in relation to demand response and integrated demand-side management strategies. Enhancing the focus on CVR could lead to more sophisticated approaches for managing energy demand, contributing to overall grid efficiency and stability.

- Integration of Advanced AI and ML Techniques

The integration of advanced Artificial Intelligence (AI) and ML techniques into voltage regulation strategies offers a promising avenue for future research. AI and ML can provide powerful tools for predicting grid behavior, optimizing energy distribution, and managing the integration of RESs. These technologies can enhance the robustness and adaptability of voltage regulation methods, allowing for more effective management of complex and dynamic grid environments.

In conclusion, while current strategies for voltage regulation in ADNs have shown significant promise, the continuous evolution of grid technologies and energy sources necessitates further research and development. By focusing on hybrid optimization techniques, leveraging emerging technologies, expanding the scope of CVR, integrating advanced AI and ML, and adopting comprehensive grid management strategies, future research can ensure the successful integration of PV and RES into a more efficient, resilient, and adaptable power system.

2.4 Conclusions

The advancements in voltage regulation for ADNs underscore the increasing importance of sophisticated, multi-objective optimization techniques and the integration of smart grid technologies. The reviewed methods demonstrate significant improvements in voltage profile management, loss minimization, and operational efficiency, particularly in networks with high PV and EV penetration. Notably, the integration of RESs, coupled with innovative control strategies and optimization algorithms, offers promising solutions for future grid management. However, challenges remain, particularly in terms of the scalability of these solutions and their adaptability to diverse and dynamic grid conditions. Future research should focus on enhancing the robustness of these strategies, further integrating artificial intelligence and machine learning techniques, and exploring more comprehensive approaches to grid management that encompass the full spectrum of RESs and advanced grid technologies. This proposed structure provides a concise, yet comprehensive overview of the key findings and methodologies discussed in the paper, while also setting a direction for future research and development in the field.

2.5 Research Gaps and Thesis Contributions

The comprehensive review of analytical and computational voltage optimization methods in Active Distribution Networks (ADNs) reveals a rapidly evolving field with significant advancements. However, several critical gaps remain unaddressed, which this thesis aims to bridge. The identified shortcomings and the corresponding contributions of this work are summarized as follows:

Gap 1: Limited Research on SOP-ES in Unbalanced Three-Phase Networks.

- *Literature Status:* While the benefits of Soft Open Points (SOPs) and Energy Storage (ES) have been explored, many studies focus on balanced or single-phase systems. There is a scarcity of research on the integrated optimal operation of SOP-ES devices in unbalanced, three-phase distribution networks under high renewable penetration.

- *Thesis Contribution:* **Chapter 3** will develop a multi-period, multi-objective optimization framework for unbalanced ADNs using SOP-ES. A key contribution is the formulation of this problem using a three-phase Semidefinite Programming (SDP) model with symmetrical components transformation, ensuring computational tractability and global optimality for a problem that has predominantly been tackled with heuristic or simplified linear methods.

Gap 2: Lack of a Unified Coordination Framework for OLTC and SOP-ES.

- *Literature Status:* Previous work often coordinates SOPs with traditional devices like OLTCs, but typically treats Energy Storage as a separate entity. A holistic, convex optimization framework that jointly coordinates OLTC tap settings, SOP power flows, and ES charging/discharging schedules in a single model is largely absent.

- *Thesis Contribution:* **Chapter 4** will introduce a unified SDP-based model for the coordinated operation of OLTC and SOP-ES. This model will demonstrate the synergistic potential of this coordination to not only improve technical performance (voltage profile, losses) but also to significantly reduce OLTC switching operations, thereby enhancing the operational lifespan of this critical asset.

Gap 3: Insufficient Integration of Detailed Economic Models in Technical Optimization.

- *Literature Status:* Many studies on SOP-ES focus on technical objectives or use

simplified economic models. A comprehensive cost-benefit analysis that simultaneously considers Time-of-Use (TOU) grid costs, battery degradation costs, and PV curtailment penalties within a convex optimization framework for SOP-ES is not thoroughly explored.

- *Thesis Contribution:* **Chapter 5** will formulate and solve a comprehensive economic operation model that integrates these three key cost components. It will quantitatively demonstrate that SOP-ES is not only a technical asset but also an economically viable one, and will analyze the trade-offs between immediate cost savings and long-term battery health.

Gap 4: Scalability Challenges for Large-Scale Network Optimization.

- *Literature Status:* Centralized optimization methods, including SDP, can become computationally prohibitive for large-scale, multi-period problems. While ADMM is recognized as a solution, its application is often slow. There is a need for accelerated distributed algorithms tailored for the non-convex and time-coupled nature of ADN optimization.

- *Thesis Contribution:* **Chapter 6** will implement and evaluate accelerated variants of the Alternating Direction Method of Multipliers (ADMM), specifically Fast ADMM (FADMM) and Adaptive ADMM (AADMM). This contribution addresses the scalability issue directly, demonstrating how the proposed models can be solved efficiently for large-scale networks, enhancing their practical real-time applicability.

In summary, this thesis moves beyond the current state-of-the-art by providing an integrated journey from device-level modeling (SOP-ES) to system-level coordination (with OLTCs), and from technical to economic optimization, all while ensuring computational scalability.

The subsequent chapters will systematically address these gaps, contributing models and strategies for the future of active distribution network management.

Chapter 3

Optimal Operation of Active Distribution Networks Using Soft Open Point Integrated with Energy Storage

Abstract

This chapter develops an integrated, multi-period optimization framework for unbalanced three-phase Active Distribution Networks (ADNs) with high penetration of renewable energy resources. The framework leverages Soft Open Points integrated with Energy Storage (SOP-ES) to address key operational challenges, including voltage unbalance, voltage violations, and power losses. A multi-objective Semidefinite Programming (SDP) model is proposed to simultaneously minimize power losses, mitigate voltage unbalance, and reduce voltage deviations. Through comprehensive case studies on the IEEE 13-bus and 123-bus systems, the results demonstrate that SOP-ES significantly outperforms SOP-only and baseline configurations, achieving superior voltage regulation, reduced system losses, and enhanced renewable energy utilization. The convex SDP formulation ensures computational tractability and global optimality, providing a robust and scalable solution for the technical optimization of modern distribution networks.

3.1 Introduction

Voltage rise, power loss, and voltage unbalance can be seen as the major impacts that occur with increasing levels of DG penetration. The use of flexible and controllable equipment in ADNs can enhance their efficiency and management capabilities. The rapid development of

power electronic technology provides an opportunity to solve these hard problems. Soft open point (SOP) is a novel power electronic device with high controllability installed to replace normally open point (NOP), realizing normal flexible connection and power transfer between feeders [5, 97].

These devices offer more precise and real-time control compared to traditional voltage regulation devices. Reference [4] introduce a time-series optimization model that coordinates SOPs with traditional regulation devices like OLTCs and capacitor banks (CBs). Building on this work, author in [28] propose the innovative Phase-Changing Soft Open Point (PC-SOP) to address three-phase imbalances in distribution networks, often exacerbated by unevenly distributed generation. The PC-SOP connects soft open points in a novel way to control active and reactive power, balancing the power flow among phases.

Further advancements in SOP control strategies are demonstrated in [29], where the author presents a novel approach combining decentralized and local control of SOPs to effectively manage voltage fluctuations.

To fully utilize the regulation ability of SOPs, the author in [31] proposes a robust optimization method involving a two-stage adjustable robust optimization model. This model generates robust operation strategies for SOPs, aiming to reduce voltage violations and minimize power losses in ADNs. Additionally, voltage stability improvement in distribution networks using SOPs was investigated in [98].

Energy Storage Systems (ESSs) have emerged as a critical component in voltage optimization within power networks, particularly in the context of integrating Renewable Energy Sources (RESs) [99]. The study in [69] proposes a two-stage methodology to optimize reactive voltage control in distribution networks with PVs and ESSs.

The recently soft open point integrated with energy storage (SOP-ES) devices [7, 8, 100-105] offer a cost-effective solution for active distribution networks by combining both spatial and temporal flexibility due to SOP and ES respectively. The spatial flexibility is achieved through SOP's power electronic converters, which enable bidirectional power flow control between different feeders, allowing real-time power redistribution to balance network loading and provide reactive power compensation at both terminals. The temporal flexibility is delivered through the integrated energy storage system, which enables time-shifting of energy to match supply and demand patterns, storing excess renewable generation during low demand periods and providing stored energy during peak demand or low generation periods. This dual flexibility is achieved using SOP converters that control the charging and discharging of the energy storage system, without the need for additional converters to connect the ES to multiple feeders in the network. This integration results in a more efficient and cost-effective approach to improve the operation of ADNs, reducing the overall capital cost compared to installing separate SOP and ES systems.

The SOP-ES device has various capabilities, including energy storage, power transfer, and reactive power regulation, which are achieved through the control of two voltage source converters and a DC-DC converter. A few studies have investigated the optimal operation of SOP-ES in active distribution networks as shown in Table 3.1. In this context, “Technical” optimization refers to objectives such as minimizing power losses, improving voltage profiles, reducing unbalance, or maximizing hosting capacity metrics that relate directly to network performance and stability. “Economic” optimization, in contrast, refers to objectives such as minimizing operational costs (e.g., energy purchase, battery degradation, curtailment penalties) or maximizing revenue metrics that relate to financial efficiency and cost-benefit analysis. Relevant literature [7] has worked on a technical optimization for single-objective (reducing power loss), while [8, 100] consider economic objectives such as the power exchange cost, loss cost, and battery degradation cost in the distribution network. A hybrid uncertainty method for managing energy storage-embedded SOPs was proposed in

[101], while multi-time-scale voltage control strategies were developed in [102]. In [103], the author focused on maximizing DG hosting capacity and operational flexibility. Reference [105] aim to optimize the operational costs of an AND and formulated as MINLP model and solved using the DICOPT solver in GAMS. An economic operation for cost reduction is proposed in [104].

However, the operation strategy and regulation ability of SOP-ES device to optimize the voltage deviation and unbalanced voltage of multiphase system in ADNs have not been considered yet. Therefore, this chapter considers the use of an optimal operation strategy for technical multi-objective optimization for unbalanced system in ADNs based on SOP-ES devices.

Table 3.1. Comparison of existing references using SOP-ES

Ref.	Phase	Model	System	Optimization-Objective
[7]	Single	Sequential Programming	Balanced	Technical (Single-Objective)
[8]	Single	Mixed-Integer Linear Programming (MILP)	Balanced	Economic
[100]	Single	Mixed-Integer Convex Programming (MICP)	Balanced	Economic
[101]	Single	Second Order Cone Programming (SOCP)	Balanced	Economic
[102]	Single	Particle Swarm Optimization (PSO) (nonlinear hybrid model)	Balanced	Technical (Multi-Objective)
[103]	Single	Second Order Cone Programming (SOCP)	Balanced	Technical (DG hosting)
[105]	Single	Mixed-Integer Non-Linear Programming (MINLP)	Balanced	Economic
[104]	Three	Second Order Cone Programming (SOCP)	Balanced	Economic
This research	Three	Semidefinite Programming (SDP)	Unbalanced	Technical (Multi-Objective)

The main contributions of this chapter can be summarized as follows:

- To our knowledge, previous literature on convexified optimal power flow has not considered the case of unbalanced distribution networks using SOP-ES devices, a critical oversight given that low-voltage networks are inherently unbalanced due to unequal single-phase loads and generation, which leads to phase-specific voltage violations and losses that balanced models cannot capture. Therefore, a multi-objective optimization model for three-phase active distribution network based on SOP-ES is developed. The model considers the optimal operation of SOP-ES to eliminate voltage violations, mitigating the voltage unbalanced condition, and minimizing the operation costs of ADNs by reducing the power loss of network.

- A convex formulation is proposed in this chapter for optimal operation of SOP-ES. The symmetrical SDP relaxation is used to convert the original non-convex nonlinear model into semidefinite programming (SDP) formulation, which can guarantee a computationally efficient and globally optimal solution by commercial solvers for radial distribution networks.

3.2 Modelling of SOP with Energy Storage

The Soft Open Point integrated with Energy Storage (SOP-ES) is a power-electronic-based grid device that combines the spatial power flow control of a Soft Open Point (SOP) with the temporal energy shifting capability of an Energy Storage System (ESS). Its operation is governed by the coordinated control of three main power electronic converters, as illustrated in Figure 3.1:

1. **Two Back-to-Back Voltage Source Converters (VSCs):** These AC-DC-AC converters are connected to different feeders (or substation buses) at points that are

traditionally kept open (Normally Open Points - NOPs). Each VSC can independently and rapidly control the active (P) and reactive (Q) power injection or absorption at its point of connection. This enables:

- **Bidirectional Active Power Flow:** Power can be transferred from one feeder to another to balance loading, alleviate congestion, and mitigate voltage issues (e.g., sending surplus PV generation from an overloaded feeder to an underloaded one).

- **Independent Reactive Power Support:** Each terminal can inject or absorb reactive power to provide localized voltage support and power factor correction, independent of the active power transfer.

2. **A DC-DC Converter:** This converter interfaces the Energy Storage system (typically a battery) with the common DC link that connects the two VSCs. It controls the charging and discharging of the battery by regulating the power flow between the DC link and the battery.

3. **The Common DC Link:** This is the crucial integration point. It electrically couples the two VSCs and the DC-DC converter, allowing for a unified power balance:

$$P_{\text{Terminal 1}} + P_{\text{Terminal 2}} + P_{\text{Battery}} + P_{\text{Losses}} = 0$$

This equation embodies the core working principle: the net active power from the two AC terminals and the battery (accounting for converter losses) must sum to zero at the DC link.

Spatial-Temporal Flexibility:

- **Spatial Flexibility (SOP Function):** The back-to-back VSCs provide real-time, controllable power transfer *between different locations* in the network, acting as a fully controllable, lossy tie-line.

- **Temporal Flexibility (ES Function):** The integrated battery stores energy when generation exceeds demand (or prices are low) and releases it when demand peaks (or prices are high), shifting energy *across time*.

Key Advantages over Separate Deployment:

- **Cost-Effectiveness:** Shares the power electronics (VSCs, controllers) and grid connection infrastructure, reducing capital cost compared to installing separate SOP and ESS units.

- **Enhanced Control:** Enables truly co-optimized dispatch where the battery's charge/discharge schedule directly influences and is influenced by the optimal power flow between feeders.

- **Efficiency:** Minimizes multiple power conversion stages (e.g., AC-DC for battery vs. AC-DC-AC for SOP) by using the common DC link.

Power balance constraints for SOP-ES device are given in equations (3.1, 3.2), while the power loss of SOPs and ES converters and ES battery are expressed in equations (3.3 - 3.6) respectively.

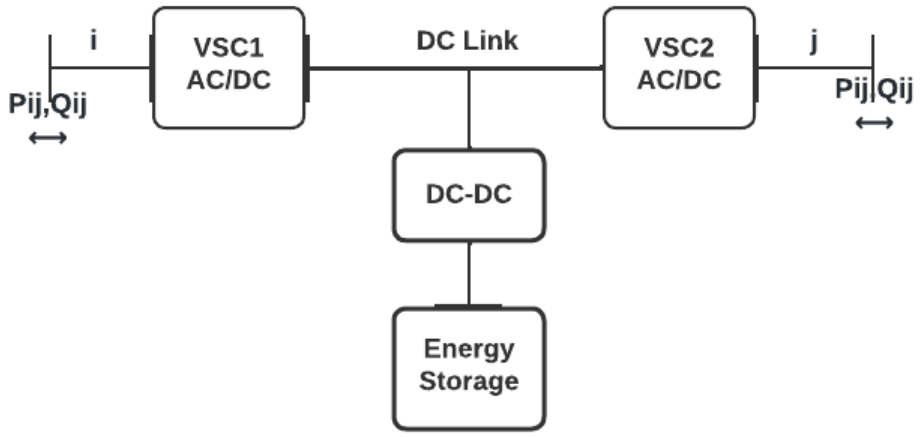

Figure 3.1: An integrated SOP-ES device in a distribution network.

$$P_{\varphi,i,t}^{\mathrm{SOP-ES}} + P_{\varphi,j,t}^{\mathrm{SOP-ES}} + P_{m,t}^{\mathrm{SOP-ES}} + P_{\varphi,i,t}^{\mathrm{SOP-ES,L}} + P_{\varphi,j,t}^{\mathrm{SOP-ES,L}} = 0 \tag{3.1}$$

$$\mathrm{P}_{\mathrm{m,t}}^{\mathrm{SOP-ES}} = -\left((\mathrm{P}_{\mathrm{m,t}}^{\mathrm{ch-ES}} - \mathrm{P}_{\mathrm{m,t}}^{\mathrm{dis-ES}}) - \mathrm{P}_{\mathrm{m,t}}^{\mathrm{ES,L}}\right) \tag{3.2}$$

$$\mathrm{P}_{\varphi,\mathrm{i,t}}^{\mathrm{SOP-ES,L}} = \mathrm{A}_{\mathrm{i}}^{\mathrm{SOP-ES}} \sqrt{\left(\mathrm{P}_{\varphi,\mathrm{i,t}}^{\mathrm{SOP-ES}}\right)^2 + \left(\mathrm{Q}_{\varphi,\mathrm{i,t}}^{\mathrm{SOP-ES}}\right)^2} \tag{3.3}$$

$$\mathrm{P}_{\varphi,\mathrm{j,t}}^{\mathrm{SOP-ES,L}} = \mathrm{A}_{\mathrm{j}}^{\mathrm{SOP-ES}} \sqrt{\left(\mathrm{P}_{\varphi,\mathrm{j,t}}^{\mathrm{SOP-ES}}\right)^2 + \left(\mathrm{Q}_{\varphi,\mathrm{j,t}}^{\mathrm{SOP-ES}}\right)^2} \tag{3.4}$$

$$\mathrm{P}_{\mathrm{m,t}}^{\mathrm{SOP-ES,L}} = \mathrm{A}_{\mathrm{m}}^{\text{SOP-ES}} \left|\mathrm{P}_{\mathrm{m,t}}^{\mathrm{SOP-ES}}\right| \tag{3.5}$$

$$\mathrm{P}_{\mathrm{m,t}}^{\mathrm{ES,L}} = \mathrm{A}_{\mathrm{m}}^{\mathrm{ES}} \left|\mathrm{P}_{\mathrm{m,t}}^{\mathrm{ES}}\right| \tag{3.6}$$

where, $P_{\varphi,i,t}^{\mathrm{SOP-ES}}$, $P_{\varphi,j,t}^{\mathrm{SOP-ES}}$represent active power injection by SOP converters at nodes i,j on phase φ at period t. $P_{m,t}^{\mathrm{SOP-ES}}$ represent active power injection by ES converter at nodes m at period t. $P_{\varphi,i,t}^{\mathrm{SOP-ES,L}}, P_{\varphi,j,t}^{\mathrm{SOP-ES,L}}$indicate active power loss of SOP converters at nodes i,j on phase φ at period t.$P_{m,t}^{\mathrm{SOP-ES,L}}$ represent active power loss of ES converters at nodes m at period t. $P_{m,t}^{\mathrm{ch-ES}}, P_{m,t}^{\mathrm{dis-ES}}$ represent charging and discharging power of ES battery at period t. $P_{m,t}^{\mathrm{ES,L}}$ represent power loss of ES battery at period t. while, $A_i^{\mathrm{SOP-ES}}$, $A_j^{\mathrm{SOP-ES}}$ $A_m^{\mathrm{SOP-ES}}$,and A_m^{ES} represent the loss coefficient.

The capacity limitations of SOPs and ES converters are expressed as in (3.7), (3.8), and (3.9), respectively, in addition to reactive power constraints of SOP-ES are considered in (3.10) and (3.11).

$$\sqrt{\left(P_{\varphi,i,t}^{SOP-ES}\right)^2 + \left(Q_{\varphi,i,t}^{SOP-ES}\right)^2} \leq S_{max}^{AC-DC} \tag{3.7}$$

$$\sqrt{\left(P_{\varphi,j,t}^{SOP-ES}\right)^2 + \left(Q_{\varphi,j,t}^{SOP-ES}\right)^2} \leq S_{max}^{AC-DC} \tag{3.8}$$

$$-S_{max}^{DC-CD} \leq P_{m,t}^{SOP-ES} \leq S_{max}^{DC-DC} \tag{3.9}$$

$$\underline{Q}_{\varphi,i}^{SOP-ES} \leq Q_{\varphi,i,t}^{SOP-ES} \leq \overline{Q}_{\varphi,i}^{SOP-ES} \tag{3.10}$$

$$\underline{Q}_{\varphi,j}^{SOP-ES} \leq Q_{\varphi,j,t}^{SOP-ES} \leq \overline{Q}_{\varphi,j}^{SOP-ES} \tag{3.11}$$

Energy storage systems must also meet the following constraints (3.12 - 3.15).

$$SoC_{t+1} = SoC_t - \left(P_{m,t}^{ES} + P_{m,t}^{ES,L}\right)\Delta t \tag{3.12}$$

$$-P_{max}^{ES} \leq P_{m,t}^{ES} \leq P_{max}^{ES} \tag{3.13}$$

$$SoC_{min} \leq SoC_t \leq SoC_{max} \tag{3.14}$$

$$SoC_1 = SoC_t \tag{3.15}$$

Equation (3.12) represents the state of charge (SoC) of the battery and how it changes based on the power of the device and its losses. Equations (3.13) and (3.14) impose limits on the power and energy of the battery, while (3.15) ensures that the initial and final SoC are kept equal.

3.3 Optimization Model

The objective of this chapter is to enhance the operation of ADNs by optimizing the deployment and control of SOP-ES devices. The formulations include objectives to

minimize power loss, voltage deviations, and unbalance voltage, supported by a set of constraints that ensure operational feasibility and network reliability.

3.3.1 Objective Functions

This research employs a multi-objective optimization strategy designed to address three primary concerns in ADNs through the strategic deployment of SOP-ES configuration. The model aims to minimize power losses, reduce voltage unbalance, and mitigate voltage deviations and fluctuations.

The multi-objective function is formulated as follows:

$$minf = W_L f^{\text{loss}} + W_U f^{V,unb} + W_D f^{V,dev} \tag{3.16}$$

where, f^{loss} represents the total power losses in the network, $f^{\text{V,unb}}$ denotes the voltage unbalance across the network, and $f^{\text{V,dev}}$ indicates the deviations from the nominal voltage. While W_L , W_U , and W_D represent the optimization wight of each component. In this technical optimization framework, photovoltaic (PV) generation is modeled as a zero-marginal cost resource with fixed active power output determined by forecasted generation profiles (Equation 3.27). The economic trade-offs associated with PV including curtailment penalties, is explicitly addressed in the economic operation model presented in Chapter 5. This separation allows for clear analysis of technical benefits (loss reduction, voltage regulation) independently from economic considerations.

These components are defined by the following specific equations:

$$f^{loss} = \sum_{t=1}^{T} \left(\sum_{ij \in \Omega_b} \operatorname{diag}\left(l_{ij,t} z_{ij}\right) \sum_{\substack{x=1,2,3 \\ \varphi=a,b,c}} P_{\varphi,x,t}^{\mathrm{SOP-ES,L}} \right) \tag{3.17}$$

$$f^{V} = \sum_{i=1}^{N_N} \sum_{\varphi=a}^{c} \left| V_{\varphi,i} - \frac{1}{3}\left(V_{a,i} + V_{b,i} + V_{c,i}\right) \right| \tag{3.18}$$

$$f^{V,\,\mathrm{deviation}} = \sum_{i=1}^{N_N} \left(\left| \boldsymbol{v}_{t,i} - V_{\mathrm{nominal}} \right| \right) \tag{3.19}$$

The nodal voltage vectors, branch current vectors, and related second-order decision variables are defined as in (3.20):

$$\begin{cases} V_{i,t} = \left[V_{i,t}^{a} \quad V_{i,t}^{b} \quad V_{i,t}^{c}\right] \\ v_{i,t} = V_{i,t} V_{i,t}^{H} \\ I_{ij,t} = \left[I_{ij,t}^{a} \quad I_{ij,t}^{b} \quad I_{ij,t}^{c}\right] \\ l_{ij,t} = I_{ij,t} I_{ij,t}^{H} \\ Sij = V_{i,t} I_{ij,t}^{H} \end{cases} \tag{3.20}$$

where the superscript *H* indicates the Hermitian transpose. $V_{i,t}$ represents the voltage vector at node *i* comprising phases *a*, *b*, and *c* at time *t*, and $I_{ij,t}$ denotes the currents of phases *a*, *b*, and *c* on branch *ij* at time *t*.

3.3.2 Power Flow and Voltage Constraints

With the foundational variables defined, the following operational constraints are established to ensure accurate modelling and control of power flows and voltages across the network.

$$\sum_{ij\in\Omega_b} \mathrm{diag}\left(S_{ij,t} - z_{ij} l_{ij,t}\right) + s_{j,t} + y_{j,t} v_{j,t} = \sum_{jk\in\Omega_b} \mathrm{diag}\left(S_{jk,t}\right) \quad (3.21)$$

$$v_{j,t} = v_{i,t} - \left(S_{ij,t} z_{ij}^H + S_{ij,t}^H z_{ij}\right) + z_{ij} l_{ij,t} z_{ij}^H \quad (3.22)$$

The voltage at each node must be maintained within specific limits to ensure safe operation and protect network equipment as in equation (3.23).

$$\underline{v_i} \leq diag\left(v_{i,t}\right) \leq \bar{v}_i \quad (3.23)$$

Where $\underline{v_i}$ and $\bar{v}_i$ represent the lower and upper voltage limits at node *i.* Equation (3.24) defines the voltage at the source node of the network.

$$v_0 = V_0^{ref} \left(V_0^{ref}\right)^H \quad (3.24)$$

Constraints (3.25) indicate the positive semidefinite constraint while (3.26) enforces that this positive semidefinite matrix should be of rank one.

$$\begin{bmatrix} v_{i,t} & S_{ij,t} \\ S_{ij,t}^H & l_{ij,t} \end{bmatrix} \geq 0 \quad i \to j \quad (3.25)$$

$$\mathrm{rank} \begin{bmatrix} v_{i,t} & S_{ij,t} \\ S_{ij,t}^H & l_{ij,t} \end{bmatrix} = 1 \quad i \to j \quad (3.26)$$

3.3.3 DG Operation Constraints

Constraint (3.27) assumes that the active power generated by DGs is equal to the given reference value.

$$P_{\varphi,i}^{\mathrm{DG}} = P_{\varphi,i}^{\mathrm{DG,re}} \quad (3.27)$$

By incorporating these comprehensive constraints, the optimization model aims to achieve a realistic and practical solution that enhances the performance of ADNs through the strategic deployment of SOP-ES configurations.

3.3.4 SDP Model Conversion

The original model of the power system's operation presents significant computational challenges due to its non-convex nature, primarily because of the rank-one constraint (3.26). To address these challenges, semidefinite programming (SDP) relaxation is adopted, which is a type of convex optimization where we optimize a linear objective function over the space of positive semidefinite matrices, subject to linear constraints, converting the complex non-convex model to an SDP model, which facilitates rapid and accurate computation [106, 107].

To convexify the problem, we employ a lifting technique. We introduce auxiliary matrix variables $v_{i,t} \in \mathbb{H}^{3\times3}$ and $l_{ij,t} \in \mathbb{H}^{3\times3}$ (Hermitian positive semidefinite matrices) to replace the outer products $V_{i,t}V_{i,t}^H$ and $I_{ij,t}I_{ij,t}^H$, respectively. The key step is to relax the rank-one equality constraints to positive semidefinite (PSD) inequality constraints as in equation (3.25). This single linear matrix inequality (LMI) convexifies the original non-convex set by:

1. SDP relaxation “lifts” quadratic relations into a higher-dimensional matrix variable defined as an outer product of the original voltage/current vectors as in (3.20).

2. Replacing the non-convex equalities $v_{i,t} = V_{i,t}V_{i,t}^H$ and $l_{ij,t} = I_{ij,t}I_{ij,t}^H$ with the convex PSD constraint (3.25), which is equivalent to requiring the matrix to be a Gram matrix of some vectors ($V_{i,t}$, $I_{ij,t}$).

3. Dropping the explicit rank-one condition equation (3.26).

Therefore, the capacity constraints of SOP-ES in (3.7-3.8) can be expressed as in (3.28).

$$\begin{bmatrix} S_{max}^{\mathrm{AC-DC}} & P_{\phi,i,t}^{\mathrm{SOP-ES}} + jQ_{\phi,i,t}^{\mathrm{SOP-ES}} \\ P_{\phi,i,t}^{\mathrm{SOP-ES}} - jQ_{\phi,i,t}^{\mathrm{SOP-ES}} & S_{max}^{\mathrm{AC-DC}} \end{bmatrix} \succeq 0 \tag{3.28}$$

Similarly, the loss constraints of SOPs in (3.3,3.4) can be transferred into an SDP model as in (3.29).

$$\begin{bmatrix} \dfrac{P_{\phi,k}^{\mathrm{SOP-ES,L}}}{A_k^{\mathrm{SOP}}} & P_{\phi,k}^{\mathrm{SOP-ES}} + jQ_{\phi,k}^{\mathrm{SOP-ES}} \\ P_{\phi,k}^{\mathrm{SOP-ES}} - jQ_{\phi,k}^{\mathrm{SOP-ES}} & \dfrac{P_{\phi,k}^{\mathrm{SOP-ES,L}}}{A_k^{\mathrm{SOP}}} \end{bmatrix} \succeq 0 \tag{3.29}$$

3.3.5 Symmetrical SDP Model Conversion

Building upon the basic SDP model, this step integrates the phase-to-phase coupling effects using symmetrical components transformation, which simplifies the three-phase unbalanced network model by reducing its complexity and enhancing the numerical stability of an SDP-based OPF method [108]. Equation (3.30) represents the transformation of voltages in phase components into symmetrical components.

$$V_{i,t}^{abc} = AV_{i,t}^{012} \tag{3.30}$$

$$A = \frac{1}{\sqrt{3}}\begin{bmatrix} 1 & 1 & 1 \\ 1 & a^2 & a \\ 1 & a & a^2 \end{bmatrix}, A^H = A^{-1} \tag{3.31}$$

and $a = 1\angle 120°$. Then, the three-phase variable in the BFM-SDP method [109] and the impedance parameters are related to the equivalent variables in symmetrical components as in equations (3.32-3.36):

$$v_{i,t}^{abc} = V_{i,t}^{abc} \times V_{i,t}^{abc,H} = AV_{i,t}^{012} \times \left(AV_{i,t}^{012}\right)^{H} = Av_{i,t}^{012}A^{H} \tag{3.32}$$

$$l_{i,t}^{abc} = Al_{i,t}^{012}A^{H} \tag{3.33}$$

$$S_{i,t}^{abc} = AS_{i,t}^{012}A^{H} \tag{3.34}$$

$$z_{i,t}^{abc} = Az_{i,t}^{012}A^{-1} = Az_{i,t}^{012}A^{H} \tag{3.35}$$

$$y_{i,t}^{abc} = Ay_{i,t}^{012}A^{-1} = Ay_{i,t}^{012}A^{H} \tag{3.36}$$

Using the symmetrical components, the power loss function in equation (3.17) and constraints in equations (3.21-3.25) are transformed as in equations (3.37-3.42).

$$f^{\text{loss}} = \sum_{t=1}^{T} \left(\sum_{ij \in \Omega_b} \text{diag}\left(A\left(l_{ij,t}^{012} z_{ij}^{012}\right)A^{H}\right) + \sum_{\varphi = 1,2,3} P_{\varphi,x,t}^{\text{SOP-ES,L}} \right) \tag{3.37}$$

$$\begin{aligned} &\sum_{ij \in \Omega_b} \text{diag}\left(A\left(S_{ij,t}^{012} - z_{ij}^{012} l_{ij,t}^{012}\right)A^{H}\right) + s_{j,t} + y_{j,t}^{012} v_{j,t}^{012} \\ &= \sum_{jk \in \Omega_b} \text{diag}\left(AS_{jk,t}^{012}A^{H}\right) \end{aligned} \tag{3.38}$$

$$\text{v}_{\text{j,t}}^{012} = \text{v}_{\text{i,t}}^{012} - \left(\text{S}_{\text{ij,t}}^{012}\text{z}_{\text{ij}}^{012,\text{H}} + \text{S}_{\text{ij,t}}^{012,\text{H}}\text{z}_{\text{ij}}\right) + \text{z}_{\text{ij}}^{012}\text{l}_{\text{ij,t}}^{012}\text{z}_{\text{ij}}^{012,\text{H}} \tag{3.39}$$

$$\underline{v_{i,t}} \leq \text{diag}\left(Av_{i,t}^{012}A^{H}\right) \leq \overline{v_{i,t}} \tag{3.40}$$

$$v_0^{012} = V_0^{012,\,\text{ref}}\left(V_0^{012,\,\text{ref}}\right)^{H} \tag{3.41}$$

$$\begin{bmatrix} v_i^{012} & S_{ij}^{012} \\ S_{ij}^{012,H} & l_{ij}^{012} \end{bmatrix} \geq 0 i \rightarrow j \tag{3.42}$$

3.3.6 Optimization Framework Overview

The optimization framework, as illustrated in Figure 3.2, follows a systematic four-step approach for power system scheduling. Initially, load forecasting and PV generation

forecasting are performed to predict energy demand and renewable generation patterns. This forecasted data feeds into the optimization model formulation stage, where the mathematical framework for the scheduling problem is established. The formulated optimization problem then undergoes convex relaxation via symmetrical SDP to transform the potentially non-convex problem into a tractable convex form that guarantees global optimality. Finally, the relaxed problem is solved through optimal scheduling of power flow over a 24-hour horizon using MOSEK as the solver, which efficiently handles the semidefinite programming constraints and provides the optimal dispatch decisions for the power system components.

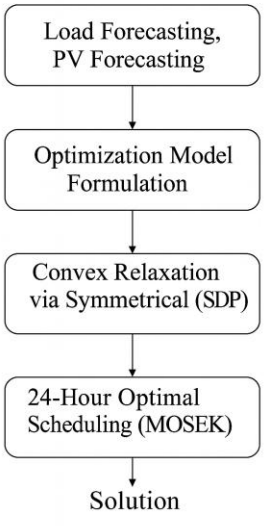

Figure 3.2: Flowchart of the Proposed Power System Scheduling

3.4 Simulations and Analysis

This section presents the simulation results and analyses the performance of the proposed model, which focuses on mitigating unbalanced voltage conditions, reducing power losses, and minimizing voltage limit violations in ADNs. The IEEE 13, and 123 node test feeder is employed as the benchmark network to validate the effectiveness of the model.

3.4.1 Simulation Setup

The proposed optimization model was implemented using the YALMIP toolbox [110] in MATLAB R2021b, and the optimization problems were solved using the MOSEK solver [111]. Voltage Source Converters (VSCs) are integrated into each SOP, with capacity of 500 kVA per phase, DC-DC converters incorporated in SOP-ES with a capacity of 500 kW and the energy storage has a capacity of 2000 kWh. Power loss coefficient is assumed to be equal 0.02 for both VSCs and DC-DC converters, reflecting conversion efficiency [4]. The system voltage is designed to operate within upper and lower voltage limits of 1.1 p.u. and 0.9 p.u., respectively, aligning with UK regulations [112]. In this work, the desired voltage range is narrowed to [0.97, 1.03] p.u., aligning with the interval thresholds applied in the voltage deviation control strategy. State of Charge (SOC) for energy storage units begin with an initial SOC of 0.5, with permissible operational ranges from 0.2 to 0.9 to maintain efficiency and battery health. The load demand and PV generation as shown in Figure 3.3 are obtained by forecasting [4] . The optimization framework presented in this chapter operates under a deterministic day-ahead scheduling paradigm, utilizing point forecasts for load demand and PV generation. The weight coefficients of each term in the objective function, obtained by using the pairwise comparison in AHP [113] as in Table 3.2 are given as follows: $W\_L = 0.61$, $W\_U = 0.13$, and $W\_D = 0.26$.

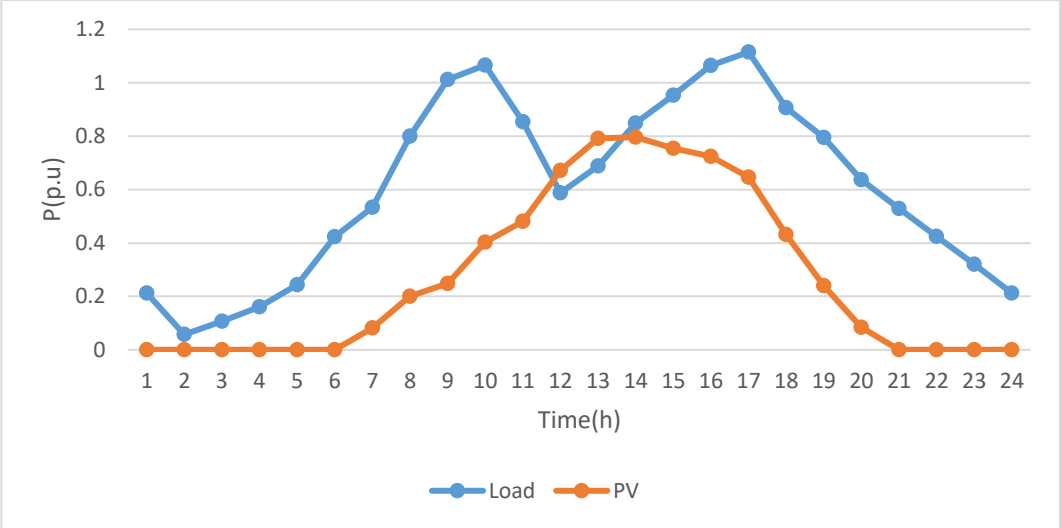

Figure.3.3: Load Demand and PV generation.

Table 3.2 Pairwise Comparisons of the Objective Function

	Power Loss	Voltage Unbalance	Voltage Deviation
Power Loss	1	5	2
Voltage Unbalance	1/5	1	1/2
Voltage Deviation	1/2	2	1

3.4.2 Performance Analysis

To evaluate the effectiveness of the proposed optimization model, three operational scenarios are considered for comparative analysis within ADN:

- Scenario I: Baseline (no SOP or SOP-ES)
- Scenario II: Using SOP only
- Scenario III: Using SOP integrated with Energy Storage (SOP-ES)

The analysis evaluates the performance based on key indicators including total power losses,

PV active power utilization, three-phase voltage unbalance condition (VUC), substation power exchange, and voltage regulation performance across the 24-hour period. All simulations are conducted on the IEEE 13-bus and IEEE 123-bus test feeders to reflect real-world operation of ADNs.

3.4.2.1 Case Study: IEEE 13-Node Test Feeder

The IEEE 13-node test feeder [114], is adopted as the simulation platform for model validation and performance analysis, as illustrated in Figure. 3.4. The network is enhanced with eight distributed PVs systems, each rated at 500 kW, summing up to a total installed capacity of 4 MW, operating at unity power factor. The technical parameters for the PV systems are summarized in Table 3.3. To facilitate advanced power flow control, two SOP-ES units are installed in the network between nodes 634 and 675, and nodes 675 and 680, respectively. In addition, OLTC is installed between buses 650 and 632. This three-phase voltage regulator is configured using fixed tap ratios consistent with the IEEE 13-bus OpenDSS standard settings:$[r_a^t, r_b^t, r_c^t] = [1.05, 1.0375, 1.04375]$, these tap ratios represent the step-up voltage settings for phases A, B, and C, respectively. The slight differences among the three phases reflect phase-specific compensation to address inherent voltage unbalances in the network.

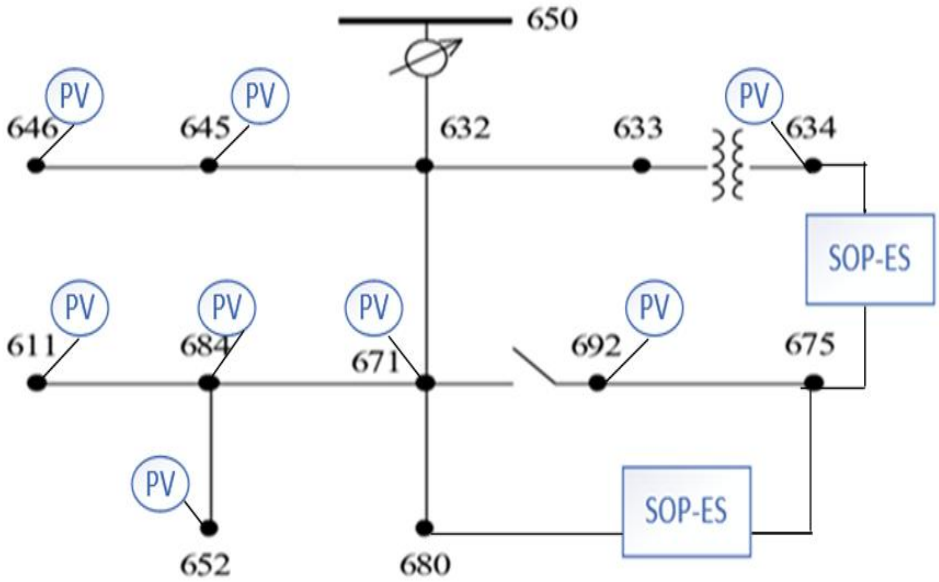

Figure. 3.4: IEEE 13-node Test Feeder.

Table 3.3. Parameters of PVs

Location	645	634	646	652	671	684	692	611
Phase	B	B	C	A	C	A	A	C
Capacity (kVA)	500	500	500	500	500	500	500	500

Table 3.4 summarizes the outcomes of the optimization under different configurations. The Baseline configuration exhibits the highest power losses and the lowest PV utilization. The SOP-ES scenario achieves the lowest power loss (0.95 MW/24 h), reflecting a 86.4% improvement over the baseline and a 5.9% reduction compared to SOP-only. The substation power values represent the total 24-hour energy imported from the main grid to supply network demand, accounting for local PV generation and losses. Lower values indicate greater self-sufficiency through local generation and improved power flow management via SOP/SOP-ES.

Figure 3.5 illustrates the active power loss across 24 hours for SOP and SOP-ES configurations. It can be seen in the early period 1-6h that SOP-ES is higher in loss due to the discharging of power from energy but, SOP-ES exhibit consistently lower power loss

during high-load intervals. For instance, between hours 9 and 11 and again from 16 to 18, SOP suffers a peak loss of over 0.07 p.u., while SOP-ES maintains significantly lower values. This demonstrates the superior energy efficiency and balancing effect provided by energy storage. In contrast, the SOP-ES configuration shows the best overall performance across all indicators.

Table 3.4 Optimization Results of the IEEE 13-Node Test Feeder

Scenario	Power Loss (MW/24 h)	PV Active Power (MW/24 h)	Substation power (MW/24 h)
Baseline	7.01	13.17	44.268
SOP	1.01	17.18	34.62
SOP-ES	0.95	17.21	34.17

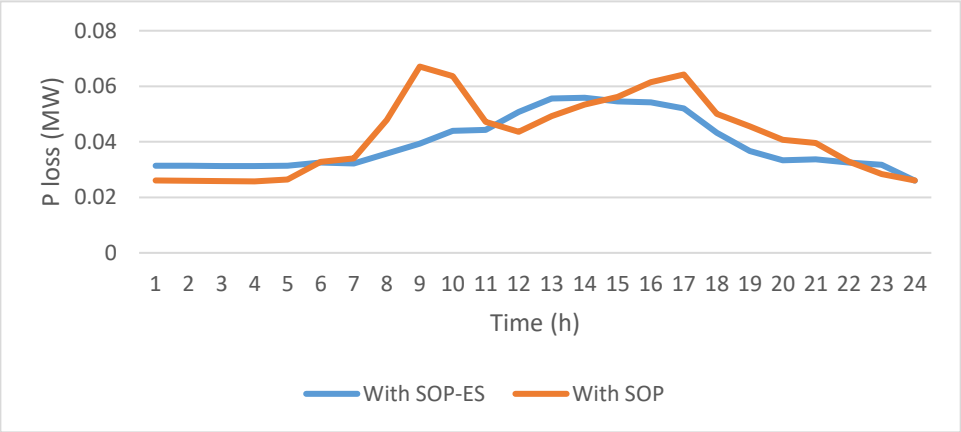

Figure 3.5: Hourly Power Loss Comparison

As shown in Figure 3.6, the SOP-ES strategy enables more consistent and smoother PV utilization, especially during midday. It reduces curtailment by absorbing excess generation into the energy storage system, thereby maximizing renewable energy usage and minimizing waste.

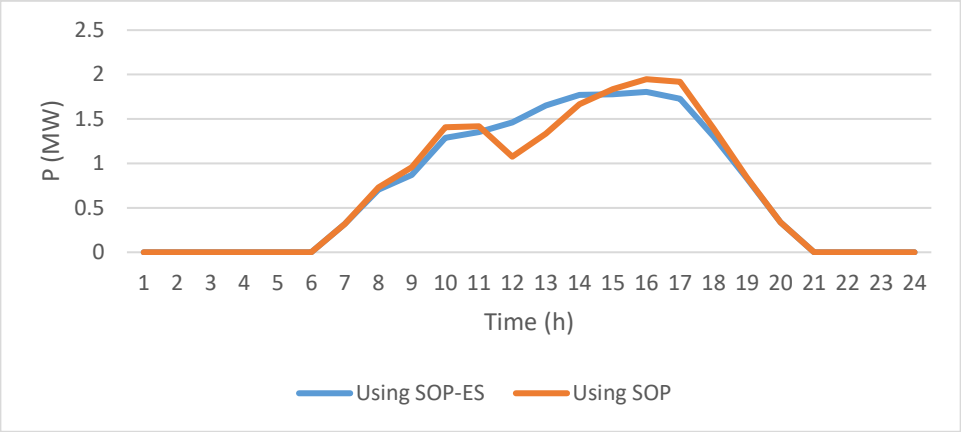

Figure 3.6: PV Utilization Profile

Figure 3.7 compares the total power imported from the substation for all scenarios. The SOP-ES strategy clearly demonstrates peak shaving and valley filling effects, with significantly lower demand during high-load periods. This reduces strain on the upstream network and lowers grid dependence.

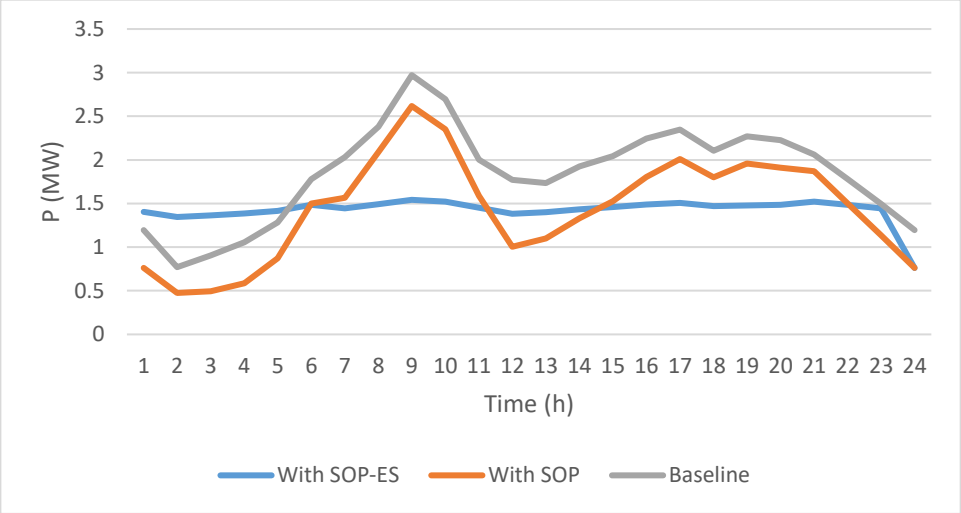

Figure 3.7: Substation Power Curve

Figures 3.8 and 3.9 present the voltage profiles on Bus 692 and 680 under the baseline scenario. When compared to the SOP and SOP-ES scenarios depicted in Figures 3.10 through 3.13 for Buses 692 and 680, the baseline case exhibits more significant and persistent voltage deviations throughout the 24-hour period. In contrast, the implementation

of SOP-ES demonstrates a notably improved voltage profile, particularly during midday peak load hours. The SOP-ES configuration results in reduced voltage deviations and a narrower spread between phases, indicating enhanced phase symmetry. This reflects the capability of the SOP-ES to effectively mitigate voltage unbalance and maintain voltage stability across the network.

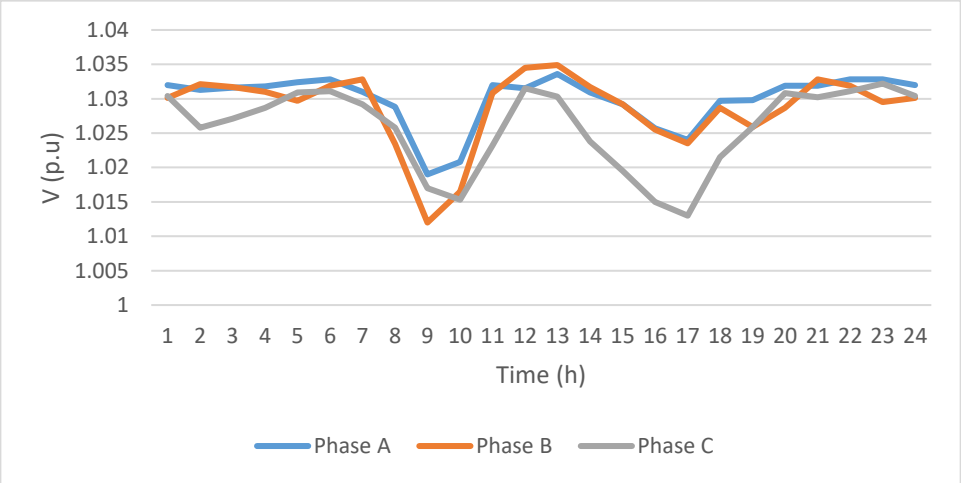

Figure 3.8: Baseline Voltage Profile at Bus 692

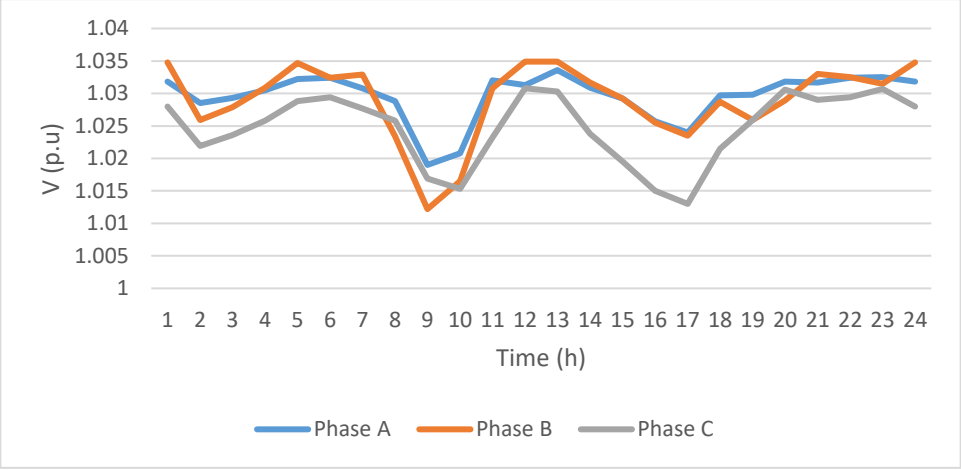

Figure 3.9: Baseline Voltage Profile at Bus 680

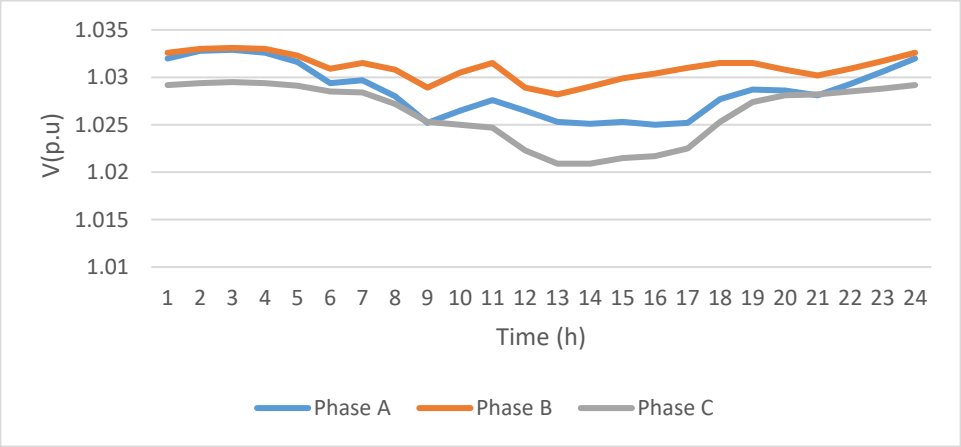

Figure 3.10: SOP Voltage Profile at Bus 692

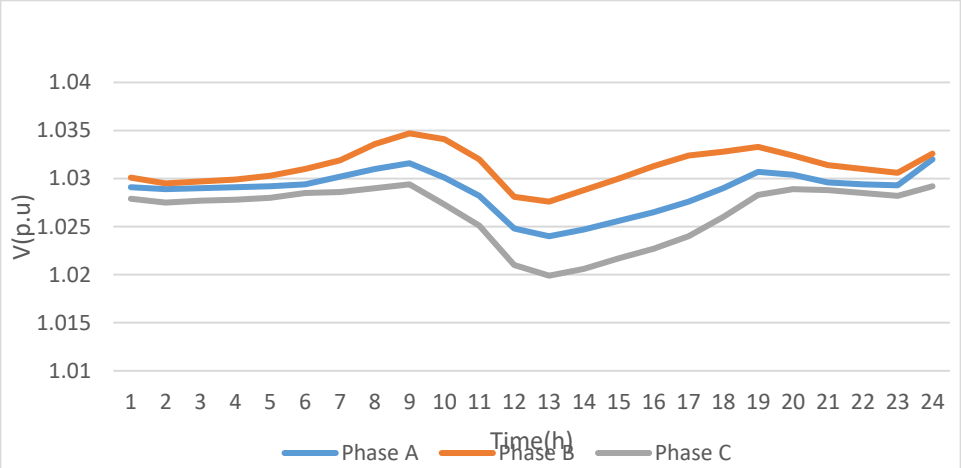

Figure 3.11: SOP-ES Voltage Profile at Bus 692

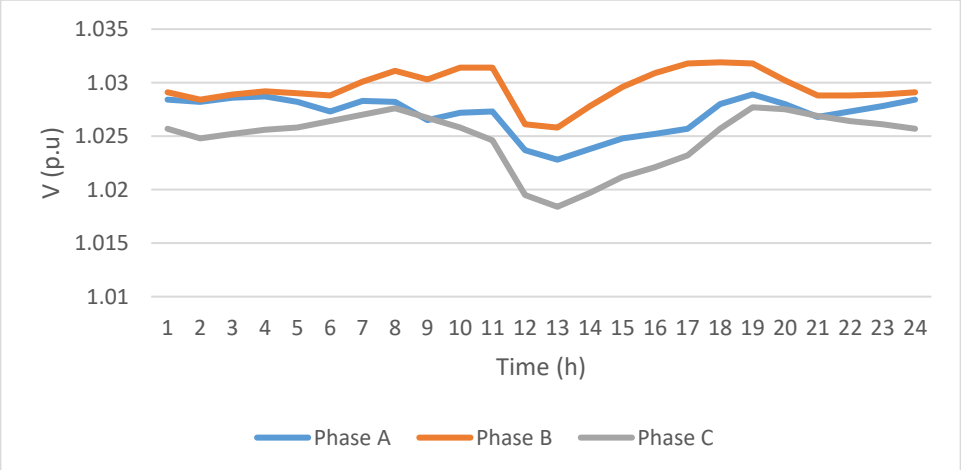

Figure 3.12: SOP Voltage Profile at Bus 680

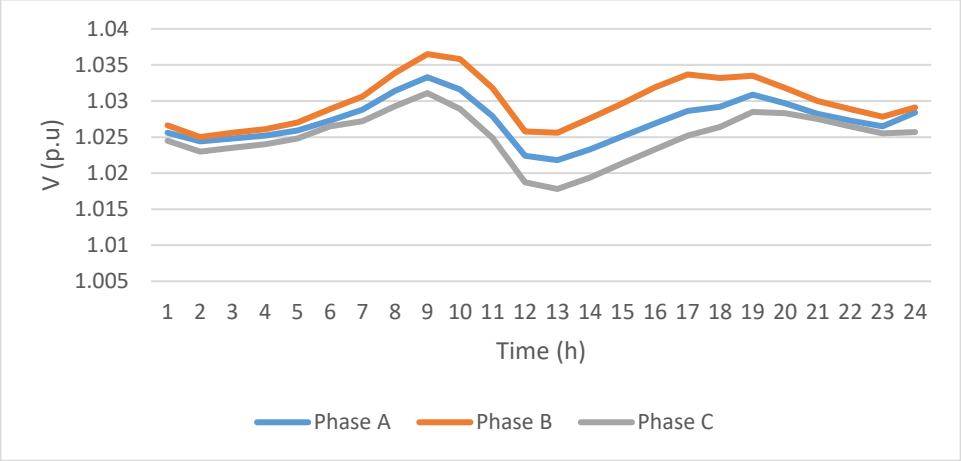

Figure 3.13: SOP-ES Voltage Profile at Bus 680

Figures 3.14 and 3.15 depict active power flows through SOP and SOP-ES respectively. Ideally, power exchange between terminal SOP1F and the other terminal SOP1S should be symmetrical (i.e., SOP1F + SOP1S = 0). However, minor asymmetries are observed during hours 2 and 3. These deviations may result from the selected objective weights or solver tolerances. Incorporating energy storage smoothens power exchange, satisfying the condition SOP1F + SOP1S + P_ES = 0 throughout, demonstrating the balancing capability of energy storage in SOP-ES configurations.

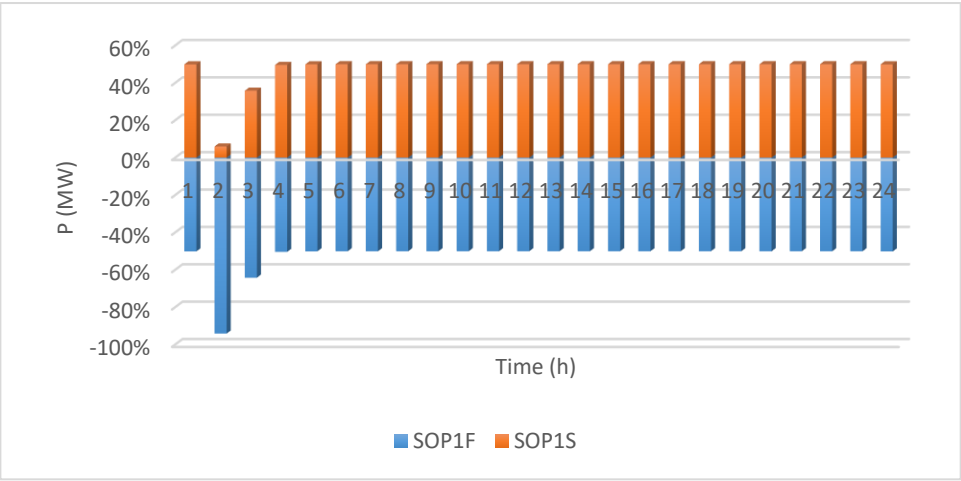

Figure 3.14: Active Power Transmission (SOP)

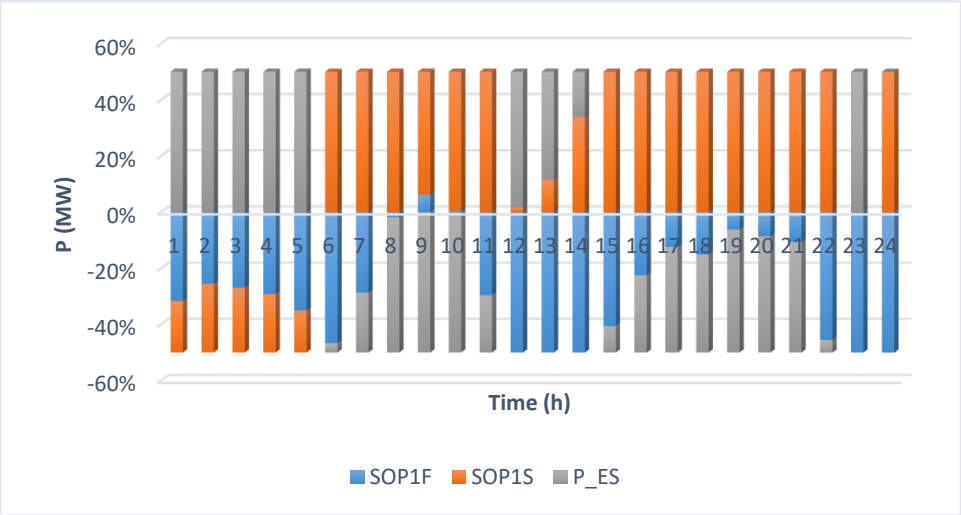

Figure 3.15: Active Power Transmission (SOP-ES)

It was observed that the SOP-only configuration exhibited asymmetric power transmission specifically during hours 2 and 3. This occurred despite the fact that these hours correspond to relatively low load demand, as confirmed by the load profile. The asymmetry suggests that factors other than load magnitude such as solver behavior under multi-objective weights or sensitivity to the voltage deviation constraint may influence SOP behavior in early low-load hours. In contrast, SOP-ES maintained symmetric operation throughout the entire time horizon.

Figures 3.16 to 3.19 compare the reactive power outputs of SOP1and SOP2 under the SOP and SOP-ES configurations over a 24-hour period. In both cases, the device alternates between reactive power absorption (negative values) and injection (positive values) to support voltage regulation. However, with SOP-ES, the magnitude of these swings is moderated, resulting in a narrower operating range compared to SOP alone. This moderation is due to the ability of the integrated energy storage to provide active power (P) support during high-load, low-voltage periods by discharging into the network, and to absorb (P) during low-load, high-voltage periods by charging from the network. In doing so, the ES

directly assists in voltage regulation, reducing the reliance on reactive power (Q) compensation alone. As a result, reactive power peaks are lower, transitions between absorption and injection are smoother, and reactive power support is more evenly distributed across the day, leading to a more balanced and efficient voltage regulation strategy.

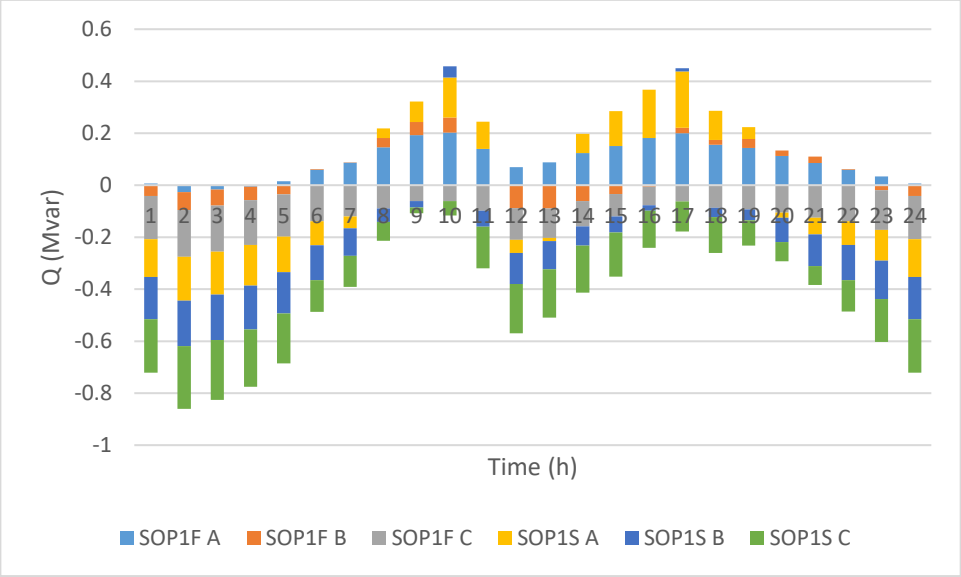

Figure 3.16: Reactive power of SOP1

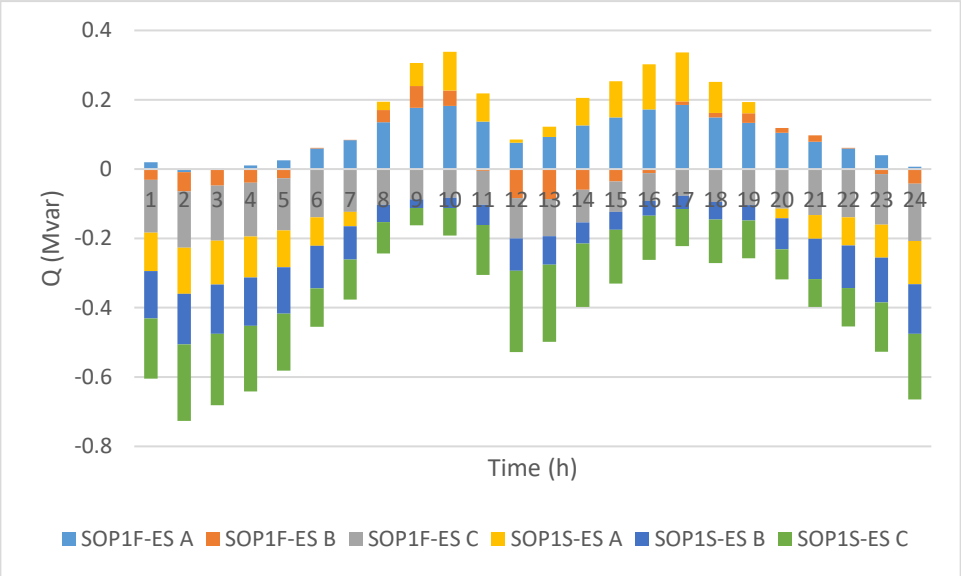

Figure 3.17: Reactive power of SOP1-ES

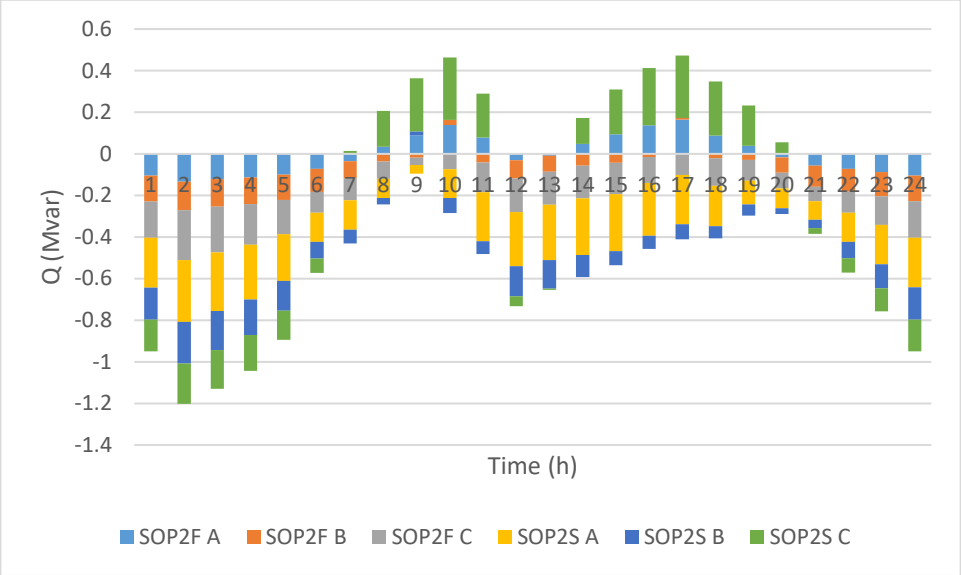

Figure 3.18: Reactive power of SOP2

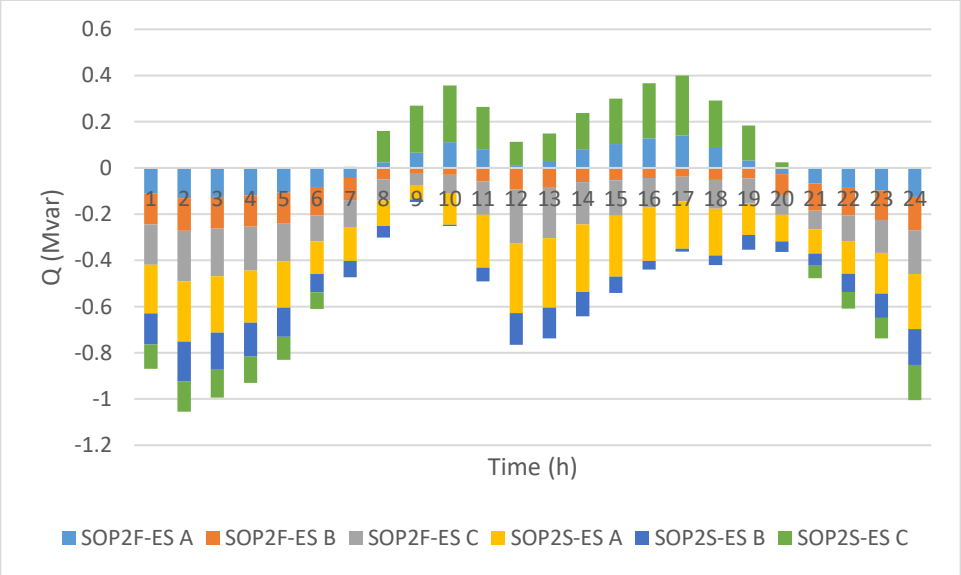

Figure 3.19: Reactive power of SOP2-ES

The Charging/Discharging profile and SoC of the ES units are shown in Figures. 3.20 to 3.23. Charging occurs during low-demand periods (hours 1–5) or excess PV periods (hours 12–14), while discharging occurs during peak demand (hours 8–11 and 16–21). Charging and discharging profiles for both ES units show coordinated operation across phases. The SoC curves confirm symmetric behavior, thus the three-phase coordination ensures that

phase balancing is maintained even during dynamic charging intervals.

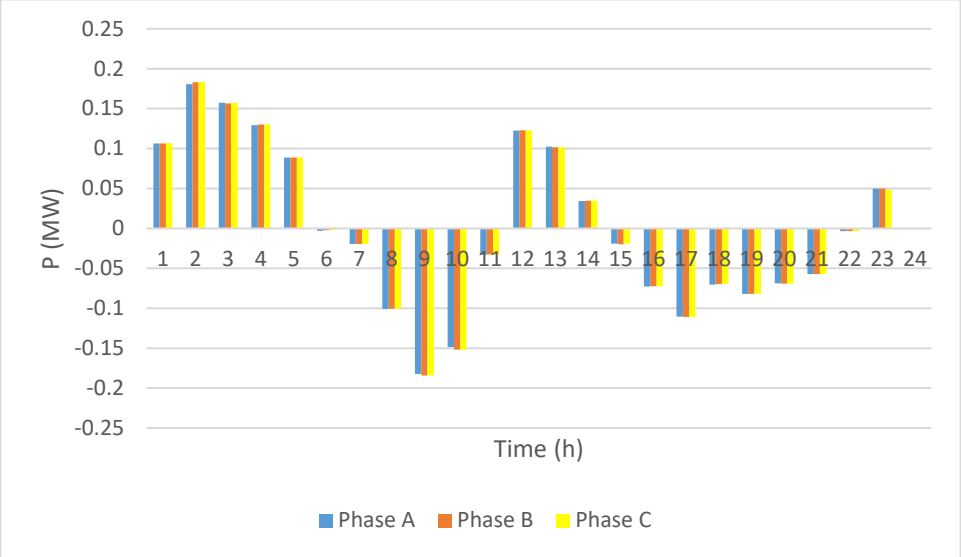

Figure 3.20: Charging Discharging Power of ES1

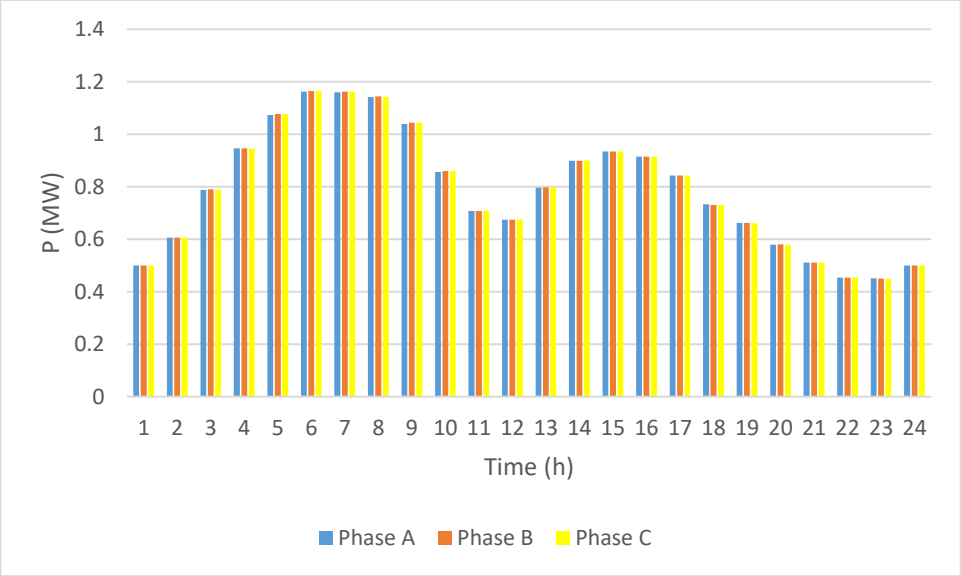

Figure 3.21: State of Charge (SoC) of ES1

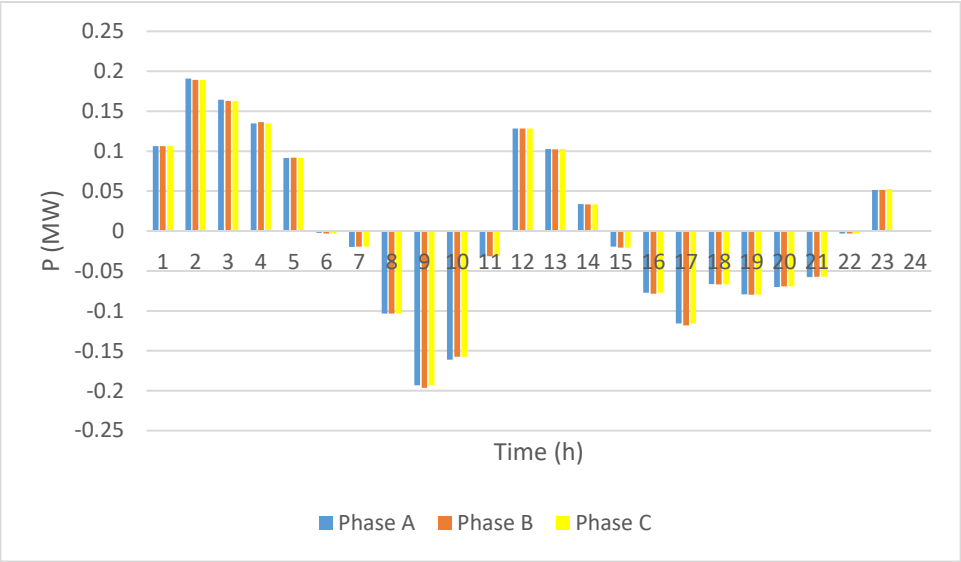

Figure 3.22: Charging Discharging Power of ES2

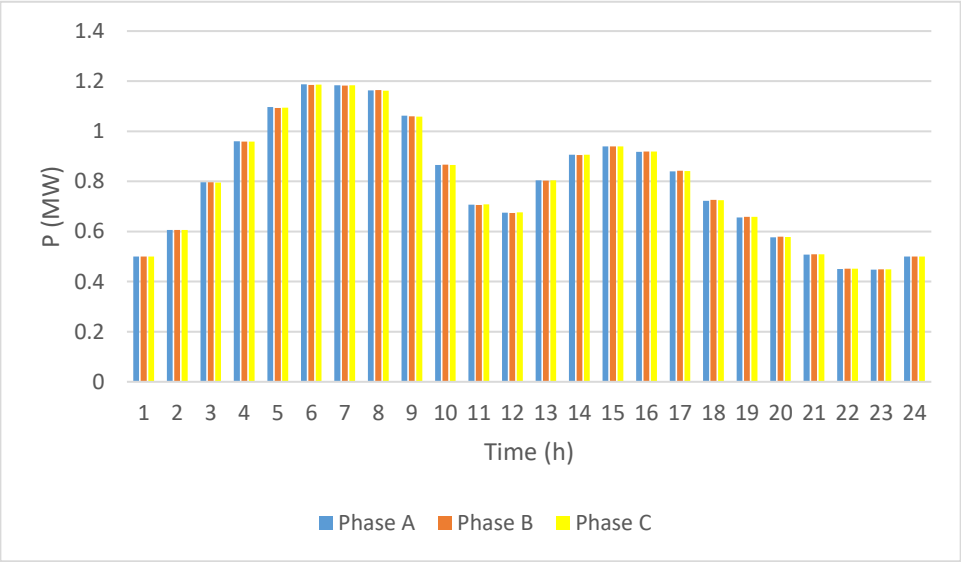

Figure 3.23: State of Charge (SoC) of ES2

3.4.2.2 Case Study: IEEE 123-Node Test Feeder

As shown in Figure 3.24, the IEEE 123-node test feeder [115] is used to test the scalability and further validate the effectiveness of SOP technologies. The rated voltage level is 4.16 kV, and the total active and reactive power loads on the system are 3,490 kW and 1,920 kvar, respectively.

To consider the impact of asymmetric access of DGs with high penetration on ADNs, ten single-phase PVs are integrated into the network with a constant power factor 1.0. the parameters are shown in Table 3.5.

Regulator tap settings are configured as follows: a three-phase regulator between buses 150 and 149 is set to $[r_a^t, r_b^t, r_c^t] = [1.05,1.0375,1.04375]$,; a single-phase regulator between buses 9 and 14 is set to $r_a^t = 0.99375$; a two-phase regulator between buses 25 and 26 is set to $[r_a^t, r_c^t] = [0,0.99375]$; and another two-phase regulator between buses 67 and 160 is set to $[r_a^t, r_b^t, r_c^t] = [1.5,1.00625,1.3125]$,following the same configurations used in the OpenDSS example case. Two sets of SOP are installed between nodes 54 and 93, and nodes 151 and 300, respectively.

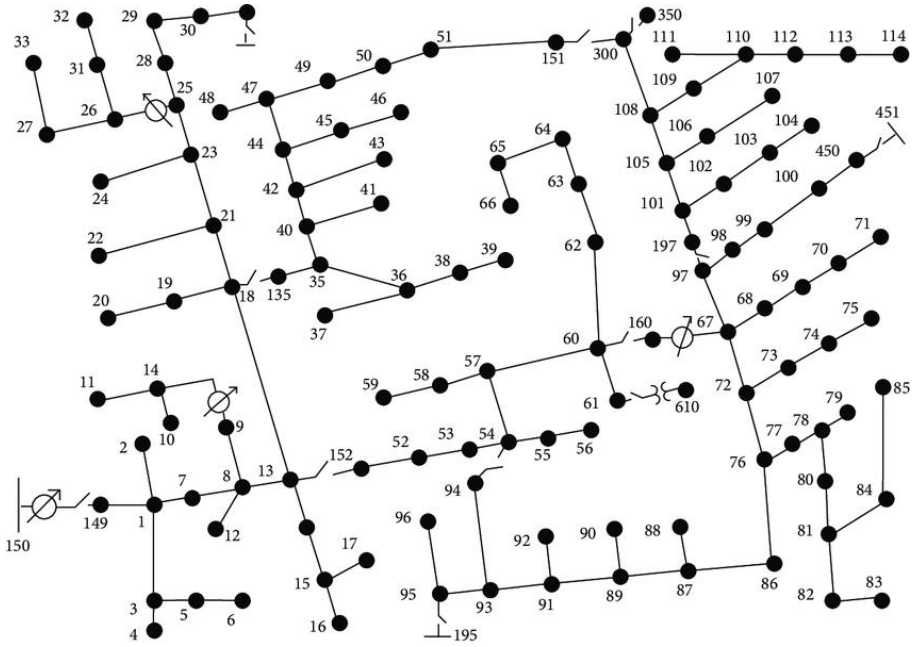

Figure 3.24: IEEE 123-bus distribution system

Table 3.5 Parameters of PVs

Location	27	41	75	85	87	93	96	107	110	450
Phase	A	C	C	C	B	B	B	B	A	C
Capacity (kVA)	200	200	300	150	300	150	300	150	150	200

The numerical results in Table 3.6 confirm the advantages of integrating energy storage with SOP. Compared to the baseline, both SOP and SOP-ES substantially reduce total feeder power losses over the 24-hour horizon (from 18.54 MW to approximately 15.5 MW), with SOP-ES achieving the lowest value (15.53 MW).

Table 3.6 Optimization Results of the IEEE 123-Node Test Feeder

Scenario	Power Loss (MW/24 h)	PV Active Power (MW/24 h)	Substation power (MW/24 h)
Baseline	18.54	9.95	63.2
SOP	15.58	10.04	62.05
SOP-ES	15.53	9.81	57.5

The hourly power loss trends in Figure 3.25 show a strong correlation with the system load profile. Losses rise during the morning demand ramp (hours 6–10), peaking near 0.69 MW under SOP and slightly lower (≈0.67 MW) under SOP-ES, before falling sharply around midday (hours 11–13) when PV generation compensates local demand. A second, smaller loss peak occurs in the late afternoon (hours 16–18), coinciding with the second load peak. The SOP-ES case consistently produces marginally lower losses during high-load periods, reflecting its ability to absorb surplus PV locally during midday and discharge during the evening peak, thereby reducing feeder current flows and associated I^2R losses. In low-load periods (e.g., early morning and late evening), the two scenarios show nearly identical loss values, indicating that storage's primary benefit occurs when demand and power transfer levels are high. This pattern aligns with the observed substation power flattening in SOP-ES as in Figure 3.26, where peak shaving reduces stress on feeder conductors and improves overall energy efficiency.

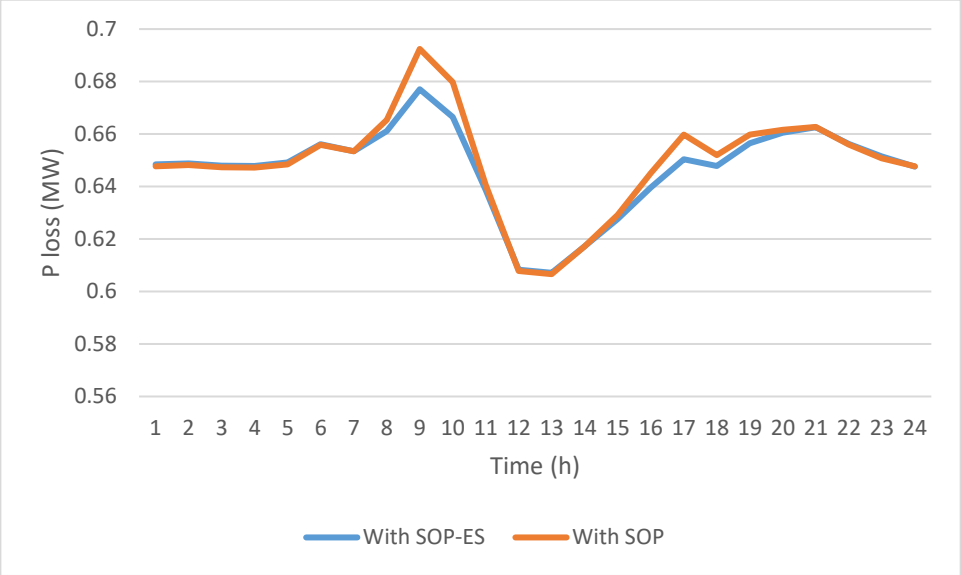

Figure 3.25: Hourly Power Loss Comparison for IEEE-123

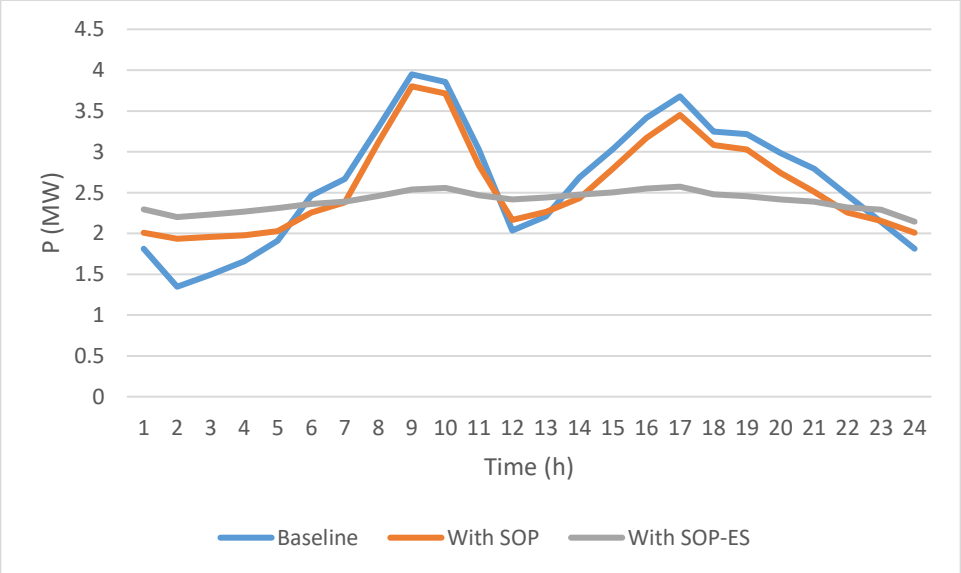

Figure 3.26: Substation Power Curve for IEEE-123

PV active power utilization increases slightly under SOP relative to baseline, while SOP-ES shows a marginal reduction compared to SOP (9.81 MW vs. 10.04 MW), consistent with its midday charging and afternoon discharging strategy observed in the PV utilization profile as in Figure 3.27, where PV utilization exhibits a time-shifting effect under SOP-ES. From 12–13 h, SOP-ES utilizes marginally more PV than SOP, reflecting storage charging during

the midday ramp, and during 14–17 h SOP shows higher PV utilization, while SOP-ES is lower because the battery discharges to support the afternoon load and maintain a flat substation profile, thereby reducing the need for instantaneous PV injection and helping manage feeder voltages. This coordinated charge–discharge strategy explains also the flatter substation curve with SOP-ES in Figure 3.26 and the slight reduction in PV utilization during the afternoon peak.

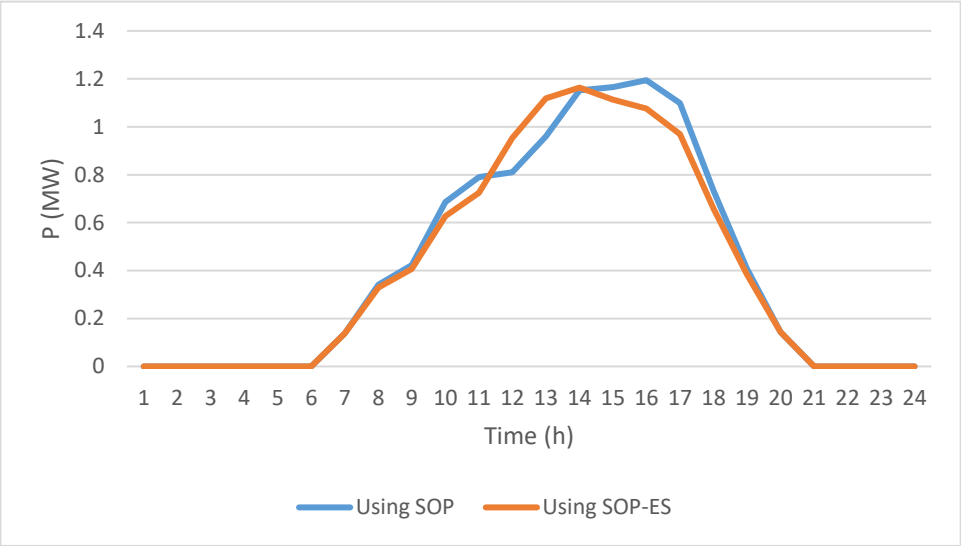

Figure 3.27: PV Utilization Profile for IEEE-123

From the voltage profiles of various buses (Figures 3.28-3.34 for Bus 35, Bus 48, Bus 114, Bus 104, and Bus 85), it can be observed that integrating ES with the SOP helps in reducing voltage fluctuations and achieving smoother voltage regulation throughout the day. This improvement is consistently seen at both near and remote buses, as well as for single-phase and three-phase points in the network. The ES charges during low-demand or high-generation periods and discharges during peak demand, effectively supporting the SOP in maintaining voltage levels. As established in the earlier section, the desired operating voltage range in this work is [0.97, 1.03] p.u., aligning with the interval thresholds applied in the voltage deviation control strategy, and all observed profiles under both SOP and SOP-ES remain within these limits.

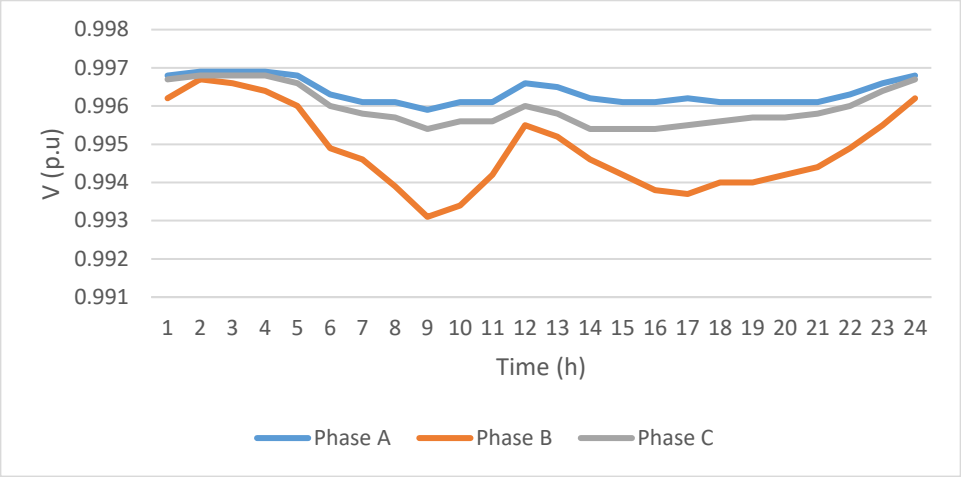

Figure 3.28: SOP Voltage Profile on Bus 35

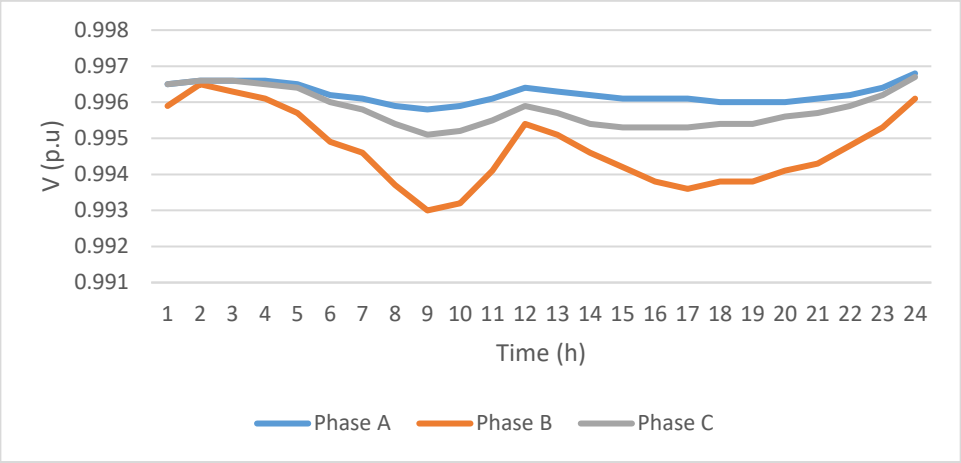

Figure 3.29: SOP-ES Voltage Profile on Bus 35

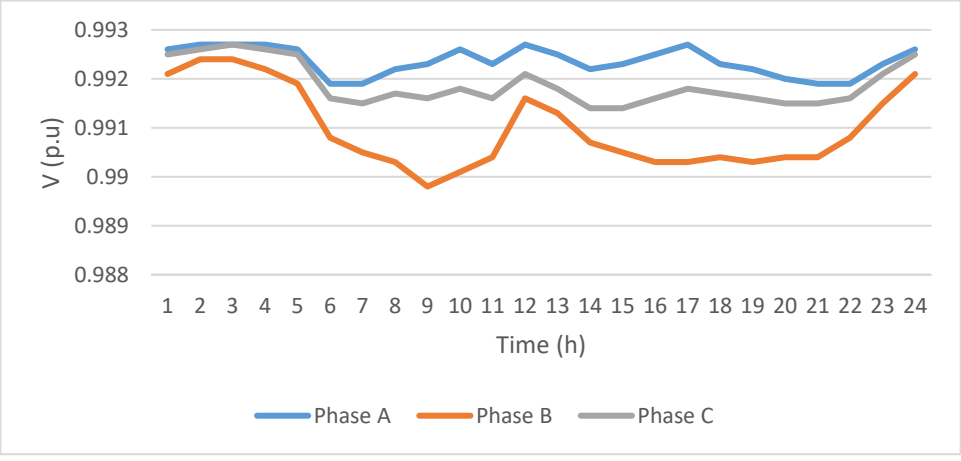

Figure 3.30: SOP Voltage Profile on Bus 48

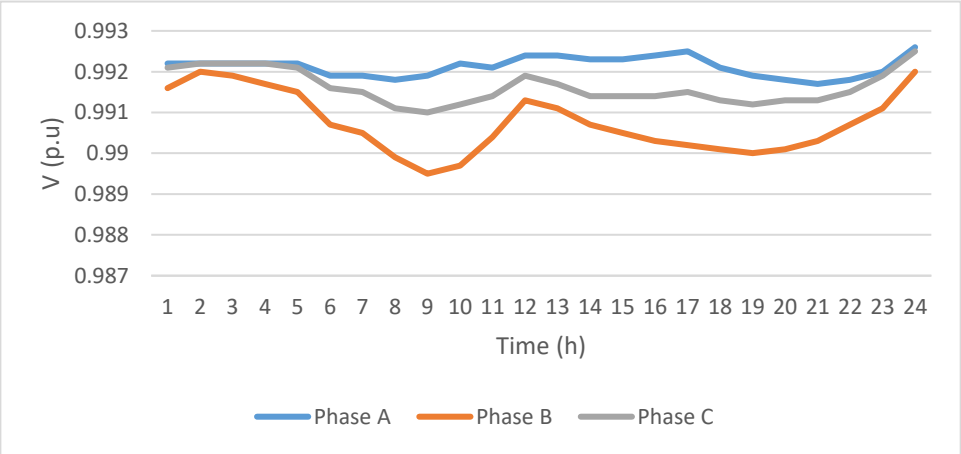

Figure 3.31: SOP-ES Voltage Profile on Bus 48

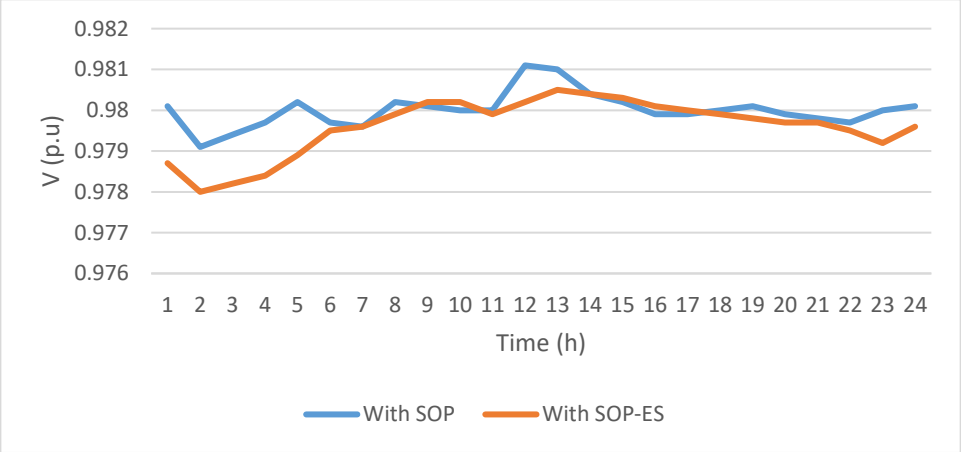

Figure 3.32: Voltage Profile Comparison on Bus 114

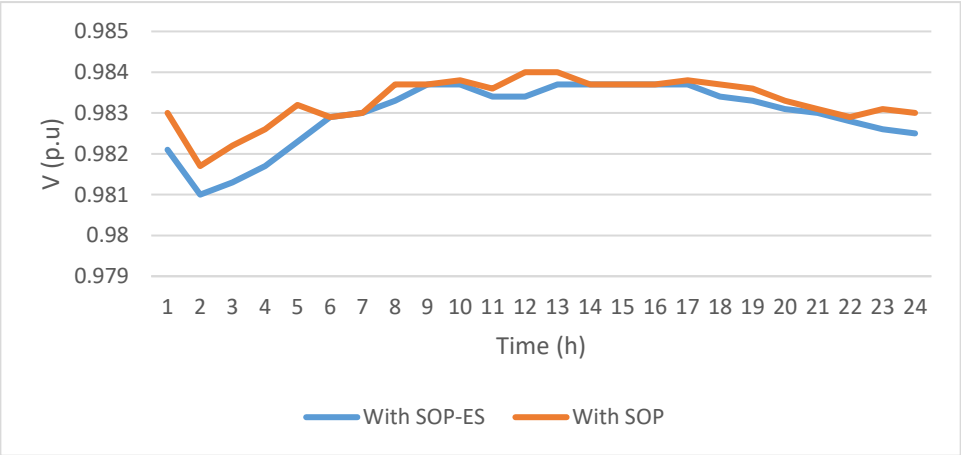

Figure 3.33: Voltage Profile Comparison on Bus 104

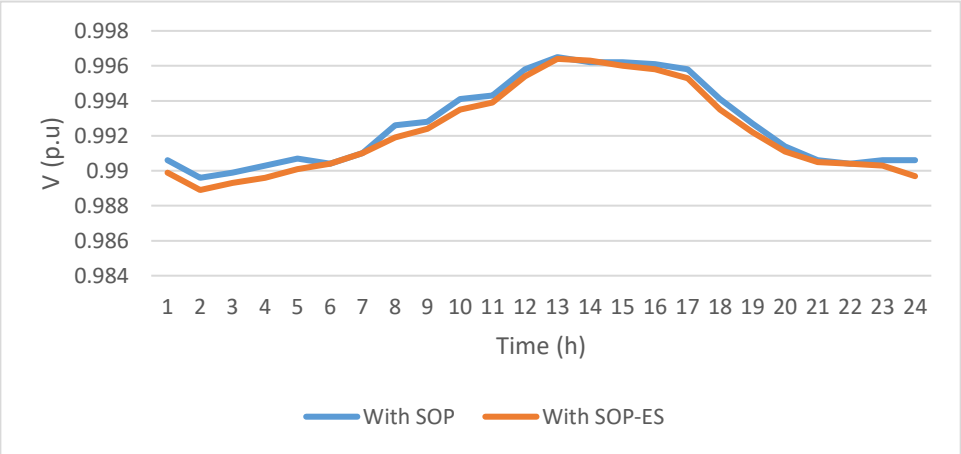

Figure 3.34: Voltage Profile Comparison on Bus 85

The active power exchanges through SOP1 and SOP2 as in Figures 3.35 to 3.38 reveal complementary behaviors between their terminals. Without storage, SOP1 predominantly transfers power from terminal (SOP1F) towards terminal (SOP1S), with magnitudes ranging between ±0.3 MW. Similarly, SOP2 exhibits higher levels of power transfer, with SOP2S consistently injecting up to 0.5 MW during midday, balanced by corresponding absorption at SOP2F. When energy storage is incorporated (SOP-ES), the profiles change substantially, the additional PES1 and PES2 components actively charge and discharge, altering the net flows at the SOP terminals. This enables SOP1 and SOP2 to mitigate imbalances and provide flexibility, as the storage absorbs excess power during high PV generation periods and discharges during evening peaks. Overall, the integration of ES with SOP under constant VRs enhances the devices' ability to balance feeder exchanges, reduce stress on the substation, and improve temporal coordination of active power across the network.

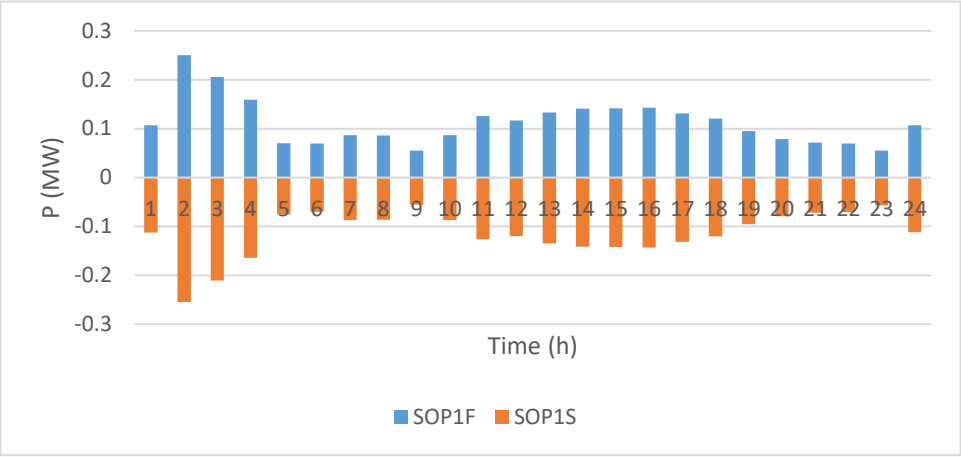

Figure 3.35: Active Power Transmission (SOP1)

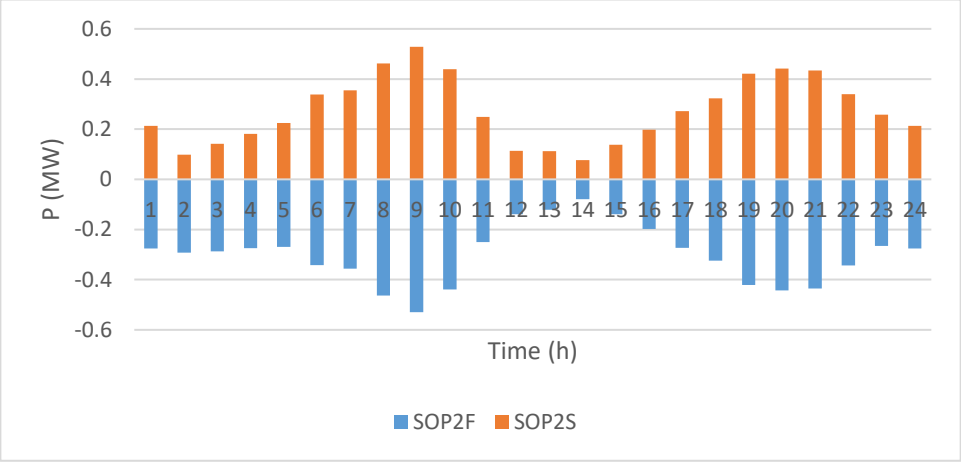

Figure 3.36: Active Power Transmission (SOP2)

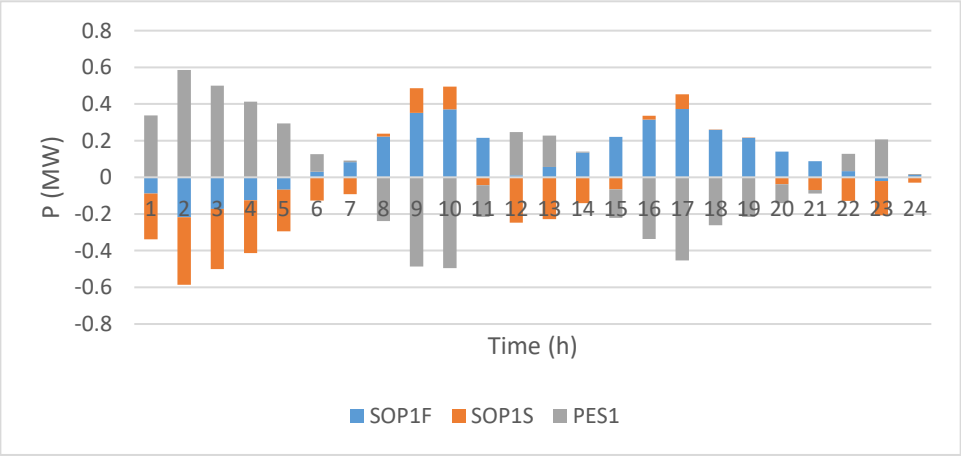

Figure 3.37: Active Power Transmission (SOP1-ES)

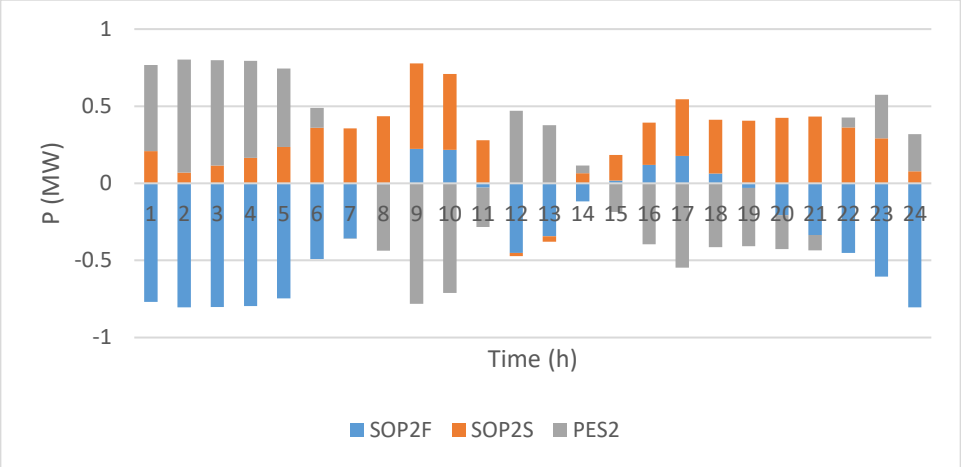

Figure 3.38: Active Power Transmission (SOP2-ES)

Figures 3.39 to 3.42 illustrate the reactive power outputs of SOP1 and SOP2 under the SOP and SOP-ES configurations across a 24-hour period. In both configurations, the devices alternate between reactive power absorption (negative values) and injection (positive values) to support voltage regulation. However, a clear difference emerges with SOP-ES: while the magnitude of reactive power injection peaks is reduced, the level of reactive power absorption is increased, particularly during midday and evening periods. This behavior arises because, when the ES charges during low-load, high-voltage hours, it draws active power (P) from the network, which tends to raise local voltages; as a result, the SOP-ES must absorb more reactive power (Q) to counteract this effect and maintain voltages within the desired [0.97, 1.03] p.u. range. Conversely, during high-load, low-voltage hours, ES discharging supplies active power support, thereby reducing the need for large reactive injections. Overall, compared to SOP alone, SOP-ES results in smoother reactive injection behavior but stronger reactive absorption, reflecting a coordinated strategy where active power support from ES complements and partially substitutes reactive power regulation.

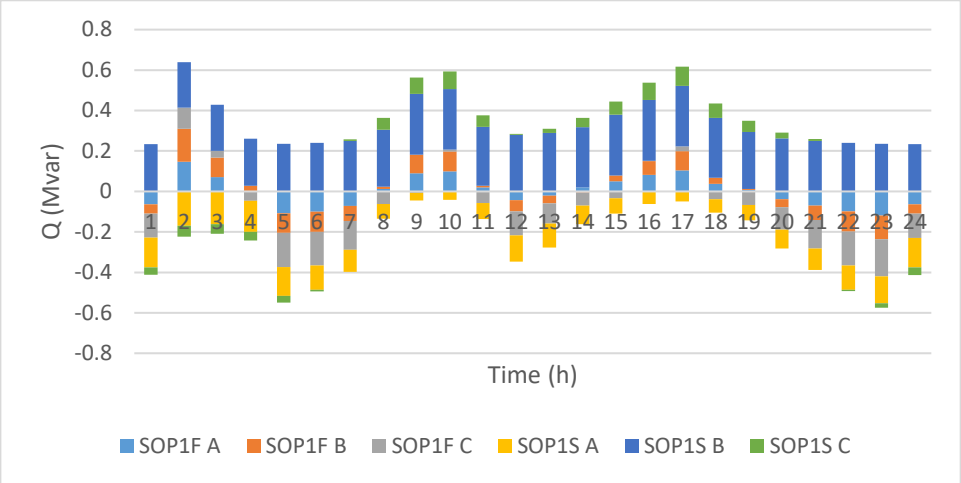

Figure 3.39: Reactive power of SOP1

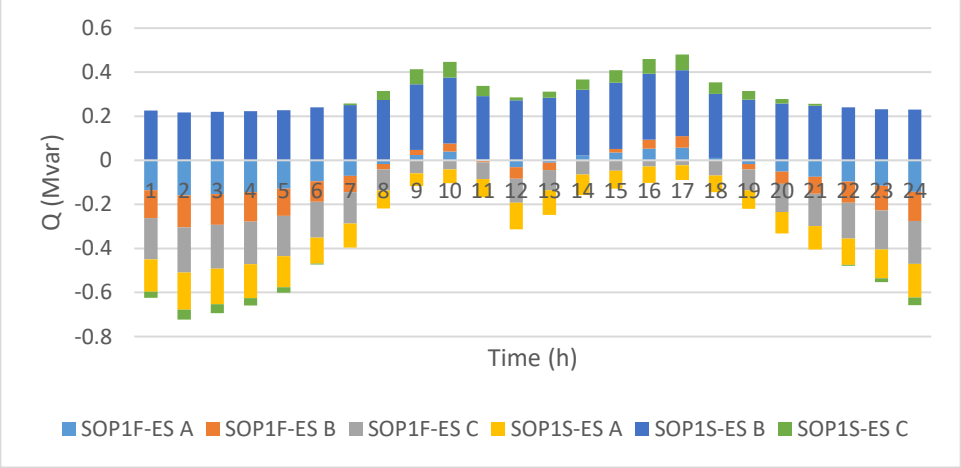

Figure 3.40: Reactive power of SOP1-ES

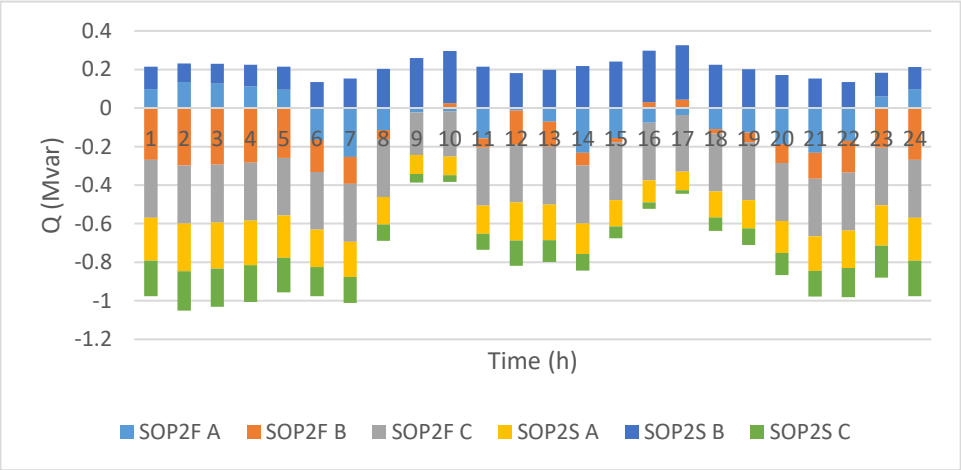

Figure 3.41: Reactive power of SOP2

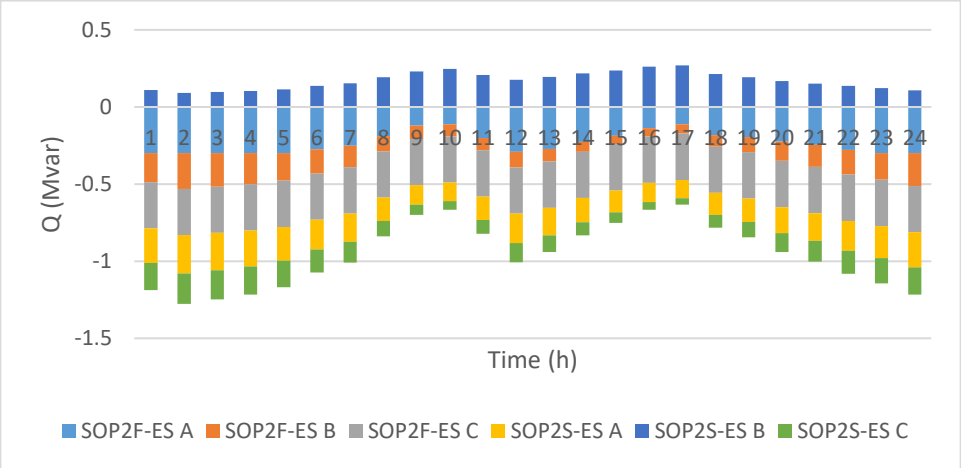

Figure 3.42: Reactive power of SOP2-ES

The charging and discharging patterns of ES1 and ES2 (Figures 3.43–3.46) explain the increased reactive power absorption observed in the SOP-ES case. During the early hours (1–6 h), when system demand is low, both ES units are charging, as seen in the positive charging power and rising SoC levels. This charging process increases active power demand at the local buses, which naturally raises voltage levels. To maintain voltages within the desired threshold range (0.97–1.03 p.u.), the SOP-ES configuration complements this charging with additional reactive power absorption. Conversely, during high-load periods (e.g., 9–11 h and 15–19 h), the ES units discharge active power into the system, directly supporting demand and mitigating voltage drops. This reduces the burden on reactive power support, resulting in more moderated Q injections compared to SOP alone. Thus, the interaction between active power exchange (through ES charging/discharging) and reactive power management leads to a coordinated strategy that enhances system voltage regulation and balances Q provision across the day.

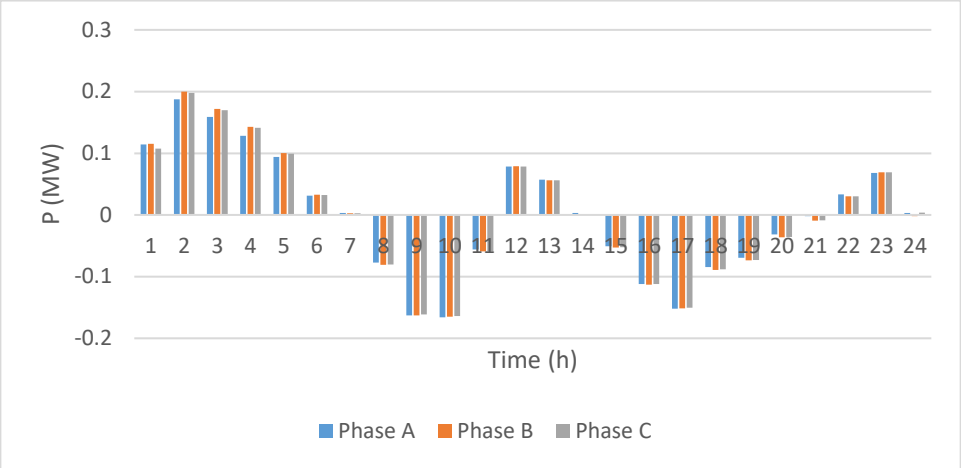

Figure 3.43: Charging Discharging Power of ES1with Fixed VRs

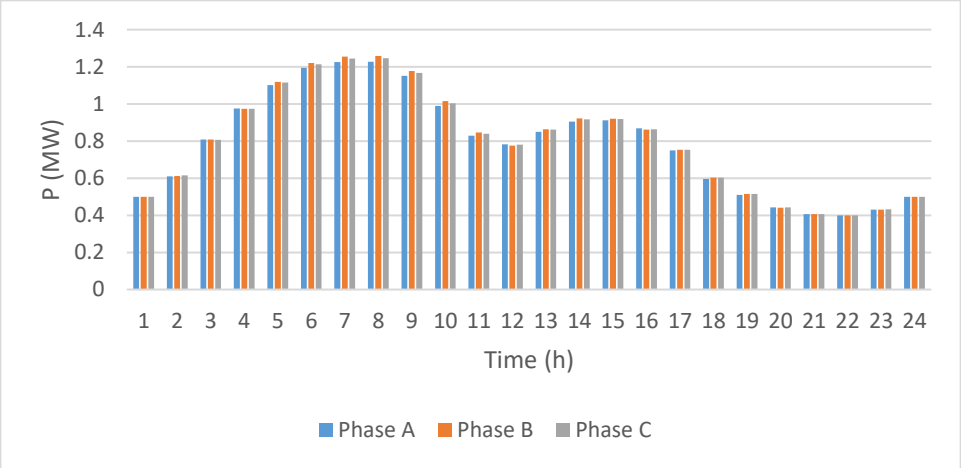

Figure 3.44: State of Charge (SoC) of ES1with Fixed VRs

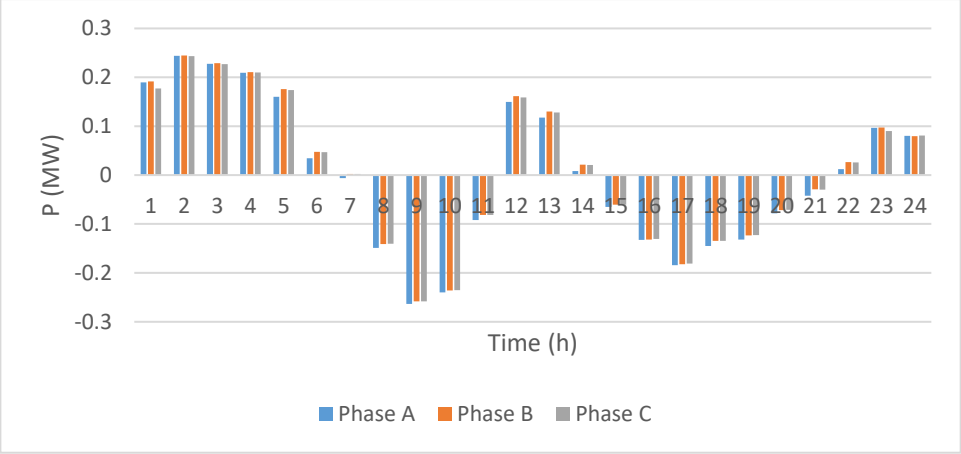

Figure 3.45: Charging Discharging Power of ES2 with Fixed VRs

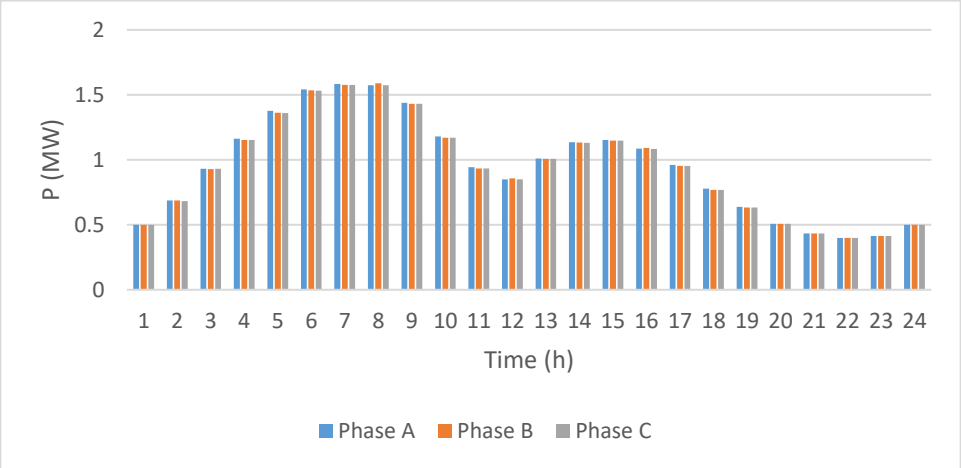

Figure 3.46: State of Charge (SoC) of ES2 with Fixed VRs

3.5 Conclusion

This chapter has demonstrated the benefits of integrating ES with SOP (SOP-ES) in the optimal operation of unbalanced active distribution networks. Through detailed case studies on the IEEE 13-bus and IEEE 123-bus systems, the analysis highlighted how the combined SOP-ES configuration achieves significant improvements over SOP alone. The results showed that SOP-ES not only reduces voltage fluctuations and maintains bus voltages within the desired control thresholds of 0.97–1.03 p.u., but also mitigates phase unbalances more effectively across the network. Furthermore, the coordinated active power support provided by ES during charging and discharging intervals was shown to reduce the reliance on reactive power compensation, leading to more balanced reactive power flows and smoother transitions between absorption and injection.

At the substation level, SOP-ES reduces peak demand and improves power exchange stability, while at the device level, the integration of ES enables SOPs to operate within narrower reactive power ranges, alleviating stress on network components. Overall, the findings confirm that SOP-ES offers a robust and flexible solution for enhancing voltage regulation, minimizing losses, and improving the operational resilience of distribution

systems under high penetration of renewable energy. This establishes SOP-ES as a more effective control strategy compared to SOP alone, paving the way for future adoption in real-world active distribution networks.

Chapter 4

Coordinated Operation of OLTC and Soft Open Point Integrated with Energy Storage Systems in Active Distribution Networks

Abstract

This chapter extends the optimization framework developed in Chapter 3 by introducing a coordinated control strategy between traditional voltage regulation devices specifically On-Load Tap Changers (OLTCs) and Voltage Regulators (VRs) and advanced Soft Open Points integrated with Energy Storage (SOP-ES). While Chapter 3 demonstrated the independent benefits of SOP-ES, this chapter addresses a critical gap in the literature by formulating a unified Semidefinite Programming (SDP) model that jointly optimizes OLTC tap settings, SOP active/reactive power flows, and battery charging/discharging schedules in unbalanced three-phase networks. Through comprehensive case studies on the IEEE 13-bus and IEEE 123-bus systems, the results demonstrate that coordinated operation significantly outperforms individual or partially coordinated schemes. Key findings include: a dramatic reduction in power losses (up to 86% vs. baseline), improved voltage profiles within tighter bounds, enhanced PV utilization, and critically a substantial reduction in OLTC switching operations, thereby extending the operational lifespan of this legacy infrastructure. The chapter validates that SOP-ES and OLTCs operate synergistically: SOP-ES provides fast, granular spatial and temporal control, while OLTCs deliver coarse network-wide voltage adjustment, together forming a robust, multi-timescale voltage regulation strategy for active

distribution networks.

4.1 Introduction

The transition toward active distribution networks with high renewable penetration, as addressed in earlier chapter, necessitates advanced voltage control strategies that coordinate new power-electronic devices with existing grid infrastructure. While Chapter 3 demonstrated the standalone benefits of Soft Open Points with Energy Storage (SOP-ES), this chapter focuses on their integrated operation with traditional On-Load Tap Changers (OLTCs).

Among the most effective methods for enhancing ADN performance are OLTCs and SOPs. OLTCs are traditionally deployed to manage voltage profiles by adjusting transformer tap ratios, thus controlling voltage magnitudes across the network [116]. Conversely, SOPs deliver granular spatial flexibility by enabling independent control of both active and reactive power exchange across interconnected feeders [98, 117]. When ESS are co-located with SOPs (forming SOP-ES systems), the capabilities are extended to include temporal shifting of energy, further stabilizing the network under dynamic load and generation conditions [118].

A growing volume of literature has explored these mechanisms separately. For instance, OLTC-based voltage regulation was effectively demonstrated in [41, 116, 119, 120], which highlighted its role in mitigating voltage rise in DER heavy networks. SOP-based coordination has been detailed in multiple works [6, 33, 121-123], where SOPs reduced power loss and enhanced power flow flexibility. A recent study investigated the coordinated operation of SOPs with OLTCs. References [4, 124] proposed a coordinated VVC method based on SOP to enhance the operational efficiency of ADNs. Recent advancements have extended this concept by integrating energy storage with SOP units, enabling both spatial

and temporal energy optimization [102, 104, 105, 118, 125]. Despite these advancements, most of studies have either addressed OLTC–SOP coordination without considering energy storage or treated SOP and ESS as independent components.

The deployment of OLTCs in modern ADNs with high DER penetration reveals significant operational limitations that necessitate coordinated control strategies. Primarily, OLTCs suffer from slow electromechanical response times and discrete tap adjustments, rendering them ineffective against rapid voltage fluctuations caused by intermittent solar generation and sudden load changes. Their reliance on single-point measurements at the substation creates visibility gaps, often missing localized overvoltage conditions at feeder ends where distributed PV is concentrated. Furthermore, frequent tap operations driven by renewable variability accelerate mechanical wear, shortening equipment lifespan and increasing maintenance costs. Perhaps most critically in unbalanced networks, OLTCs typically adjust all three phases simultaneously, which limits their ability to address phase-specific voltage issues arising from uneven single-phase PV and load connections. These challenges underscore the need to integrate OLTCs with faster, more granular power-electronic devices like SOP-ES to achieve effective voltage regulation while preserving the longevity of legacy grid infrastructure.

This chapter addresses these gaps by introducing an optimization framework for the coordinated operation of OLTC and SOP-ES systems in unbalanced ADNs. To the best of our knowledge, this is the first study that systematically integrates OLTC devices with SOP-ES using a symmetrical SDP formulation. The model jointly optimizes OLTC tap settings, SOP power exchange (active and reactive), and ESS charging/discharging schedules over a 24-hour scheduling horizon. The use of SDP relaxation ensures convexity and guarantees global optimality within practical computation times, and the problem becomes mixed integer semidefinite programming (MISDP) solved using the MOSEK solver.

While Chapter 3 demonstrated the independent benefits of SOP-ES deployment, this chapter extends the framework by incorporating OLTC coordination into the model. This enables a more comprehensive control scheme that unifies spatial (SOP), temporal (ESS), and voltage-level (OLTC) optimization. Additionally, the co-location of ESS with SOP terminals smooths net injections and damps short-term fluctuations, thereby reducing OLTC switching frequency, and improve overall power quality especially under high PV penetration and during low-load periods.

Case studies on the IEEE 13 and 123-bus system validate the effectiveness of the proposed coordination scheme. Compared to OLTC-only, SOP-only, and SOP-ES-only configurations, the joint optimization of OLTC and SOP-ES results in superior performance in terms of power loss reduction, voltage deviation minimization, and improved PV utilization. Additionally, results show that energy storage buffers SOP operations, reducing the OLTC switching frequency and mitigating SOP asymmetry in low-load periods.

4.2 Optimization Model and Mathematical Formulation

The optimization model determines the coordinated operation of OLTC and SOP-ES systems across a 24-hour horizon. The objective is to minimize network power losses while maintaining voltages within statutory limits and mitigating unbalance. In contrast to Chapter 1, where OLTC taps were fixed, here tap ratios are optimization variables within their discrete bounds. This allows simultaneous determination of OLTC tap positions, SOP power flows, and battery charging/discharging profiles.

Mathematical formulation extends the SDP-based OPF from Chapter 3 by incorporating OLTC decision variables. The optimization model determines the coordinated operation of OLTC and SOP-ES systems across a 24-hour horizon. The same multi-objective function from Chapter 3 is employed, minimizing a weighted sum of power losses, voltage unbalance,

and voltage deviation while maintaining all operational constraints.

4.2.1 Voltage Regulator and On-Load Tap Changer Modeling

Voltage regulators, particularly OLTC, are among the most widely used control devices in distribution networks. By dynamically adjusting the transformer turns ratio, they regulate downstream voltages and maintain network stability under varying operating conditions. To incorporate these devices within the convex SDP–based OPF framework, their mathematical modeling must be carefully reformulated in terms of lifted variables and linear matrix inequalities (LMIs). This section presents the modeling framework for voltage regulators and OLTCs suitable for unbalanced multiphase active distribution networks.

4.2.2 Basic Voltage Regulator Model

The operation of a voltage regulator is characterized by the relationship between primary and secondary voltages through adjustable tap positions. For a three-phase regulator, the tap ratio vector is defined as:

$$\text{ratio } = [r_a, r_b, r_c]^T \tag{4.1}$$

with each phase ratio given by:

$$r_\phi = 1 + 0.00625 \times \text{Tap}_\phi \quad \forall \in \{a, b, c\}. \tag{4.2}$$

The tap position Tap_ϕ is a discrete integer variable, typically ranging from [−16,+16], corresponding to a voltage regulation range of approximately ±10% in increments of 0.625%. In Chapter 3, the OLTC was fixed to [1.05, 1.0375, 1.04375] following the OpenDSS IEEE 13-bus case, but here the tap ratios are decision variables within their bounds.

The phase-specific voltage transformation can be expressed as:

$$\mathbf{V}_{\text{sec}}^{T} = [V_{\text{sec}}^{a}, V_{\text{sec}}^{b}, V_{\text{sec}}^{c}]^{T} = \left[r_a V_{\text{pri}}^{a}, r_b V_{\text{pri}}^{b}, r_c V_{\text{pri}}^{c}\right]^{T}. \tag{4.3}$$

This formulation allows independent regulation of each phase, which is particularly advantageous in unbalanced distribution systems.

4.2.3 SDP Formulation for Voltage Regulators

In SDP-based OPF, the lifted voltage matrices are used to convexify the problem. The primary $\mathbf{u}_{\text{pri}}$ and secondary $\mathbf{u}_{\text{sec}}$ voltages matrix are defined as:

$$\mathbf{u}_{\text{pri}} = \mathbf{V}_{\text{pri}}\mathbf{V}_{\text{pri}}^{H} \quad , \quad \mathbf{u}_{\text{sec}} = \mathbf{V}_{\text{sec}}\mathbf{V}_{\text{sec}}^{H}$$

Substituting the tap ratios gives:

$$\mathbf{u}_{\text{sec}} = \begin{bmatrix} r_a^2 V_i^a V_i^{aH} & r_a r_b V_i^a V_i^{bH} & r_a r_c V_i^a V_i^{cH} \\ r_b r_a V_i^b V_i^{aH} & r_b^2 V_i^b V_i^{bH} & r_b r_c V_i^b V_i^{cH} \\ r_c r_a V_i^c V_i^{aH} & r_c r_b V_i^c V_i^{bH} & r_c^2 V_i^c V_i^{cH} \end{bmatrix} \tag{4.4}$$

A more compact representation is obtained by defining the transformation matrix:

$$\mathbf{A}_i = [r_a, r_b, r_c]^T [r_a, r_b, r_c] = \begin{bmatrix} r_a^2 & r_a r_b & r_a r_c \\ r_b r_a & r_b^2 & r_b r_c \\ r_c r_a & r_c r_b & r_c^2 \end{bmatrix} \tag{4.5}$$

so that:

$$\mathbf{u}_{\text{sec}} = \mathbf{A}_i \odot \mathbf{u}_{pri}, \tag{4.6}$$

Where $\odot$ denotes the Hadamard (element-wise) product. This formulation preserves convexity while embedding the regulator transformation into the SDP relaxation.

4.2.4 Integration with the Branch Flow Model

When integrated into the branch flow model, the regulator is treated as a special branch with voltage transformation capability. The voltage relationship along branch *ij* containing a regulator is expressed as:

$$u_j = u_{sec}^{\phi_{ij}} - \left(S_{ij} z_{ij}^H + z_{ij} S_{ij}^H\right) + z_{ij} l_{ij} z_{ij}^H \tag{4.7}$$

where $u_{sec}^{\phi_{ij}}$ denotes the secondary voltage matrix corresponding to the phases of branch *ij*, S_{ij} is the power flow matrix, z_{ij} is the branch impedance, and l_{ij} is the current outer-product matrix. The convex relaxation for branches with regulators is enforced via the LMI:

$$\begin{bmatrix} u_{sec}^{\phi_{ij}} & S_{ij} \\ S_{ij}^H & l_{ij} \end{bmatrix} \geq 0 \tag{4.8}$$

4.2.5 Symmetrical Components Transformation

For improved numerical stability and reduced problem size, the regulator model can be expressed in symmetrical components. Using the Clarke transformation matrix A, the

secondary voltage Gram matrix in symmetrical components is given by:

$$Av_{sec,t}^{012}A^H = A\left(v_{i,t}^{012} - \left(S_{reg,t}^{012}z_{reg}^{012^H} + S_{reg,t}^{012^H}z_{reg}^{012}\right) + z_{reg}^{012}l_{reg,t}^{012}z_{reg}^{012^H}\right)A^H.ratio \quad (4.9)$$

This transformation allows the optimization to be solved in the symmetrical domain, which can simplify computation while still ensuring accurate modeling of unbalanced systems.

4.2.6 Operational Constraints

The regulator must satisfy practical operating limits and network constraints:

- Tap position bounds

$$\text{Tap}_{\phi,min} \leq \text{Tap}_{\phi} \leq \text{Tap}_{\phi,max} \quad \forall\phi \in \{a,b,c\} \quad (4.10)$$

- Voltage limits

$$V_{min} \leq \left|V_{\text{sec}}^{\phi}\right| \leq V_{max}, \quad \forall\phi \in \{a,b,c\} \quad (4.11)$$

The regulator must satisfy Kirchhoff's current and power balance laws, consistent with other network branches.

4.2.7 Discrete vs. Continuous Modeling

In practice, tap positions are discrete, making the OLTC problem inherently mixed integer. However, in convex SDP formulations, continuous relaxation of tap ratios is often adopted:

$$r_\phi \in [0.9,1.1], \quad \forall \phi \in \{a,b,c\} \tag{4.12}$$

which greatly enhances tractability. For operational decision-making, the resulting continuous tap ratios can be post-processed to select the nearest feasible discrete tap settings. This trade-off ensures that planning and optimization studies remain computationally efficient while still capturing realistic regulator behavior.

4.3 Simulations and Analysis

4.3.1 Comparative Scenarios

To evaluate the effectiveness of the proposed coordinated control scheme, six scenarios are considered in both the IEEE 13-bus and IEEE 123-bus test feeders. The first three scenarios are based on the assumption of fixed OLTC tap ratios, consistent with the IEEE 13-bus OpenDSS standard configuration $[r_a^t, r_b^t, r_c^t] = [1.05,1.0375,1.04375]$. In the first scenario, only the OLTC is used to regulate voltages, providing a benchmark case without SOP devices. The second scenario incorporates SOP devices while maintaining the OLTC at its fixed ratios, enabling spatial flexibility through feeder interconnection. The third scenario extends this configuration by integrating energy storage with SOP (SOP-ES), also under fixed OLTC taps. These three scenarios essentially replicate the modeling framework established in Chapter 3.

The remaining three scenarios allow the OLTC to operate as a decision variable within its tap bounds. In the fourth scenario, OLTC control alone is optimized, capturing its full flexibility. The fifth scenario combines OLTC with SOP devices, highlighting the complementary role of spatial and voltage-level regulation. Finally, the sixth scenario implements the full proposed coordination of OLTC with SOP-ES, simultaneously leveraging OLTC tap adjustment, SOP active/reactive power control, and energy storage

scheduling. Each scenario is simulated over a 24-hour horizon to capture the interaction between load variation and photovoltaic generation.

4.3.2 Case Study Setup

The case studies are carried out on the IEEE 13-bus and IEEE 123-bus unbalanced distribution feeders, which are widely adopted as benchmarks for ADN optimization research. In both systems, SOP-ES devices are placed strategically at network tie points: between buses 634–675 and 675–680 for the IEEE 13-bus feeder, and buses 300-151 and 54-93 for the IEEE 123-bus feeder. Time-series profiles of load demand and photovoltaic generation are applied across the 24-hour horizon to reflect realistic daily operating conditions under high renewable penetration. The OLTC is located between bus RG60 and bus 650 in the IEEE 13-bus feeder, while the IEEE 123-bus model includes the regulator placements defined in its OpenDSS test case.

All optimization problems are formulated in MATLAB using YALMIP and solved with the MOSEK solver, employing the SDP relaxation framework described in Section 4.2. The comparative scenarios provide a systematic basis to quantify the incremental benefits of SOP, SOP-ES, OLTC, and their coordination.

4.3.2.1 Case Study Results: IEEE 13-Bus System

The IEEE 13-bus test feeder was used to evaluate the six comparative scenarios introduced in Sub-section 4.3.1. Tables 4.1 and 4.2 summarize the performance in terms of total power loss, PV active power utilization, and substation power exchange over the 24-hour horizon.

Table 4.1: Results with Fixed OLTC Tap Ratios

Scenario (Fixed OLTC)	Power Loss (MW/24 h)	PV Active Power (MW/24 h)	Substation power (MW/24 h)
OLTC	7.01	13.17	44.268
OLTC + SOP	1.01	17.18	34.62
OLTC + SOP-ES	0.95	17.21	34.17

Table 4.2: Results with Variable OLTC Tap Ratios

Scenario (Variable OLTC)	Power Loss (MW/24 h)	PV Active Power (MW/24 h)	Substation power (MW/24 h)
OLTC	2.38	13.62	39.19
OLTC + SOP	0.52	18.96	32
OLTC + SOP-ES	0.46	19. 1	31.8

The results highlight the incremental benefits of SOP and SOP-ES integration, as well as the importance of OLTC flexibility as shown in Figure 4.1. Under fixed tap ratios, the only OLTC scenario suffers from significant losses (7.01 MW/24h) and limited PV utilization (13.17 MW/24h). The introduction of SOP devices reduces losses by nearly 86% and increases PV output by about 23%. Further integration of energy storage (SOP-ES) yields modest but consistent improvements, with losses reduced to 0.95 MW/24h and substation demand lowered to 34.17 MW/24h.

When the OLTC is treated as a decision variable, substantial improvements are observed even without SOP, with power loss decreasing from 7.01 MW/24h to 2.38 MW/24h compared to the fixed-tap case. However, the greatest benefits arise from joint optimization of OLTC with SOP-ES, which reduces losses to 0.46 MW/24h, enhances PV utilization to 19.1 MW/24h, and minimizes substation demand to 31.8 MW/24h.

These findings confirm that the proposed coordinated OLTC + SOP-ES model outperforms

all other configurations, validating its role as the most effective strategy for ADN operation under high PV penetration.

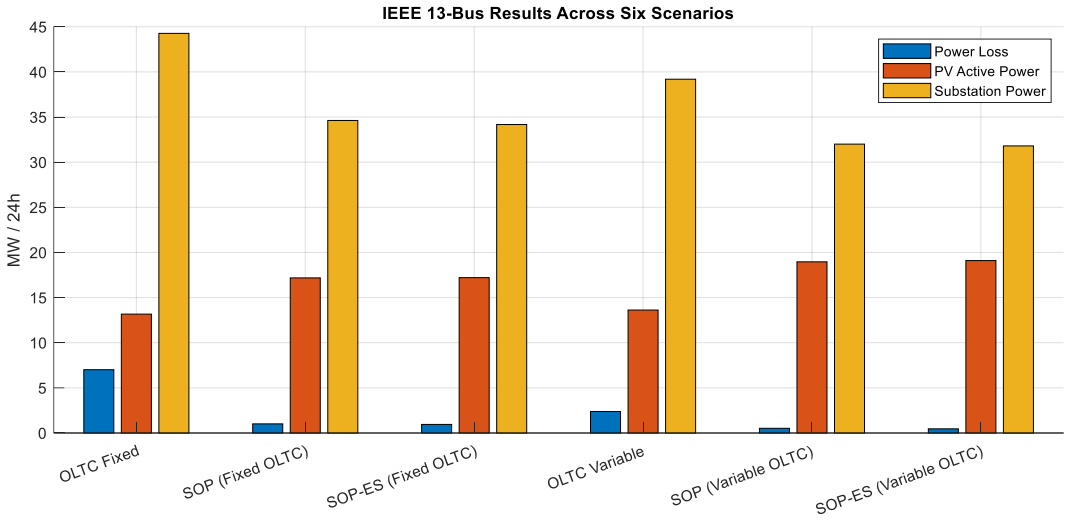

Figure 4.1: All Scenarios Results

Power losses. Figure 4.2 shows that allowing the OLTC to vary already lowers losses compared to the fixed-tap scenario, but the profile still exhibits a strong morning peak (≈h9–h10) under Only OLTC. Introducing OLTC+SOP substantially suppresses that peak and keeps losses low for most hours. The full OLTC+SOP-ES coordination provides the flattest curve and the lowest loss levels across the day, consistent with the 24-h totals (2.38 → 0.52 → 0.46 MW/24 h for Only-OLTC, OLTC+SOP, and OLTC+SOP-ES, respectively).

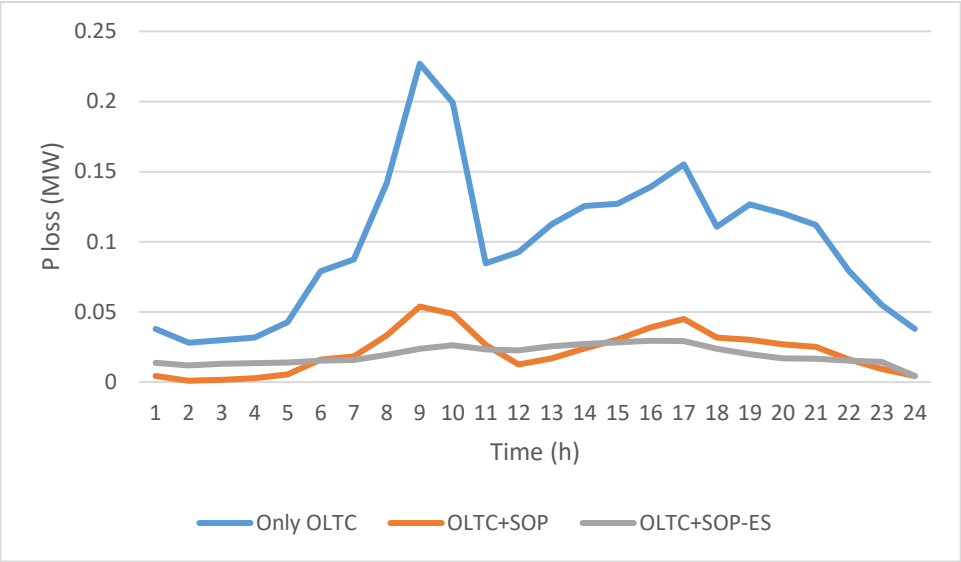

Figure 4.2: Hourly Power Loss Comparison with variable OLTC Tap ratios

PV utilization. Figure 4.3 highlights that OLTC+SOP and OLTC+SOP-ES both release more PV export at mid-day compared with Only OLTC. The SOP enables spatial re-dispatch between feeders, while the ES buffers short-term PV variability and local voltage constraints, yielding the highest PV throughput overall (13.62 → 18.96 → 19.10 MW/24 h).

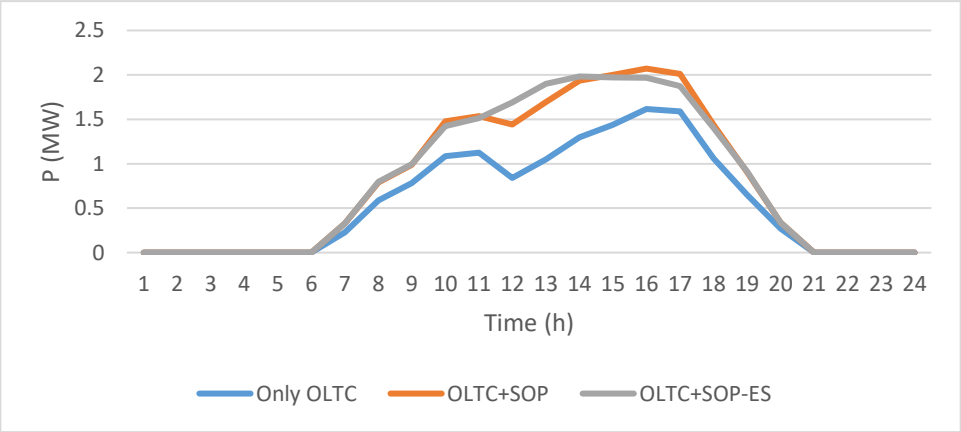

Figure 4.3: PV Utilization Profile with variable OLTC Tap ratios

Substation power. As shown in Figure 4.4, Only OLTC exhibits pronounced peaks (≈h8–

h10 and late afternoon). With OLTC+SOP, those peaks are reduced as the SOP redistributes feeder flows. OLTC+SOP-ES further flattens the profile, ES charges around PV peaks and discharges in shoulder periods leading to the lowest daily substation energy (39.19 → 32.00 → 31.80 MW/24 h) and a obviously smoother trajectory.

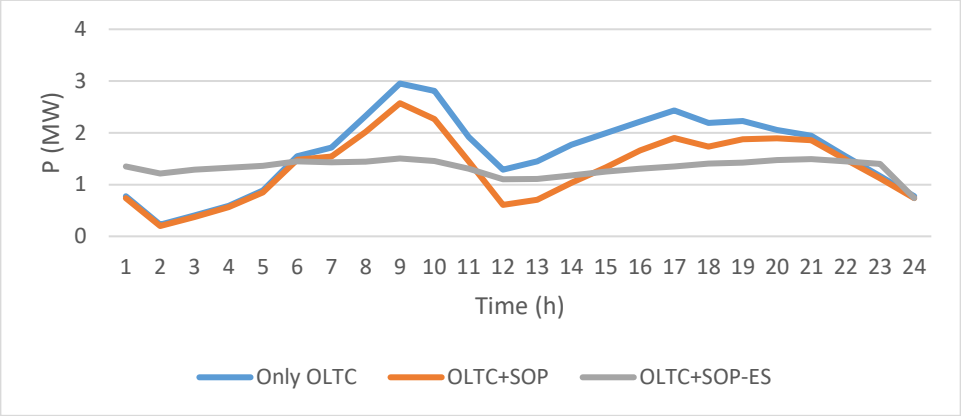

Figure 4.4: Substation Power Curve with variable OLTC Tap ratios

Key Observation:

Moving from fixed to variable OLTC improves technical performance, but the coordinated OLTC+SOP-ES strategy is consistently best on an hourly and daily basis: it suppresses loss spikes, maximizes PV utilization, and smoother substation demand. This confirms the value of combining voltage-level regulation (OLTC) with spatial flexibility (SOP) and temporal flexibility (ES) in a single optimization framework.

The optimal tap movements. The tap position under Only OLTC as in Figure 4.5 shows multiple adjustments during the 24-hour operation. Initially, the regulator is set at a low position of –2 p.u., reflecting the need to counteract over-voltage conditions during low-load hours. As demand increases, the OLTC adjusts upwards, reaching +1 and later stabilizing at +2. Toward the end of the horizon, the tap returns to –2, highlighting the regulator's role as the single voltage balancing mechanism. However, this frequent shifting indicates higher mechanical stress on the OLTC and limited adaptability under high PV penetration.

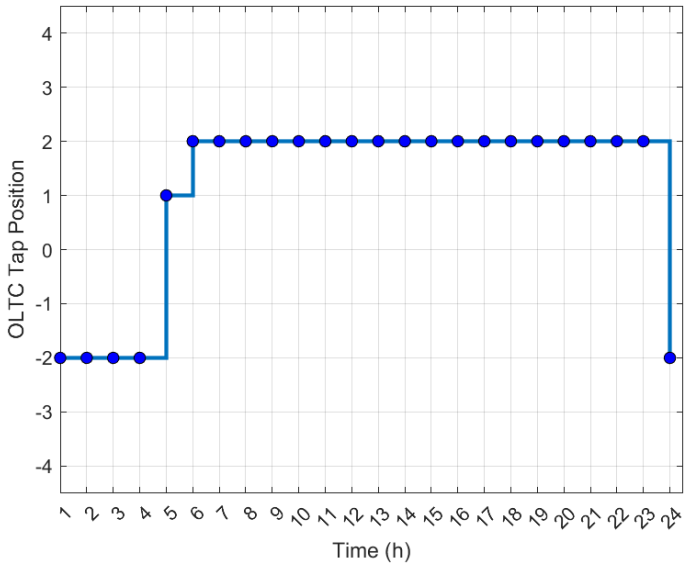

Figure 4.5 Hourly OLTC Tap Position under Only OLTC

With the addition of the SOP, the OLTC exhibits significantly reduced movement as shown in Figure 4.6. Although the regulator still changes position once (from –2 to +2), it remains stable for most of the scheduling horizon. This behavior suggests that the SOP provides spatial flexibility by redistributing power flows between feeders, thereby alleviating part of the burden from the OLTC. As a result, the OLTC does not need to adjust tap ratios as frequently, reducing switching stress and improving long-term device reliability.

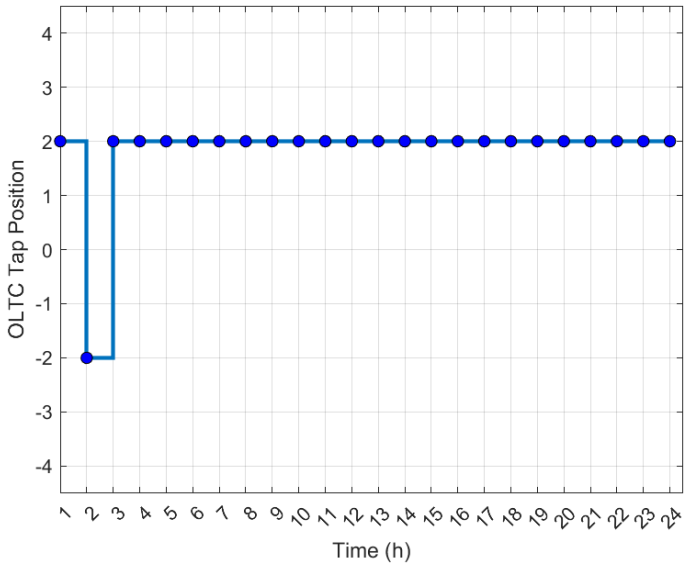

Figure 4.6 Hourly OLTC Tap Position for SOP + OLTC

In the coordinated operation with SOP-ES, the OLTC tap ratio remains fixed at +2 for the entire 24-hour period as in Figure 4.7. The presence of energy storage, co-located with SOP terminals, enhances temporal flexibility by shifting excess PV generation to later periods and smoothing demand fluctuations. Consequently, voltage deviations are effectively managed without requiring OLTC adjustments. This outcome highlights the cooperation between SOP and ESS, which not only improves network performance but also significantly reduces OLTC wear by eliminating unnecessary tap movements.

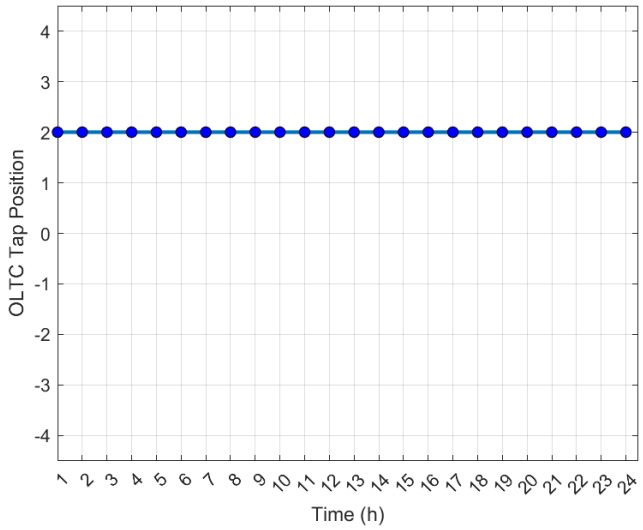

Figure 4.7 Hourly OLTC Tap Position for SOP-ES + OLTC

Key Observation:

The comparison reveals that Only OLTC operation leads to frequent tap changes, while OLTC+SOP reduces regulator activity, and OLTC+SOP-ES eliminates OLTC movements entirely. This demonstrates the importance of SOP-ES in not only improving technical performance (loss reduction, PV utilization, voltage balancing) but also in extending the operational lifespan of OLTC devices through minimized switching frequency.

Voltage profile. The comparative analysis of voltage profile for all scenarios are shown in Figures (4.8-4.15) for node 634. It confirms that coordinated optimization of SOP-ES with variable OLTC provides superior voltage regulation and power quality across the distribution

system. Unlike constant-tap operation, which biases the network towards the upper limit and reduces PV headroom, the variable-tap strategy recenters voltages and complements SOP-ES flexibility to maintain both U_{min} and U_{max} well within the admissible band [0.97, 1.03]. This reduces phase unbalance, lowers worst-phase deviations, and enhances PV hosting capacity without reliance on curtailment. These findings underline the critical role of joint OLTC–SOP–ES optimization in achieving reliable and sustainable operation of active distribution networks.

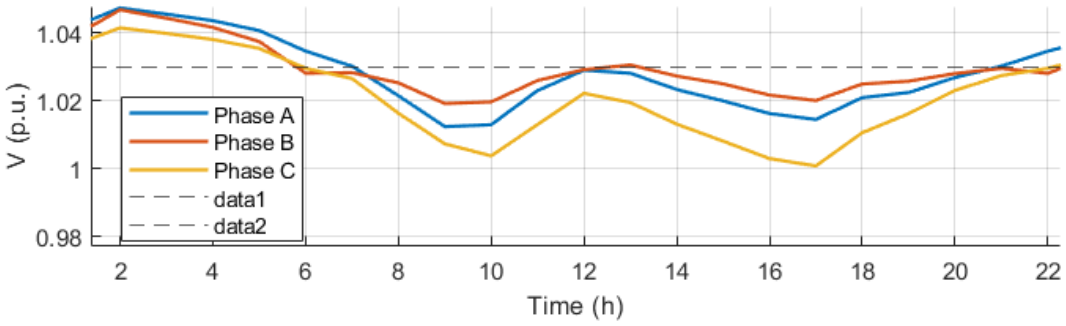

Figure 4.8. Voltage profile of node 634 – Only OLTC (Fixed)

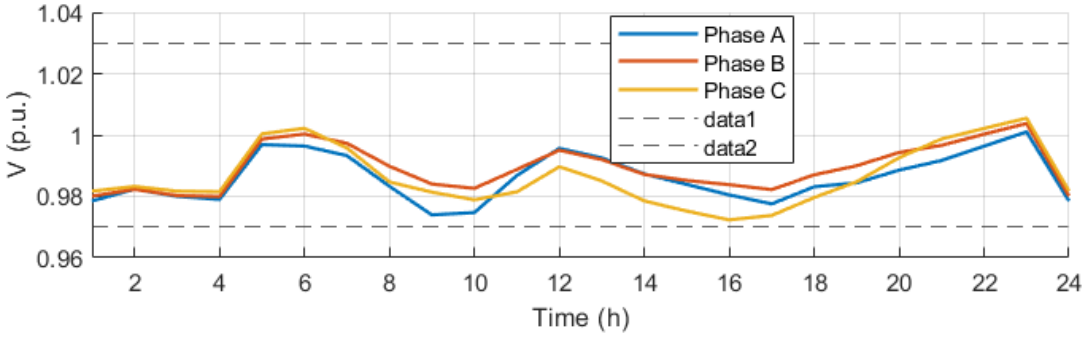

Figure 4.9. Voltage profile of node 634 – Only OLTC (Variable)

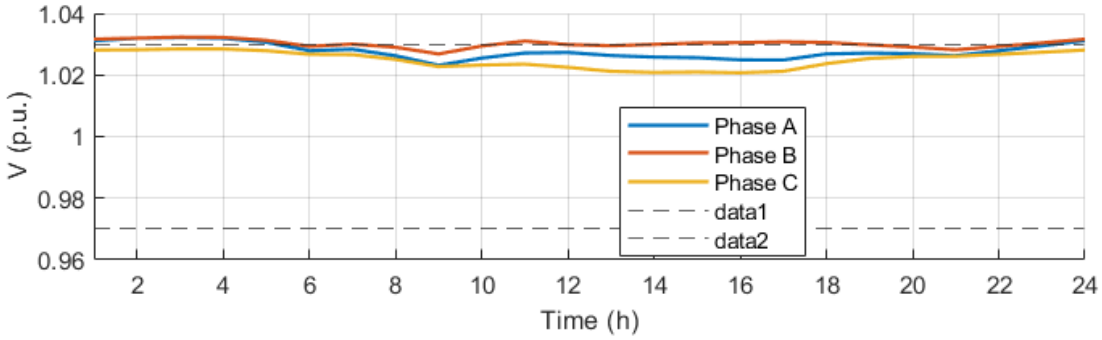

Figure 4.10. Voltage profile of node 634 – SOP + OLTC (Fixed)

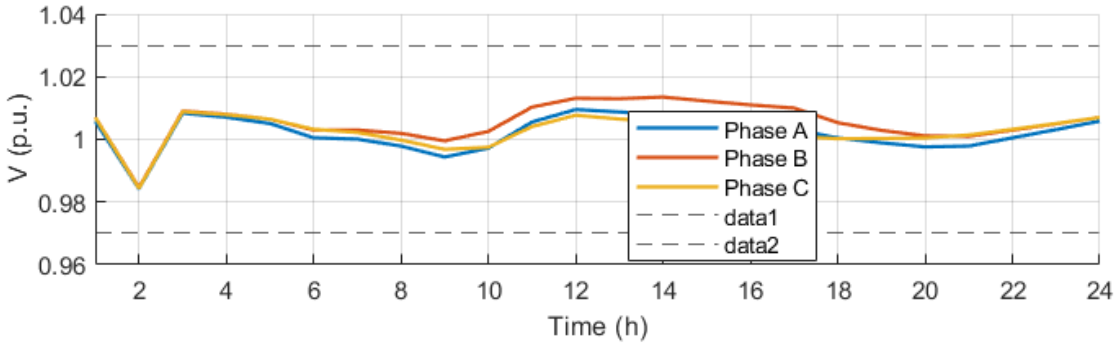

Figure 4.11. Voltage profile of node 634 – SOP + OLTC (Variable)

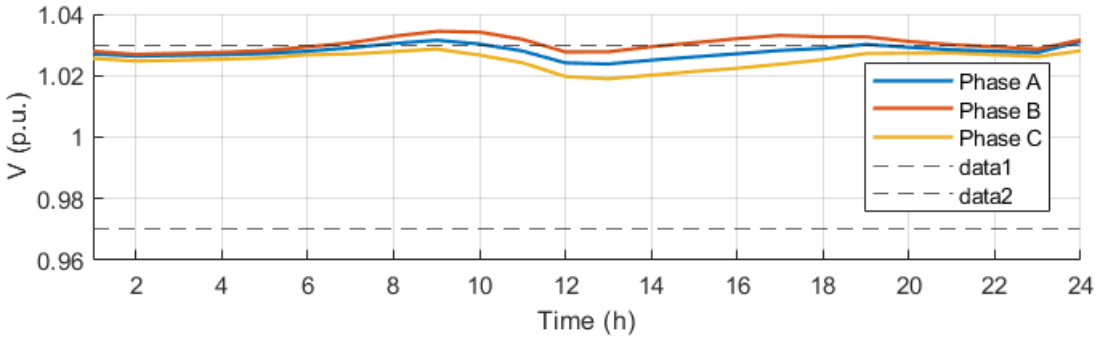

Figure 4.12. Voltage profile of node 634 – SOP-ES + OLTC (Fixed)

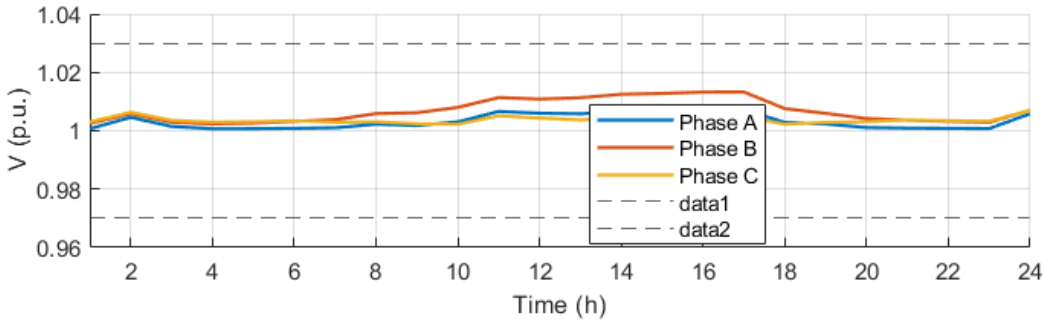

Figure 4.13. Voltage profile of node 634 – SOP-ES + OLTC (Variable)

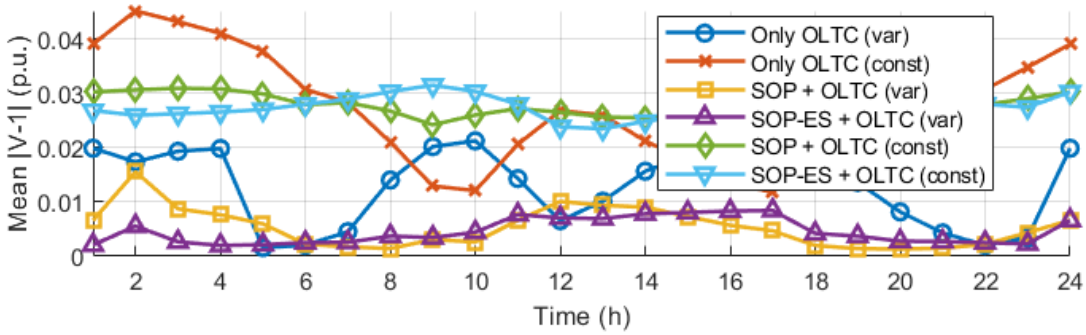

Figure 4.14. Mean voltage deviation of node 634

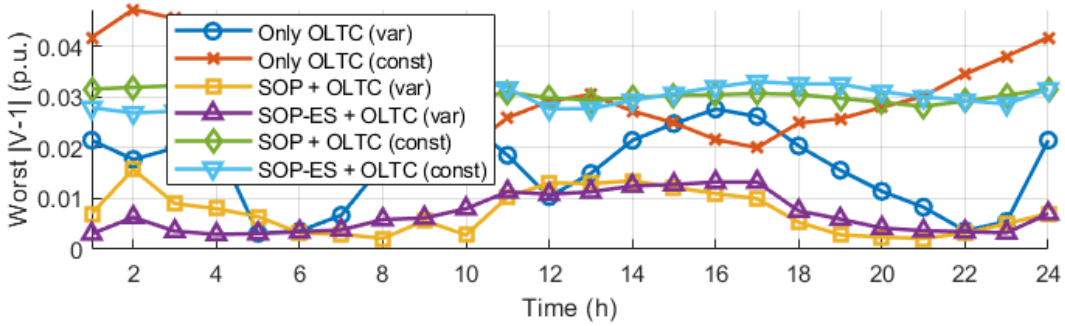

Figure 4.15. Worst-phase deviation of node 634

Figure 4.16 shows the comparison of system-wide maximum and minimum voltages across all scenarios. The SOP-ES with variable OLTC configuration maintains voltages within the admissible band [0.97–1.03 p.u.], whereas constant OLTC exhibits a persistent upward bias, with U_{max} frequently exceeding 1.03 p.u. The variable-tap strategy recenters voltages around

1.0 p.u. and narrows the max–min spread, while constant-tap operation leaves the feeder elevated close to the upper band limit.

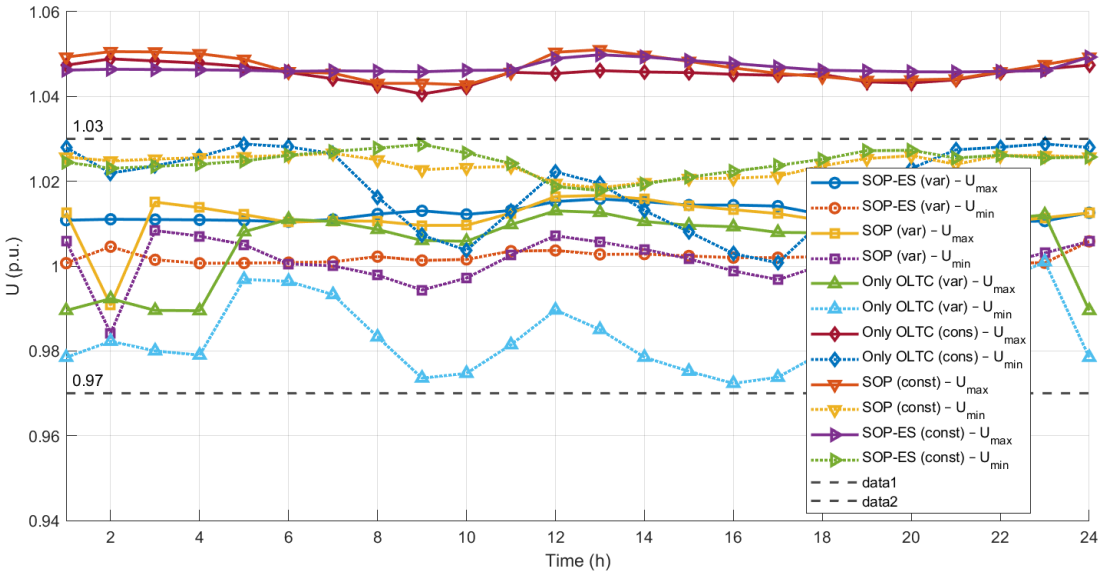

Figure 4.16. Maximum and minimum system voltage for all scenarios

The Figures (4.17-4.20) illustrate the active power transmission patterns through SOP1 and SOP2 under constant OLTC tap ratios. With constant OLTC settings, SOP1 and SOP2 show pronounced active power exchanges throughout the day. In the SOP with constant OLTC case, the transmission patterns are more symmetrical, however, occasional asymmetry arises due to phase imbalances and local demand–generation mismatches. When SOP-ES is added, the energy storage buffers these exchanges, leading to smoother profiles and enhanced balancing between feeder ends. This confirms the ability of SOP-ES to provide both spatial and temporal flexibility.

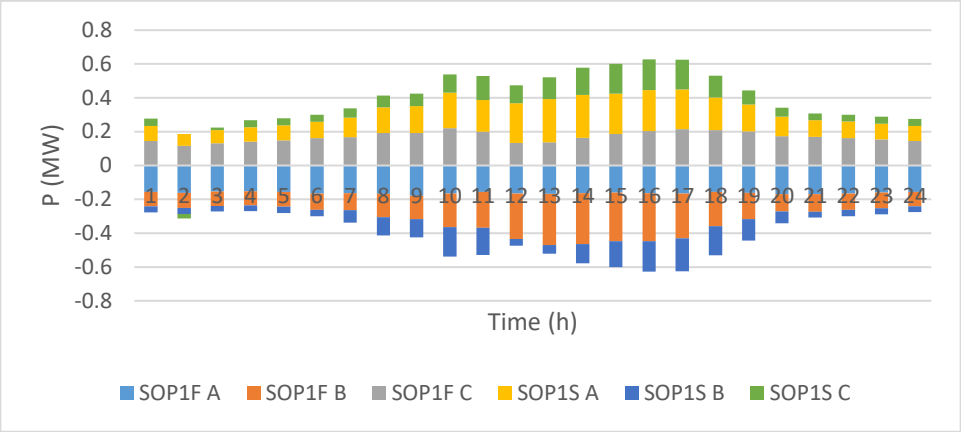

Figure 4.17: Active Power Transmission (SOP1+ Fixed OLTC)

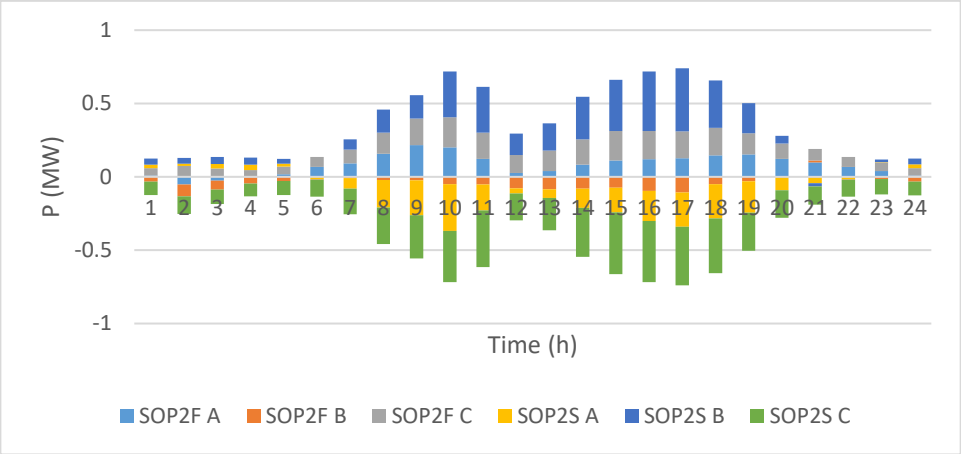

Figure 4.18: Active Power Transmission (SOP2 + Fixed OLTC)

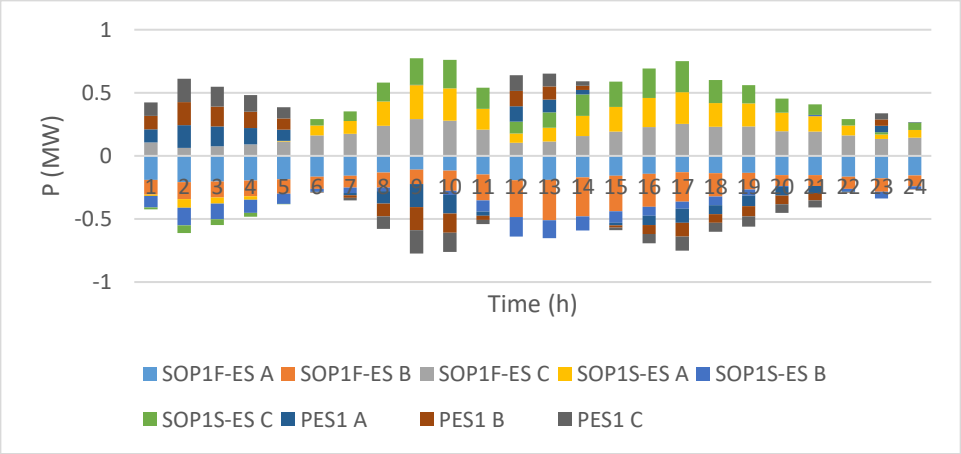

Figure 4.19: Active Power Transmission (SOP1-ES + Fixed OLTC)

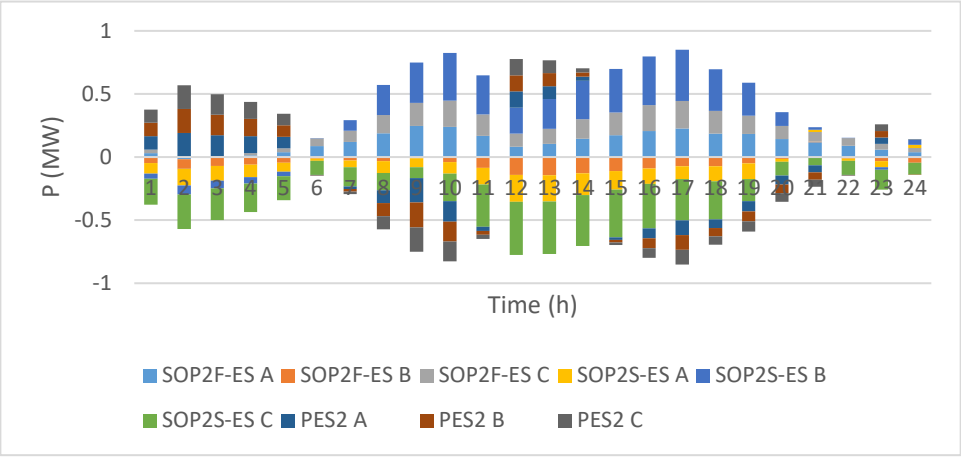

Figure 4.20: Active Power Transmission (SOP2-ES + Fixed OLTC)

The Figures (4.21-4.24) illustrate the active power transmission patterns through SOP1 and SOP2 under variable OLTC tap ratios. Allowing OLTC tap ratios to vary reduces the burden on SOP units. Compared to constant taps, the magnitude of SOP power transfer is notably lower, as part of the voltage regulation is absorbed by the OLTC. For SOP-only with variable OLTC, the flows become more distributed, and peak transfers are mitigated. With SOP-ES + variable OLTC, the most coordinated pattern emerges. Energy storage effectively absorbs surplus PV generation (midday) and discharges during evening peaks, minimizing extreme SOP flows. This leads to smaller oscillations and a well-balanced exchange across feeders.

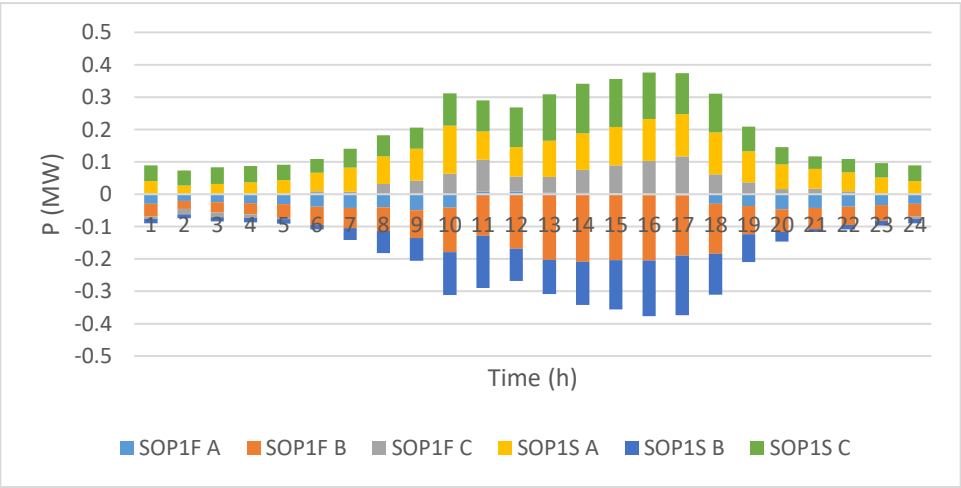

Figure 4.21: Active Power Transmission (SOP1+ Variable OLTC)

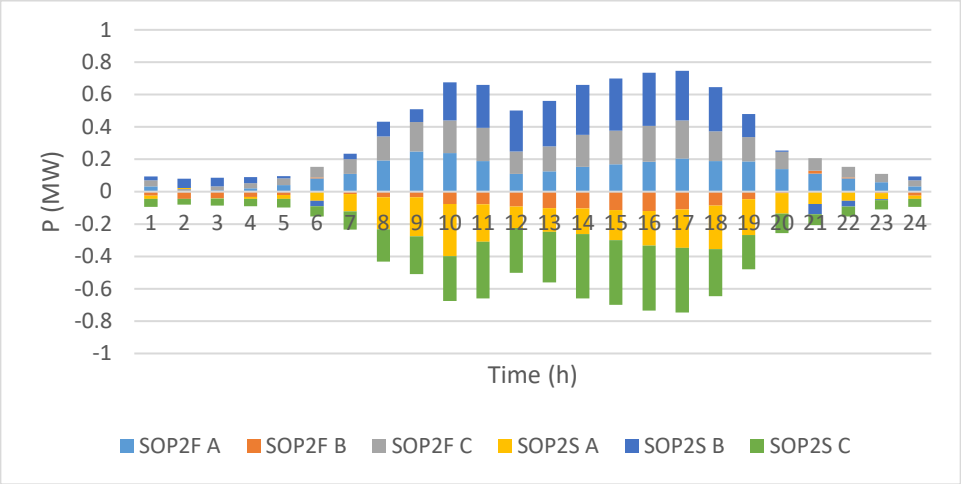

Figure 4.22: Active Power Transmission (SOP2+ Variable OLTC)

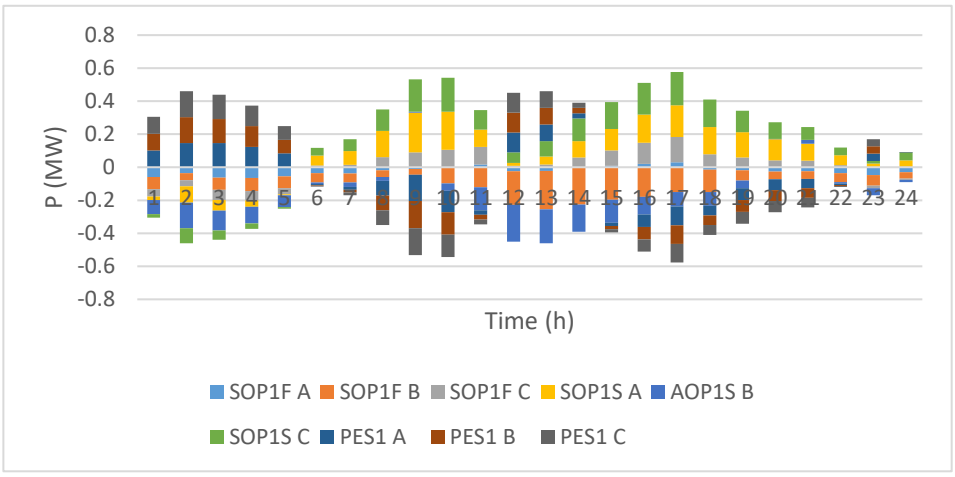

Figure 4.23: Active Power Transmission (SOP1-ES + Variable OLTC)

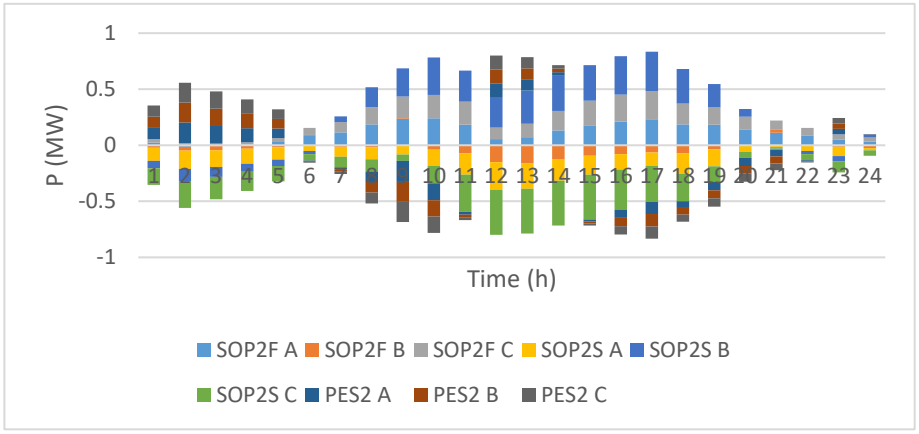

Figure 4.24: Active Power Transmission (SOP2-ES + Variable OLTC)

In general, SOP with constant OLTC strong reliance on inter-feeder exchanges, occasionally asymmetric in low-load hours, while SOP-ES balanced and smoothed profiles, particularly around PV peaks, due to temporal shifting from energy storage. Using variable OLTC coordination reduces SOP stress, with SOP-ES providing the most stable exchange pattern. This shows that OLTC tap control and SOP-ES coordination are complementary, OLTC addresses network-wide voltage magnitude, while SOP-ES balances feeder-to-feeder and temporal mismatches.

The results in Figures 4.25 and 4.26 illustrate the aggregated 24-hour reactive power exchange (injection and absorption) of SOP-ES devices across both terminals (SOP1 and SOP2) under fixed tap ratios (Fixed OLTC). Each figure shows the total injected (blue) and absorbed (orange) reactive power for all three phases (A, B, and C).

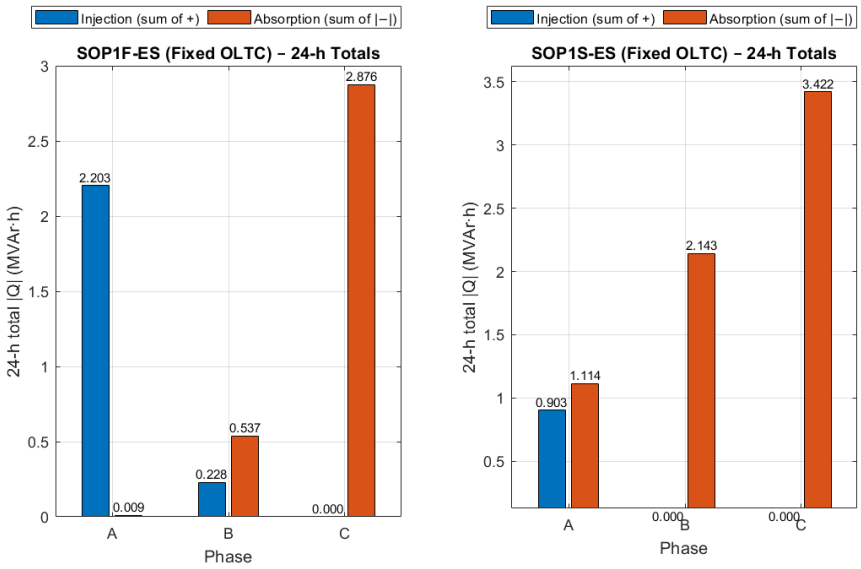

Figure 4.25 Reactive Power for Fixed OLTC+SOP1-ES

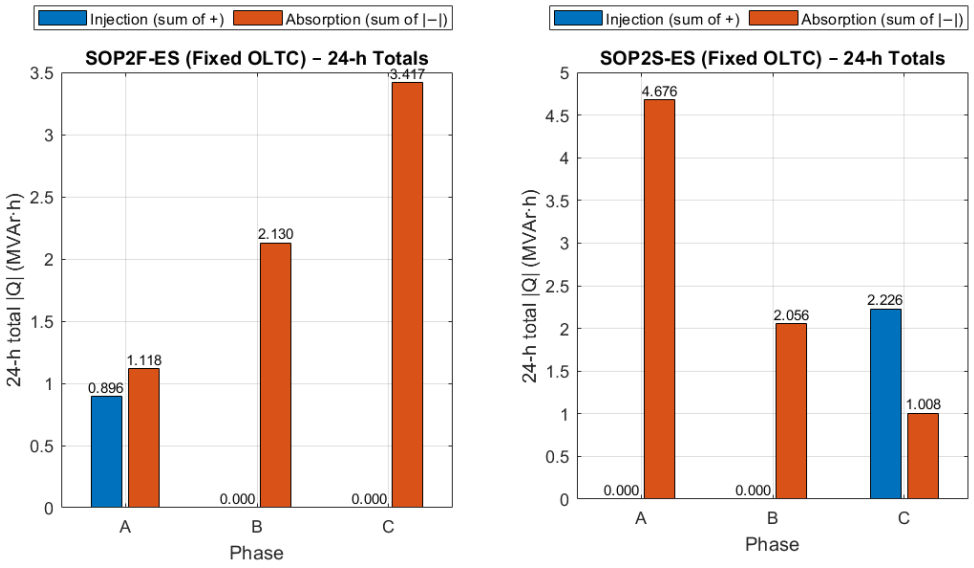

Figure 4.26 Reactive Power for Fixed OLTC+SOP2-ES

Using fixed OLTC (constant tap ratio), as shown in Figure 4.25, SOP1F-ES and SOP1S-ES exhibit significant reactive power absorption, particularly in Phase C, reaching nearly 2.9 Mvar·h (SOP1F-ES) and 3.4 Mvar·h (SOP1S-ES), respectively. SOP2F-ES and SOP2S-ES in Figure 4.26 also display dominant absorption, with maximum values of 3.4 Mvar·h (SOP2F-ES Phase C) and 4.7 Mvar·h (SOP2S-ES Phase A). Injection values remain relatively small compared to absorption, highlighting that fixed OLTC operation forces SOP-ES units to frequently act as reactive sinks to reduce voltage rise from PV generation.

Using variable OLTC (coordinated tap ratios), as in Figure 4.27 and 4.28, a change in behavior is observed: SOP-ES units show greater injection capability, particularly in Phase A of both SOP1F-ES (≈2.3 Mvar·h) and SOP1S-ES (≈2.4 Mvar·h), as well in SOP2F-ES (≈2.5 Mvar·h), and Phase C of SOP2S-ES (≈4.6 Mvar·h). Reactive power absorption is reduced significantly, with only moderate absorption in selected phases (e.g., SOP1S-ES Phase C ≈1.4 Mvar·h, and SOP2F-ES Phase C ≈1.5 Mvar·h). This indicates that variable OLTC alleviates the burden on SOP-ES, allowing them to provide reactive support (injection) instead of continuous absorption. This demonstrates the complementary relationship: OLTC

adjusts voltage levels globally, while SOP-ES fine-tunes local reactive exchanges. Coordinated operation therefore reduces the over-reliance on SOP-ES for absorption and enhances their supporting role in injection.

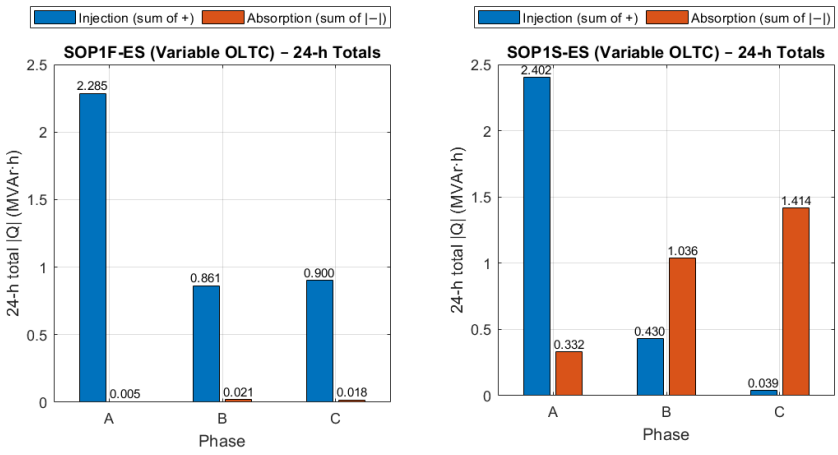

Figure 4.27 Reactive Power for Variable OLTC+SOP1-ES

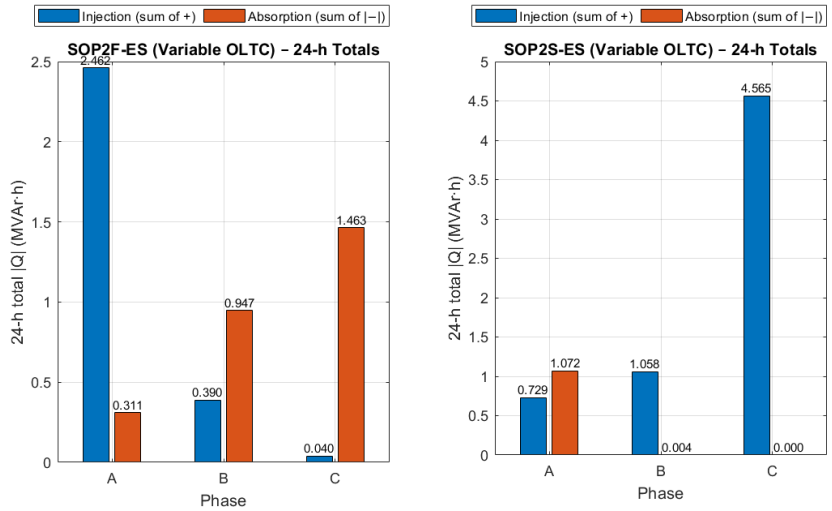

Figure 4.28 Reactive Power for Variable OLTC+SOP2-ES

In general, the complementary action between Variable OLTC and SOP-ES reduces the SOP's net absorption requirement, preserves converter headroom for active power transfer, and ultimately enables higher PV hosting capacity.

The SoC traces of ES1 and ES2 highlight how OLTC operation mode directly influences the charging–discharging coordination of the integrated storage. Under constant OLTC as in Figures 4.29, and 4.30, both ES1 and ES2 experience relatively steeper charging profiles in the morning, reaching their maximum SoC (~1.2–1.5 MW) earlier in the day (around hours 6–8). This reflects the converters being forced to absorb excess PV generation more aggressively, since the fixed tap does not lower feeder voltage sufficiently during peak PV periods. The discharge phases are shorter and less pronounced, with SoC declining only moderately in the late afternoon and evening.

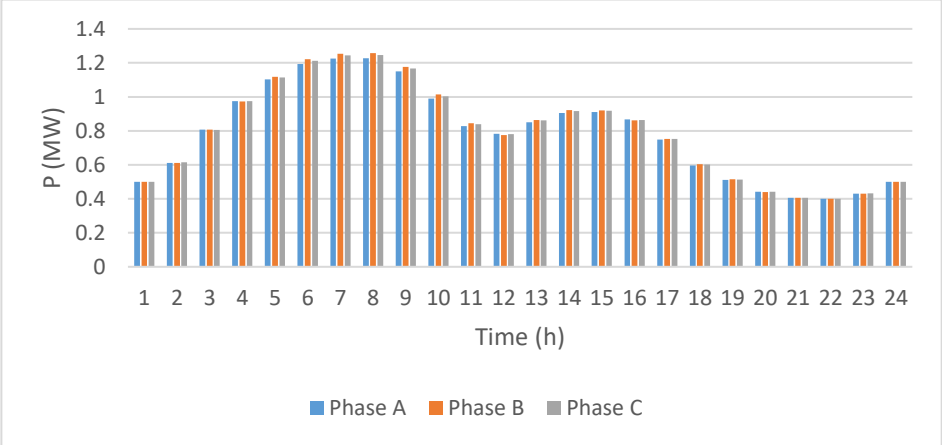

Figure 4.29: State of Charge (SoC) of ES1 with Fixed OLTC

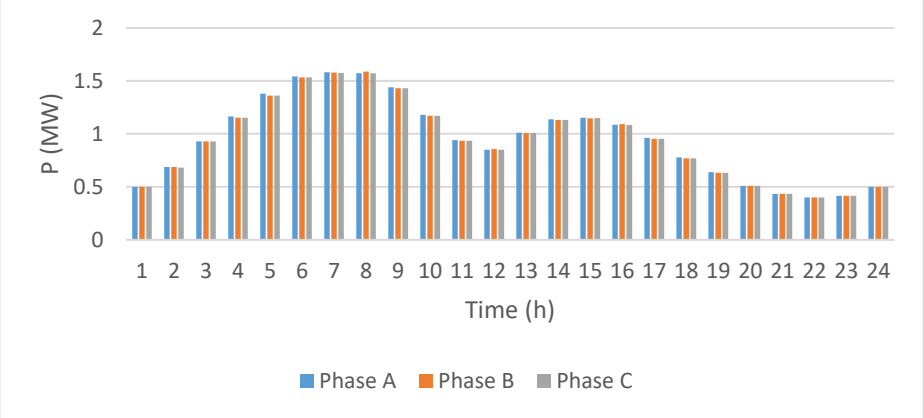

Figure 4.30: State of Charge (SoC) of ES2 with Fixed OLTC

By contrast, under variable OLTC as in Figures 4.31, and 4.32, the SoC peaks (~1.0–1.2

MW) are slightly lower than in the constant case (~1.2–1.5 MW). This indicates that the OLTC, by adjusting the feeder voltage dynamically, absorbs part of the PV-induced voltage rise, thereby reducing the burden on the storage units to absorb surplus generation. The resulting headroom in the ESS can be reserved for other operational needs e.g., evening peak shaving, fast voltage support during transients, or contingencies thereby improving overall flexibility.

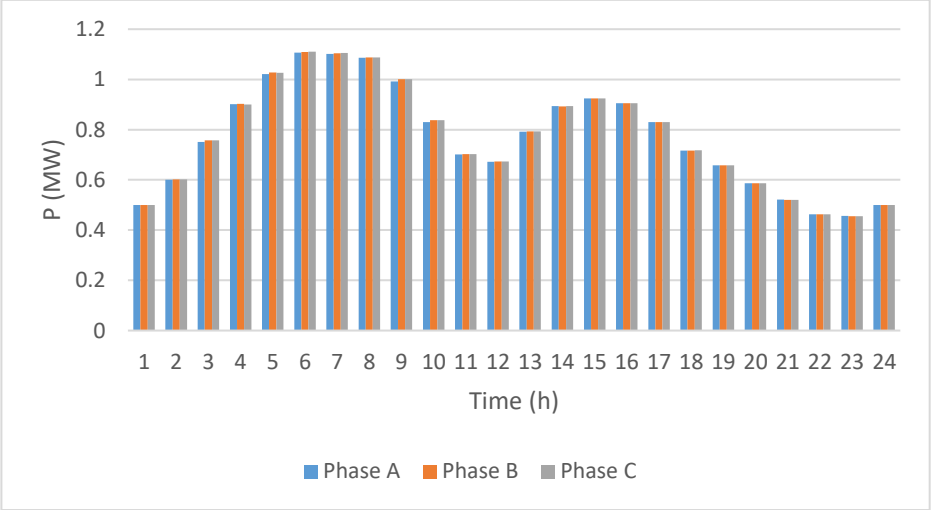

Figure 4.31: State of Charge (SoC) of ES1 with Variable OLTC

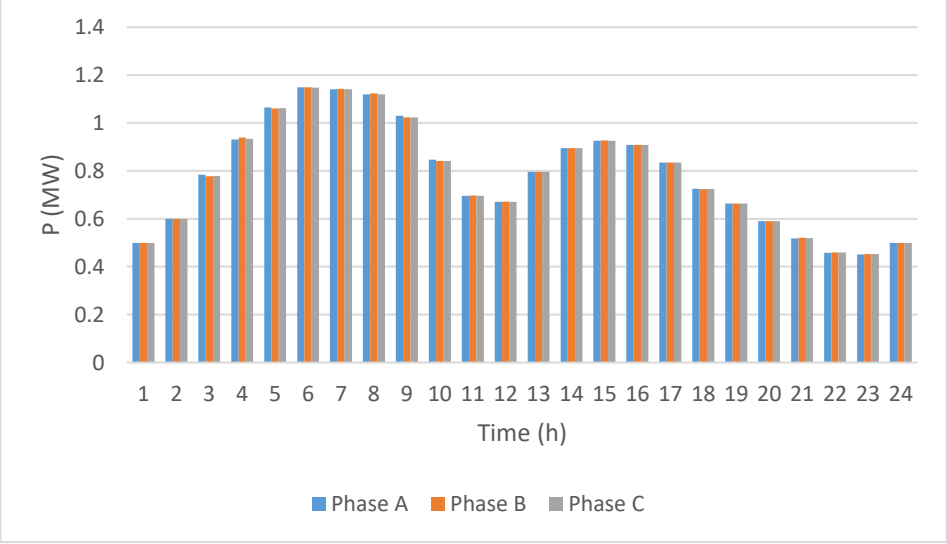

Figure 4.32: State of Charge (SoC) of ES2 with Variable OLTC

4.3.2.2 Case Study Results: IEEE 123-Bus System

In Chapter 3, four voltage-regulator locations were modeled with fixed taps: a three-phase unit between buses 150–149 with $[r_a^t, r_b^t, r_c^t] = [1.05, 1.0375, 1.04375]$; a single-phase unit between buses 9-14 with $r_a^t = 0.99375$; a two-phase regulator between buses 25-26 is set to $[r_a^t, r_c^t] = [0, 0.99375]$; and another two-phase regulator between buses 67 and 160 is set to $[r_a^t, r_b^t, r_c^t] = [1.5, 1.00625, 1.3125]$. In this chapter, these taps are promoted to decision variables and jointly coordinated with SOP and SOP-ES. To demonstrate scalability beyond the IEEE-13 case studied earlier, we now validate the approach on the larger, more heterogeneous IEEE-123 test feeder, highlighting performance under realistic multi-phase topology and multiple regulator placements.

Tables 4.3 and 4.4 compares the system performance under constant regulator taps as in (Chapter 3) and variable regulator taps (this chapter) across three scenarios: only VRs, VRs + SOP, and VRs + SOP-ES.

Table 4.3: Results with Fixed Tap Ratios

Scenario (Constant VRs)	Power Loss (MW/24 h)	PV Active Power (MW/24 h)	Substation power (MW/24 h)
VRs	18.54	9.95	63.2
VRs + SOP	15.58	10.04	62.05
VRs + SOP-ES	15.53	9.81	57.5

Table 4.4: Results with Variable Tap Ratios

Scenario (Variable VRs)	Power Loss (MW/24 h)	PV Active Power (MW/24 h)	Substation power (MW/24 h)
VRs	4.02	8.47	46.6
VRs + SOP	3.15	9.85	44.3
VRs + SOP-ES	3.08	9.57	44

With constant VRs, daily power losses remain high (≈18.5 MW/24 h for VRs), although SOP and SOP-ES reduce losses slightly to ~15.5 MW/24 h, the improvement is modest. Substation power exchange is also heavy (≈63 MW/24 h with VRs, dropping to 57.5 MW/24 h with SOP-ES), while PV utilization sits around 9.8–10.0 MW/24 h.

In contrast, when voltage regulators are treated as decision variables, performance improves dramatically. Power losses fall by nearly 80% in all cases (down to 3–4 MW/24 h), while substation power is cut by almost 30% (from ~63 MW/24 h with fixed taps to ~44–46 MW/24 h with variable taps). PV utilization is also more effectively supported by SOP and SOP-ES: compared with the only VRs variable case (8.47 MW/24 h), the SOP increases PV throughput to 9.85 MW/24 h, while SOP-ES delivers 9.57 MW/24 h with the added benefit of energy shifting.

Overall as shown in Figure 4.33, the results demonstrate that variable VRs coordination fundamentally changes the system operating point: losses are minimized, substation dependency is reduced, and PV integration is enhanced. Moreover, while SOP and SOP-ES provide benefits under both strategies, their impact is magnified when operating alongside optimizable voltage regulators, confirming the importance of joint VRs+SOP–ES coordination for efficient and renewable-friendly distribution network operation.

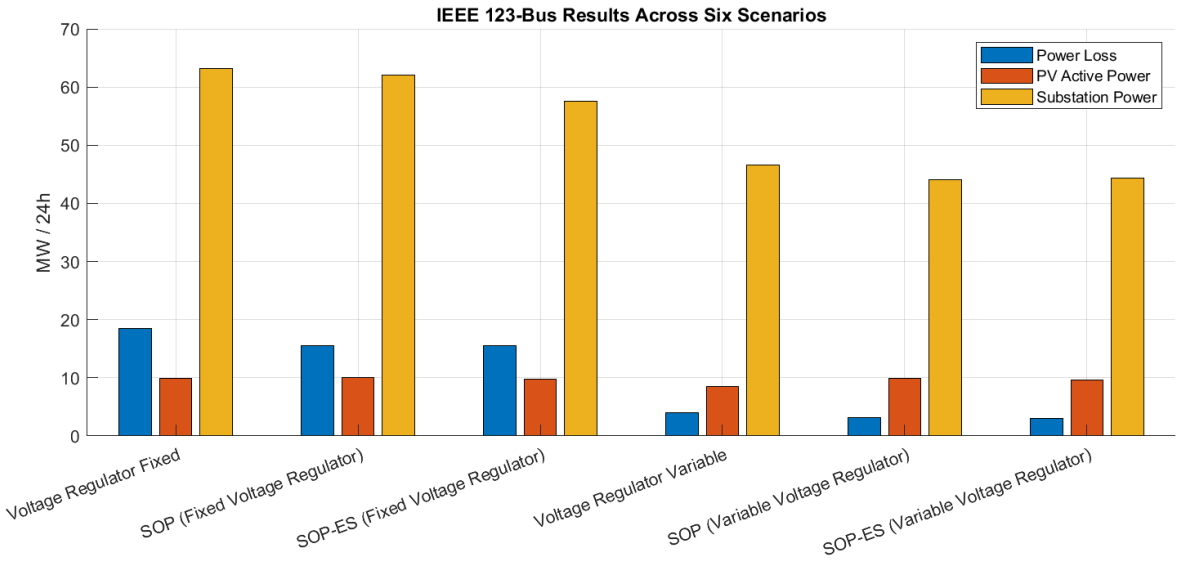

Figure 4.33: All Scenarios Results

The tap movement results as in Figures (4.34-4.37) show clear differences between the three scenarios. With only VRs, regulators exhibit frequent and sometimes wide tap changes as they attempt to maintain feeder voltages under varying load and PV generation. When SOPs are introduced, the tap movements become somewhat smoother, but the VRs are still required to adjust regularly, especially during PV peaks and evening load periods. In contrast, with SOP-ES coordination, the tap profiles are noticeably more stable, with fewer and smaller adjustments. This indicates that the storage-enhanced SOPs effectively absorb midday PV surplus and discharge during evening peaks, providing local support that reduces the burden on VRs. As a result, the VRs act more as coarse, background controllers, while the SOP-ES takes on the finer, dynamic regulation role. This coordinated action not only reduces regulator wear and operation but also improves voltage stability and system efficiency compared with the other cases.

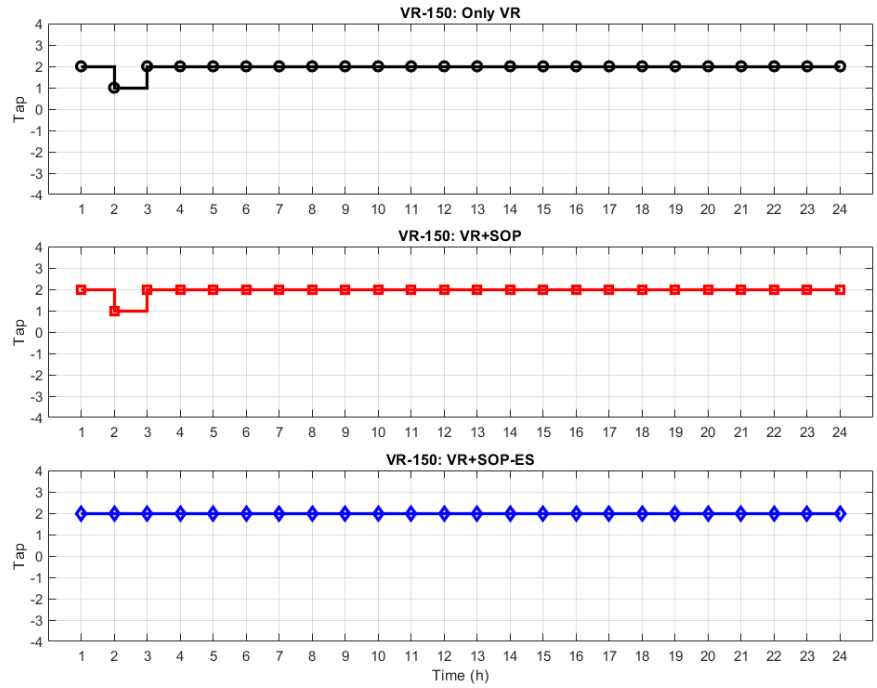

Figure 4.34 Tap Position for VR-150

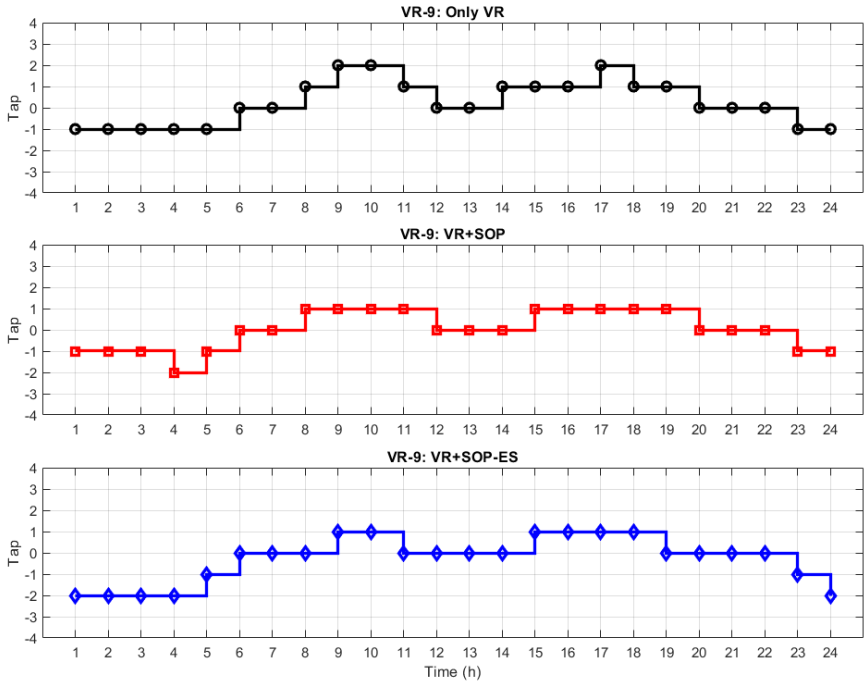

Figure 4.35 Tap Position for VR-9

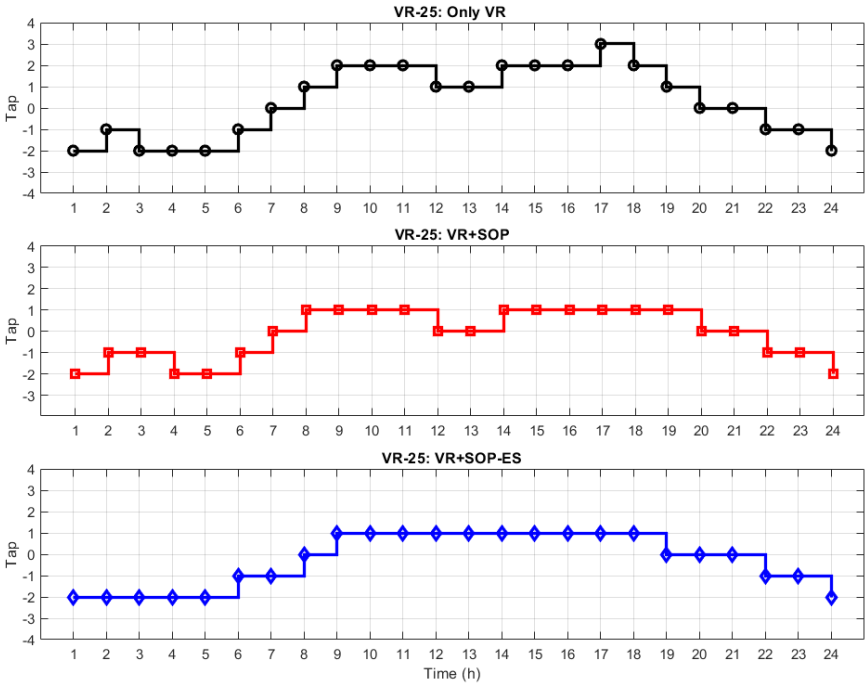

Figure 4.36 Tap Position for VR-25

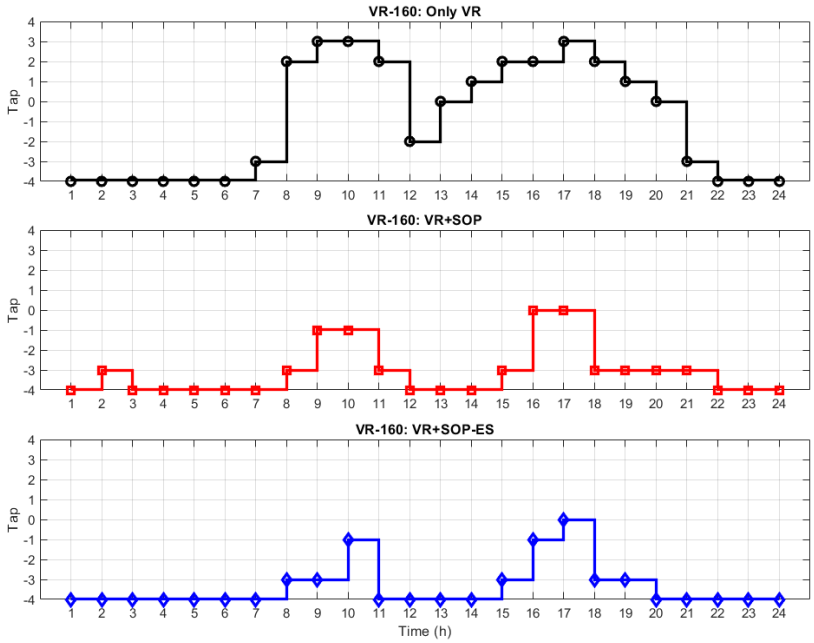

Figure 4.37 Tap Position for VR-160

At Bus 8, the voltage trajectories under different control strategies as in Figure 4.38 show clear differences between constant and variable regulator operations. With only VRs under constant taps, the three-phase voltages remain nearly flat but biased close to the upper

admissible limit, which restricts flexibility. By contrast, variable VR control dynamically adjusts the tap positions, keeping voltages closer to 1.0 p.u. and reducing daily excursions. When SOPs are added, further improvements are observed: SOP + VRs (variable) smoothens phase deviations and maintains voltages within a narrower band compared to the constant-tap case. The integration of SOP-ES provides the best performance, delivering balanced voltages across phases with minimal fluctuation. This is confirmed by the mean and worst-phase deviation plots, where SOP-ES + VRs (variable) consistently yields the lowest deviation values throughout the day. Similarly, the Voltage Unbalance Factor (VUF) at Bus 8 is highest under only VRs (both constant and variable) but drops significantly when SOP and especially SOP-ES are included, demonstrating the coordinated benefit of distributed flexibility resources and variable regulator settings. Overall, the results highlight that combining SOP-ES with variable VRs achieves superior voltage regulation and unbalance mitigation.

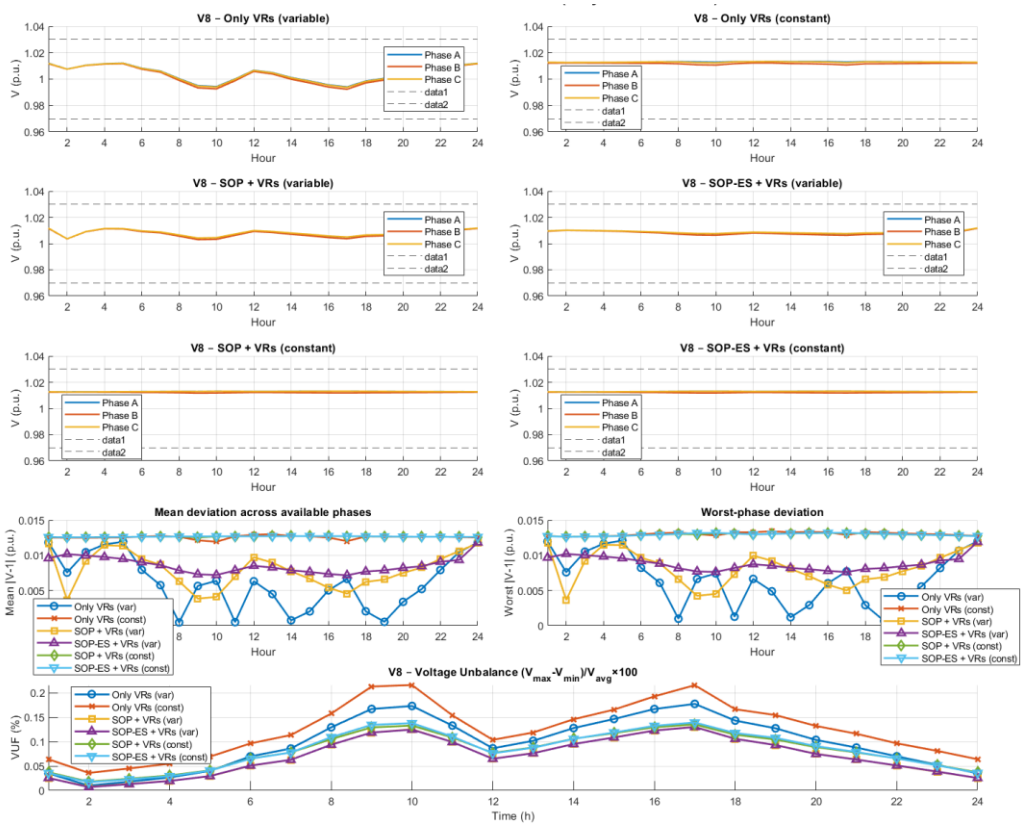

Figure 4.38 Voltage Profile of All Scenarios for Bus 8

Figure 4.39 compares the 24-h system maximum (U_{max}) and minimum (U_{min}) voltages when SOP-ES is operated under constant versus variable VRs settings. With constant VRs, the maximum voltage remains elevated at around 1.045 p.u., consistently exceeding the desired control range of 1.03 p.u. The minimum voltage simultaneously falls below 0.97 p.u. for most of the day, reaching as low as 0.955 p.u., which indicates persistent under-voltage conditions in weaker parts of the feeder. In contrast, when VRs are optimized as decision variables, the voltage band is significantly tightened: (U_{max}) stabilizes close to 1.015 p.u. while (U_{min}) is maintained above 0.975 p.u. throughout the horizon. This demonstrates that variable VRs coordination with SOP-ES not only reduces over-voltage at heavily loaded or PV-dominated nodes but also alleviates under-voltage at remote buses, ensuring the entire network operates comfortably within the admissible [0.97–1.03] p.u. band. Overall, the results confirm that making VRs controllable provides a complementary role to SOP-ES in enforcing voltage security and improving feeder robustness.

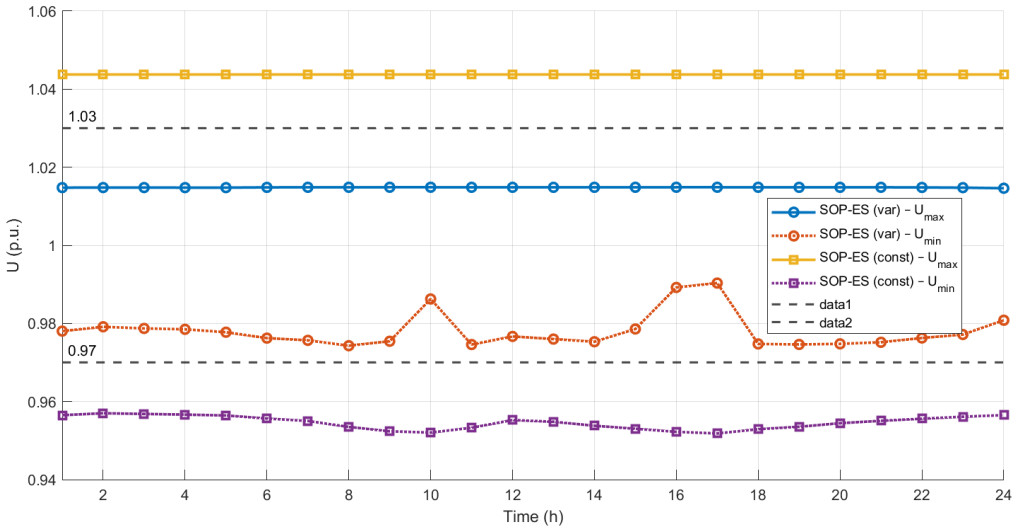

Figure 4.39 Maximum and minimum system voltage for all scenarios

The active power exchanges of SOPs depend strongly on whether VRs are fixed or variable. Under constant VRs as shown in Figures (3.35-3.38) from chapter 3, SOP1 and SOP2 exhibit relatively rigid inter-feeder transfers: SOP1 exchanges are modest (±0.3 MW), while SOP2

supports larger inter-feeder power flows (up to ±0.5 MW). With SOP-ES, additional charging and discharging activity appears at PES1 and PES2, but under constant VRs these storage actions mainly reshape the local SOP flows without significantly altering the magnitude of feeder-to-feeder exchanges.

When VRs are variable, as in Figures (4.40-4.43) the SOPs operate more dynamically. SOP1 supports higher bidirectional flows between its connected feeders, reaching up to –0.6 MW on one terminal with corresponding export on the other during midday PV peaks. SOP2 also adapts its transfers more flexibly, though at smaller magnitudes (±0.1 MW). The integration of storage under variable VRs opens much greater flexibility: PES1 and especially PES2 undertake substantial charge–discharge cycles (up to ±1 MW), which directly shape the SOP flows. This temporal shifting smooths peak inter-feeder transfers and enables better coordination with VR tap movements.

In summary, constant VRs limit SOPs to relatively fixed feeder-to-feeder exchanges, with storage playing only a local balancing role. By contrast, variable VRs enable SOPs and SOP-ES to work in tandem, enhancing both spatial balancing (redistributing active power across feeders) and temporal balancing (via storage), which improves PV hosting and reduces feeder stress.

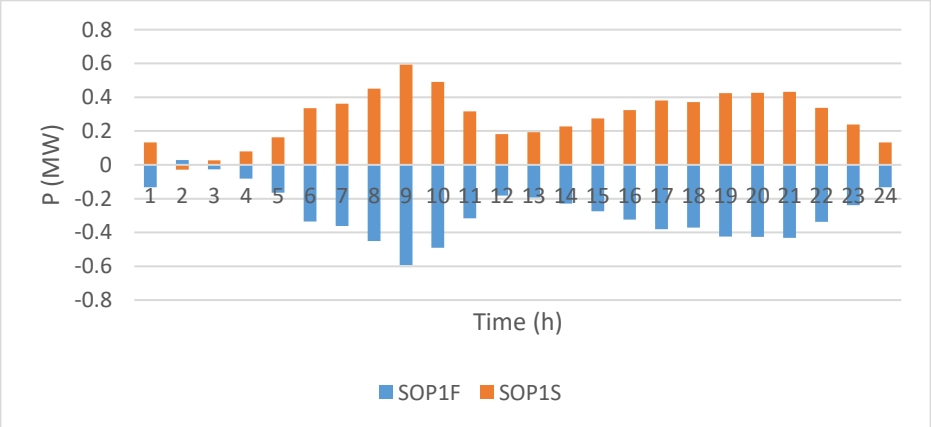

Figure 4.40: Active Power Transmission (SOP1+ Variable VRs)

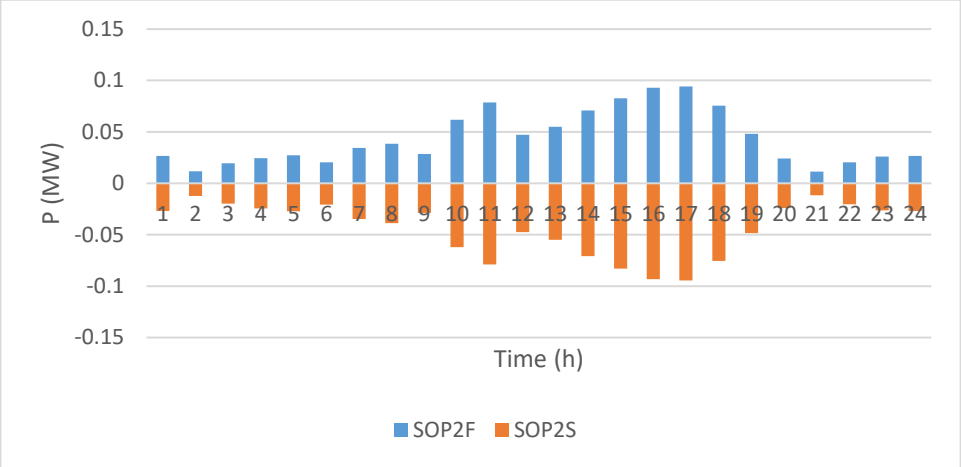

Figure 4.41: Active Power Transmission (SOP2+ Variable VRs)

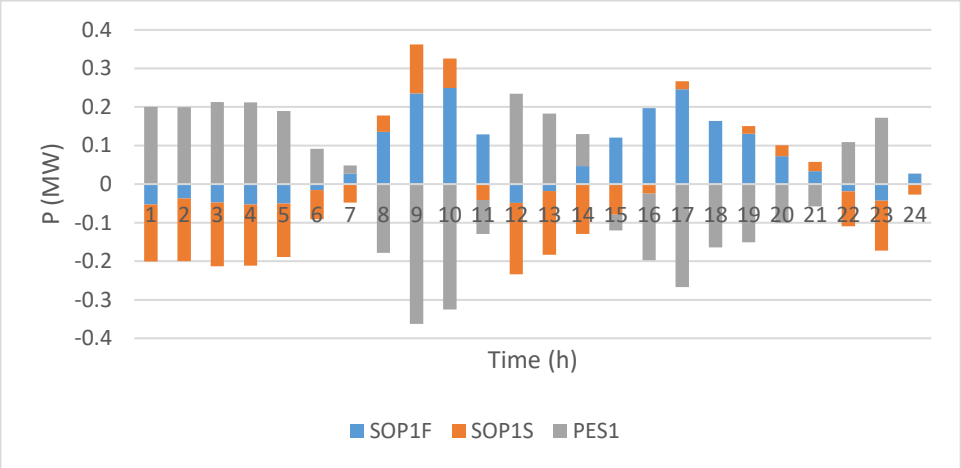

Figure 4.42: Active Power Transmission (SOP1-ES+ Variable VRs)

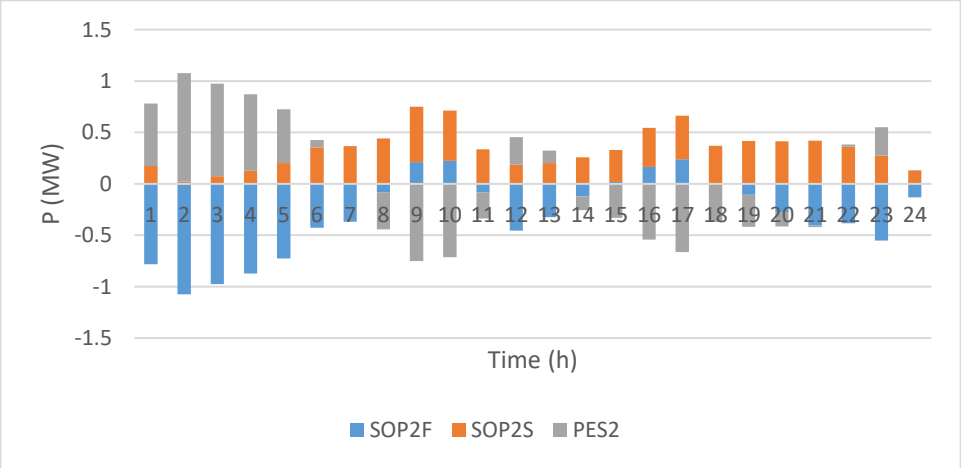

Figure 4.43: Active Power Transmission (SOP2-ES+ Variable VRs)

When VRs are kept constant, SOP-ES is forced to compensate for voltage rise primarily through reactive absorption, which dominates across most terminals and phases as in Figures (4.44 - 4.45). This results in a less flexible and more phase-skewed contribution, since the fixed tap settings limit the system's ability to adapt.

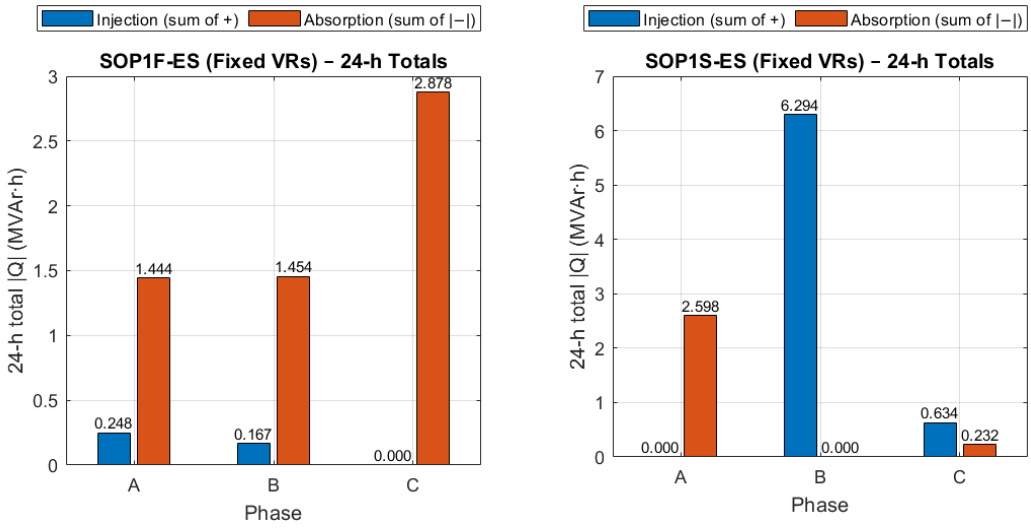

Figure 4.44 Reactive Power Fixed VRs+SOP1-ES

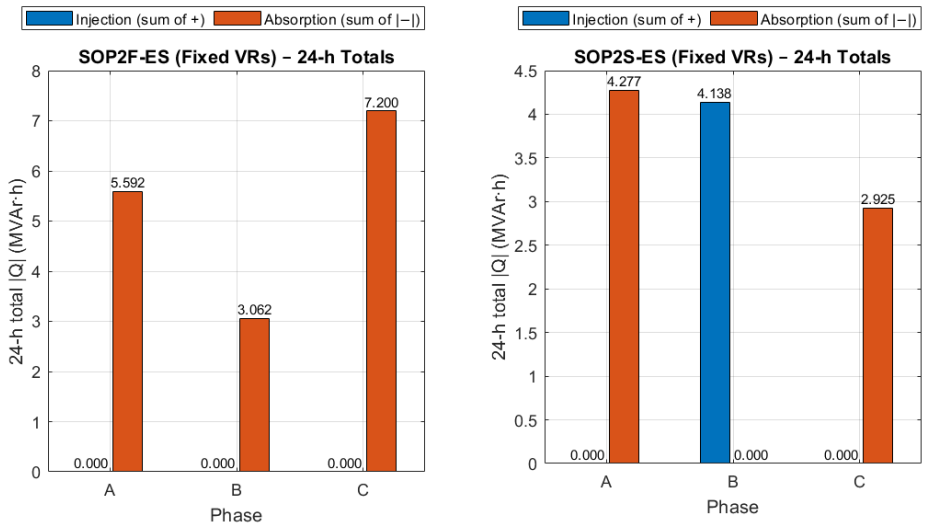

Figure 4.45 Reactive Power Fixed VRs+SOP2-ES

By contrast, with variable VRs as shown in Figures (4.46 - 4.47), the voltage rise can be actively managed through tap-ratio adjustments. This relieves SOP-ES from having to act mainly as an absorber, allowing it instead to operate predominantly in injection mode. In this coordinated setup, SOP-ES contributes more dynamically, supporting feeder voltages with greater flexibility and balance across phases. Hence, integrating SOP-ES with variable VRs not only improves voltage regulation but also releases the device's potential to provide sustained reactive injections rather than being constrained to absorption.

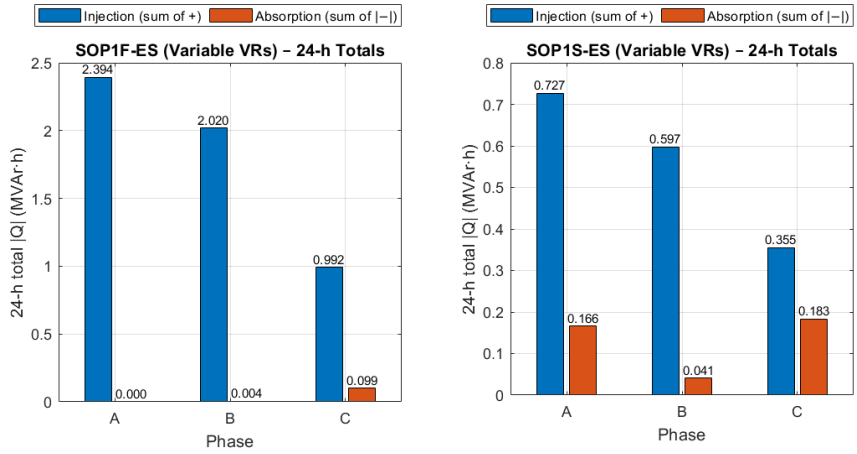

Figure 4.46 Reactive Power Variable VRs+SOP1-ES

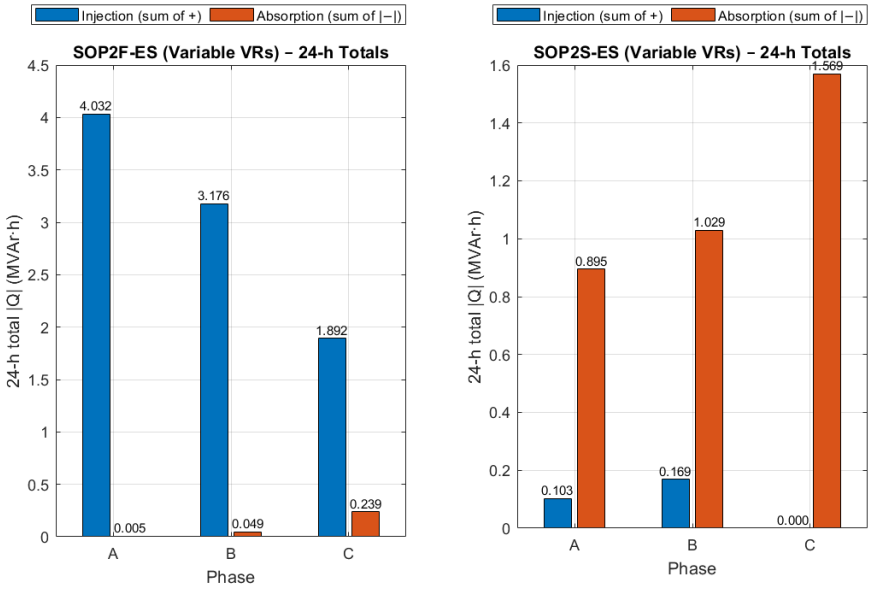

Figure 4.47 Reactive Power Variable VRs+SOP2-ES

When comparing the charging/discharging and state of charge (SoC) behavior of both ES units under fixed VRs (Figures 3.43–3.46) and variable VRs (Figures 4.48–4.51), the daily traces follow a similar pattern shaped by PV generation and load. However, the key difference lies in the amplitude of power exchange. For ES1, the use of variable VRs reduces the magnitude of both charging and discharging, leading to shallower cycles and a smoother SoC profile. Under fixed VRs, ES1 is subjected to stronger charging and deeper discharging, since it must absorb a larger share of the voltage regulation task. In the case of ES2, variable VRs enable higher charging peaks in the morning while limiting the depth of afternoon discharges compared to the fixed scenario.

Overall, variable VRs moderate the cycling intensity of the storage units by reducing extreme discharges and balancing charging demands, thereby alleviating stress on the batteries and enhancing their role in supporting PV integration more effectively.

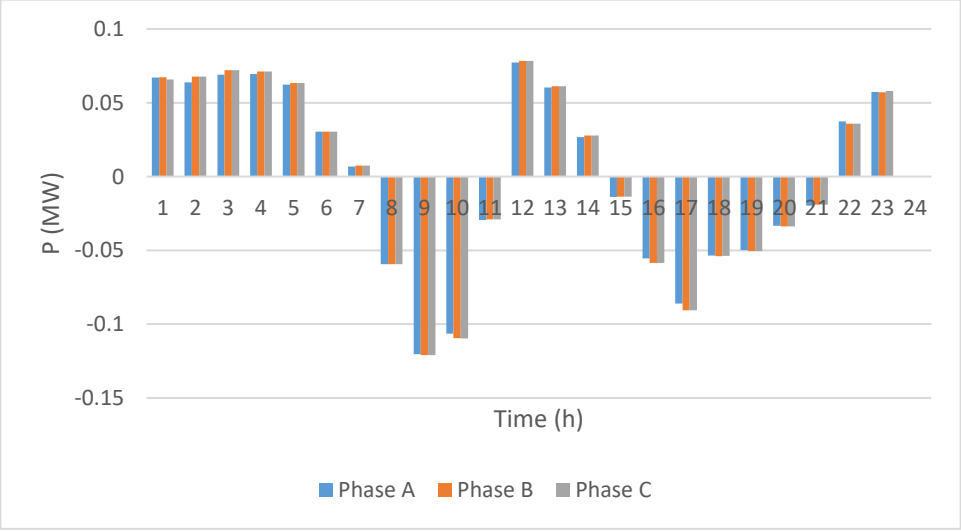

Figure 4.48: Charging Discharging Power of ES1 with Variable VRs

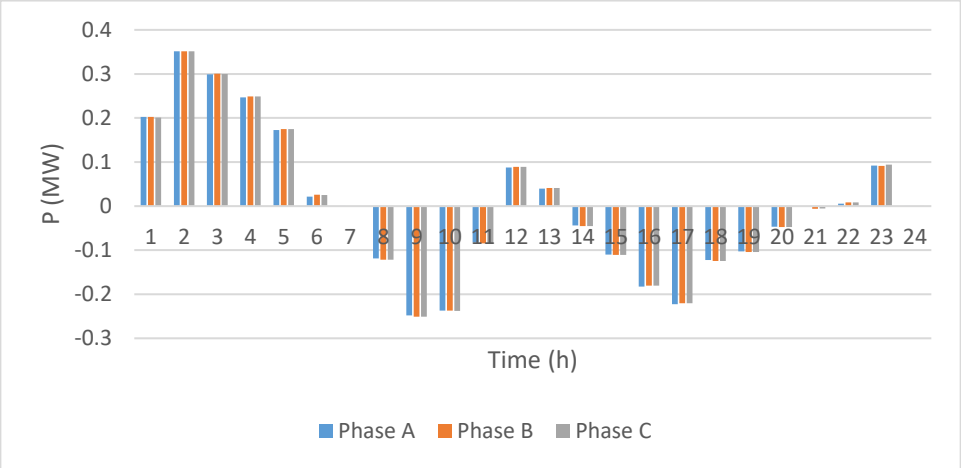

Figure 4.49: Charging Discharging Power of ES2 with Variable VRs

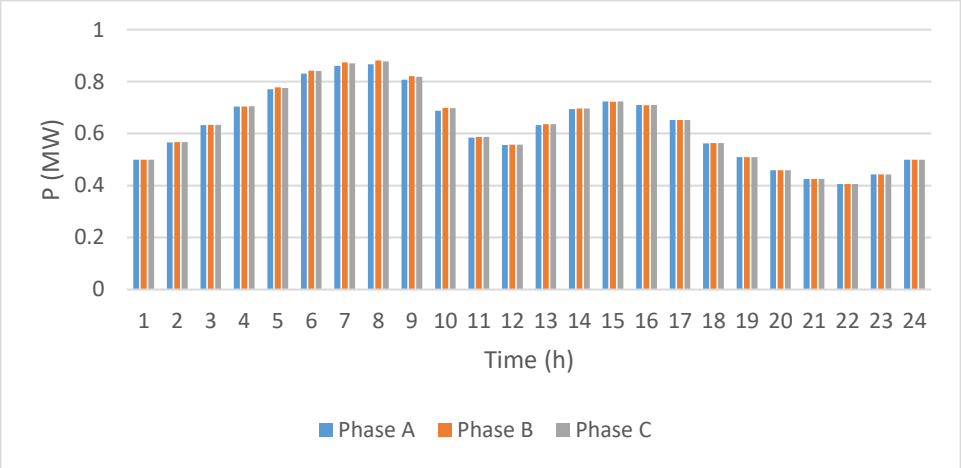

Figure 4.50: State of Charge (SoC) of ES1 with Variable VRs

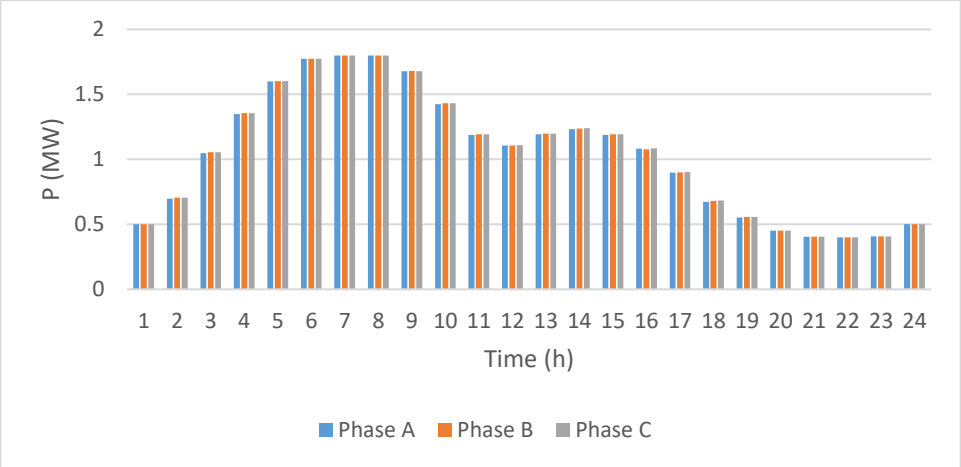

Figure 4.51: State of Charge (SoC) of ES2 with Variable VRs

4.4 Conclusion

This Chapter presented a comprehensive investigation into the coordinated operation of voltage regulators (VRs/OLTCs) and SOPs, both with and without integrated energy storage, in ADNs. The results demonstrated that when VRs/OLTCs are fixed, SOPs and SOP-ES provide valuable reactive support and power exchange capabilities, but their operation is often unbalanced across phases and places greater cycling demands on the storage units. By contrast, when VRs/OLTCs are treated as decision variables, tap ratio adjustments effectively control voltage rise, allowing SOPs and SOP-ES to operate more flexibly. In this case, SOP-ES units shift from predominantly absorptive behavior to more frequent injection, while their charging and discharging cycles exhibit reduced amplitude and shallower SoC fluctuations. This not only alleviates stress on the storage but also enhances the overall utilization of PV generation and improves system-wide voltage regulation.

Overall, the coordinated optimization of variable VRs/OLTCs with SOP and SOP-ES delivers a more balanced, efficient, and resilient distribution network, reducing power losses, improving voltage profiles, increasing renewable hosting capacity, and supporting reliable operation.

Chapter 5

Economic Operation Analysis of Soft Open Point Integrated with Energy Storage Systems

Abstract

This chapter transitions from technical optimization to economic analysis, developing a cost-driven operational framework for Soft Open Points integrated with Energy Storage (SOP-ES) in Active Distribution Networks (ADNs). While Chapters 3 and 4 focused on loss reduction, voltage regulation, and device coordination, this chapter formulates and solves a comprehensive economic model that integrates three key cost components: time-of-use (TOU) grid purchase costs, battery degradation costs, and PV curtailment penalties. Using a convex Semidefinite Programming (SDP) formulation, the model co-optimizes SOP power flows and battery charging/discharging schedules to minimize total daily operational expenditure. Case studies on the IEEE 13-bus and 123-bus systems demonstrate that SOP-ES achieves substantial cost savings (22–37% vs. baseline) through energy arbitrage, peak shaving, and loss reduction. Crucially, the analysis reveals that explicitly pricing battery degradation moderates storage cycling without significantly compromising energy-cost benefits, thereby extending battery lifetime while maintaining economic efficiency. The results establish SOP-ES not only as a technical asset but as an economically viable investment that balances immediate operational savings with long-term asset sustainability.

5.1 Introduction

Day-ahead operation of modern distribution networks is increasingly driven by economic objectives: minimizing energy procurement costs under time-of-use (TOU) tariffs, accounting for network and converter losses, avoiding renewable curtailment penalties, and managing battery degradation so that short-term savings do not compromise long-term asset life. SOPs enhance spatial flexibility by steering power between feeders, and when combined with ES, SOP-ES units add temporal flexibility by performing energy arbitrage charging during low-price hours and discharging during peak-price periods. As a result, an extensive body of research now formulates the economic scheduling of SOP-ES as an optimization problem that jointly balances grid purchases, loss costs, degradation, and, in some cases, curtailment penalties.

Several studies have highlighted the potential economic benefits of SOP-ES. For example, the authors in [8] developed an optimal operation model for SOP-based energy storage that explicitly considers battery lifetime costs through a mixed-integer linear programming (MILP) approach. Their IEEE-33 feeder case study showed that SOP-ES reduces grid purchase costs and loss costs compared with SOP-only operation, while degradation modeling prevents excessive cycling and lowers overall cost. Similarly, [126] proposed an SOCP-based economic operation model for ES-integrated SOPs, demonstrating that ES integration relaxes feeder power-coupling constraints and enhances arbitrage opportunities, leading to improved economic performance on a modified IEEE-33 system.

A more detailed cost modeling approach was adopted in [100], which developed a robust mixed-integer convex framework explicitly incorporating subsystem losses (AC-DC, DC-DC, and battery interface). This study revealed that constant-efficiency assumptions underestimate true converter costs, leading to suboptimal arbitrage schedules, and demonstrated the value of loss-dependent cost modeling. Other works, such as [105], extend

the scope to mixed-integer nonlinear economic models that co-optimize grid purchase costs, DG utilization, and demand-side management (DSM) actions, confirming the flexibility of SOP-ES in diverse economic contexts.

Beyond deterministic optimization, [125] investigated the planning economics of multi-port SOPs (MSOPs) and ESS, employing a tri-layer stochastic–robust framework to balance profitability in normal conditions with resilience under extreme scenarios. Their results reinforce the complementary value of spatial SOP and temporal ESS flexibility under realistic price and renewable uncertainty.

Furthermore, multi-time-scale operational studies (e.g., [102]) show that economically guided SoC management enables SOP-ES units to better absorb PV fluctuations, reduce curtailment, and lower purchase costs, even when integrated within broader operational frameworks.

However, existing research exhibits several limitations that this chapter addresses. Previous studies primarily focus on single optimization or using simplified degradation models without comprehensive multi-objective frameworks that systematically balance immediate costs against long-term sustainability.

To address these limitations, this chapter proposes a comprehensive economic optimization framework for SOP-ES in ADNs. The model is based on semidefinite programming (SDP), ensuring convex relaxation of the original nonlinearities and guaranteeing tractable solutions. The framework integrates TOU tariffs, PV generation profiles, degradation costs, and curtailment penalties into a single objective function. By jointly coordinating SOP power flows and ES schedules, the method minimizes total operating cost while satisfying network constraints.

While the previous chapters of this thesis demonstrated the technical benefits of SOP-ES, in terms of loss reduction, voltage regulation, and unbalance mitigation, this chapter examines the economics of SOP-ES independently of technical performance. Specifically, it quantifies cost savings achievable under SOP-ES operation, explores the trade-off between degradation costs and curtailment avoidance, and compares baseline, SOP-only, and SOP-ES scenarios. To the best of our knowledge, this represents one of the first systematic studies to apply an SDP-based convex economic optimization of SOP-ES in unbalanced distribution networks with realistic time-series PV and load profiles. Case studies confirm that SOP-ES can deliver substantial cost reductions (up to 22-37% relative to baseline), while simultaneously improving PV utilization and moderating storage cycling.

Contributions of This Chapter

This chapter advances the state of the art on SOP-ES economic operation by providing:

- **A comprehensive cost formulation** that integrates grid purchase costs (under TOU tariffs), explicit PV-curtailment penalties, and annualized degradation costs into a single objective function.

- **An SDP-based convex optimization framework** that ensures tractability while capturing the nonlinear relationships inherent in SOP-ES scheduling.

- **Scenario-wise cost decompositions** (baseline, SOP, SOP-ES) to explicitly attribute savings to arbitrage, loss reduction, and curtailment avoidance.

- **Validation on unbalanced IEEE-13 and IEEE-123 feeders**, extending beyond the balanced IEEE-33 case commonly used in prior studies.

5.2 Modeling of Economic Components

The economic operation of SOP-ES is evaluated by considering three main cost components: (i) grid purchase cost, (ii) battery degradation cost, and (iii) PV curtailment penalty. Each of these elements contributes to the overall economic performance of the distribution network and is mathematically formulated as follows.

5.2.1 Grid Purchase Cost

The cost of electricity purchased from the main grid is modeled under a time-of-use (TOU) pricing scheme [126]. At each time interval *h*, the purchase cost is expressed as:

$$C_{\text{grid}} = \sum_{h=1}^{H} \pi_h \, . P_h^{grid} \tag{5.1}$$

where:

- π_h is the unit electricity price at time interval *h* (£/MWh),
- P_h^{grid} is the active power drawn from the grid (MW),
- *H* is the total number of time intervals in the scheduling horizon.

This term represents the direct expenditure for energy procurement. Minimization of grid purchases during high-price hours incentivizes the use of SOP-ES for arbitrage and local balancing.

5.2.2 Battery Degradation Cost

Battery cycling leads to wear, capacity fade, and reduced lifetime. To capture this effect, the degradation cost is modeled as a function of energy throughput:

$$C_{deg} = \sum_{h=1}^{H} c_{deg} \cdot \left(\left|P_h^{ES,ch}\right| + \left|P_h^{ES,dis}\right|\right) \tag{5.2}$$

where:

- c_{deg} is the degradation cost coefficient (£/MWh),
- $P_h^{ES,ch}$ and $P_h^{ES,dis}$ are charging and discharging powers at time interval h.

This cost discourages excessive charging/discharging cycles and balances short-term arbitrage savings with long-term battery health. The economic lifetime (years) is modeled as:

$$E_{\text{life}}^{(\text{econ})} = \frac{C_{\text{rep}}}{c_{\text{deg}}} \tag{5.3}$$

$$\text{Years} \approx \frac{E_{\text{life}}^{(\text{econ})}}{365 \times E_{\text{day}}^{ES}} \tag{5.4}$$

$$E_{\text{day}}^{ES} = \sum_{h=1}^{H} \left(\left|P_h^{ES,ch}\right| + \left|P_h^{ES,\text{ dis}}\right|\right) \cdot \Delta t \tag{5.5}$$

Where C_{rep} is the assumed installed replacement cost (£), and Δt is the time step in hours.

5.2.3 PV Curtailment Penalty

Curtailment of PV generation reduces renewable energy utilization and may be associated with economic or environmental penalties. The curtailment penalty coefficient c_{curt} is held constant as this study employs a deterministic day-ahead scheduling framework, where fixed penalties are standard for reflecting average opportunity costs of curtailed renewable energy, consistent with related economic dispatch studies [8, 126]. The penalty is modeled as:

$$C_{\text{curt}} = \sum_{h=1}^{H} c_{\text{curt}} \cdot P_h^{\text{curt}} \tag{5.6}$$

where:

- c_{curt} is the curtailment penalty factor (£/MWh),
- P_h^{curt} is the curtailed PV power at time interval h.

Including this term ensures that the optimization favors maximum PV utilization whenever possible, thereby aligning economic operation with sustainability objectives.

5.3 Economic Objective Function

By combining the three cost components defined in Section 5.2, the total operating cost of the network is expressed as:

$$C_{\text{total}} = C_{\text{grid}} + C_{\text{deg}} + C_{\text{curt}} \tag{5.7}$$

Substituting the individual terms gives the final single-objective optimization problem:

$$minC_{\text{total}} = \sum_{h=1}^{H} \left(\pi_h P_h^{\text{grid}} + c_{\text{deg}} \left(\left| P_h^{ES,\,\text{ch}} \right| + \left| P_h^{ES,\,\text{dis}} \right| \right) + c_{\text{curt}} P_h^{\text{curt}} \right) \quad (5.8)$$

Interpretation:

- The first term captures energy procurement cost from the grid.
- The second term accounts for battery degradation, preventing myopic overuse of storage.
- The third term penalizes PV curtailment, promoting renewable integration.

Thus, the objective function jointly optimizes the trade-offs among energy cost reduction, renewable utilization, and long-term asset sustainability. These costs are not treated as separate objectives but are combined into a single unified cost function.

5.4 Constraints and SOP-ES Operational Model

The economic optimization framework of Section 5.3 is subject to the same electrical and operational constraints introduced in the technical operation chapter (Chapter 3). For completeness, the key elements are briefly summarized here:

5.4.1 Power Flow Constraints

- Active and reactive power balance across each feeder segment is enforced through semidefinite relaxation of the branch flow model.
- Bus voltage magnitudes are maintained within statutory limits [0.9,1.1] p.u.

5.4.2 SOP-ES Operating Limits

- Power exchange between terminals follows DC-link conservation, i.e., total injected active power equals total absorbed active power, minus converter losses.

$$P_{\varphi,i,t}^{\mathrm{SOP-ES}} + P_{\varphi,j,t}^{\mathrm{SOP-ES}} + P_{m,t}^{\mathrm{SOP-ES}} + P_{\varphi,i,t}^{\mathrm{SOP-ES,L}} + P_{\varphi,j,t}^{\mathrm{SOP-ES,L}} = 0 \tag{3.1}$$

- Each SOP-ES terminal must satisfy converter capacity constraints:

$$\sqrt{\left(\mathrm{P}_{\varphi,\mathrm{i,t}}^{\mathrm{SOP-ES}}\right)^2 + \left(\mathrm{Q}_{\varphi,\mathrm{i,t}}^{\mathrm{SOP-ES}}\right)^2} \leq \mathrm{S}_{\mathrm{max}}^{\mathrm{AC-DC}} \tag{3.7}$$

5.4.3 Energy Storage Constraints

- Charging/discharging power is bounded by device ratings:

$$-\mathrm{P}_{\mathrm{max}}^{\mathrm{ES}} \leq \mathrm{P}_{\mathrm{m,t}}^{\mathrm{ES}} \leq \mathrm{P}_{\mathrm{max}}^{\mathrm{ES}} \tag{3.13}$$

- State of charge (SoC) dynamics are enforced by:

$$\mathrm{SoC}_{\mathrm{t+1}} = \mathrm{SoC}_{\mathrm{t}} - \left(\mathrm{P}_{\mathrm{m,t}}^{\mathrm{ES}} + \mathrm{P}_{\mathrm{m,t}}^{\mathrm{ES,L}}\right)\Delta\mathrm{t} \tag{3.12}$$

- SoC must remain within minimum and maximum bounds.

$$\mathrm{SoC}_{\min} \leq \mathrm{SoC}_{t} \leq \mathrm{SoC}_{\max} \tag{3.14}$$

5.4.4 OLTC/Voltage Regulator Constraints

In this chapter, only fixed-tap operation is considered; tap settings follow the OpenDSS IEEE test-feeder defaults. A detailed derivation of the SDP relaxation, SOP converter modeling, was presented in Chapter 3, these constraints are retained unchanged as defined in Section 3.3.

5.5 Case Studies and Results

To ensure consistency and comparability, the same distribution feeders, PV penetration levels, and SOP placements as in Chapter 3 are used for the economic analysis. Specifically, the IEEE 13-bus and IEEE 123-bus systems are employed, with PVs and SOPs allocated at the same buses as in technical operation studies. The optimization horizon remains 24 hours with identical load and PV generation profiles.

TOU tariffs are adopted to capture the variability of electricity prices across the day, following the formulation principle in [126], in which the peak price is £0.9/kWh (10:00-13:00,17:00-21:00), and the normal price is £0.6/kWh (6:00-10:00,13:00-17:00,21:00-24:00), and £0.3/kWh (0:00-6:00). This pricing structure incentivizes load shifting and arbitrage, thereby enabling SOP-ES units to reduce grid purchase costs by charging during low-price hours and discharging when prices peak.

Following prior studies [8], [127], [126], the battery degradation cost coefficient is set to £20/MWh, while the PV curtailment penalty is set to £50/MWh. Each energy storage unit

has a rated capacity of 2000 kWh (2 MWh) and an installed replacement cost of £200/kWh, i.e., £400,000 per unit. The SoC starts at 0.5 and is constrained to 0.2–0.9, implying a usable DoD of 0.7. These settings align with typical SOP-ES economic optimization studies and ensure tractable scheduling under TOU tariffs.

While Chapter 3 examined the technical impacts of SOP-ES integration (loss reduction, voltage deviation, and unbalance), this chapter focuses exclusively on economic performance, evaluating grid purchase costs, battery degradation costs, and PV curtailment penalties under different coordination scenarios.

5.5.1 Case Study: IEEE 13-Node Test Feeder

Table 5.1 summarizes the daily cost breakdown for the baseline, SOP, and SOP-ES scenarios. In the baseline, total expenditure is £18,941.7/day, dominated by grid purchases (£17,082.2/day) and notable line-loss cost (£1,859.5/day), with no storage flexibility and zero curtailment penalties. Adding SOP alone delivers a modest saving of £325.3/day (~1.72%), mainly by trimming resistive losses (line-loss cost falls to £1,678.4/day), while grid purchases although have been reduced but not that much (£16,938/day) because SOP cannot arbitrage time-varying prices.

In contrast, SOP-ES significantly reshapes the cost profile. Considering degradation priced in the objective, grid purchases drop to £11,204.2/day (≈−34% vs baseline) and line-loss cost collapses to £300.7/day (≈−84%), yielding a total cost of £11,879.95/day, a reduction of £7,061.75/day (≈37.3%) relative to baseline. PV curtailment remains zero in all cases, indicating that available flexibility was sufficient to fully accommodate renewable output without penalties. Finally, comparing the two SOP-ES variants shows that including degradation cost leads the optimizer to cycle the batteries less (degradation £375.06/day vs £443.58/day without the penalty) and, importantly, achieves a slightly lower total cost

(£11,879.95/day vs £11,931.86/day). In short, SOP-ES delivers large economic gains via TOU arbitrage and loss reduction, and explicitly pricing battery wear improves not harms overall economic efficiency.

Table 5.1: Results with Fixed OLTC Tap Ratios

Scenario	Grid (£/day)	Curtail (£/day)	Degradation (£/day)	Line Loss (£/day)	Total (£/day)	Savings vs Baseline
Baseline	17,082.20	0.00	—	1,859.50	18,941.70	—
SOP	16,938.00	0.00	—	1,678.40	18,616.40	£325.30 (1.72%)
SOP-ES (degradation not considered)	11,196.21	0.00	443.58	292.07	11,931.86	£7,009.84 (37.00%)
SOP-ES (degradation considered)	11,204.19	0.00	375.06	300.70	11,879.95	£7,061.75 (37.28%)

Comparing Tables 5.2 and 5.3 shows that including degradation cost in the objective leads the optimizer to cycle the batteries less: the total daily throughput falls from 22.179 MWh/day (no degradation priced) to 18.753 MWh/day (with degradation priced). Thus, lower energy throughput directly reduces wear on both units—ES1 drops from 9.906 → 8.882 MWh/day and ES2 from 12.273 → 9.870 MWh/day. Given the same lifetime energy budget (20,000 MWh per unit), the lower daily throughput lengthens the implied economic life, ES1 increases from 5.53 → 6.17 years and ES2 from 4.46 → 5.55 years.

These results are lower daily degradation cost, longer service life, and nearly the same (slightly better) total operating cost, demonstrating that valuing degradation guides the schedule toward a more sustainable use of storage.

Table 5.2. SOP-ES without degradation priced in the objective

ES Unit	Daily Throughput (MWh)	Annual Throughput (MWh/y)	Implied Economic Life (years)
ES1	9.906	3,615.6	5.53
ES2	12.273	4,479.8	4.46

Table 5.3. SOP-ES with degradation priced in the objective

ES Unit	Daily Throughput (MWh)	Annual Throughput (MWh/y)	Implied Economic Life (years)
ES1	8.882	3,242.0	6.17
ES2	9.870	3,602.7	5.55

Figure 5.1 shows ES1–ES2 SoC trajectories alongside the TOU tariff [126]. Both units charge progressively during the low-price window (≈ h1–h6), reaching a high SoC plateau around h7–h9 when the tariff steps up. During the midday high-price period (≈ h11–h13) the schedules avoid grid purchases and partially discharge to support the feeder. They then recharge at mid-tariff (≈h14–h18) to stage for the peak, followed by evening discharge (≈h18–h21) that serves local demand and reduce substation imports.

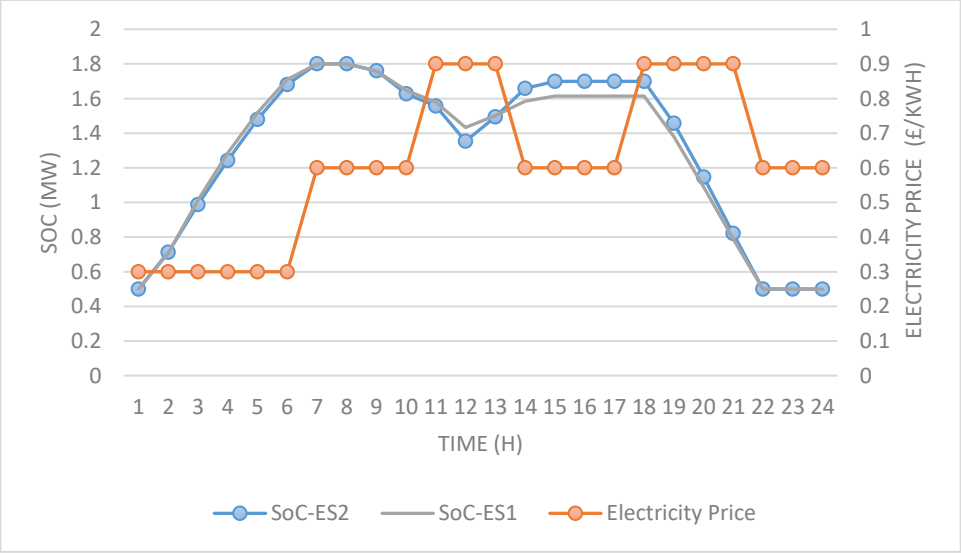

Figure 5.1. SoC of ES1 and ES2 over 24 h with TOU price

Figure 5.2 shows that, unlike the baseline which imports heavily in the morning/evening and swings at midday, SOP-ES charges during low-price hours and discharges during high-price hours. This reduces purchases when prices peak and shifts them to cheaper periods.

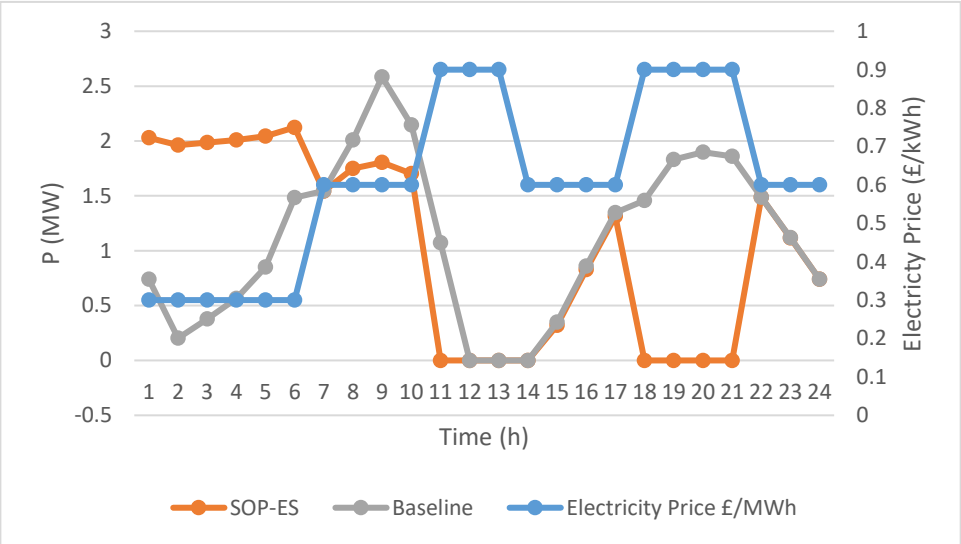

Figure 5.2. Substation Purchases with SOP-ES vs Baseline

Figures (5.3, 5.4) compare SoC trajectories with and without explicit degradation cost. With degradation priced, both ES units display lower midday dips and slightly softer evening peaks, i.e., fewer deep cycles and shorter time near the bounds. The schedules still exploit the major price spreads but avoid marginal trades that add wear for minimal savings.

This visual behavior is consistent with the quantitative result reported earlier (daily throughput falls from 22.179 → 18.753 MWh/day), and with the corresponding extension of implied lifetime under the same lifetime-energy budget.

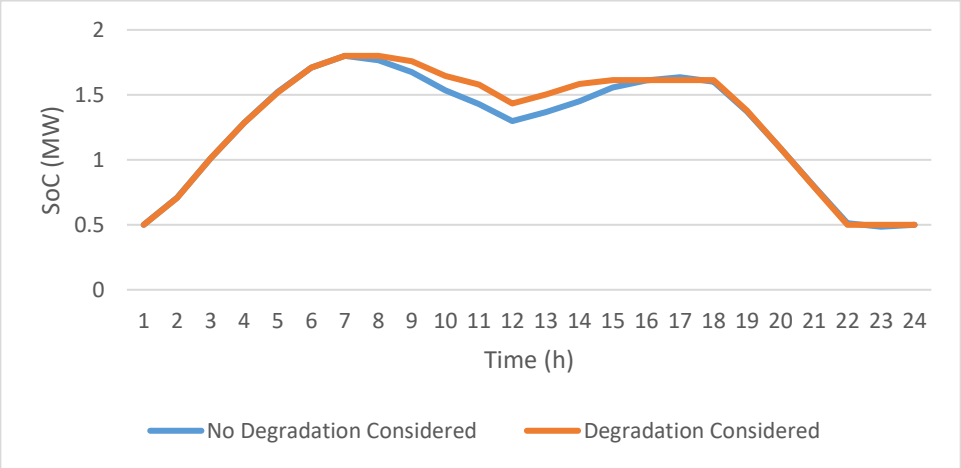

Figure 5.3. SoC of ES1 with and without degradation pricing

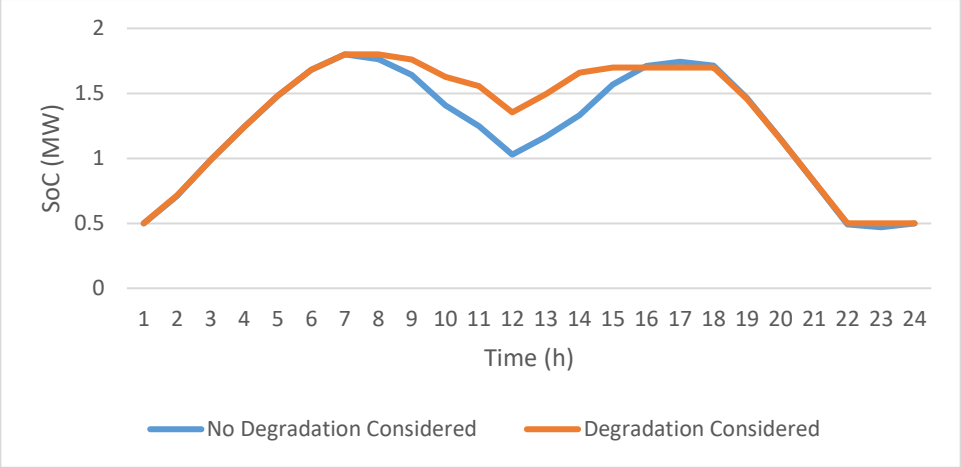

Figure 5.4. SoC of ES2 with and without degradation pricing

Figure 5.5 plots hourly U_{max} and U_{min} across scenarios. All cases stay well within the statutory limits [0.90, 1.10] p.u. The SOP-ES case yields the tightest envelope, keeping U_{min} elevated and lowering U_{max}, thus sitting closest to the preferred operating band [0.97, 1.03] p.u. By contrast, baseline shows the widest spread with a deeper midday dip; SOP narrows this spread, and SOP-ES narrows it further.

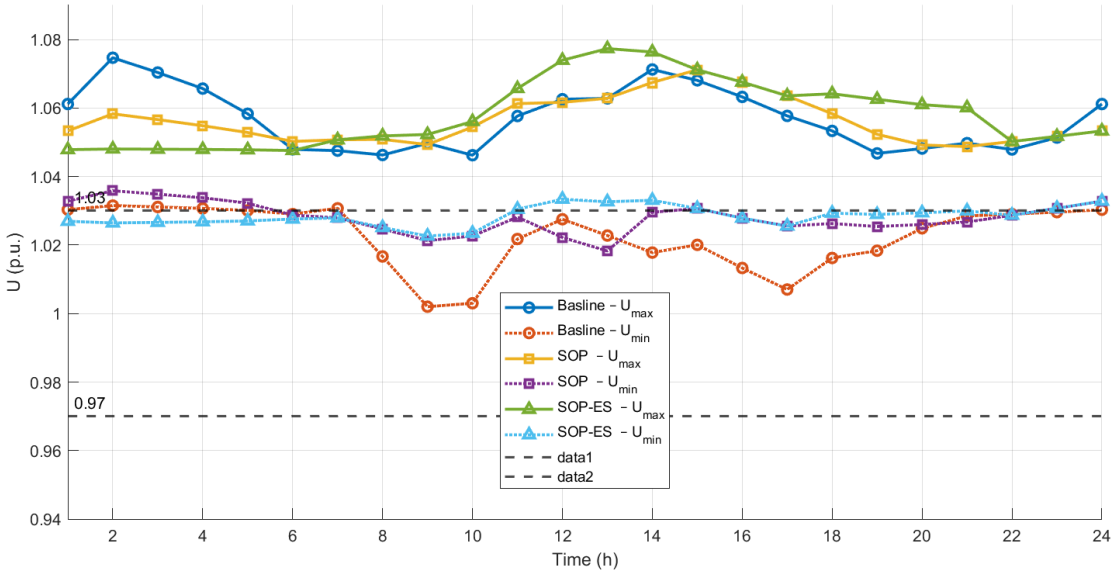

Figure 5.5. Maximum and minimum system voltage for all scenarios

5.5.2 Case Study: IEEE 123-Node Test Feeder

Table 5.4 reports the daily cost breakdown for the Baseline, SOP, and SOP-ES scenarios on the IEEE-123 bus feeder. SOP delivers a modest saving over Baseline £324/day (1.3%) driven mainly by reduced line losses. Adding ES produces the step change: grid cost drops from £24,507.94 to £18,540/day, lowering the total to £19,363.85/day. With degradation priced, the total improves slightly to £19,349.18/day as the degradation charge falls (478.15 → 462.92 £/day) while grid and loss costs remain essentially unchanged. PV curtailment costs are zero across all scenarios, indicating that the feeder can absorb available PV without curtailment; in SOP-ES, this is enabled by shifting/redistribution via storage and SOP. Overall savings reach £5,667.95/day (22.65%) versus Baseline, showing that degradation pricing regulates cycling and wear without reducing the core energy-cost benefits of SOP-ES.

Table 5.4: Results with Fixed OLTC Tap Ratios for Case Study IEEE-123

Scenario	Grid (£/day)	Curtail (£/day)	Degradation (£/day)	Line Loss (£/day)	Total (£/day)	Savings vs Baseline
Baseline	24,507.94	0.00	—	509.19	25,017.13	—
SOP	24,346.84	0.00	—	346.13	24,692.97	£324.16 (1.3%)
SOP-ES (degradation not considered)	18,539.96	0.00	478.15	345.74	19,363.85	£5,653.28 (22.6%)
SOP-ES (degradation considered)	18,540.23	0.00	462.92	346.03	19,349.18	£5,667.95 (22.65%)

Comparing Tables 5.5 and 5.6 (IEEE-123) shows that pricing degradation modestly reduces daily cycling while extending estimated life. ES1 throughput falls from 9.985 → 9.532 MWh/day (≈4.54%), increasing its estimated economic life from 5.49 → 5.75 years; ES2 drops from 13.922 → 13.614 MWh/day (≈2.21%), with life rising from 3.94 → 4.02 years. Aggregated over both units, daily throughput decreases by 0.761 MWh/day (≈3.18%). The reduction is more pronounced for ES1, suggesting stronger locational or sensitivity benefits from softer cycling at its placement. Overall, degradation-aware scheduling preserves economic performance while reducing wear, yielding longer estimated service life with only minor changes to dispatch profiles.

Table 5.5. SOP-ES without degradation priced in the objective for IEEE-123 case

ES Unit	Daily Throughput (MWh)	Annual Throughput (MWh/y)	Implied Economic Life (years)
ES1	9. 985	3,644.7	5.49
ES2	13.922	5,081.6	3.94

Table 5.6. SOP-ES with degradation priced in the objective for IEEE-123 case

ES Unit	Daily Throughput (MWh)	Annual Throughput (MWh/y)	Implied Economic Life (years)
ES1	9.532	3,479.3	5.75
ES2	13.614	4,969	4.02

Figure 5.6 shows SoC of ES with TOU tariff. Both ES units charge during low-price hours (h1–h6) and hold near the upper band through h7–h10. They partially discharge across the midday high-price block (≈h11–h14), charging at mid tariff (≈h15–h18), then discharge again during the evening high price (≈h18–h20) before returning to the lower bound overnight.

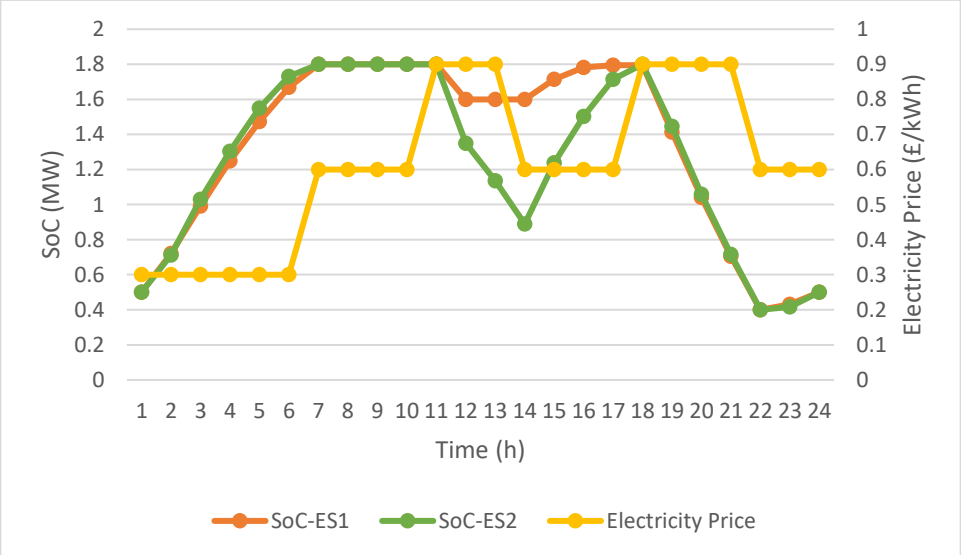

Figure 5.6. SoC of ES1 and ES2 over 24 h with TOU price

The substation purchased electricity (Baseline vs SOP-ES) with TOU tariff is shown in Figure 5.7. Relative to Baseline, SOP-ES shifts purchases into low-price periods and drives them toward zero across high-price windows (≈h11–h13 and ≈h18–h21). Baseline shows pronounced peaks that persist into expensive hours, whereas SOP-ES suppresses these by

charging off-peak and discharging on-peak.

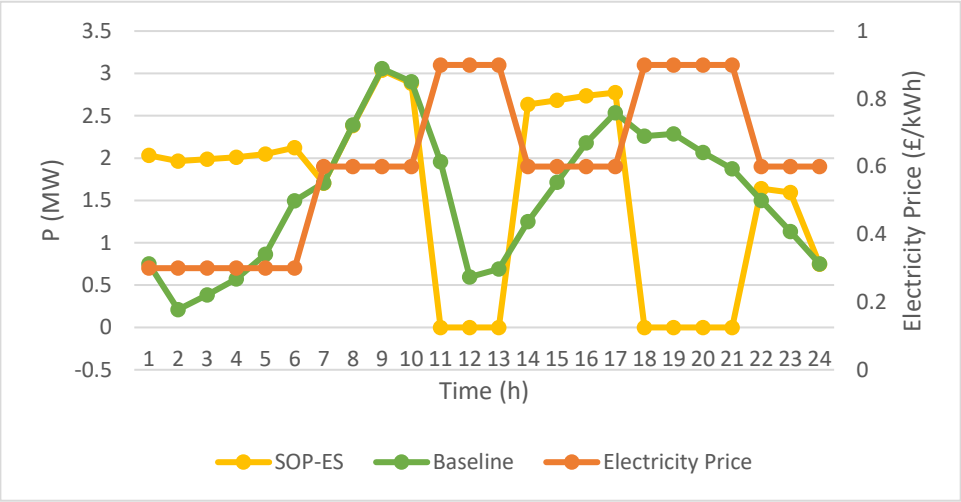

Figure 5.7. Substation Purchases with SOP-ES vs Baseline for IEEE-123 Case

Figures (5.8, 5.9) compare SoC with and without degradation cost. The two curves largely coincide in timing; with degradation priced, SoC shows slightly shallower midday dips and softer evening peaks, reflecting reduced cycling depth with unchanged dispatch schedule.

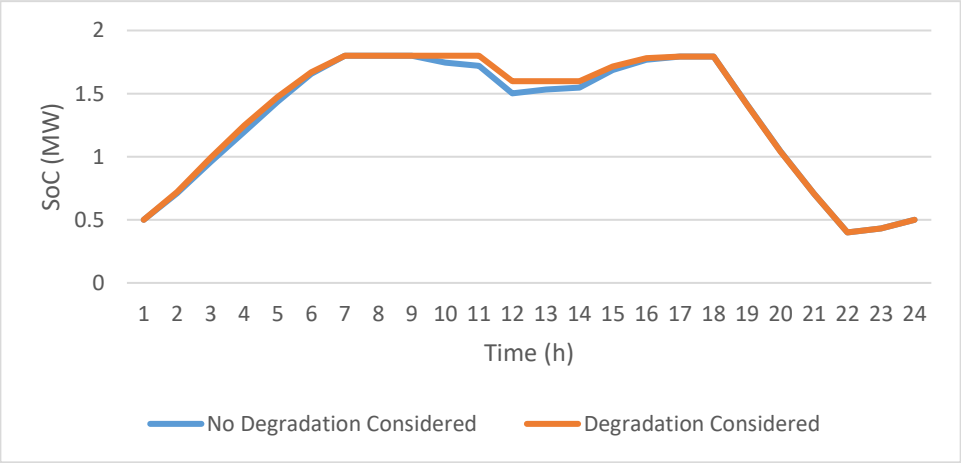

Figure 5.8. SoC of ES1 with and without degradation pricing

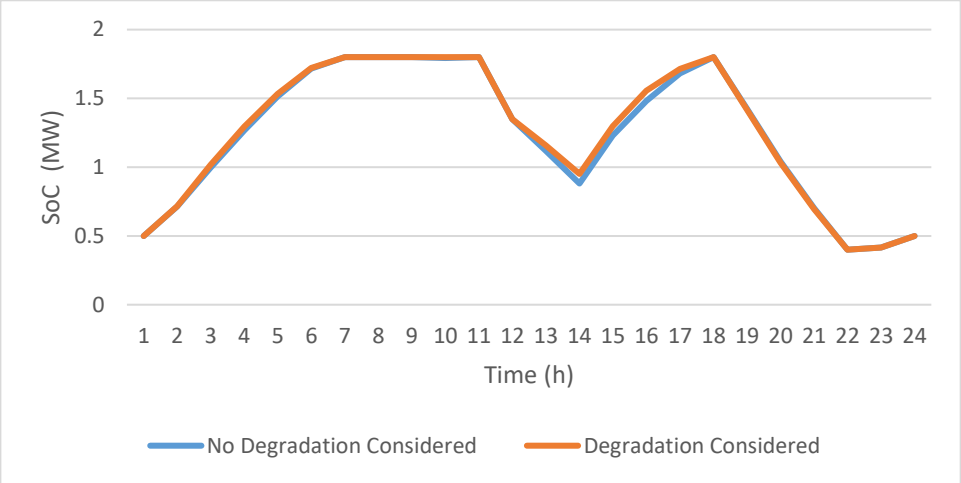

Figure 5.9. SoC of ES2 with and without degradation pricing

Figure 5.10 shows hourly voltage profile U_{max} and U_{min} across scenarios. All cases satisfy the statutory limits [0.90,1.10] p.u. The Baseline exhibits shallow midday dips in U_{min} (≈0.99 p.u. around h9–10 and h16–17) and a wider max–min spread. Introducing SOP lifts U_{min} to ~1.00 p.u. throughout the day. SOP-ES further tightens the envelope: U_{min} remains pinned near 1.00 p.u. while U_{max} stays below ~1.10 p.u., yielding the most centered and compact voltage range relative to the reference band [0.97,1.03] p.u.

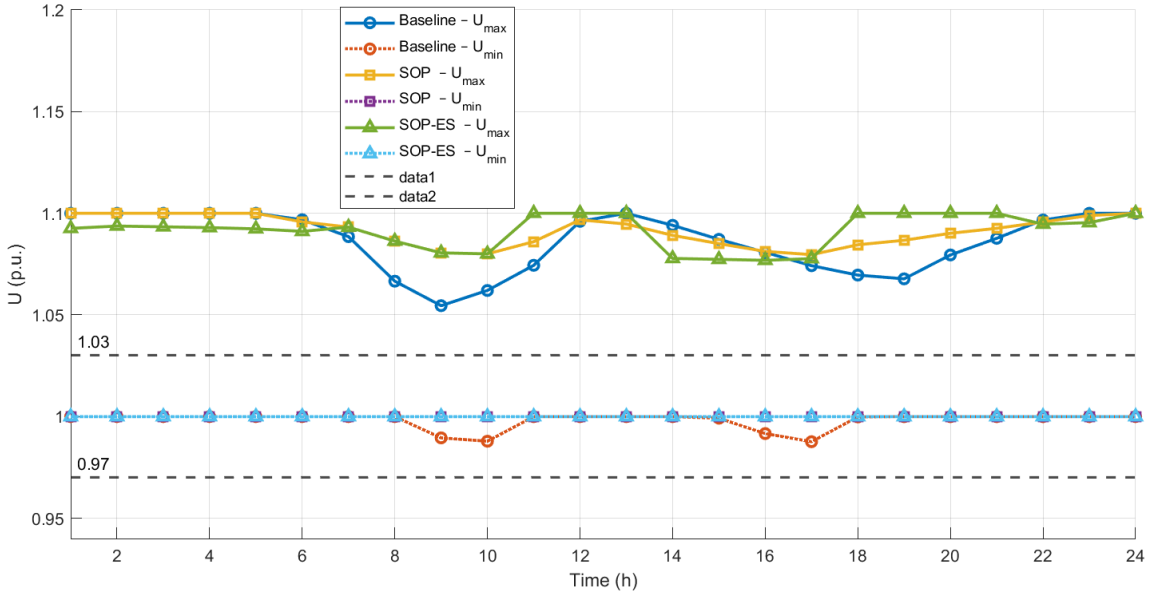

Figure 5.10. Maximum and minimum system voltage of IEEE-123 for all scenarios

5.6 Conclusion

This chapter showed that coupling storage with SOP delivers the dominant economic gains while preserving technical quality on both IEEE-13 and IEEE-123 feeders. Relative to Baseline, SOP alone provides only modest savings (≈1.3-1.7%) mainly from lower line losses, whereas SOP-ES achieves a step change by time-shifting energy: it charges in low-price hours and discharges in high-price hours, drives purchases toward zero across peak-tariff windows, a 37.3% saving versus Baseline, and keeps voltages within limits. When degradation is priced, cycling moderates (total daily throughput 22.179 → 18.753 MWh/day), and the estimated life extends (ES1: 5.53 → 6.17 years; ES2: 4.46 → 5.55 years) with negligible loss of energy-cost benefit. Voltages remain within limits and PV curtailment is not required.

On IEEE-123, SOP-ES reduces total daily cost to £19,349/day (with degradation priced), a 22.65% saving versus Baseline, with zero PV curtailment and only small differences in line-loss cost across scenarios. Explicitly valuing degradation moderates cycling (total daily throughput ↓ ≈3.2%), which extends the batteries' estimated life (e.g., ES1: 5.49→5.75 years; ES2: 3.94→4.02 years) while not reducing the core energy-cost benefits—grid and loss costs remain essentially unchanged.

Overall, the results establish SOP-ES with degradation-aware scheduling as an economically efficient and asset-friendly operating strategy: it captures most arbitrage value, avoids low-yield wear, and maintains a tight voltage envelope. The findings are consistent across feeders, indicating scalability. Practical implications include lower operating expenditure, better utilization of embedded PV without curtailment, and gentler duty on storage assets. Future work should examine tariff/price uncertainty, alternative degradation models, battery replacement economics, and coordination with discrete regulation (e.g., variable OLTC) to further refine the cost–lifetime trade-off.

Chapter 6

Accelerated ADMM-Based Distributed Optimization for Real-Time Control

Abstract

This chapter addresses the scalability challenge of centralized optimization for large-scale Active Distribution Networks (ADNs) by developing a distributed, accelerated optimization framework based on the Alternating Direction Method of Multipliers (ADMM). While Chapters 3–5 presented centralized Semidefinite Programming (SDP) models for SOP-ES operation and coordination, this chapter decomposes the three-phase SDP-OPF problem into partitioned subproblems that can be solved in parallel. To overcome the slow convergence of conventional ADMM, we implement and evaluate accelerated variants, including Fast ADMM (FADMM) with Nesterov momentum and Adaptive ADMM (AADMM) with penalty parameter tuning. A hybrid stopping criterion combining absolute and relative tolerances is introduced to improve convergence detection. Case studies on the IEEE 13-bus (two-area) and IEEE 123-bus (four-area) systems demonstrate that the proposed accelerated methods reduce iteration counts by 30–50% compared to standard ADMM while maintaining solution accuracy comparable to centralized benchmarks.

6.1 Introduction

As active distribution networks (ADNs) grow in complexity with widespread DERs, power-electronic controls, and granular operational requirements centralized OPF approaches

become computationally prohibitive and lack scalability. Decomposed methods are attractive because they exploit network sparsity and locality, allow parallel solves across areas or device groups, and reduce the need for large-scale centralized solvers. Among these methods, the Alternating Direction Method of Multipliers (ADMM) has emerged as a workhorse for distributed optimization in electric power systems because it decomposes large OPF problems into smaller subproblems that can be solved locally with minimal boundary information exchange [10, 107]. Despite its simplicity, vanilla ADMM can converge slowly when residuals are ill-conditioned or when penalty/relaxation parameters are poorly tuned [128, 129].

Recent contributions in the power systems literature demonstrate that acceleration mechanisms can substantially reduce ADMM iteration counts in distributed OPF. Two families stand out. Adaptive-penalty (AADMM) schemes update the penalty parameter using residual-balancing or curvature-aware rules, achieving order-of-magnitude speedups on difficult AC-OPF instances while preserving the decentralized architecture [130, 131]. Nesterov-type accelerated ADMM (FAADMM / N-ADMM) [132], augments ADMM with predictor–corrector extrapolation to exploit momentum, often yielding significantly faster convergence in convex settings and with restart safeguards when necessary [128, 130, 133, 134].

Within three-phase distribution OPF, FAADMM with adaptive penalty has been proposed to address slow convergence and to maintain performance under non-ideal data transfer (bad/noisy measurements). That work shows that combining Nesterov extrapolation with per-area adaptive penalties markedly reduces iterations on the IEEE-123 test feeder, even when communication imperfections are present, highlighting the practical value of joint acceleration and adaptivity in realistic ADN settings [134].

Complementary advances target how to select or adapt algorithmic parameters. For quadratic

and related classes, theory provides optimal or near-optimal choices of ADMM step sizes and over-relaxation that minimize worst-case convergence factors, offering guidance to specialists about tuning beyond ad-hoc heuristics. In parallel, weighted and auto-tuned penalty designs exploit power-system structure (e.g., admittance/Hessian information) to stabilize and accelerate distributed OPF without delicate manual parameter search. These insights demonstrate that parameter adaptation whether global, or local can be as crucial to performance as the underlying decomposition structure itself. [129, 130, 135].

Building on these developments, this chapter focuses on single-time, three-phase distributed OPF formulated as a convex semidefinite program (SDP), and investigates a hybrid acceleration that combines:

(i) Nesterov-type extrapolation (FAADMM/N-ADMM style) and,

(ii) adaptive penalty updates, together with,

(iii) hybrid scaled stopping criteria and practical penalty clipping.

The accelerated ADMM literature from the previous studies, largely targets linearized OPF with vector variables and scalar consensus, whereas our setting involves an SDP relaxation with matrix-valued consensus and positive semidefinite (PSD) constraints. This introduces cone projections, Frobenius-norm residuals, and PSD-feasibility safeguards that are not covered by prior FAADMM formulations [134]. We integrate adaptive penalty adjustment with safeguarded momentum to enhance ADMM convergence for SDP-based OPF. The penalty parameter is updated globally by comparing the relative sizes of the primal and dual residuals increasing it when primal feasibility lags and decreasing it when dual feasibility dominates which maintains balanced progress toward consensus. Concurrently, when using Nesterov-type acceleration, we implement a monotonicity-aware restart rule: if residuals

begin to rise, indicating oscillatory overshoot, the momentum sequence is reset. This combined strategy of residual-balanced penalty tuning and cautious momentum control ensures stable, accelerated convergence without the numerical instability often observed in conventional accelerated ADMM applied to non-strongly convex problems like three-phase OPF.

Contributions. The chapter (i) formulates a matrix-consensus, SDP-based distributed OPF amenable to ADMM; (ii) integrates Nesterov-type extrapolation with residual-balanced adaptive penalties under scaled stopping rules; and (iii) provides implementation guidelines (penalty clipping, restart, and initialization) and empirical evidence of reduced iteration counts relative to baseline ADMM. These results complement earlier distributed OPF studies (SOCP/SDP and AC formulations) by showing how combined acceleration and adaptivity translate into practical gains in a convex three-phase setting.

6.2 Mathematical Preliminaries of ADMM

We summarize the ADMM machinery used throughout the chapter, in a form that matches the matrix-consensus structure of our distributed OPF (with semidefinite variables at area interfaces).

6.2.1 Canonical Form and Augmented Lagrangian

Consider,

$$\min_{x,z} f(x) + g(z) \text{ s.t. } Ax + Bz = c, \tag{6.1}$$

with closed, proper, convex f, g. The (scaled) augmented Lagrangian with penalty $\rho > 0$

and scaled dual u is,

$$\mathcal{L}_\rho(x,z,u) = f(x) + g(z) + \frac{\rho}{2}\|Ax + Bz - c + u\|_2^2 - \frac{\rho}{2}\|u\|_2^2. \tag{6.2}$$

The ADMM iterations are,

$$x^{k+1} := \arg\min_x f(x) + \frac{\rho}{2}\|Ax + Bz^k - c + u^k\|_2^2, \tag{6.3}$$

$$z^{k+1} := \arg\min_z g(z) + \frac{\rho}{2}\|Ax^{k+1} + Bz - c + u^k\|_2^2, \tag{6.4}$$

$$u^{k+1} := u^k + (Ax^{k+1} + Bz^{k+1} - c). \tag{6.5}$$

6.2.2 Consensus ADMM

Let $\mathcal{B}$ be the set of inter-area interfaces and let the global consensus variable be block-structured $z = \{z_e\}_{e\in\mathcal{B}}$. For G areas with local variables x_g and global boundary copies z, the consensus ADMM form is:

$$\min_{\{x_g\},z} \sum_{g=1}^{G} f_g(x_g) \text{ s.t. } A_g x_g - z = 0, \forall g, \tag{6.6}$$

where A_g selects boundary blocks (voltages/power flows) from x_g that must agree with the corresponding global copies in z.

With scaled duals u_g and penalty $\rho > 0$, one ADMM iteration reads:

$$\text{(Local)} \qquad x_g^{k+1} := \arg\min_{x_g\in\mathcal{X}_g} f_g(x_g) + \frac{\rho}{2}\left\|A_g x_g - z^k + u_g^k\right\|_F^2, \tag{6.8}$$

(Consensus) (6.9)

$$z^{k+1} := \arg\min_{z} \sum_{g=1}^{G} \frac{\rho}{2} \left\| A_g x_g^{k+1} - z + u_g^k \right\|_F^2$$

(Dual) $$u_g^{k+1} := u_g^k + \left(A_g x_g^{k+1} - z^{k+1} \right), \forall g. \tag{6.10}$$

Writing the consensus step per interface $e \in \mathcal{B}$ gives the closed form

$$z_e^{k+1} = \frac{1}{G_e} \sum_{g \in \mathcal{N}(e)} \left(A_g x_g^{k+1} + u_g^k \right)_e \tag{6.11}$$

Where:

- $\mathcal{N}(e)$ = the set of areas that meet at interface e
- $G_e = |\mathcal{N}(e)|$
- u_g is the scaled dual for area g at that interface.

All norms are Frobenius ($\| \cdot \|_F$) to reflect matrix-valued consensus at interfaces blocks (e.g., submatrices of *W* in the SDP).

Given: areas $\{\mathcal{A}_g\}_{g=1}^{G}$; local feasible sets $\mathcal{X}_g$ (BFM-SDP); selectors A_g; penalty $\rho > 0$.

In the context of our three-phase SDP-OPF problem, this decomposition is applied as follows:

- **Network Partitioning:** The distribution network is divided into G geographical areas based on feeder topology. Each area g contains its own buses, branches.
- **Local Variables (x_g):** These include all voltage (v_i), current (l_{ij}), and power (S_{ij})

matrices for buses and branches inside area g.

- **Consensus Variables (z):** These represent the boundary voltages and power flows at the interfaces between adjacent areas. All areas sharing a boundary must agree on the same voltage and power flow values at that interface.

- **Selector Matrix (A_g):** This matrix extracts from x_g only the voltage and power flow submatrices corresponding to the boundary buses and tie-lines that area g shares with its neighbors.

- **Local Objective ($f_g(x_g)$):** This is typically the sum of power losses within area g, optionally including local voltage deviation terms.

- **Local Constraints (X_g):** These enforce the three-phase BFM-SDP equations, device operational limits, and voltage bounds only for components inside area g.

The consensus constraint $A_g x_g - z = 0$ thus ensures physical consistency across area boundaries: all areas must agree on the same voltages and power flows where they connect.

6.2.3 Residuals and Stopping Rules

To improve convergence detection in the distributed optimization process, we adopt a hybrid stopping criterion that combines absolute and relative tolerances for both voltage and power variables. Although this approach is recommended in general ADMM literature [10], it is not commonly applied in power system ADMM implementations. Our results show that this hybrid rule significantly reduces the required iterations compared to using fixed values, thereby improving computational efficiency without sacrificing solution quality.

Hybrid (absolute + relative) stopping thresholds make termination scale-aware: tolerances grow with the magnitude of the current iterates, so the same rule works across feeders, unit choices, and loading levels. Compared with fixed 10^{-3} thresholds, the scaled criteria avoid over-iteration on small problems and prevent premature stopping on large-magnitude variables, typically reducing iterations while preserving accuracy. This mirrors best practice in ADMM where stopping is tied to the norms of $A_g x_g$ and z, yielding more consistent convergence behavior across cases.

We monitor the primal and dual residuals:

$$r_{\text{pri}}^{k+1} := \max_g \left\| A_g x_g^{k+1} - z^{k+1} \right\|_F, r_{\text{dual}}^{k+1} := \rho \max_e \| z_e^{k+1} - z_e^k \|_F. \tag{6.11}$$

We employ hybrid (scaled) tolerances (absolute + relative):

$$\begin{aligned} \varepsilon_{\text{pri}} &= \sqrt{2}\varepsilon_{\text{abs}} + \varepsilon_{\text{rel}} \cdot \max\left(\max_g \left\| A_g x_g^{k+1} \right\|_F, \| z^{k+1} \|_F \right), \\ \varepsilon_{\text{dual}} &= \sqrt{2}\varepsilon_{\text{abs}} + \varepsilon_{\text{rel}} \cdot \max(\| z^{k+1} \|_F, \| z^k \|_F), \end{aligned} \tag{6.12}$$

and stop when $r_{\text{pri}}^{k+1} \le \varepsilon_{\text{pri}}$ and $r_{\text{dual}}^{k+1} \le \varepsilon_{\text{dual}}$. (Typical: $\varepsilon_{\text{abs}} = 10^{-4}, \varepsilon_{\text{rel}} = 10^{-3}$.)

Algorithm 1: Consensus ADMM

For $k = 0,1,2, \ldots$ do

1. Local solves (area g, parallelizable):

$$x_g^{k+1} \leftarrow \arg \min_{x_g \in \mathcal{X}_g} f_g(x_g) + \frac{\rho}{2} \left\| A_g x_g - z^k + u_g^k \right\|_F^2 \text{ for all } g.$$

2. Consensus (per interface e):

$$z_e^{k+1} \leftarrow \frac{1}{G_e} \sum_{g \in \mathcal{N}(e)} \left(A_g x_g^{k+1} + u_g^k \right)_e$$

3. Dual update (per area g):

$$u_g^{k+1} \leftarrow u_g^k + \left(A_g x_g^{k+1} - z^{k+1}\right).$$

4. Residuals:

$$r_{\text{pri}}^{k+1} \leftarrow \max_g \left\| A_g x_g^{k+1} - z^{k+1} \right\|_F,$$

$$r_{\text{dual}}^{k+1} \leftarrow \rho \max_e \| z_e^{k+1} - z_e^k \|_F.$$

if $r_{\text{pri}}^{k+1} \le \varepsilon_{\text{pri}}$ and $r_{\text{dual}}^{k+1} \le \varepsilon_{\text{dual}} \rightarrow$ STOP.

end for

else next iteration $k = 1,2,3, \ldots$

6.2.4 Adaptive Penalty for ADMM

The ADMM penalty ρ scales how strongly the algorithm enforces consensus versus progressing along local objectives. If ρ is too small, primal agreement (consensus) is weak and the primal residual decays slowly; if ρ is too large, the method over-penalizes disagreement, causing the dual residual to dominate and local subproblems to become ill-conditioned. The adaptive rule (6.13) balances the residuals by increasing ρ when primal feasibility lags and decreasing it when dual progress lags, while clipping $\rho \in [\ \rho_{\min},\ \rho_{\max}]$ preserves numerical stability across iterations.

$$\rho \leftarrow \begin{cases} \tau_\uparrow \rho & r_{\text{pri}} > \mu r_{\text{dual}}, \\ \rho / \tau_\downarrow & r_{\text{dual}} > \mu r_{\text{pri}}, \rho \leftarrow \min(\max(\rho, \rho_{\min}), \rho_{\max}), \\ \rho & \text{otherwise}, \end{cases} \tag{6.13}$$

with $\mu = 10, \tau_\uparrow = \tau_\downarrow = 2, \rho_{\min} = 10^{-3}, \rho_{\max} = 10^3$.

Algorithm 2: Adaptive Penalty ADMM

Given: μ = 10, $\tau_\uparrow$ = 2, $\tau_\downarrow$= 2; bounds: $\rho_{\min} = 10^{-3}, \rho_{\max} = 10^3$.

for $k = 0,1,2, \ldots$ do

1. Local solves (area g, parallelizable):

$$x_g^{k+1} \leftarrow \arg \min_{x_g \in X_g} f_g(x_g) + \frac{\rho}{2} \left\| A_g x_g - z^k + \right.$$

$u_g^k\|_F^2$ for all g.

2. Consensus (per interface e):

$$z_e^{k+1} \leftarrow \frac{1}{G_e} \sum_{g \in \mathcal{N}(e)} \left(A_g x_g^{k+1} + u_g^k\right)_e$$

3. Dual update (per area g):

$$u_g^{k+1} \leftarrow u_g^k + \left(A_g x_g^{k+1} - z^{k+1}\right).$$

4. Residuals:

$$r_{\text{pri}}^{k+1} \leftarrow \max_g \left\|A_g x_g^{k+1} - z^{k+1}\right\|_F,$$

$$r_{\text{dual}}^{k+1} \leftarrow \rho \max_e \left\|z_e^{k+1} - z_e^k\right\|_F.$$

if $r_{\text{pri}}^{k+1} > \mu \cdot r_{\text{dual}}^{k+1}$ then $\rho \leftarrow \tau_\uparrow \cdot \rho$

elseif $r_{\text{dual}}^{k+1} > \mu \cdot r_{\text{pri}}^{k+1}$ then $\rho \leftarrow \rho \,/\, \tau_\downarrow$

if $r_{\text{pri}}^{k+1} \le \varepsilon_{\text{pri}}$ and $r_{\text{dual}}^{k+1} \le \varepsilon_{\text{dual}} \rightarrow$ STOP.

end for

else next iteration $k = 1,2,3, \ldots$

6.2.5 Fast ADMM (Nesterov / FAADMM) with Restart

Nesterov-type Fast ADMM (FAADMM) expands standard ADMM with a momentum (extrapolation) step that leverages the trend of recent iterates to accelerate convergence often cutting the number of iterations substantially in convex problems. The restart safeguard preserves robustness: if the extrapolation worsens the primal/dual residuals (e.g., due to oscillation or a sudden change in ρ), momentum is reset, preventing divergence and letting the method revert to the stable baseline ADMM until acceleration becomes beneficial again. This coupling speed from momentum, stability from restart typically yields faster yet reliable convergence in practice.

Define momentum sequence:

$$\phi_{k+1} = \left(1 + \sqrt{1 + 4\phi_k^2}\right)/2 \tag{6.14}$$

And,

$$\theta_k = (\phi_k - 1)/\phi_{k+1} \tag{6.15}$$

Equations (6.16)–(6.17) apply that momentum to ADMM's consensus and dual variables after a full baseline ADMM sweep.

$$\tilde{z}^{k+1} = z^{k+1} + \theta_k(z^{k+1} - z^k) \tag{6.16}$$

$$\tilde{u}_g^{k+1} = u_g^{k+1} + \theta_k\left(u_g^{k+1} - u_g^k\right) \tag{6.17}$$

Monotone safeguard: accept $(\tilde{z}^{k+1}, \tilde{u}^{k+1})$ only if both residuals decrease, e.g., $r_{\text{pri}}^{k+1} \leq \eta r_{\text{pri}}^k$ and $r_{\text{dual}}^{k+1} \leq \eta r_{\text{dual}}^k$ with $\eta \approx 0.9999$; otherwise restart ($\phi_{k+1} \leftarrow 1$, use non-extrapolated z^{k+1}, u^{k+1}).

Algorithm 3: Fast ADMM

Given: $\eta \approx 0.9999$. Initialize:$\phi_1 = 1$.

for $k = 0,1,2,\ldots$ do

1. Local solves (area g, parallelizable):

$$x_g^{k+1} \leftarrow \arg\min_{x_g \in \mathcal{X}_g} f_g(x_g) + \frac{\rho}{2}\left\|A_g x_g - z^k + u_g^k\right\|_F^2 \text{ for all } g.$$

2. Consensus (per interface e):

$$z_e^{k+1} \leftarrow \frac{1}{G_e} \sum_{g \in \mathcal{N}(e)} \left(A_g x_g^{k+1} + u_g^k\right)_e$$

3. Dual update (per area g):

$$u_g^{k+1} \leftarrow u_g^k + \left(A_g x_g^{k+1} - z^{k+1}\right).$$

4. Residuals:

$r_{\text{pri}}^{k+1} \leftarrow \max_g \left\| A_g x_g^{k+1} - z^{k+1} \right\|_F$,

$r_{\text{dual}}^{k+1} \leftarrow \rho \max_e \| z_e^{k+1} - z_e^k \|_F$.

4. Monotone acceptance (restart test):

if ($r_{\text{pri}}^{k+1} < \eta r_{\text{pri}}^k$ and $r_{\text{dual}}^{k+1} < \eta r_{\text{dual}}^k$) then

$\phi_{k+1} = \left(1 + \sqrt{1 + 4\phi_k^2}\right)/2$, $\theta_k = (\phi_k - 1)/\phi_{k+1}$

$\tilde{z}^{k+1} \leftarrow z^{k+1} + \theta_k \cdot (z^{k+1} - z^k)$

$\tilde{u}_g^{k+1} \leftarrow u_g^{k+1} + \theta_k \left(u_g^{k+1} - u_g^k\right)$ for all g

else

$\phi_{k+1} \leftarrow 1$ (restart; $\theta_k = 0$)

$\tilde{z}^{k+1} = z^{k+1}$, $\tilde{u}_g^{k+1} = u_g^{k+1}$

end

end for

6.2.6 Proposed Method — Hybrid Accelerated ADMM for BFM–SDP

We propose a hybrid accelerated ADMM tailored to matrix-consensus SDP OPF in three-phase distribution networks. The method keeps the standard consensus ADMM backbone (local SDP solves + interface consensus + dual ascent) and couples it with three practical enhancements:

1. **Hybrid (scaled) stopping**: absolute + relative tolerances that scale with iterate magnitudes, avoiding over-iteration on small cases and premature stopping on large ones.

2. **Adaptive penalty with clipping (AADMM)**: residual balancing updates of the ADMM penalty ρ, with simple lower/upper bounds to preserve numerical stability.

3. **Nesterov extrapolation with restart (FAADMM)**: momentum on consensus and

dual variables to reduce iterations; a monotone restart rule resets momentum if residuals worsen.

Why this combination?

- Hybrid stopping typically cuts iterations versus fixed 10^{-3} thresholds by aligning tolerances to problem scale.

- Adaptive ρ balances primal and dual progress; clipping avoids runaway/vanishing ρ that can destabilize SDP solves.

- Nesterov momentum adds look-ahead and often yields further iteration reductions; restart preserves robustness in the presence of noisy residuals or sudden ρ changes.

For convex BFM–SDP with feasible consensus constraints, baseline ADMM converges under the usual assumptions for convex problems. Hybrid stopping does not alter fixed points; AADMM with clipping is a heuristic that preserves convergence in practice; FAADMM uses restart to retain the stability of vanilla ADMM while offering acceleration.

Algorithm 4: Proposed Fast ADMM

Given: μ = 10, $\tau_{\uparrow}$ = 2, $\tau_{\downarrow}$= 2; bounds: $\rho_{\min} = 10^{-3}, \rho_{\max} = 10^{3}$. $\varepsilon_{\text{abs}} = 10^{-4}, \varepsilon_{\text{rel}} = 10^{-3}$
$\eta \approx 0.9999$. Initialize:ϕ_1 = 1. penalty $\rho > 0$, count k=0

for $k = k + 1$

1. Local SDP solves (per area g):

$$x_g^{k+1} \leftarrow \arg\min_{x_g \in \mathcal{X}_g} f_g(x_g) + \frac{\rho}{2}\left\|A_g x_g - z^k + u_g^k\right\|_F^2 \text{ for all } g.$$

2. Consensus (per interface e):

$$z_e^{k+1} \leftarrow \frac{1}{G_e} \sum_{g \in \mathcal{N}(e)} \left(A_g x_g^{k+1} + u_g^k\right)_e$$

3. Dual update (per area g):

$$u_g^{k+1} \leftarrow u_g^k + \left(A_g x_g^{k+1} - z^{k+1}\right).$$

4. Residuals (Frobenius):

$$r_{\text{pri}}^{k+1} \leftarrow \max_g \left\| A_g x_g^{k+1} - z^{k+1} \right\|_F,$$
$$r_{\text{dual}}^{k+1} \leftarrow \rho . \max_e \| z_e^{k+1} - z_e^k \|_F .$$

5. Hybrid (scaled) stopping:

$$\varepsilon_{\text{pri}} \leftarrow \sqrt{2}\varepsilon_{\text{abs}} + \varepsilon_{\text{rel}} \cdot \text{ax}\left(\max_g \left\| A_g x_g^{k+1} \right\|_F, \| z^{k+1} \|_F \right)$$

$$\varepsilon_{\text{dual}} \leftarrow \sqrt{2}\varepsilon_{\text{abs}} + \varepsilon_{\text{rel}} \cdot \max(\| z^{k+1} \|_F, \| z^k \|_F)$$

if $r_{\text{pri}}^{k+1} \le \varepsilon_{\text{pri}}$ and $r_{\text{dual}}^{k+1} \le \varepsilon_{\text{dual}}$ → STOP.

end for

else

6. Fast ADMM (Nesterov extrapolation with restart):

if ($r_{\text{pri}}^{k+1} < \eta r_{\text{pri}}^k$ and $r_{\text{dual}}^{k+1} < \eta r_{\text{dual}}^k$) then

$$\phi_{k+1} = \left(1 + \sqrt{1 + 4\phi_k^2}\right)/2 \, , \theta_k = (\phi_k - 1)/\phi_{k+1}$$

$$\tilde{z}^{k+1} \leftarrow z^{k+1} + \theta_k \cdot (z^{k+1} - z^k)$$
$$\tilde{u}_g^{k+1} \leftarrow u_g^{k+1} + \theta_k \left(u_g^{k+1} - u_g^k \right) \quad \text{for all } g$$

else

$$\phi_{k+1} \leftarrow 1 \text{ (restart; } \theta_k = 0)$$
$$\tilde{z}^{k+1} = z^{k+1} \, , \quad \tilde{u}_g^{k+1} = u_g^{k+1}$$

end if

7. Adaptive ρ (residual balancing)

if $r_{\text{pri}}^{k+1} > \mu \cdot r_{\text{dual}}^{k+1}$ then $\rho \leftarrow \tau_\uparrow \cdot \rho$

else if $r_{\text{dual}}^{k+1} > \mu \cdot r_{\text{pri}}^{k+1}$ then $\rho \leftarrow \rho \, / \, \tau_\downarrow$

if $r_{\text{pri}}^{k+1} \le \varepsilon_{\text{pri}}$ and $r_{\text{dual}}^{k+1} \le \varepsilon_{\text{dual}}$ → STOP.

end for

else next iteration k=1,2,3,….

6.3 Problem Statement: BFM–SDP OPF

The same three-phase Branch-Flow Model (BFM) formulated as a Semidefinite Program (SDP), as developed in Section 3.3, is adopted here. This model based on the convex relaxation of the Baran Wu branch-flow equations for radial networks ensures exactness under typical operating conditions [106, 107]. For completeness, we restate only the items needed for the distributed decomposition; the full derivation and symbol definitions remain as in Chapter 3.

- Variables (lifted): per-bus three-phase voltage moment $W_n \in \mathbb{H}_+^3$; per-branch moments for currents/flows as defined previously.

- Objective: convex combination of loss proxy $f_{\text{loss}}(W,$ flows $)$, voltage deviation $f_{\text{volt}}(W)$.

- Constraints: three-phase branch-flow equalities/inequalities in lifted variables; voltage bounds $\underline{V}^2 I \preceq W_n \preceq \bar{V}^2 I$; line ampacity limits; device constraints; and $W_n \succeq 0$ for all n.

6.3.1 Area Partition and Interface Definition

Let the feeder be partitioned into G areas $\{\mathcal{A}_g\}$ (as specified in the case study). Each area g carries its local copy x_g of all variables indexed by $\mathcal{N}_g, \mathcal{E}_g$, plus boundary blocks (subset of W and/or flow moments) on inter-area tie lines. For each interface $e \in \mathcal{B}$, z_e collects the boundary block(s) to be shared (e.g., specific rows/cols of W_n).

Linear selection maps A_g pick from x_g the exact block matching z_e. Consensus requires $A_g x_g = z$ at every interface.

6.3.2 Distributed Formulation for BFM-SDP

$$\min_{\{x_g\},z} \sum_{g=1}^{G} f_g(x_g) \tag{6.18}$$

$$\text{s.t. } x_g \in \mathcal{X}_g(\text{BFM} - \text{SDP constraints on } \mathcal{A}_g)$$

$$A_g x_g - z = 0 \forall g. \tag{6.19}$$

Here f_g is the local contribution of losses, voltage deviation on $\mathcal{A}_g; \mathcal{X}_g$.

With the foundational variables defined in Chapter 3, the following operational constraints are established to ensure accurate modelling and control of power flows and voltages across the network.

$$\sum_{ij\in\Omega_b} \mathrm{diag}\left(S_{ij,t} - z_{ij} l_{ij,t}\right) + s_{j,t} + y_{j,t} v_{j,t} = \sum_{jk\in\Omega_b} \mathrm{diag}\left(S_{jk,t}\right) \quad (3.21)$$

$$v_{j,t} = v_{i,t} - \left(S_{ij,t} z_{ij}^H + S_{ij,t}^H z_{ij}\right) + z_{ij} l_{ij,t} z_{ij}^H \quad (3.22)$$

The voltage at each node must be maintained within specific limits to ensure safe operation and protect network equipment as in equation (6.22).

$$\underline{v_i} \leq diag\left(v_{i,t}\right) \leq \bar{v}_i \quad (3.23)$$

Where $\underline{v_i}$ and $\bar{v}_i$ represent the lower and upper voltage limits at node *i.* Equation (3.24) defines the voltage at the source node of the network.

$$v_0 = V_0^{ref}\left(V_0^{ref}\right)^H \quad (3.24)$$

Constraints (3.25) indicate the positive semidefinite constraint while the rank-1 constraint has been removed for relaxation the model.

$$\begin{bmatrix} v_{i,t} & S_{ij,t} \\ S_{ij,t}^H & l_{ij,t} \end{bmatrix} \succeq 0 \quad i \to j \quad (3.25)$$

6.4 Case Study and Results

We evaluate the proposed Hybrid Accelerated ADMM (Hybrid stop + AADMM + FAADMM) on two standard distribution feeders under a single-time operating snapshot:

- IEEE-13 bus (radial): partitioned into 2 areas connected at one tie/boundary.

- IEEE-123 bus (radial with multiple laterals): partitioned into 4 areas (consistent with geographic clustering and feeder branches).

Partition boundaries define the interfaces used by the matrix-consensus constraints. All tests use the three-phase BFM–SDP formulation from Chapter 3 but for (single time), with identical device and constraint models across methods. Power loss was used as the objective function for evaluating the performance analysis of the proposed algorithm.

We compare three ADMM algorithms:

- Baseline ADMM: fixed penalty ρ.

- AADMM (Adaptive ρ + clipping): residual-balancing update of ρ with bounds.

- FAADMM: AADMM + Nesterov extrapolation with monotone restart.

Common settings:

- Hybrid (scaled) stopping (for AADMM/FAADMM): $(\varepsilon_{\text{abs}},\varepsilon_{\text{rel}}) = (10^{-4},10^{-3})$ with Frobenius norms.

- Penalty ρ: $\rho = 1$

- AADMM parameters: $\mu = 10$, $\tau_{\uparrow} = 2$, $\tau_{\downarrow} = 2$; clip $\rho \in [10^{-3}, 10^{3}]$

- FAADMM parameters: $\phi_1 = 1$, $\eta \approx 0.999$

The proposed optimization model was implemented using the YALMIP toolbox in MATLAB R2021b, and the optimization problems were solved using the MOSEK solver.

6.4.1 Results on IEEE-13

For IEEE-13 we adopt the two-area split shown in Figure. 6.1: Area 1 (650–632–633–634 and 645–646) and Area 2 (611–684–652 and 671–680–692–675). The areas share a single interface at the 632–671 boundary, where ADMM enforces matrix-consensus on the three-phase voltage (and associated boundary blocks) via the global variable $\mathbf{z}_e$. This one-tie partition keeps communication minimal only interface quantities are exchanged each iteration while still capturing meaningful inter-area coupling.

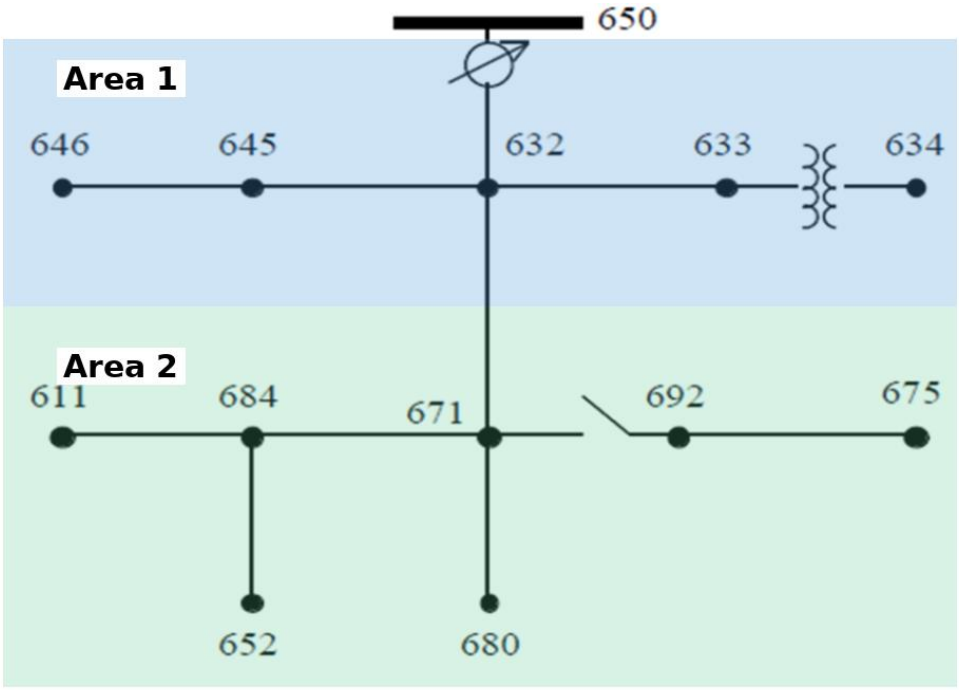

Figure 6.1: IEEE 13-bus test system with two areas

On the IEEE-13 feeder with ρ=1, all distributed variants converged to essentially the same optimum as the centralized solver total loss ≈ 0.425−0.426 kW and objective 0.54 but with markedly different iteration counts and wall-clock times. As reported in Table 6.1, baseline ADMM (fixed ρ) required 113 iterations and 41.7 s. Introducing adaptive penalty (AADMM) reduced this to 104 iterations (–8.0 %) and 37.5 s (–10.1 %), while the proposed N-ADMM + AADMM achieved the best performance at 97 iterations (–14.2 %) and 32.84 s (–21.3 %) with no loss of optimality. The convergence traces in Figures 6.2 and 6.3 validate these trends: all curves settle to the centralized loss and final objective level, but the adaptive and accelerated variants reach that neighborhood sooner and with fewer oscillations. In short, parameter adaptation already delivers measurable speed-ups over fixed-ρ ADMM, and adding Nesterov momentum on top yields the fastest convergence in both iterations and runtime without sacrificing solution quality.

Table 6.1: Performance Comparison

Method (ρ = 1)	Iterations	Total time [s]	Loss (MW)	Total-Objective
ADMM (Fixed ρ)	113	41.7	0.426	0.54
AADMM	104	37.5	0.425	0.54
N-ADMM+AADMM	97	32.84	0.426	0.54

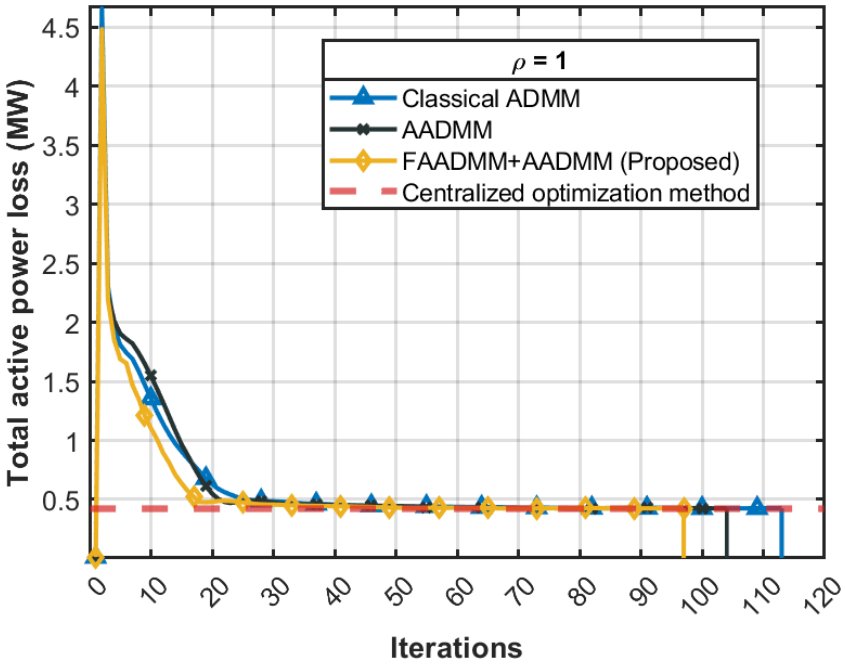

Figure 6.2: Convergence curves for loss of different ADMM methods

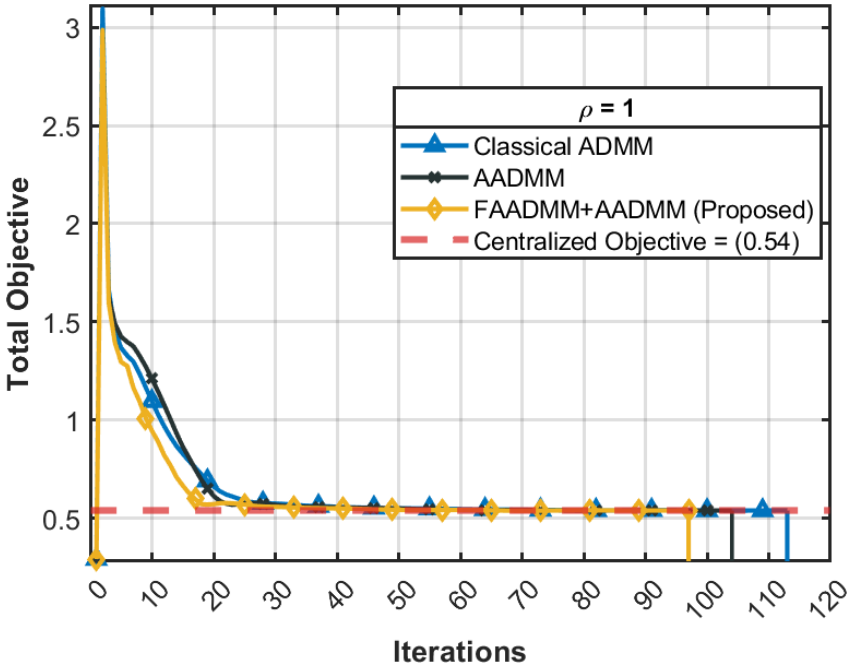

Figure 6.3: Convergence curves of different ADMM methods

Figure. 6.4 reports the primal and dual residuals versus iteration (log scale) for three distributed solvers with initial ρ =1: Classical ADMM, AADMM (residual-balanced, clipped ρ), and the proposed FAADMM+AADMM (Nesterov–type extrapolation with monotone restart plus adaptive ρ). Vertical dashed lines mark the iteration at which each run satisfied the scaled stopping test ($r_{\text{pri}}^{k} \leq \varepsilon_{\text{pri}}$, $r_{\text{dual}}^{k} \leq \varepsilon_{\text{dual}}$). These results confirm that adding momentum + adaptive penalty with clipping reduces iterations on the convex BFM–SDP IEEE-13 case without degrading solution quality.

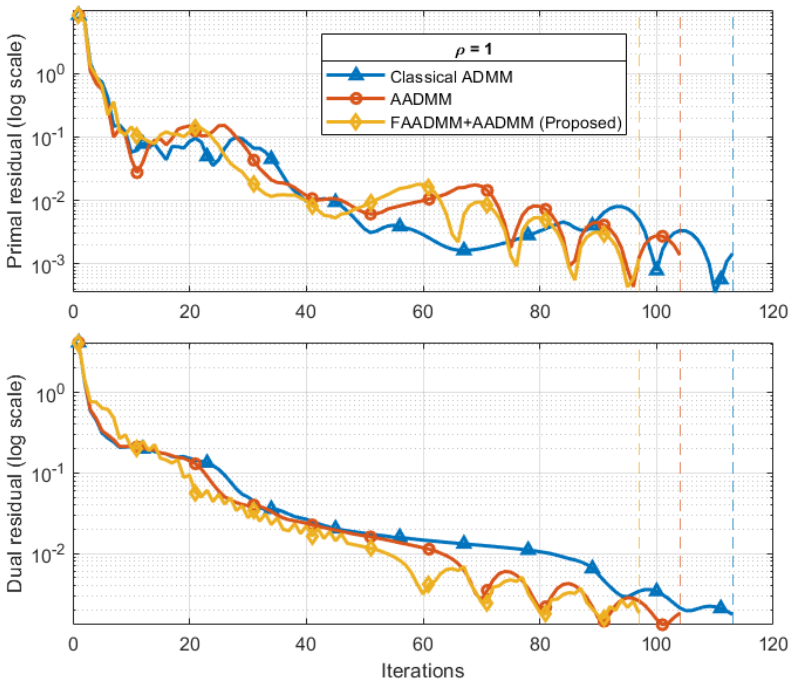

Figure 6.4: Convergence curve of primal and dual residuals

6.4.2 Results on IEEE-123

We evaluate the proposed accelerated distributed OPF on the IEEE-123 test feeder under a single operating snapshot. The feeder is partitioned into four areas as shown in Figure 6.5, reflecting a realistic multi-operator split. Each area preserves radiality internally, while tie-buses across cuts enforce matrix-valued consensus on three-phase voltage moments v and complex branch powers S via ADMM. Typical interfaces include, for example, Area 1–Area 2 (e.g., at buses 18/135), Area 1–Area 3 (e.g., 13/152), and Area 3–Area 4 (e.g., 60/160). A centralized BFM–SDP solve provides the reference objective and feasibility.

We compare three methods: (i) Classical ADMM with fixed ρ; (ii) AADMM using residual balancing with ρ-clipping; and (iii) FAADMM+AADMM (Proposed), which enhances ADMM with Nesterov-type extrapolation and a monotone restart safeguard. For each method we report iteration count, wall-clock time, total active-power loss, and primal/dual residual trajectories.

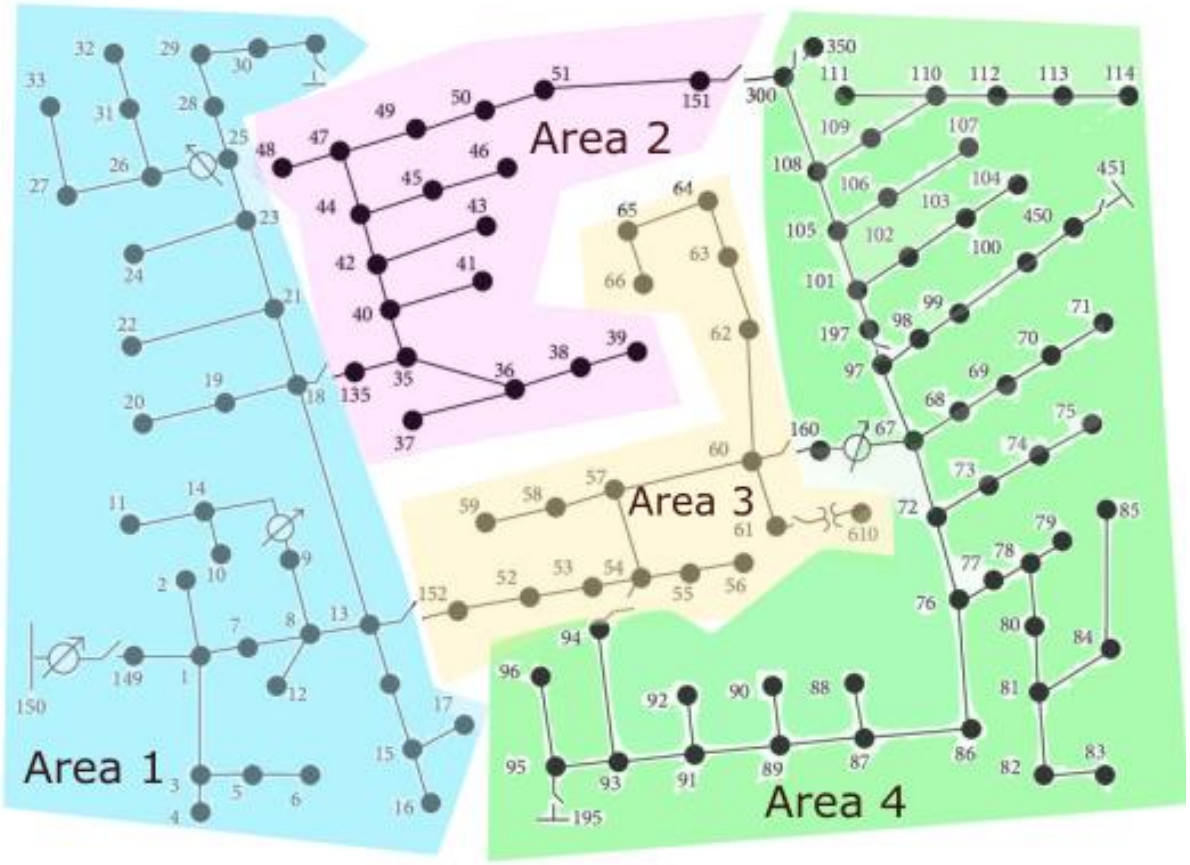

Figure 6.5: IEEE 123-bus test system with four areas

This case aims to (1) confirm that all distributed variants match the centralized objective within tolerance despite four-way coupling, and (2) quantify how adaptive ρ and momentum plus restart reduce iterations and runtime in a large, unbalanced three-phase network with multiple matrix-consensus interfaces.

Table 6.2. summarizes iteration/time improvements. Relative to Classical ADMM (91 iters, 193.6 s), AADMM converges in 57 iters (−37%) and 111s (−43%), while FAADMM+AADMM reaches feasibility in 54 iters (−41%) and 109.4 s (−44%). Loss is higher with AADMM likely because it converges in fewer iterations, potentially stopping before fully minimizing the loss function. Each iteration of ADMM can be computationally expensive, so early stopping or fewer iterations may lead to a suboptimal, higher-loss

solution compared to methods that run longer or refine more gradually.

Table 6.2: Performance Comparison for IEEE-123

Method ($\rho = 1$)	Iterations	Total time [s]	Loss (MW)	Total-Objective
ADMM (Fixed ρ)	91	193.6	0.175	0.52
AADMM	57	111	0.18	0.52
N-ADMM+AADMM	54	109.407	0.178	0.52

Figure 6.6 shows loss trajectories with vertical dashes marking the detected stop iteration; Figure 6.7 overlays primal and dual residuals on a log scale. All distributed runs land very close to the centralized loss (0.17 MW): Classical ADMM 0.175 MW, AADMM 0.180 MW, FAADMM+AADMM 0.178 MW. The small gap (≤ 0.01 MW) is expected from consensus-relaxed, area-coupled solves and remains within operational tolerance.

On the IEEE-123 four-area split, residual-balanced AADMM substantially reduces iterations vs. fixed-ρ ADMM; adding Nesterov with restart gives a further, modest reduction in iteration count and runtime, with stability ensured by restart and ρ-clipping. All methods reach the same centralized optimum.

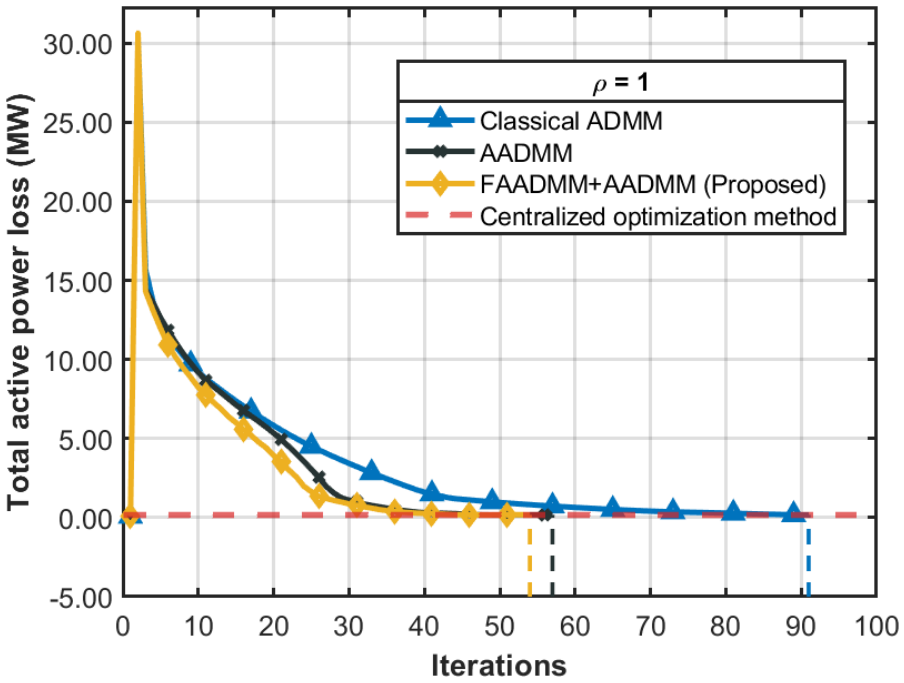

Figure 6.6: Convergence curves for loss of different ADMM methods

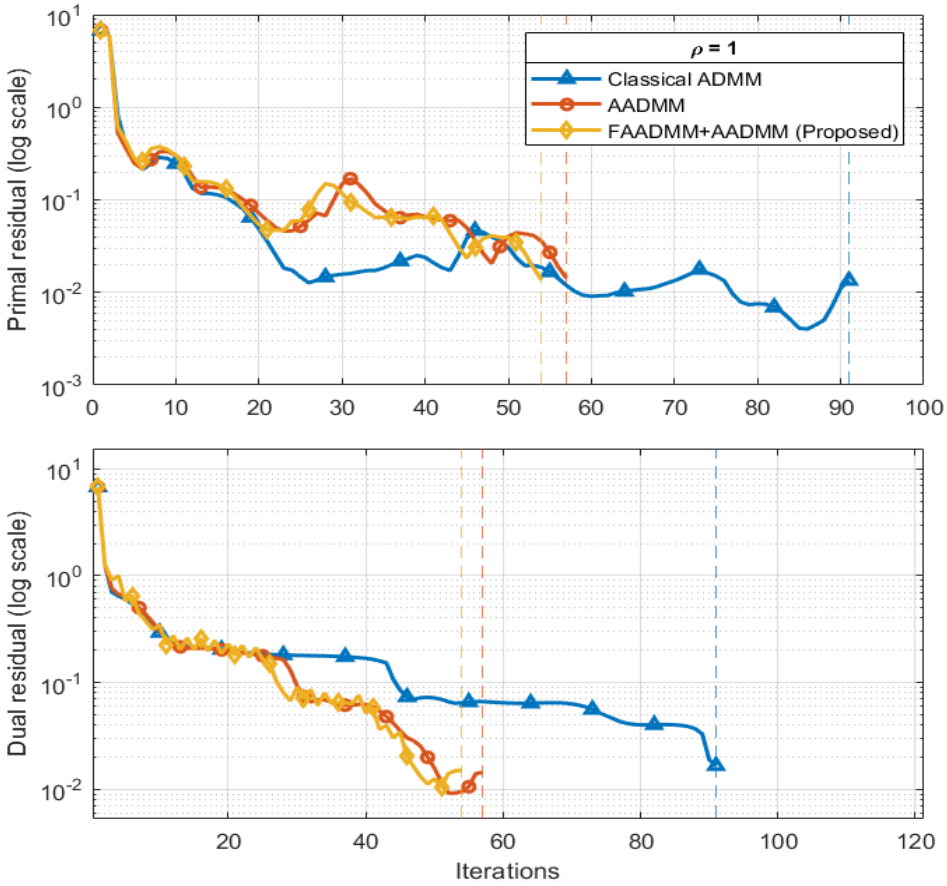

Figure 6.7: Convergence curve of primal and dual residuals

With ρ = 1, all three distributed methods drive the total objective toward the centralized benchmark (0.52) but with markedly different iteration counts as in figure 6.8 and Table 6.2. Classical ADMM converges the slowest, stabilizing near the centralized objective after ~91 iterations, whereas AADMM reaches the same neighborhood in ~57 iterations and the proposed FAADMM+AADMM does so in ~54 iterations. Vertical dashed markers in the figure highlight the detected stopping iterations for each method, and all runs terminate at essentially the same final objective (~0.52), confirming that acceleration/adaptivity primarily reduce iterations and time, without altering the optimality of the solution.

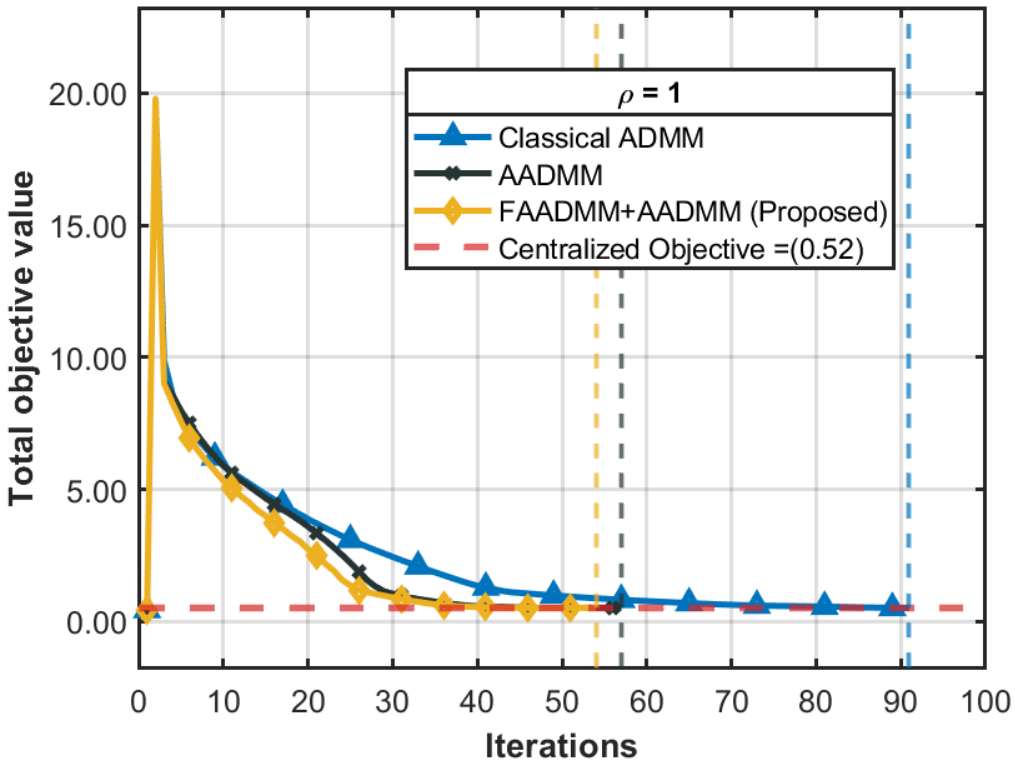

Figure 6.8: Convergence curves of different ADMM methods

6.5 Conclusion

This chapter developed, justified, and tested a practical acceleration framework for distributed OPF based on ADMM. Starting from a convex three-phase BFM–SDP with

matrix-valued consensus, we showed that plain ADMM can be made obviously more effective by combining residual-balanced adaptive penalties with clipping, Nesterov-type extrapolation equipped with a monotone restart, and scaled hybrid stopping rules tailored to Frobenius-norm residuals.

Implementation is straightforward: penalty clipping in $[\rho_{\min}, \rho_{\max}]$, simple residual-ratio thresholds for adjusting ρ, and a restart that only accepts momentum when both residuals decrease. On IEEE-13 (two areas) and IEEE-123 (four areas), these ingredients consistently reduced iteration counts and wall-clock time relative to fixed-ρ ADMM, while matching the centralized optimal objective. In both feeders, adaptive penalties delivered the largest single improvement; adding Nesterov with restart produce a further, modest reduction in both iterations and runtime; and the hybrid strategy offered the best overall convergence–time trade-off without inducing oscillations in the residuals.

The present scope remains single-time BFM–SDP with synchronous iterations over reliable communication links, and parameter ranges follow standard practice from the literature rather than mathematically optimal choices for SDP consensus. Future work includes extending the approach to multi-period and uncertainty aware OPF (e.g., PV/load variability) and incorporating discrete devices via convex surrogates or mixed-integer relaxations.

Chapter 7

Conclusions and Future Work

7.1 Conclusions

This thesis has presented a comprehensive investigation into the optimization of Active Distribution Networks (ADNs) with high penetration of renewable energy resources. The primary focus has been on developing and validating advanced control strategies that coordinate power electronic-based devices like Soft Open Points (SOPs) with traditional infrastructure such as On-Load Tap Changers (OLTCs) and Energy Storage Systems (ESS). The research successfully addressed critical challenges in voltage regulation, power loss minimization, phase balancing, and economic operation through a series of integrated optimization frameworks.

The key conclusions derived from this work are summarized as follows:

1. **Superiority of SOP-ES Integration (Chapter 3):** The integration of Energy Storage with Soft Open Points (SOP-ES) was demonstrated to be significantly more effective than SOPs alone. Case studies on the IEEE 13-bus and 123-bus systems showed that SOP-ES configurations provide not only spatial flexibility (through power transfer between feeders) but also crucial temporal flexibility (through energy time-shifting). This dual capability resulted in a substantial reduction in total power losses (up to 86.4% on the 13-bus system compared to the baseline), enhanced voltage profile stability by maintaining voltages within the desired band of [0.97, 1.03] p.u., and improved mitigation of three-phase voltage unbalance. SOP-ES increased PV active power utilization from 13.17 MW/24h (baseline) to 17.21

MW/24h, representing a 30.7% improvement, achieved through effective spatial and temporal flexibility.

Validation on the larger IEEE 123-bus system confirmed the approach's scalability, achieving similar relative improvements: power losses reduced from 18.54 MW/24h (baseline) to 15.53 MW/24h (SOP-ES), a 16.2% reduction.

2. **Synergistic Benefits of OLTC and SOP-ES Coordination (Chapter 4):** A major contribution of this thesis is the development of a unified optimization framework for the coordinated operation of OLTCs and SOP-ES systems. The results conclusively show that this coordination delivers synergistic benefits that surpass the capabilities of each device operating independently. By jointly optimizing OLTC tap settings, SOP power flows, and ESS charging/discharging schedules:

- **System Performance was Enhanced:** The coordinated strategy achieved the lowest power losses, minimized voltage deviations, and maximized PV utilization across all tested scenarios.

- **Variable vs. Fixed Tap Operation**: Transitioning from fixed OLTC tap ratios to variable optimization dramatically improved performance on the IEEE 13-bus system. Total daily power losses fell from 7.01 MW/24h (fixed-tap, OLTC-only) to 0.46 MW/24h (variable-tap, OLTC+SOP-ES), representing a 93.4% reduction.

- **OLTC Lifespan was Extended:** The presence of SOP-ES dramatically reduced the need for frequent OLTC tap changes. In the optimal coordinated case, the OLTC remained at a fixed tap position for the entire 24-hour horizon, thereby reducing mechanical wear and tear and enhancing the long-term reliability of this traditional asset.

- **Voltage Envelope Tightening**: The coordinated approach maintained system-wide voltages within a narrow band around 1.0 p.u., with $U\_{max} < 1.03$ p.u. and $U\_{min} > 0.97$ p.u. throughout the day. In contrast, constant-tap operation exhibited persistent upward bias, frequently exceeding the upper limit.

- **Reactive Power Management was Optimized:** The coordination allowed the OLTC to handle broader voltage adjustments, freeing the SOP-ES to provide more balanced reactive power support, shifting from predominantly absorptive behavior to a more dynamic mix of injection and absorption.

On the IEEE 123-bus system with four voltage regulators, similar patterns emerged: power losses decreased from 18.54 MW/24h (fixed-tap baseline) to 3.08 MW/24h (variable-tap, OLTC+SOP-ES), an 83.4% reduction, while substation demand dropped by approximately 30%.

3. **Economic Viability of SOP-ES Systems (Chapter 5):** The transition from technical to economic optimization revealed that SOP-ES systems are not only technically beneficial but also economically advantageous. The proposed economic model, which incorporates Time-of-Use (TOU) grid purchase costs, battery degradation costs, and PV curtailment penalties, demonstrated that SOP-ES can achieve substantial cost savings—up to 37.3% on the IEEE 13-bus system and 22.65% on the IEEE 123-bus system compared to the baseline. Explicitly modeling battery degradation cost within the optimization was shown to guide the scheduling towards more sustainable storage use, slightly reducing total cost while extending the implied economic lifetime of the batteries by minimizing excessive cycling. SOP-ES effectively exploited TOU tariff structure by charging during low-price hours (h1-h6) and discharging during high-price periods (h11-h13, h18-h21), substantially reducing grid purchases when electricity prices peaked while maintaining voltage stability.

The economic analysis validated that incorporating battery degradation costs into the optimization does not compromise and slightly improves overall economic performance by guiding the schedule toward sustainable asset utilization.

4. **Scalability through Distributed Optimization (Chapter 6):** To address the computational challenges of large-scale networks, Chapter 6 successfully implemented accelerated variants of the Alternating Direction Method of Multipliers (ADMM), namely Fast ADMM (FADMM) and Adaptive ADMM (AADMM). These distributed algorithms effectively decomposed the centralized SDP problem into manageable sub-problems, achieving near-optimal solutions with significantly improved convergence speed and reduced computational burden. This demonstrates a viable pathway for the real-time application of the proposed optimization models in extensive distribution networks.

5. **Effectiveness of the Convex Optimization Framework:** The application of a Semidefinite Programming (SDP) approach, enhanced with symmetrical components transformation for unbalanced networks, proved to be a robust and computationally efficient method for solving the complex, non-convex Optimal Power Flow (OPF) problem. This formulation guaranteed global optimal solutions for the relaxed problem and was successfully implemented using the MOSEK solver, demonstrating its practicality for planning and operational studies in ADNs.

In summary, this thesis provides a holistic set of models and strategies that validate the critical role of coordinated power electronic and storage technologies in future distribution networks. The findings offer concrete evidence that the integrated operation of OLTCs, SOPs, and ESS, solved via advanced centralized and distributed optimization techniques, is a viable and highly effective pathway towards managing the complexities introduced by high renewable energy penetration, ensuring both technical efficiency, economic sustainability,

and operational scalability.

7.2 Future work

While this research has addressed several important aspects of ADN optimization, it also opens numerous avenues for future investigation. The following directions are proposed to build upon the findings of this thesis:

- **Uncertainty and Stochastic Optimization:** This work utilized forecasted profiles for load and PV generation. A critical next step is to explicitly model the uncertainties inherent in these forecasts, as well as in electricity prices and component availability. Future research could develop a stochastic or robust optimization framework to derive operating strategies that are resilient against forecast errors and variability, thereby enhancing the real-world robustness of the proposed methods. This could be integrated with the distributed ADMM framework for scalable uncertainty management.

- **Real-Time and Multi-Timescale Control:** The optimization models presented are primarily suited for day-ahead scheduling. To bridge the gap between planning and real-time operation, future work should investigate a multi-timescale control architecture. This could involve a hierarchical framework where day-ahead schedules (solved via SDP) are adjusted in a receding horizon manner using distributed ADMM for intra-day and real-time control, incorporating real-time measurements to handle rapid fluctuations.

- **Advanced Battery Degradation and Asset Health Models:** The battery degradation model used in the economic chapter was a linear cost based on energy throughput. Future studies could incorporate more sophisticated, non-linear health

models that account for factors such as C-rate, depth of discharge, temperature, and calendar aging. Furthermore, the framework could be extended to include condition-based maintenance scheduling for both the battery and the OLTC, optimizing operational costs alongside long-term asset health.

- **Fully Decentralized Optimization with Privacy Preservation:** Building on the ADMM work, future research could explore a fully decentralized architecture where different areas of the network (or even different asset owners) solve their local problems with minimal information exchange. Fully decentralized architecture refers to a system design where no single central authority, controller, or server is needed. Each node operates independently, makes decisions autonomously, and communicates directly with peers, ensuring resilience, scalability, and fault tolerance without a central point of failure. This would enhance data privacy and security while still achieving near-global optimality, a key consideration for future smart grids with multiple stakeholders.

- **Hardware-in-the-Loop (HIL) Validation:** To further validate the practical applicability of the proposed coordination strategies, HIL simulations are recommended. This would involve implementing the distributed ADMM-based control algorithms on a real-time digital simulator coupled with physical controllers for SOPs and OLTCs, testing their performance, communication requirements, and convergence under dynamic and transient conditions.

By pursuing these research directions, the promising foundations laid by this thesis can be further developed into comprehensive tools and strategies for the secure, efficient, and intelligent operation of the next-generation power grid.

References

[1] M. A. Hurayra *et al.*, "A Comprehensive Review: Distribution Network Management Strategy, Impact and Future," *European Journal of Applied Science, Engineering and Technology,* vol. 3, no. 3, pp. 309-328, 2025.

[2] M. M. Haque and P. Wolfs, "A review of high PV penetrations in LV distribution networks: Present status, impacts and mitigation measures," *Renewable and Sustainable Energy Reviews,* vol. 62, pp. 1195-1208, 2016.

[3] M. Yao, I. A. Hiskens, and J. L. Mathieu, "Mitigating voltage unbalance using distributed solar photovoltaic inverters," *IEEE Transactions on Power Systems,* vol. 36, no. 3, pp. 2642-2651, 2020.

[4] P. Li, H. Ji, C. Wang, J. Zhao, G. Song, F. Ding, and J. Wu, "Coordinated control method of voltage and reactive power for active distribution networks based on soft open point," *IEEE Transactions on Sustainable Energy,* vol. 8, no. 4, pp. 1430-1442, 2017.

[5] W. Cao, J. Wu, N. Jenkins, C. Wang, and T. Green, "Operating principle of Soft Open Points for electrical distribution network operation," *Applied Energy,* vol. 164, pp. 245-257, 2016.

[6] Z. Ma and F. Cao, "Optimization of Active Distribution Network Operation with SOP Considering Reverse Power Flow," *Applied Sciences,* vol. 14, no. 24, p. 11797, 2024.

[7] C. Yao, C. Zhou, J. Yu, K. Xu, P. Li, and G. Song, "A Sequential Optimization Method for Soft Open Point Integrated with Energy Storage in Active Distribution Networks," *Energy Procedia,* vol. 145, pp. 528-533, 2018, doi: 10.1016/j.egypro.2018.04.077.

[8] J. Wang, N. Zhou, A. Tao, and Q. Wang, "Optimal Operation of Soft Open Points-Based Energy Storage in Active Distribution Networks by Considering the Battery Lifetime," *Frontiers in Energy Research,* vol. 8, 2021, doi: 10.3389/fenrg.2020.633401.

[9] M. Farivar and S. H. Low, "Branch flow model: Relaxations and convexification—Part I," *IEEE Transactions on Power Systems,* vol. 28, no. 3, pp. 2554-2564, 2013.

[10] S. Boyd, N. Parikh, E. Chu, B. Peleato, and J. Eckstein, "Distributed optimization and statistical learning via the alternating direction method of multipliers," *Foundations and Trends® in Machine learning,* vol. 3, no. 1, pp. 1-122, 2011.

[11] R. A. Jabr, "Linear decision rules for control of reactive power by distributed photovoltaic generators," *IEEE Transactions on Power Systems,* vol. 33, no. 2, pp. 2165-2174, 2017.

[12] R. A. Jabr, "Robust Volt/VAr Control With Photovoltaics," *IEEE Transactions on Power Systems,* vol. 34, no. 3, pp. 2401-2408, 2019, doi: 10.1109/tpwrs.2018.2890767.

[13] I. P. I. T. S. T. Force, "Impact of IEEE 1547 Standard on Smart Inverters," May 18, 2018 2018.

[14] W. Lu, M. Liu, and Q. Liu, "Increment-Exchange-Based Decentralized Multiobjective Optimal Power Flow for Active Distribution Grids," *IEEE Systems Journal,* vol. 14, no. 3, pp. 3695-3704, 2020, doi: 10.1109/jsyst.2019.2956820.

[15] C. Zhang, Y. Xu, Z. Y. Dong, and R. Zhang, "Multi-Objective Adaptive Robust Voltage/VAR Control for High-PV Penetrated Distribution Networks," *IEEE Transactions on Smart Grid,* vol. 11, no. 6, pp. 5288-5300, 2020, doi: 10.1109/tsg.2020.3000726.

[16] K. Christakou, M. Paolone, and A. Abur, "Voltage Control in Active Distribution Networks Under Uncertainty in the System Model: A Robust Optimization Approach," *IEEE Transactions on Smart Grid,* vol. 9, no. 6, pp. 5631-5642, 2018, doi: 10.1109/tsg.2017.2693212.

[17] N. Daratha, B. Das, and J. Sharma, "Robust voltage regulation in unbalanced radial distribution system under uncertainty of distributed generation and loads," *International Journal of Electrical Power & Energy Systems,* vol. 73, pp. 516-527, 2015, doi: 10.1016/j.ijepes.2015.05.046.

[18] Q. Zhang, K. Dehghanpour, and Z. Wang, "Distributed CVR in Unbalanced Distribution Systems With PV Penetration," *IEEE Transactions on Smart Grid,* vol. 10, no. 5, pp. 5308-5319, 2019, doi: 10.1109/tsg.2018.2880419.

[19] B. A. Robbins and A. D. Dominguez-Garcia, "Optimal Reactive Power Dispatch for Voltage Regulation in Unbalanced Distribution Systems," *IEEE Transactions on Power Systems,* vol. 31, no. 4, pp. 2903-2913, 2016, doi: 10.1109/tpwrs.2015.2451519.

[20] S. S. Guggilam, E. Dall'Anese, Y. C. Chen, S. V. Dhople, and G. B. Giannakis, "Scalable Optimization Methods for Distribution Networks With High PV Integration," *IEEE Transactions on Smart Grid,* vol. 7, no. 4, pp. 2061-2070, 2016, doi: 10.1109/tsg.2016.2543264.

[21] B. A. Robbins, H. Zhu, and A. D. Domínguez-García, "Optimal tap setting of voltage regulation transformers in unbalanced distribution systems," *IEEE Transactions on Power Systems,* vol. 31, no. 1, pp. 256-267, 2015.

[22] E. Dall'Anese, S. V. Dhople, B. B. Johnson, and G. B. Giannakis, "Decentralized Optimal Dispatch of Photovoltaic Inverters in Residential Distribution Systems," *IEEE Transactions on Energy Conversion,* vol. 29, no. 4, pp. 957-967, 2014, doi: 10.1109/tec.2014.2357997.

[23] M. Nick, R. Cherkaoui, and M. Paolone, "Optimal siting and sizing of distributed energy storage systems via alternating direction method of multipliers," *International Journal of Electrical Power & Energy Systems,* vol. 72, pp. 33-39, 2015, doi: 10.1016/j.ijepes.2015.02.008.

[24] C. Zhong, A. P. S. Meliopoulos, B. Xie, J. Xie, and K. Liu, "Multi-Stage Quadratic Flexible Optimal Power Flow With a Rolling Horizon," *IEEE Transactions on Smart Grid,* vol. 12, no. 4, pp. 3128-3137, 2021, doi: 10.1109/tsg.2021.3059255.

[25] X. Sun, J. Qiu, and J. Zhao, "Real-Time Volt/Var Control in Active Distribution Networks With Data-Driven Partition Method," *IEEE Transactions on Power Systems,* vol. 36, no. 3, pp. 2448-2461, 2021, doi: 10.1109/tpwrs.2020.3037294.

[26] Y. Guo, Q. Wu, H. Gao, S. Huang, B. Zhou, and C. Li, "Double-Time-Scale Coordinated Voltage Control in Active Distribution Networks Based on MPC," *IEEE Transactions on Sustainable Energy,* vol. 11, no. 1, pp. 294-303, 2020, doi: 10.1109/tste.2018.2890621.

[27] X. Ge, L. Shen, C. Zheng, P. Li, and X. Dou, "A Decoupling Rolling Multi-Period Power and Voltage Optimization Strategy in Active Distribution Networks," *Energies,* vol. 13, no. 21, 2020, doi: 10.3390/en13215789.

[28] C. Lou, J. Yang, T. Li, and E. Vega-Fuentes, "New phase-changing soft open point and impacts on optimising unbalanced power distribution networks," *IET Generation, Transmission & Distribution,* vol. 14, no. 23, pp. 5685-5696, 2020, doi: 10.1049/iet-gtd.2019.1660.

[29] P. Li, H. Ji, H. Yu, J. Zhao, C. Wang, G. Song, and J. Wu, "Combined decentralized and local voltage control strategy of soft open points in active distribution networks," *Applied Energy,* vol. 241, pp. 613-624, 2019, doi: 10.1016/j.apenergy.2019.03.031.

[30] C. Long, J. Wu, L. Thomas, and N. Jenkins, "Optimal operation of soft open points in medium voltage electrical distribution networks with distributed generation," *Applied Energy,* vol. 184, pp. 427-437, 2016, doi: 10.1016/j.apenergy.2016.10.031.

[31] H. Ji, C. Wang, P. Li, F. Ding, and J. Wu, "Robust Operation of Soft Open Points in Active Distribution Networks With High Penetration of Photovoltaic Integration," *IEEE Transactions on Sustainable Energy,* vol. 10, no. 1, pp. 280-289, 2019, doi: 10.1109/tste.2018.2833545.

[32] R. Hu, W. Wang, X. Wu, Z. Chen, and W. Ma, "Interval optimization based coordinated control for distribution networks with energy storage integrated soft open points," *International Journal of Electrical Power & Energy Systems,* vol. 136, 2022, doi: 10.1016/j.ijepes.2021.107725.

[33] Y. Zheng, Y. Song, and D. J. Hill, "A general coordinated voltage regulation method in distribution networks with soft open points," *International Journal of Electrical Power & Energy Systems,* vol. 116, 2020, doi: 10.1016/j.ijepes.2019.105571.

[34] P. Li, H. Ji, G. Song, M. Yao, C. Wang, and J. Wu, "A combined central and local voltage control strategy of soft open points in active distribution networks," *Energy Procedia,* vol. 158, pp. 2524-2529, 2019.

[35] H. Ji, H. Yu, G. Song, P. Li, C. Wang, and J. Wu, "A decentralized voltage control strategy of soft open points in active distribution networks," *Energy Procedia,* vol. 159, pp. 412-417, 2019.

[36] V. Calderaro, V. Galdi, F. Lamberti, and A. Piccolo, "A Smart Strategy for Voltage Control Ancillary Service in Distribution Networks," *IEEE Transactions on Power Systems,* vol. 30, no. 1, pp. 494-502, 2015, doi: 10.1109/tpwrs.2014.2326957.

[37] A. Kulmala, S. Repo, and P. Jarventausta, "Coordinated Voltage Control in Distribution Networks Including Several Distributed Energy Resources," *IEEE Transactions on Smart Grid,* vol. 5, no. 4, pp. 2010-2020, 2014, doi: 10.1109/tsg.2014.2297971.

[38] N. Daratha, B. Das, and J. Sharma, "Coordination Between OLTC and SVC for Voltage Regulation in Unbalanced Distribution System Distributed Generation," *IEEE Transactions on Power Systems,* vol. 29, no. 1, pp. 289-299, 2014, doi: 10.1109/tpwrs.2013.2280022.

[39] M. Nick, R. Cherkaoui, and M. Paolone, "Optimal Allocation of Dispersed Energy Storage Systems in Active Distribution Networks for Energy Balance and Grid Support," *IEEE Transactions on Power Systems,* vol. 29, no. 5, pp. 2300-2310, 2014, doi: 10.1109/tpwrs.2014.2302020.

[40] H. Ji, C. Wang, P. Li, J. Zhao, G. Song, F. Ding, and J. Wu, "A centralized-based method to determine the local voltage control strategies of distributed generator operation in active distribution networks," *Applied Energy,* vol. 228, pp. 2024-2036, 2018, doi: 10.1016/j.apenergy.2018.07.065.

[41] C. Li, V. R. Disfani, Z. K. Pecenak, S. Mohajeryami, and J. Kleissl, "Optimal OLTC voltage control scheme to enable high solar penetrations," *Electric Power Systems Research,* vol. 160, pp. 318-326, 2018, doi: 10.1016/j.epsr.2018.02.016.

[42] Z. Tian, W. Wu, B. Zhang, and A. Bose, "Mixed-integer second-order cone programing model for VAR optimisation and network reconfiguration in active distribution networks," *IET Generation, Transmission & Distribution,* vol. 10, no. 8, pp. 1938-1946, 2016, doi: 10.1049/iet-gtd.2015.1228.

[43] F. Ding, Y. Zhang, J. Simpson, A. Bernstein, and S. Vadari, "Optimal Energy Dispatch of Distributed PVs for the Next Generation of Distribution Management Systems," *IEEE Open Access Journal of Power and Energy,* vol. 7, pp. 287-295, 2020, doi: 10.1109/oajpe.2020.3009684.

[44] B. Zhang, A. Y. S. Lam, A. D. Dominguez-Garcia, and D. Tse, "An Optimal and Distributed Method for Voltage Regulation in Power Distribution Systems," *IEEE Transactions on Power Systems,* vol. 30, no. 4, pp. 1714-1726, 2015, doi: 10.1109/tpwrs.2014.2347281.

[45] S.-I. Go, S.-Y. Yun, S.-J. Ahn, and J.-H. Choi, "Voltage and Reactive Power Optimization Using a Simplified Linear Equations at Distribution Networks with DG," *Energies,* vol. 13, no. 13, 2020, doi: 10.3390/en13133334.

[46] M. Ammar and A. M. Sharaf, "Optimized Use of PV Distributed Generation in Voltage Regulation: A Probabilistic Formulation," *IEEE Transactions on Industrial Informatics,* vol. 15, no. 1, pp. 247-256, 2019, doi: 10.1109/tii.2018.2829188.

[47] X. Su, M. A. S. Masoum, and P. J. Wolfs, "Optimal PV Inverter Reactive Power Control and Real Power Curtailment to Improve Performance of Unbalanced Four-Wire LV Distribution Networks," *IEEE Transactions on Sustainable Energy,* vol. 5, no. 3, pp. 967-977, 2014, doi: 10.1109/tste.2014.2313862.

[48] C. Li, V. R. Disfani, H. V. Haghi, and J. Kleissl, "Coordination of OLTC and smart inverters for optimal voltage regulation of unbalanced distribution networks," *Electric Power Systems Research,* vol. 187, 2020, doi: 10.1016/j.epsr.2020.106498.

[49] H. Ahmadi and J. R. Marti, "Distribution System Optimization Based on a Linear Power-Flow Formulation," *IEEE Transactions on Power Delivery,* vol. 30, no. 1, pp. 25-33, 2015, doi: 10.1109/tpwrd.2014.2300854.

[50] A. Borghetti, M. Bosetti, S. Grillo, S. Massucco, C. A. Nucci, M. Paolone, and F. Silvestro, "Short-Term Scheduling and Control of Active Distribution Systems With High Penetration of Renewable Resources," *IEEE Systems Journal,* vol. 4, no. 3, pp. 313-322, 2010, doi: 10.1109/jsyst.2010.2059171.

[51] S. Kundu, S. Backhaus, and I. A. Hiskens, "Distributed control of reactive power from photovoltaic inverters," in *2013 IEEE International Symposium on Circuits and Systems (ISCAS)*, 2013: IEEE, pp. 249-252.

[52] W. Ma, W. Wang, Z. Chen, and R. Hu, "A centralized voltage regulation method for distribution networks containing high penetrations of photovoltaic power," *International Journal of Electrical Power & Energy Systems,* vol. 129, 2021, doi: 10.1016/j.ijepes.2021.106852.

[53] W. Ma, W. Wang, Z. Chen, X. Wu, R. Hu, F. Tang, and W. Zhang, "Voltage regulation methods for active distribution networks considering the reactive power optimization of substations," *Applied Energy,* vol. 284, 2021, doi: 10.1016/j.apenergy.2020.116347.

[54] M. Jafari, T. O. Olowu, and A. I. Sarwat, "Optimal smart inverters volt-var curve selection with a multi-objective volt-var optimization using evolutionary algorithm approach," in *2018 North American Power Symposium (NAPS)*, 2018: IEEE, pp. 1-6.

[55] T. O. Olowu, M. Jafari, and A. I. Sarwat, "A multi-objective optimization technique for volt-var control with high pv penetration using genetic algorithm," in *2018 North American Power Symposium (NAPS)*, 2018: IEEE, pp. 1-6.

[56] H. Lee, J.-C. Kim, and S.-M. Cho, "Optimal Volt–Var Curve Setting of a Smart Inverter for Improving Its Performance in a Distribution System," *IEEE Access,* vol. 8, pp. 157931-157945, 2020, doi: 10.1109/access.2020.3019794.

[57] C. Li, Y.-A. Chen, C. Jin, R. Sharma, and J. Kleissl, "Online PV Smart Inverter Coordination using Deep Deterministic Policy Gradient," *Electric Power Systems Research,* vol. 209, 2022, doi: 10.1016/j.epsr.2022.107988.

[58] M. Alrashidi and S. Rahman, "A bi-level optimization method for voltage control in distribution networks using batteries and smart inverters with high wind and photovoltaic penetrations," *International Journal of Electrical Power & Energy Systems,* vol. 151, 2023, doi: 10.1016/j.ijepes.2023.109217.

[59] P. Diaz, M. Perez-Cisneros, E. Cuevas, O. Camarena, F. A. Fausto Martinez, and A. Gonzalez, "A Swarm Approach for Improving Voltage Profiles and Reduce Power Loss on Electrical Distribution Networks," *IEEE Access,* vol. 6, pp. 49498-49512, 2018, doi: 10.1109/access.2018.2868814.

[60] A. Abessi, V. Vahidinasab, and M. S. Ghazizadeh, "Centralized Support Distributed Voltage Control by Using End-Users as Reactive Power Support," *IEEE Transactions on Smart Grid,* vol. 7, no. 1, pp. 178-188, 2016, doi: 10.1109/tsg.2015.2410780.

[61] O. Ceylan, G. Liu, and K. Tomsovic, "Coordinated distribution network control of tap changer transformers, capacitors and PV inverters," *Electrical Engineering,* vol. 100, no. 2, pp. 1133-1146, 2017, doi: 10.1007/s00202-017-0563-x.

[62] Y. Chen, M. Strothers, and A. Benigni, "Day-ahead optimal scheduling of PV inverters and OLTC in distribution feeders," in *2016 IEEE Power and Energy Society General Meeting (PESGM)*, 2016: IEEE, pp. 1-5.

[63] O. Ceylan, G. Liu, Y. Xu, and K. Tomsovic, "Distribution system voltage regulation by distributed energy resources," in *2014 North American power symposium (NAPS)*, 2014: IEEE, pp. 1-5.

[64] Q. Qi, J. Wu, and C. Long, "Multi-objective operation optimization of an electrical distribution network with soft open point," *Applied Energy,* vol. 208, pp. 734-744, 2017, doi: 10.1016/j.apenergy.2017.09.075.

[65] C. Han, S. Song, Y. Yoo, J. Lee, G. Jang, and M. Yoon, "Optimal operation of soft-open points for high penetrated distributed generations on distribution networks," in *2019 10th International Conference on Power Electronics and ECCE Asia (ICPE 2019-ECCE Asia)*, 2019: IEEE, pp. 806-812.

[66] M. B. Shafik, H. Chen, G. I. Rashed, R. A. El-Sehiemy, M. R. Elkadeem, and S. Wang, "Adequate Topology for Efficient Energy Resources Utilization of Active Distribution Networks Equipped With Soft Open Points," *IEEE Access,* vol. 7, pp. 99003-99016, 2019, doi: 10.1109/access.2019.2930631.

[67] M. Shafik, G. Rashed, H. Chen, M. Elkadeem, and S. Wang, "Reconfiguration strategy for active distribution networks with soft open points," in *2019 14th IEEE Conference on Industrial Electronics and Applications (ICIEA)*, 2019: IEEE, pp. 330-334.

[68] H.-T. Yang and J.-T. Liao, "MF-APSO-Based Multiobjective Optimization for PV System Reactive Power Regulation," *IEEE Transactions on Sustainable Energy,* vol. 6, no. 4, pp. 1346-1355, 2015, doi: 10.1109/tste.2015.2433957.

[69] G. Huang, H. Wu, Z. Feng, Y. Ding, and J. Wang, "Day-ahead reactive-voltage optimization for active distribution network with energy storage," presented at the 2021 3rd International Conference on Electrical Engineering and Control Technologies (CEECT), 2021.

[70] K. Tantrapon, P. Jirapong, and P. Thararak, "Mitigating microgrid voltage fluctuation using battery energy storage system with improved particle swarm optimization," *Energy Reports,* vol. 6, pp. 724-730, 2020, doi: 10.1016/j.egyr.2019.11.145.

[71] Q. Li, F. Zhou, F. Guo, F. Fan, and Z. Huang, "Optimized Energy Storage System Configuration for Voltage Regulation of Distribution Network With PV Access," *Frontiers in Energy Research,* vol. 9, 2021, doi: 10.3389/fenrg.2021.641518.

[72] G. Lei, Y. Huang, N. Dai, L. Cai, L. Deng, S. Li, and C. He, "Optimization Strategy of Hybrid Configuration for Volatility Energy Storage System in ADN," *Processes,* vol. 10, no. 9, 2022, doi: 10.3390/pr10091844.

[73] G. Shaoyun, X. Zhengyang, L. Hong, L. Mengyi, Y. Zan, and Z. Chenghao, "Coordinated voltage control for active distribution network considering the impact of energy storage," *Energy Procedia,* vol. 158, pp. 1122-1127, 2019.

[74] H. Li, C. Hong, Y. Yang, Y. Yi, X. Chen, and Y. Zhang, "Multi-objective extended reactive power optimization in distribution network with photovoltaic-storage systems," in *2016 IEEE International Conference on Power System Technology (POWERCON)*, 2016: IEEE, pp. 1-5.

[75] R. Su *et al.*, "Optimal placement and capacity sizing of energy storage systems via NSGA-II in active distribution network," *Frontiers in Energy Research,* vol. 10, 2023, doi: 10.3389/fenrg.2022.1073194.

[76] B. Ahmadi, J. S. Giraldo, G. Hoogsteen, M. E. T. Gerards, and J. L. Hurink, "A multi-objective decentralized optimization for voltage regulators and energy storage devices in active distribution systems," *International Journal of Electrical Power & Energy Systems,* vol. 153, 2023, doi: 10.1016/j.ijepes.2023.109330.

[77] B. Ahmadi, O. Ceylan, and A. Ozdemir, "Voltage profile improving and peak shaving using multi-type distributed generators and battery energy storage systems in distribution networks," in *2020 55th International Universities Power Engineering Conference (UPEC)*, 2020: IEEE, pp. 1-6.

[78] Y. Zhang, J. Li, K. Meng, Z. Y. Dong, Z. Yu, and K. Wong, "Voltage regulation in distribution network using battery storage units via distributed optimization," in *2016 IEEE International Conference on Power System Technology (POWERCON)*, 2016: IEEE, pp. 1-6.

[79] T. Niknam, M. Zare, and J. Aghaei, "Scenario-Based Multiobjective Volt/Var Control in Distribution Networks Including Renewable Energy Sources," *IEEE Transactions on Power Delivery,* vol. 27, no. 4, pp. 2004-2019, 2012, doi: 10.1109/tpwrd.2012.2209900.

[80] D. Jin, H.-D. Chiang, and P. Li, "Two-Timescale Multi-Objective Coordinated Volt/Var Optimization for Active Distribution Networks," *IEEE Transactions on Power Systems,* vol. 34, no. 6, pp. 4418-4428, 2019, doi: 10.1109/tpwrs.2019.2914923.

[81] D. Jin and H.-D. Chiang, "Multi-objective look-ahead reactive power control for active distribution networks with composite loads," in *2018 IEEE Power & Energy Society General Meeting (PESGM)*, 2018: IEEE, pp. 1-5.

[82] D. O. Sidea, I. I. Picioroaga, A. M. Tudose, C. Bulac, and I. Tristiu, "Multi-objective particle swarm optimization applied on the optimal reactive power dispatch in electrical distribution systems," in *2020 International Conference and Exposition on Electrical and Power Engineering (EPE)*, 2020: IEEE, pp. 413-418.

[83] S. Singh, V. Babu Pamshetti, A. K. Thakur, and S. P. Singh, "Multistage Multiobjective Volt/VAR Control for Smart Grid-Enabled CVR With Solar PV

Penetration," *IEEE Systems Journal,* vol. 15, no. 2, pp. 2767-2778, 2021, doi: 10.1109/jsyst.2020.2992985.

[84] R. Sun, Y. Shu, Z. Lv, B. Chen, and Z. Wei, "Research on the multiple timescale reactive power optimization of receiving power grid based on model predictive control," in *2020 12th IEEE PES Asia-Pacific Power and Energy Engineering Conference (APPEEC)*, 2020: IEEE, pp. 1-6.

[85] X. Su, J. Liu, S. Tian, P. Ling, Y. Fu, S. Wei, and C. SiMa, "A multi-stage coordinated volt-Var optimization for integrated and unbalanced radial distribution networks," *Energies,* vol. 13, no. 18, p. 4877, 2020.

[86] A. Ramadan, M. Ebeed, and S. Kamel, "Performance assessment of a realistic egyptian distribution network including PV penetration with DSTATCOM," in *2019 International Conference on Innovative Trends in Computer Engineering (ITCE)*, 2019: IEEE, pp. 426-431.

[87] Y. Chen, B. Luckey, J. Wigmore, M. Davidson, and A. Benigni, "Real-time volt/var optimization for distribution systems with photovoltaic integration," in *IECON 2017-43rd Annual Conference of the IEEE Industrial Electronics Society*, 2017: IEEE, pp. 2658-2663.

[88] V. B. Pamshetti and S. P. Singh, "Optimal coordination of PV smart inverter and traditional volt-VAR control devices for energy cost savings and voltage regulation," *International Transactions on Electrical Energy Systems,* vol. 29, no. 7, 2019, doi: 10.1002/2050-7038.12042.

[89] H.-J. Lee, K.-H. Yoon, J.-W. Shin, J.-C. Kim, and S.-M. Cho, "Optimal Parameters of Volt–Var Function in Smart Inverters for Improving System Performance," *Energies,* vol. 13, no. 9, 2020, doi: 10.3390/en13092294.

[90] R. Wu and S. Liu, "Deep Learning Based Muti-Objective Reactive Power Optimization of Distribution Network with PV and EVs," *Sensors (Basel),* vol. 22, no. 12, Jun 7 2022, doi: 10.3390/s22124321.

[91] Y.-D. Lee, W.-C. Lin, J.-L. Jiang, J.-H. Cai, W.-T. Huang, and K.-C. Yao, "Optimal Individual Phase Voltage Regulation Strategies in Active Distribution Networks with High PV Penetration Using the Sparrow Search Algorithm," *Energies,* vol. 14, no. 24, 2021, doi: 10.3390/en14248370.

[92] H. Xiao, W. Pei, Z. Dong, L. Kong, and D. Wang, "Application and Comparison of Metaheuristic and New Metamodel Based Global Optimization Methods to the Optimal Operation of Active Distribution Networks," *Energies,* vol. 11, no. 1, 2018, doi: 10.3390/en11010085.

[93] R. Xu, C. Zhang, Y. Xu, Z. Dong, and R. Zhang, "Multi-Objective Hierarchically-Coordinated Volt/Var Control for Active Distribution Networks With Droop-Controlled PV Inverters," *IEEE Transactions on Smart Grid,* vol. 13, no. 2, pp. 998-1011, 2022, doi: 10.1109/tsg.2021.3126761.

[94] M. M. Othman, M. H. Ahmed, and M. M. A. Salama, "A Coordinated Real-Time Voltage Control Approach for Increasing the Penetration of Distributed

Generation," *IEEE Systems Journal,* vol. 14, no. 1, pp. 699-707, 2020, doi: 10.1109/jsyst.2019.2904532.

[95] C. K. Das, O. Bass, G. Kothapalli, T. S. Mahmoud, and D. Habibi, "Optimal placement of distributed energy storage systems in distribution networks using artificial bee colony algorithm," *Applied Energy,* vol. 232, pp. 212-228, 2018, doi: 10.1016/j.apenergy.2018.07.100.

[96] T. Senjyu, Y. Miyazato, A. Yona, N. Urasaki, and T. Funabashi, "Optimal Distribution Voltage Control and Coordination With Distributed Generation," *IEEE Transactions on Power Delivery,* vol. 23, no. 2, pp. 1236-1242, 2008, doi: 10.1109/tpwrd.2007.908816.

[97] J. M. Bloemink and T. C. Green, "Increasing distributed generation penetration using soft normally-open points," in *IEEE PES general meeting*, 2010: IEEE, pp. 1-8.

[98] K. Mardanimajd, S. Karimi, and A. Anvari-Moghaddam, "Voltage stability improvement in distribution networks by using soft open points," *International Journal of Electrical Power & Energy Systems,* vol. 155, p. 109582, 2024.

[99] D. M. Greenwood, N. S. Wade, P. C. Taylor, P. Papadopoulos, and N. Heyward, "A probabilistic method combining electrical energy storage and real-time thermal ratings to defer network reinforcement," *IEEE Transactions on Sustainable Energy,* vol. 8, no. 1, pp. 374-384, 2016.

[100] I. Sarantakos *et al.*, "A Robust Mixed-Integer Convex Model for Optimal Scheduling of Integrated Energy Storage—Soft Open Point Devices," *IEEE Transactions on Smart Grid,* vol. 13, no. 5, pp. 4072-4087, 2022, doi: 10.1109/tsg.2022.3145709.

[101] K. Gholami *et al.*, "Hybrid uncertainty approach for management of energy storage-embedded soft open points in distribution grids," *Journal of Energy Storage,* vol. 87, p. 111394, 2024.

[102] X. Ding, X. Chen, K. Yu, F. Cao, and B. Wang, "Multi-time-scale voltage control of the distribution network with energy storage equipped soft open points," *Frontiers in Energy Research,* vol. 12, p. 1374704, 2024.

[103] H. Ji, C. Wang, P. Li, J. Zhao, G. Song, and J. Wu, "Quantified flexibility evaluation of soft open points to improve distributed generator penetration in active distribution networks based on difference-of-convex programming," *Applied Energy,* vol. 218, pp. 338-348, 2018, doi: 10.1016/j.apenergy.2018.02.170.

[104] H. Li, Z. Li, B. Wang, and K. Sun, "Stochastic Optimal Operation of SOP-Assisted Active Distribution Networks with High Penetration of Renewable Energy Sources," *Sustainability,* vol. 16, no. 13, p. 5808, 2024.

[105] S. P. Singh, N. Kanwar, and A. Saraswat, "Optimal Operation of Active Distribution Network Considering Energy Storage-Equipped Soft Open Points," *e-Prime-Advances in Electrical Engineering, Electronics and Energy,* p. 101082, 2025.

[106] E. Dall'Anese, H. Zhu, and G. B. Giannakis, "Distributed optimal power flow for smart microgrids," *IEEE Transactions on Smart Grid,* vol. 4, no. 3, pp. 1464-1475, 2013.
[107] S. Boyd and L. Vandenberghe, *Convex optimization*. Cambridge university press, 2004.
[108] Z. Wang, D. S. Kirschen, and B. Zhang, "Accurate semidefinite programming models for optimal power flow in distribution systems," *arXiv preprint arXiv:1711.07853,* 2017.
[109] L. Gan and S. H. Low, "Convex relaxations and linear approximation for optimal power flow in multiphase radial networks," in *2014 Power Systems Computation Conference*, 2014: IEEE, pp. 1-9.
[110] J. Lofberg, "YALMIP: A toolbox for modeling and optimization in MATLAB," in *2004 IEEE international conference on robotics and automation (IEEE Cat. No. 04CH37508)*, 2004: IEEE, pp. 284-289.
[111] M. ApS, "Mosek optimization toolbox for matlab," *User's Guide and Reference Manual, Version,* vol. 4, no. 1, p. 116, 2019.
[112] A. Smith, "Electricity Safety, Quality and Continuity Regulations 2002," *Lighting Journal,* vol. 68, no. 2, pp. 35-36, 2003.
[113] T. L. Saaty, "Decision making—the analytic hierarchy and network processes (AHP/ANP)," *Journal of systems science and systems engineering,* vol. 13, pp. 1-35, 2004.
[114] D. T. Feeders, "IEEE PES Distribution System Analysis Subcommittee's, Distribution Test Feeder Working Group," *ed,* 2013.
[115] C. Lou, J. Yang, E. Vega-Fuentes, N. K. Meena, and L. Min, "Multi-terminal phase-changing soft open point SDP modeling for imbalance mitigation in active distribution networks," *International Journal of Electrical Power & Energy Systems,* vol. 142, 2022, doi: 10.1016/j.ijepes.2022.108228.
[116] B. Kumar, A. Kumar, R. Agrawal, and S. Rai, "Voltage Regulation for Load Balancing Using OLTC Transformer," in *2023 IEEE Renewable Energy and Sustainable E-Mobility Conference (RESEM)*, 2023: IEEE, pp. 1-5.
[117] Z. Li, F. Gao, C. ZHAO, Z. Wang, H. Zhang, P. Wang, and Y. Li, "Research review of power electronic transformer technologies," *Proceedings of the CSEE,* vol. 38, no. 5, 2018.
[118] M. Alshehri, J. Yang, C. Lou, and L. Min, "Optimal Operation in Active Distribution Networks Using Soft Open Point Integrated with Energy Storage," in *2025 IEEE Texas Power and Energy Conference (TPEC)*, 2025: IEEE, pp. 1-6.
[119] S. Baek, B. Lim, C. Han, and Y. Yoo, "A Study on Real-Time OLTC Control in PV-Integrated Distribution Systems Using Machine Learning," in *2025 IEEE International Conference on Consumer Electronics (ICCE)*, 2025: IEEE, pp. 1-6.
[120] W. Huang, T. Guo, Y. Gao, and L. Hua, "A Coordinated Voltage Control Strategy for Coordination of Wind Turbines Variable Mode control and OLTC in

Distribution Grid," in *2019 IEEE Innovative Smart Grid Technologies-Asia (ISGT Asia)*, 2019: IEEE, pp. 2544-2549.

[121] R. Hu, W. Wang, Z. Chen, X. Wu, L. Jing, W. Ma, and G. Zeng, "Coordinated voltage regulation methods in active distribution networks with soft open points," *Sustainability,* vol. 12, no. 22, p. 9453, 2020.

[122] C. Li, Y. Dai, P. Wang, and S. Xia, "Active and reactive power coordinated optimization of active distribution networks considering dynamic reconfiguration and SOP," *IET Renewable Power Generation,* vol. 19, no. 1, p. e12814, 2025.

[123] J. Zhang *et al.*, "Optimal operation strategy for distribution network with high-penetration distributed PV based on soft open point and multi-device collaboration," *Energy,* vol. 325, p. 136191, 2025.

[124] W. Cao, J. He, and Y. Zhou, "Voltage control in distribution networks with soft open point and on-load tap changer," in *2021 IEEE 4th International Conference on Electronics Technology (ICET)*, 2021: IEEE, pp. 446-451.

[125] H. Diao, P. Li, K. Liu, J. Xiao, and Z. Mao, "Co-deployment of energy storage systems and soft open points in distribution networks considering normal and extreme conditions," *Journal of Energy Storage,* vol. 125, p. 116806, 2025.

[126] J. Shang, H. Liu, R. Zhang, and J. Wang, "Optimal economic operation of active distribution networks with energy storage integrated SOP," in *2022 IEEE 3rd China International Youth Conference on Electrical Engineering (CIYCEE)*, 2022: IEEE, pp. 1-5.

[127] M. Amini, M. H. Nazari, and S. H. Hosseinian, "Optimal energy management of battery with high wind energy penetration: A comprehensive linear battery degradation cost model," *Sustainable Cities and Society,* vol. 93, p. 104492, 2023.

[128] T. Goldstein, B. O'Donoghue, S. Setzer, and R. Baraniuk, "Fast alternating direction optimization methods," *SIAM Journal on Imaging Sciences,* vol. 7, no. 3, pp. 1588-1623, 2014.

[129] C. Mavromatis, M. Foti, and M. Vavalis, "Auto-tuned weighted-penalty parameter ADMM for distributed optimal power flow," *IEEE Transactions on Power Systems,* vol. 36, no. 2, pp. 970-978, 2020.

[130] R. Zhang, Y. Song, and R. Qu, "Distributed optimal Volt/Var control in power electronics dominated AC/DC hybrid distribution network," *IET Renewable Power Generation,* vol. 18, no. 15, pp. 2978-2990, 2024.

[131] W. Zheng, W. Wu, B. Zhang, H. Sun, and Y. Liu, "A fully distributed reactive power optimization and control method for active distribution networks," *IEEE Transactions on Smart Grid,* vol. 7, no. 2, pp. 1021-1033, 2015.

[132] Y. Nesterov, "Smooth minimization of non-smooth functions," *Mathematical programming,* vol. 103, no. 1, pp. 127-152, 2005.

[133] S. Mhanna, G. Verbič, and A. C. Chapman, "Adaptive ADMM for distributed AC optimal power flow," *IEEE Transactions on Power Systems,* vol. 34, no. 3, pp. 2025-2035, 2018.

[134] S. Paul, B. Ganguly, and S. Chatterjee, "Nesterov-type accelerated admm (n-admm) with adaptive penalty for three-phase distributed opf under non-ideal data transfer scenarios," in *2023 IEEE 3rd International Conference on Smart Technologies for Power, Energy and Control (STPEC)*, 2023: IEEE, pp. 1-6.

[135] E. Ghadimi, A. Teixeira, I. Shames, and M. Johansson, "Optimal parameter selection for the alternating direction method of multipliers (ADMM): Quadratic problems," *IEEE Transactions on Automatic Control,* vol. 60, no. 3, pp. 644-658, 2014.